Interplay between peripheral signals, behaviour and the central clock

Claire Gizowski

Integrated Program in Neuroscience, McGill University

October 2019

A thesis submitted to McGill University in partial fulfillment of the requirements of the degree of Doctor of Philosophy

TABLE OF CONTENTS

Abstract

Almost all living organisms exhibit circadian rhythms, ranging from complex humans to simple cyanobacteria. Circadian rhythms are critical to adapt an organism's physiology and behaviour to the constraints of earth's 24h light-dark cycle. In mammals, the suprachiasmatic nucleus (SCN) serves as the body's master circadian clock and provides anticipatory homeostatic benefits. For example, the SCN opposes overnight adipsia by driving anti-diuretic hormone secretion and lowering body temperature to reduce water loss during sleep. Maintaining optimal body fluid balance is essential to sustain life and such rhythms are indispensable to prevent life-threatening pathologies. However, very little is known about how changes in the electrical activity of clock neurons actually mediate central rhythms. Likewise, we know almost nothing about how their activity can be altered by unanticipated changes in an organism's physiology. Throughout my PhD, I investigated the bidirectional interactions between the central clock and central osmosensors. Specifically, how (i) the clock can regulate water intake prior to sleep to prevent overnight dehydration and (ii) how an acute rise in osmolality can alter clock time and its output-networks to drive homeostatic responses. Collectively, the findings of this thesis significantly advance our understanding of how the central clock functions.

Résumé

Presque tous les organismes vivants démontrent des rythmes circadiens, aussi bien les humains dans toute leur complexité que les cyanobactéries simples. Les rythmes circadiens sont primordiaux pour adapter la physiologie et les comportements d'un organisme au cycle de 24h sur terre. Chez les mammifères, le noyau suprachiasmatique (NSC) est reconnu comme étant l'horloge centrale responsable du contrôle des rythmes circadiens fournissant des avantages homéostatiques anticipatifs. Par exemple, le NSC contrecarre la déshydratation survenant durant la nuit en stimulant la sécrétion de l'hormone antidiurétique et en réduisant la température corporelle afin de réduire la perte d'eau durant le sommeil. Maintenir une balance des fluides corporels optimale est essentielle à la vie et de tels rythmes sont indispensables pour prévenir des pathologies mortelles. Toutefois, on n'en connaît que très peu sur la façon dont les changements dans l'activité électrique des

neurones-horloge modèrent les rythmes centraux. Pareillement, on ne connaît presque rien sur la façon dont leur activité peut être altérée par des changements inattendus de la physiologie d'un organisme. Tout au long de mon doctorat, j'ai étudié les interactions bidirectionnelles entre l'horloge centrale et les osmosenseurs centraux. Plus précisément, comment (i) l'horloge peut régulariser la prise d'eau avant le sommeil pour empêcher la déshydratation pendant la nuit et (ii) comment une augmentation aiguë en osmolalité peut altérer l'horloge et entraîner des réponses homéostatiques de ses réseaux de sortie. Ensemble, les résultats de cette thèse amènent des progrès significatifs sur notre compréhension du fonctionnement de l'horloge centrale.

Acknowledgements

First, and foremost, I want to thank my supervisor, Dr. Charles Bourque, for helping me along this wild adventure. Without your unwavering support, none of this would have been possible. I want to thank you for always believing in me and giving me the confidence to ask bold questions and tackle problems from head-to-toe. Anyone who is lucky enough to have you as a mentor and friend will undoubtedly become a better scientist and person.

Next, I would like to thank my parents, Nicole Régis and Jim Gizowski. Even though you do not entirely understand what I do, you have always supported my dreams. Without your love, sense of humour and support, I would not be where I am and who I am today.

Merci à Mathieu Dionne pour ton aide avec la traduction de mon résumé scientifique en résumé poétique, car la science c'est d'la poésie!

I also want to thank my current and former lab mates, Josh, Cristian, Zahra, Eric, Daniel, Nick, Nate, Masha, David and Katrina for your kindness and support throughout the years. We can only truly grow as scientists when we surround ourselves with people who challenge us to think differently.

I want to thank my advisory committee members Drs. Keith Murai and Jesper Sjöström, the CRN, BRaIN program and the MNG for the thoughtful discussions and support offered to me throughout my degree. In addition, I want to thank CIHR and the RIMUHC for generously funding this work.

Lastly, I want to thank the animal technicians and vets for taking care of my animals, giving me a circadian room, letting me modify cages and use their equipment to complete my experiments. Even though one of you did make me cry, you still helped me a lot.

Peer-reviewed publications arising from this work

***GIZOWSKI C,** and BOURQUE CW (2019) Salt regulates clock time and output via an excitatory GABAergic neural circuit. *Submitted.*

***GIZOWSKI C,** and BOURQUE CW (2018) Hypothalamic neurons controlling water homeostasis: it's about time. *Current Opinion in Physiology*. 5: 45-50

ZAEZLER C, **GIZOWSKI C,** SALMON C, MURAI, KK, & BOURQUE, CW (2018) Detection of activity-dependent vasopressin release from neuronal dendrites and axon terminals using sniffer cells. *Journal of Neurophysiology*. 120: 1386-1396

***GIZOWSKI C,** ZAELZER C, and BOURQUE CW (2018) Activation of organum vasculosum neurons and water intake in mice by vasopressin neurons in the suprachiasmatic nucleus. *Journal of Neuroendocrinology*, (Epub ahead of print)

***GIZOWSKI C** and BOURQUE CW (2018) The neural basis of homeostatic and anticipatory thirst. *Nature Reviews Nephrology* 14, 11-25

***GIZOWSKI C**, TRUDEL E, and BOURQUE CW (2017) Central and peripheral roles of vasopressin in the circadian defense of body hydration. *Best Practice & Research Clinical Endocrinology & Metabolism*, 31, 535-546

***GIZOWSKI C** and BOURQUE CW (2017) Neurons that drive and quench thirst. *Science* 357, 1092-1093

***GIZOWSKI C**, ZAELZER C and BOURQUE CW (2016) Clock-driven vasopressin neurotransmission mediates anticipatory thirst prior to sleep. *Nature* 537, 685-688.

Contribution to original knowledge

This is a manuscript-based thesis built from published and submitted works. This thesis was written according to guidelines by McGill University.

Chapter 1 – Introduction

This chapter provides a review of the scientific literature on circadian biology. How the SCN is organized, how neurons in the SCN fire autonomously and are synchronized with each other are described. The mechanisms by which the clock controls rhythms and can be mediated by photic and non-photic rhythms are also outlined. Furthermore, how thirst can be regulated is introduced in this chapter.

Chapter 2 – The neural basis of homeostatic and anticipatory thirst

In this chapter, we provide a highly detailed overview of the different mechanisms by which fluid homeostasis is regulated in animals. I consider this chapter to be part of my introduction, however it is presented as a standalone chapter as it has been published:

GIZOWSKI C and BOURQUE CW (2018) The neural basis of homeostatic and anticipatory thirst. *Nature Reviews Nephrology* 14, 11-25

Chapter 3 – Clock-driven vasopressin neurotransmission mediates anticipatory thirst prior to sleep

In this chapter we provide the first detailed mechanism by which the circadian clock can regulate water intake. In addition, we provide the first definitive evidence demonstrating that neuropeptides can act as neurotransmitters. We also demonstrate a new kind of thirst, termed "anticipatory thirst", and reveal that the circadian clock drives thirst prior to sleep in anticipation of the reduction in water intake overnight to prevent overnight dehydration in mice. This work was published in the following article:

GIZOWSKI C, ZAELZER C and BOURQUE CW (2016) Clock-driven vasopressin neurotransmission mediates anticipatory thirst prior to sleep. *Nature* 537, 685-688.

Chapter 4 – Salt regulates clock time and output via an excitatory GABAergic neural circuit

In this chapter, we describe how a physiologically relevant non-photic cue can alter clock time and output. Specifically, we show that salt can mediate SCN^{VP} neuron activity via an input from $OVLT^{GAD}$ neurons. We demonstrate that this pathway is mediated by an excitatory GABAergic projection and can mediate adaptive changes in body temperature via regulation of non-shivering thermogenesis. A manuscript containing these results are currently under consideration:

GIZOWSKI C and BOURQUE CW (2019) Salt regulates clock time and output via an excitatory GABAergic neural circuit.

Chapter 5: **General Discussion**

This chapter represents a general discussion of how experimental findings in the previous chapters relate to one another and to current literature, identification of remaining questions and suggestions for future studies.

Contribution of Authors

Chapter 2

GIZOWSKI C. (McGill University, Montreal, Quebec, Canada)

Although this review is co-authored with Dr. Bourque, I performed 85% of the writing and preparation of the figures.

Chapter 3

GIZOWSKI C. (McGill University, Montreal, Quebec, Canada)

Experimental design; performed all experiments except single cell RT-PCR, and quantified and interpreted data. I performed 90% of the experiments and 80% of the writing.

ZAELZER C. (McGill University, Montreal, Quebec, Canada)

Single cell RT-PCR and quantification of data.

Chapter 4

GIZOWSKI C. (McGill University, Montreal, Quebec, Canada)

Experimental design; performed all experiments, and quantified and interpreted data. I performed 100% of the experiments and 90% of the writing.

List of abbreviations

$[Na^+]$ − Sodium concentration
3V − Third ventricle
AC − Anterior commissure
ACC − Anterior cingulate cortex
ACSF − Artificial cerebrospinal fluid
AMCSF − Artificial mouse cerebrospinal fluid
Ang II − Angiotensin II
ANOVA − Analysis of variance
ANP − Atrial natriuretic peptide
AP − Anticipatory period
AP − Area postrema
ArchT − Archaerhodopsin-3
ARCSF − Artificial rat cerebrospinal fluid
AVP − Vasopressin
AVP^{Cre} − Cre expression in vasopressin cells
BAT − Brown adipose tissue
Bic − Bicuculline
BL − Blue light
BNP − B-type natriuretic peptide
BNST − Bed nucleus of the stria terminalis
BP − Basal period
ChETA − E123T mutant channelrhodopsin 2
Cl− − Chloride
CNO − Clozapine-N-oxide
Cs+ − Cesium
CSF − Cerebrospinal fluid
DD − Dark:Dark
DREADD − Designer receptors exclusively activated by designer drugs
ECF − Extracellular fluid
E_{GABA} − Reversal potential of GABA
ENaC − Epithelial-like Na^+ channel
E_{rev} − Reversal potential
fMRI − Functional magnetic resonance imaging
FO − Fiberoptic
FR − Firing rate
G − Conductance
GABA − γ-Aminobutyric acid
$GABA_AR$ − $GABA_A$ receptor
GAD^{Cre} − Cre expression in glutamic acid decarboxylase expressing cells
GBZ − Gabazine
GFP − Green fluorescent protein
GHT − Geniculohypothalamic tract
GluR − Glutamate
GPCR − G-protein coupled receptor

GRP − Gonadotropin releasing peptide
H^+ − Hydrogen
hDBB − Horizontal Diagonal Band of Broca
HEK293 − Human embryonic kidney 293 cell
IC − Insular cortex
IGL − Intergeniculate leaflet
IPSP − Inhibitory postsynaptic potential
IRT − Infrared thermography
I-V − Current-voltage
K^+ − Potassium
Kyn − Kynurenate
LD − Light:Dark
ME − Median eminence
MnPO − Median preoptic nucleus
$MnPO^{nNOS}$ – nNos expressing MnPO neurons
mOsm − Milliosmoles
MS − Medial septum
Na^+ − Sodium
NaCl − Sodium chloride
Nav − Voltage-gated Na^+ channel
Na_X − Voltage-sensitive Na^+ channel
nNO – Nitric oxide synthase
NMDA − *N*-methyl-d-aspartate; glutamate receptor agonist
NSC − Noyau suprachiasmatique
NST − Non-shivering thermogenesis
NTS − Nucleus of the tractus solitaries
OC − Optic chiasma
OVLT − Organum vasculosum lamina terminalis
$OVLT^{GABA}$ – OVLT neurons expressing GABA
F − Fluorescence
$OVLT^{GAD}$ – OVLT GAD neurons
$OVLT^{nNOS}$ – nNOS expressing OVLT neurons
$OVLT^{V1aR}$ − V1aR expressing OVLT neurons
$OVLT^{Vglut}$ – Vesicular glutamate transporter 1 expressing OVLT neurons
PACAP − Pituitary adenylate cyclase-activating polypeptide
PBN − Parabrachial nucleus
PBS − Phosphate buffered saline
PET − Positron emission tomography
PFA − Paraformaldehyde
POA − Preoptic area
PP − Posterior pituitary
PSC − Post synaptic current
PVN − Hypothalamic paraventricular nucleus
PVT − Paraventricular nucleus of the thalamus
RAAS − Renin–angiotensin–aldosterone system
RGC − Retinal ganglion cells

RHT − Retinohypothalamic tract
RT-PCR − Reverse transcriptase polymerase chain reaction
s.c. − Subcutaneous
S.D. − Standard deviation
s.e.m. − Standard error of the mean
SCN STIM − Electrical stimulation of the SCN
SCN − Suprachiasmatic nucleus
SCN^{VIP} − SCN VIP neurons
SCN^{VP} − SCN VP
SFO − Subfornical organ
SFO^{nNOS} − nNOS expressing SFO neurons
SON − Supraoptic nucleus
sOsm − Serum osmolality
sPSC − Spontaneous post synaptic current
SR − SR49059
T_b − Core body temperature
T_{BAT} − BAT temperature
tdTOM – tdTomato
T_{EYE} − Eye temperature
THAL − Thalamus
TRPV1 − Transient receptor potential vanilloid 1
TTFL − Transcription-translation feedback loop
TTX − Tetrodotoxin
V1aR − Vasopressin 1 a receptor
$V1aR^{-/-}$ − V1a receptor knockout
V1bR − Vasopressin 1 b receptor
vDBB − Ventral Diagonal Band of Broca
$Vgat^{Flp}$ − Flipase expression in vesicular inhibitory amino acid transporter cells
VIP − Vasoactive Intestinal Peptide
VLM − Ventrolateral medulla
VLM − Ventrolateral medulla
Vm − Membrane voltage
vmPOA − Ventral medial part of the POA
VP − Vasopressin
$VPAC_2$ − VIP receptor 2
WT − Wild type
ZT − Zeitgeber time
Δ − Delta

Chapter 1 – Introduction

1.0 – Foreword

The introduction to this thesis (Chapter 1) is perhaps briefer than most of its counterparts in the field of life sciences. This is because, as will be mentioned in section 1.2, I consider chapter 2 to provide significant standalone introduction material that would have otherwise been incorporated within this chapter.

1.1 – General introduction

Circadian rhythms have evolved to produce cyclic changes in behaviour, hormone secretion and metabolism that adapt the body to changing requirements throughout the earth's 24-hour light/dark cycle. While individual cells and tissues, both centrally and peripherally located, are endowed with cell-autonomous clocks, appropriate timing and synchronization of these clocks requires signals derived from the brain master circadian clock, the suprachiasmatic nucleus (SCN). The SCN is a bilateral hypothalamic structure that comprises approximately 20,000 neurons that form a highly interconnected network. SCN neurons display prominent daily rhythms in both gene expression and action potential firing rate, and the timing of these rhythms is entrained primarily by light input via axonal inputs from the retina. Although the clock is best known for being the primary pacemaker that regulates circadian rhythms, almost nothing is known about how the clock achieves this. For example, are target axonal projections emerging from SCN neurons required to mediate rhythms? Are changes in the firing rate of SCN output projection neurons required to mediate rhythms? And, do neuropeptides mediate SCN-dependent rhythms? Moreover, there is a vast body of literature describing how different non-photic cues, such as drugs, can alter clock time and output, however it is poorly understood how this information is transmitted to the clock's timing and how clock-outputs are influenced by these cues. For example, do such cues cause acute changes in the electrical activity of SCN neurons, or impact the long-term circadian timing of their electrical activity? Can non-photic cues mediate physiologically relevant functions? My PhD thesis investigates such questions in rodents; specifically, (i) how the clock can regulate circadian rhythms of body fluid homeostasis and (ii) how homoeostatic perturbations affect clock time and clock outputs.

1.1.1 – The clock

Roughly 300 years ago, in 1729 in an essay entitled *Observation botanique*, Jean-Jacques Dortous de Mairan reported the observation that *Mimosa pudica* plants exhibited a daily pattern in the state of their leaves: when the sun was out, the leaves were spread open, and when the sun went down, the leaves and stems of the plant folded up. To determine whether this behaviour was simply a response to the sun, he placed the plant in a dark closet; de Mairan observed the same rhythmic pattern of leaf movements in the absence of light or to the open air[1,2]. This simple, but crucial observation is recognized as the intellectual foundation establishing the fundamental principle of chronobiology: a 24-hour rhythm that persists in the absence of recurrent daily fluctuations in the external environment (e.g. light vs. dark) is a rhythm driven by an endogenous circadian clock (Latin: *circa* "approximately" *diēm* "day")[3]. It was also noted in this publication that the daily rhythms of the plant leaves in the absence of light were reminiscent of bedridden people that were able to tell the difference between day and night without seeing changes in daylight, suggesting that de Mairan probably also had somewhat of an idea that animals could also "tell time". However, it was not until the 1970s that researchers discovered the SCN, the master circadian pacemaker. The role of the SCN as a master clock in mammals was revealed by several studies showing that SCN lesions abolished circadian rhythms in locomotor activity[4], corticosterone levels[5] and water intake[6]. Furthermore, experiments showed that locomotor rhythmicity could be restored by implanting SCN tissue from donor animals into the third ventricle of SCN-lesioned hamsters. Remarkably, it was observed that the circadian periodicity characteristics of the donor, in this case a period shorter than 24h, became expressed by the host, which established that the SCN is an autonomous oscillator that has the capacity to drive overt behavioural circadian rhythms[4]. Furthermore, transplanting encapsulated SCN grafts into SCN lesioned animals revealed that some circadian rhythms could be sustained by diffusible factors. However, in animals with encapsulated SCN grafts, endocrine and reproductive response rhythms were not restored using this approach [7,8], indicating that some functions require direct neural input from the clock.

1.1.2 – Organization of the SCN

The mammalian SCN is a bilateral football shaped nucleus in the hypothalamus that extends rostrocaudally and lies dorsal to the optic chiasm on either side of the third ventricle. The nucleus

is densely packed by a chemically heterogenous population of 10,000 neurons in each nucleus[9,10]. Most, if not all, SCN neurons produce the inhibitory neurotransmitter γ-aminobutyric acid (GABA; single amino acid) but also coexpress one or more neuropeptide (multi-amino acid peptide chain). Most neurons in the SCN coexpress vasopressin (VP ~30%) or vasoactive-intestinal peptide (VIP; ~20%), or various other peptides such as gonadotropin-releasing peptide (GRP), calretinin enkephalin, substance P, somatostatin, neuropeptide Y, neuromedin U, angiotensin II, thyrotropin-releasing hormone, and neurotensin. Each neuropeptide has at least one type of G-protein coupled receptor (GPCR) that can potentially engage a multitude of second messenger systems, and cause changes in gene expression and ion channel activity in post synaptic targets. Over 100 endogenous peptides have been identified in the SCN[11], which easily illustrates the potential for diverse signalling methods offered by this complex nucleus[10,12,13]. There are two striking anatomically distinct compartments within the SCN that are characterized by a high density of neurons expressing specific peptides. These are known as the *shell*, spanning the dorsomedial region, and the *core*, comprising of the ventrolateral area, which predominantly contain VP, and VIP and GRP neurons, respectively.

Anatomical antero- and retrograde tracing studies demonstrate that the clock densely innervates and is innervated by brain-wide sites [14,15]. The main afferent inputs originate from the retina (see section 1.1.4), which entrain the clock to the environmental light cycle, however the clock also receives abundant afferent inputs from non-photic regions. For example, the limbic system, the extraretinal visual system, and the hypothalamus (the latter will be further discussed in section 1.1.5)[15]. These inputs are organized topographically within the SCN[15]. For instance, the retina and the extraretinal visual system densely innervate VIP neurons within the core region, whereas the limbic and hypothalamic regions innervate dorsal regions[15]. This organization likely permits VIP neurons to function as the primary synchronizers of the SCN to environmental light cycles, whereas the non-retinal inputs to the shell allows VP neurons to potentially receive information about physiological need and use this information to alter homeostatic responses accordingly[14-17].

Within the SCN, neurons in the shell and core project ipsilaterally, and project to neurons in the homologous contralateral nucleus[16]. There are dense ipsilateral projections from the core to the

shell, however very sparse inputs from shell to core[16], further reinforcing the notion that the core serves as the primary pacemaker that synchronizes neurons within the SCN (see section 1.1.3), whereas the shell drives output-networks.

1.1.3 – Circadian oscillators

The classic pacemaker electrical activity of SCN neurons is characterized by a high firing rate during the light period and low during the dark period in both diurnal and nocturnal animals[18-24]. A unique property of these neurons is their ability to generate daily electrical activity rhythms even in isolation from the rest of the organism as observed in both brain slice preparations[25] and in dispersed cell cultures made from SCN tissue[24,26,27]. In dispersed cell cultures, the firing of individual SCN neurons is endogenously rhythmic, however they are not necessarily synchronized with one another or to the light cycle (further discussed in section 1.1.4). Interestingly, application of tetrodotoxin (TTX), a voltage-gated sodium channel blocker, blocks the firing activity of cultured SCN neurons, and following washout, their individual firing patterns re-emerge unperturbed. This finding indicates that individual clock neurons do not rely on intercellular communication to drive endogenous rhythmic firing patterns, but instead intrinsically generate circadian oscillations [23,24,28]. However, how these neurons generate intrinsic firing patterns is not known.

Recent Nobel Prize winning work has established that the molecular clock work is underpinned by a transcription-translation feedback loop (TTFL)[29]. The transcription, translation, and degradation of key clock genes in an autoregulatory loop with an endogenous period of ~24h have been hypothesized to drive daily cycles in electrical firing. During the light period, CLOCK/BMAL1 protein dimers act at E-box elements to promote transcription of a family of three period genes (*per1*, *per2*, *per3*) and two cryptochrome genes (*cry1*, *cry2*), leading to the increase in PER and CRY levels, whereby PER/CRY dimers inhibit transcription of their own genes. The progressive degradation of PER/CRY proteins during the dark period relieves the inhibition and permits a new cycle to begin. The TTFL is thought to drive cyclic electrical activity by driving rhythmic changes in ion channel expression in SCN neurons. For example, it has been shown that voltage-dependent potassium (K^+) channels are more prominently expressed during the dark period[30-32,33]. These currents likely contribute to overall membrane hyperpolarization and to the decrease in firing of

SCN neurons at this time[34-36]. It has also been speculated that the TTFL exerts rhythmic control over intracellular calcium, which can influence membrane excitability[37]. However, how this might occur is entirely unknown. Conversely, electrical activity is thought to reciprocally contribute to the stability of the SCN TTFL mechanism, as TTX application significantly dampens PER2 expression[38], revealing a chicken and egg situation. Ultimately, these potential mechanisms are speculative and the lack of mechanistic evidence explaining how SCN neurons rhythmically fire presents a critical gap in our knowledge of the SCN and the mammalian circadian system.

1.1.4 – Synchronization of clock time

As discussed in the previous section, SCN neurons are capable of generating cell-autonomous oscillations. However, even in the presence of abundant functional synapses between dispersed neurons in culture, individual neurons do not fire synchronously as they normally would in intact slice preparations *in vitro* or *in vivo*[24]. SCN neurons were not designed to function alone, instead synchronous firing observed during the light/dark cycle depends on precise spatiotemporal organization, intercellular signaling and glial-neuron interaction to reinforce the collective rhythmicity of the network.

As a whole, to maintain rhythmicity within the entire SCN, connectivity between the shell and core regions is required[39]. For instance, when the core and shell are physically separated *in vitro*, the core region maintains synchronous firing, however the shell region becomes arrhythmic. Restoration of function by SCN transplants in animals rendered arrhythmic by SCN lesions is made possible by transplants that predominantly contain VIP neurons (core), whereas transplants mainly containing VP neurons (shell) do not restore rhythmicity[40]. Moreover, mice lacking VIP or its receptor, $VPAC_2$ (VIP receptor 2), exhibit severe deficits in circadian behaviour, clock gene oscillations and SCN firing rhythms, indicating VIPergic neurons promote synchronized rhythmicity in other cell types via neuropeptide signalling[41]. Moreover, there is evidence suggesting that electrical synapses (gap junctions) are present in the SCN and may contribute to neuronal synchrony[42]. For example, connexin36 (gap junction protein) knockout mice show dampened circadian activity rhythms *in vivo*[43], and inhibition of gap junctions by nonspecific agents disrupt circadian rhythms of neuronal firing[44] and neuropeptide release[45] *in vitro*. Electrical synapses are

proposed to facilitate intercellular coupling within VIP or VP subpopulations[45] and glial-neuron interactions within the SCN[44], however it remains unclear whether gap junctions are important for synchronization. Recent evidence shows that glutamatergic signals from astrocytes with functional TTFLs can reinstate circadian oscillations of clock gene expression in SCN neurons *in vitro* and initiate and sustain robust circadian patterns of locomotor activity *in vivo* in *Cry*-null mice[46]. Interestingly, specific inhibition of hemichannel function in astrocytes, which prevents glutamatergic gliotransmission without altering gap junction communication in astrocytes, prevented the resynchronization of SCN neurons[46]. Although there is still much to be discovered on what makes the SCN fire synchronously, collectively, the evidence strongly suggests that classic chemical synapses alone are not sufficient for synchronizing the clock. Instead, this is achieved through several diverse signaling mechanisms.

1.1.5 – Clock inputs – photic

As mentioned above, light is the most potent synchronizer of the circadian clock. For instance, a single 10-minute light pulse delivered at the beginning of the active period can induce a phase delay in the onset of activity rhythms on following days observed in constant darkness. Conversely, a light pulse delivered toward the end of the active period, phase advances subsequent onsets of activity[47]. Light information is relayed to the SCN via a direct retinohypothalamic tract (RHT) pathway originating from the retina which almost exclusively terminates within the core[48,49]. It has recently been shown that mice lacking rods and cones are still capable of entraining to light cycles[50]. This observation led to the discovery of a subset of retinal ganglion cells (RGC) that express the photosensitive pigment melanopsin[51], which is capable of mediating extra-visual function such as pupillary reflex and entrainment of the circadian clock. Indeed, in experiments where RGCs were specifically ablated, animals lost the ability to photoentrain their circadian activity rhythms to the light cycle, whereas their normal outer retinal function was unaffected[52]. RGCs transmit light information to the core by secreting glutamate and pituitary adenylate cyclase-activating polypeptide (PACAP), which is co-expressed with glutamate in a subset of cells[53-55]. *In vitro* administration of glutamate, NMDA (*N*-methyl-d-aspartate; glutamate receptor agonist)[56] or PACAP[57] on SCN slices causes phase shifts in the firing pattern of neurons, and *in vivo* intraventricular delivery of NMDA antagonists prevent phase shifts induced by light[58,59]. Recent

work has revealed that a number of RGCs also coexpress VP[60], and VP receptor knockout mice show accelerated recovery from jet lag[61], suggesting a potential role for retinal-VP in mediating photic entrainment. Photic input can also be relayed via the geniculohypothalamic tract (GHT) from the intergeniculate leaflet (IGL). The IGL receives direct input from the retina via a separate branch of the RHT, whereby GHT afferents terminate within the core, overlapping with RHT inputs. The GHT also provides an alternate input, which has been implicated in non-photic circadian entrainment (discussed in section 1.1.6). Collectively, the data favours glutamatergic afferents as being the primary mediators of circadian photoentrainment, however there is strong evidence that non-glutamatergic inputs can also relay photic information. Ultimately, further work is required to fully elucidate the mechanisms by which the clock keeps time with the daily light cycle.

1.1.6– Clock inputs – non-photic

The idea that the clock can be synchronized by non-photic stimuli goes back to the early 1950s[62]. Much attention has been focused on how periodic feeding[63], social interaction[64], restricted wheel running activity[65], and various drugs such as opioids[66,67], benzodiazepines[68,69] and melatonin[70] can phase shift the circadian clock. It has been proposed that inputs from the IGL via the GHT can mediate non-photic input to the clock. Indeed, IGL lesions prevent the phase shifts induced by novel wheel running activity and benzodiazepines[71], however the specific neural circuits underlying the mechanisms by which non-photic stimuli are relayed to the clock remain unclear. The SCN also receives abundant direct afferent input from various brain areas, including the hypothalamus, however it is not known what role these inputs serve or if they can relay non-photic information to the clock. The ethological significance for why the central pacemaker can be shifted by stimuli other than the light cycle is not yet clear. The most convincing argument for why this entrainment occurs stems from studies of maternal synchronization of the clock in utero. For instance, although light can penetrate the hamster uterus[72], entrainment of the foetus to prevailing LD cycles is mediated exclusively by maternal signals such as melatonin and dopamine[73-75]. In animals that are not directly or regularly exposed to light, maternal entrainment cues enable newly born pups to exhibit circadian rhythms phase locked to local time. While the adaptive significance of non-photic signals is clear for neonates, in adults it is less clear. Alternatively, the field may be looking for answers to this question in the wrong places. Instead of thinking of the clock as a simple pacemaker, there is potential for the clock to serve as an integrative hub, whereby it can receive information

about physiological need (i.e. non-photic cues) and acutely regulate its output to adapt to changes in an organism's internal environment. This question was explored as part of my PhD work and is further discussed in Chapter 4.

1.1.7 Clock outputs

As mentioned in section 1.1.1, the clock can exert control over certain rhythms via what appears to be volume transmission of neuropeptidergic signals (grafts encapsulated in SCN-lesioned animals), however certain rhythms are not restored, indicating the need for direct neural input from the clock[7,8]. The control of rhythmic function is thought to be mediated primarily by VP neurons in the SCN. Several lines of evidence support this theory. First, to this day, central VP is still the only known SCN humoral output secreted in the cerebrospinal fluid (CSF) with a marked circadian rhythm *in vivo*[76]. Indeed, specific SCN lesion experiments result in arrhythmic VP secretion in the CSF[77]. Next, VP deficient rats, known as the Brattleboro rat, exhibit coherent rhythms in activity and sleep/wake cycles in cyclic light and constant light, however they show overall reduced activity[78] and reduced amplitudes of circadian sleep rhythms, such as slow-wave and paradoxical sleep[79]. Furthermore, central VP has also been shown to exert circadian control over the hypothalamo-pituitary-adrenal system. For example, intraventricular administration of a VP receptor antagonist increases circulating plasma corticosterone levels when delivered during the middle of the light period, whereas administration of VP toward the end of the light period prevents the rise in corticosterone[80,81]. Moreover, previous work from the Bourque Lab has shown that the excitation of VP neurons in the supraoptic nucleus, which secrete VP in the periphery, is thought to be mediated in part by a neural pathway between VP neurons in the SCN and the supraoptic nucleus[82,83]. Collectively, the literature strongly supports the theory that VP neurons are the main output of the SCN, however, heretofore the lack of genetic tools available has prevented the study of identified neuron populations and how they can mediate circadian rhythms. As part of my PhD, I explore how identified VP neurons in the SCN mediate homeostatic behaviours in defined neural circuits (Chapter 3 and 4). Specifically, my thesis will explore the possibility that the SCN can exert circadian influence on water intake for homeostatic benefit.

1.2 Regulation of thirst

A critical component of this thesis examined the possibility that the central clock regulates a specific form of need-free water intake. Because thirst is a complex topic that incorporates potentially many types of physiological stimuli, I performed an exhaustive review of the field to ascertain my ability to master the area and provide conclusive evidence for describing what I ultimately termed "anticipatory thirst". Because of its significant scope, this review was published as a full article in Nature Reviews Nephrology. This scholarly article is a full synthesis of our understanding of the mechanisms of fluid homeostasis and is included as a formal contribution to new knowledge in the form of Chapter 2 in this thesis, rather than being included within the introduction. However, for clarity, I will quickly cover some basic key points in this section.

There are two major ways in which thirst can be regulated in organisms. The first is via negative homeostatic feedback responses to rises is blood osmolality or decreases in blood volume. For instance, the loss of water caused by thermoregulatory sweating, panting, or saliva spreading during prolonged physical activity results in a rise in osmolality in animals as secreted fluids, including alveolar exudate, are hypoosmotic, thereby stimulating thirst to maintain extracellular fluid near ideal set-points[84]. Central osmosensory neurons, such as those located in the organum vasculosum lamina terminalis (OVLT) and subfornical organ (SFO), monitor changes in blood osmolality[85-89], solute load[90-94] and hormone circulation[95-100], and engage cortical areas such as the anterior cingulate cortex (ACC) and insular cortex (IC) to orchestrate the necessary responses to drive water intake [101-106]. Much of the way we think about thirst is based on the notion that it is simply a reflex of need; however, recent evidence indicates a clear role for thirst as a need-free feedforward adaptive anticipatory response that precedes physiological challenges. For example, neurons in the SFO are rapidly activated by food intake and drive water intake before any detectable rises in plasma osmolality can occur[107]. The occurrence of need-free water intake is a remarkable evolutionary behaviour which prompted me to question whether the circadian clock might drive water intake to anticipate physiological need associated with the daily light cycle (Chapter 3). Indeed, it was hypothesized almost half a century ago that drinking is controlled by "*an independent (presumably neural) programmer which has a marked circadian rhythm*"[108].

1.3 Aims of the thesis

As mentioned in the sections above, there is a notable lack of evidence demonstrating how neural projections emanating from the central clock can mediate overt circadian behaviours. In addition, there is almost nothing known about how neural circuits transmit non-photic information to the clock. As such, there is no evidence indicating non-photic stimuli can regulate clock-output networks to mediate physiologically relevant responses.

The first hypothesis, which is explored and fully stated in Chapter 3, investigates the possibility that the central clock can drive need-free water intake. Specifically, we wondered if SCN VP neurons (SCN^{VP}) excite OVLT thirst neurons to mediate an increase in water intake prior to sleep to mitigate the impact of reduced water intake overnight.

The second hypothesis, stated in Chapter 4, explores the possibility that a physiologically relevant non-photic stimulus can alter clock time and mediate its outputs. Specifically, we wondered whether a rise in osmolality, achieved by injection of a physiologically relevant dose of salt, can drive an increase in the electrical activity of SCN^{VP} neurons via osmo and sodium-sensitive OVLT neurons at a time during which SCN^{VP} neurons are normally silent. Furthermore, we explored the hypothesis that a change in SCN^{VP} neuron activity could mediate acute changes in homeostatic responses, such as temperature and non-shivering thermogenesis.

Chapter 2 – The neural basis of homeostatic and anticipatory thirst

As explained in section 1.2, I performed an exhaustive review of the literature regarding the control of thirst. Although, this subject could have been incorporated into the general introduction (Chapter 1), it has been redacted as a major review published in Nature Reviews Nephrology and is therefore being presented as a standalone chapter because I consider it to be a significant scholarly contribution to knowledge. Although this review is co-authored with Dr. Bourque, I performed 85% of the writing and preparation of the figures.

Published in Nature Reviews Nephrology, November 25, 2018

The neural basis of homeostatic and anticipatory thirst

Claire Gizowski and Charles W. Bourque

Centre for Research in Neuroscience, Research Institute of the McGill University Health Center and Montreal General Hospital, 1650 Cedar Avenue, Montreal H3G1A4, Canada.

ABSTRACT

Water intake is one of the most basic physiological responses and is essential to sustain life. The perception of thirst has a critical role in controlling body fluid homeostasis, and if neglected or dysregulated can lead to life-threatening pathologies. Clear evidence suggests that the perception of thirst occurs in higher order centres, such as the anterior cingulate cortex (ACC) and insular cortex (IC), which receive information from midline thalamic relay nuclei. Multiple brain regions, notably circumventricular organs such as the organum vasculosum lamina terminalis (OVLT) and subfornical organ (SFO), monitor changes in blood osmolality, solute load and hormone circulation, and are thought to orchestrate appropriate responses to maintain extracellular fluid near ideal set-points by engaging the medial thalamic–ACC/IC network. Thirst has long been thought of as a negative homeostatic feedback response to increases in blood solute concentration or decreases in blood volume. However, emerging evidence suggests a clear role for thirst as a feed-forward adaptive anticipatory response that precedes physiological challenges. These anticipatory responses are promoted by rises in core body temperature, food intake (prandial) and signals from the circadian clock. Feed-forward signals are also important mediators of satiety, inhibiting thirst well before the physiological state is restored by fluid ingestion. In this Review, we discuss the importance of thirst for body fluid balance and outline our current understanding of the neural mechanisms that underlie the various types of homeostatic and anticipatory thirst.

INTRODUCTION

Mammals experience continual water losses through the production of urine and the evaporation of hypotonic fluid during breathing or sweating [109-111]. Consequently, the intermittent ingestion of water is essential to sustain life[112] and individuals with chronic adipsia must follow a disciplined regimen of voluntary fluid intake to remain healthy[113-118]. Although often overlooked as an instinctive process, the perception of thirst is critical to the control of body fluid homeostasis[84,119-122] and its dysregulation can result in life-threatening pathologies[114,118,123-125]. Although clear evidence demonstrates that the perception of thirst is primarily orchestrated by central neural networks,, adaptive changes in thirst can be induced by systemic processes, for instance in response to alterations in kidney function or pharmacological treatment with agents such as the vasopressin receptor 2 antagonist, tolvaptan[126]. Here we Review the importance of thirst as a regulated system and outline our current understanding of the neural mechanisms that underlie its control by homeostatic and anticipatory signals. Since our focus is on the control of hydration, we employ herein the term 'thirst' to designate specifically a drive to ingest water and do not consider factors involved in the choice or motivation to drink other types of fluid[127]. Moreover, for simplicity, we refer to thirst as any drive that can motivate water intake, regardless of cause.

Fluid balance in health and disease

Disturbances in the balance of body fluid encompass a spectrum of changes that can occur in the composition or volume of extracellular fluid (ECF)[123,128], and are frequently encountered in emergency medicine because they can be triggered by drugs[129-133], or by the ingestion of inappropriate amounts of water [134-136] or salt[137,138]. Disorders of fluid balance also occur secondary to acute conditions such as cerebral trauma[139], heart failure[140] and sepsis[141], and in chronic ailments that affect the kidneys[142] or liver [143]. Indeed, perturbations in fluid balance feature among the top 10 causes for patient admission at hospital emergency departments in the United States[144].

Small changes in ECF volume are well tolerated due to dynamic compensatory changes in vasomotor tone that modulate the compliance and capacity of the vascular system[145]. For example, decreases in blood volume of up to 15% can be experienced without significant changes in mean arterial pressure in humans[146]; however, progressively greater reductions in blood volume induce a

reflex increase in cardiac output[145]. Therefore, very large increases or decreases in ECF volume will ultimately cause arterial pressure to rise or fall, respectively, and thus under physiological conditions a series of volume-regulated homeostatic mechanisms maintain ECF volume near a desired set point (FIG. 1a).

Pathological symptoms can also be induced by changes in the solute concentration (that is, osmolality) of ECF. Sodium is the dominant ion in ECF and in healthy animals its concentration varies in direct proportion to osmolality[147]. Therefore, changes in either osmolality or sodium concentration ($[Na^+]$) can serve as indicators of tonicity in otherwise healthy individuals. Acute changes in extracellular tonicity are poorly tolerated because they cause swelling or shrinking of cells and organs due to osmosis[148]. Notably, acute decreases in ECF $[Na^+]$ (hyponatraemia) or osmolality (hypoosmolality) cause significant increases in brain volume[149], whereas acute hypernatraemia or hyperosmolality cause shrinking[150]. The brain is particularly sensitive to such insults and changes in ECF tonicity can result in the development of neurological symptoms. In otherwise healthy individuals, acute changes in tonicity of ±7% are asymptomatic [151], whereas changes greater than ±10% will cause weakness and lethargy, followed by nausea. More severe insults will lead to mental confusion and ultimately to convulsions and coma[132,151,152]. In healthy organisms, ECF osmolality is normally maintained near an optimal set point by osmotic or sodium-dependent mechanisms (FIG. 1b).

Thirst as a central homeostatic mechanism

As mentioned above, the overall control of fluid balance is achieved by the regulation of several behavioural and physiological responses that are orchestrated to maintain the volume and osmolality of ECF near ideal set-points (FIG. 1). Thirst, as a behavioural regulator of water intake, is a central player in this regulation. As discussed later, the control of thirst is not mediated exclusively by negative feedback signals. Rather, the intensity of its perception can also be enhanced or suppressed through feed-forward mechanisms that anticipate an impending gain or deficit in hydration status[153].

In 1821 Rullier described thirst as “le sentiment le plus vif et le plus impérieux de la vie” (the strongest sense and the most imperative of life)[154]. It is a physiological urge to oppose the continual

fluid loss that occurs through daily activities, which if neglected for prolonged periods becomes one of the most painful and difficult sensations to ignore[119]. Most humans have experienced thirst at some point in their lives, and it has been a subject of study for centuries. In 1867, Schiff hypothesized that thirst was a general sensation that arose from a deficiency of water content in the body[155]; however, whether thirst was a general or a localized sensation was much debated. The involvement of the central nervous system in the sensation of the thirst was proposed as early as the 19th century and in 1901, Wettendorff hypothesized that the brain was the "seat of the conscious perception of the sensation"[119,156].

A putative thalamo–cortical thirst module

The anterior cingulate and insular cortices

Experiments in rhesus monkeys provided the first evidence that activation of prefrontal cortical neurons might be responsible for the conscious perception of thirst in mammals. In a classic study, Robinson and Mishkin[157] showed water intake could be evoked by delivering current pulses through a stimulating electrode placed in the anterior cingulate cortex (ACC) of awake animals. Unlike responses sometimes evoked by stimulation in other regions, which were often delayed and outlasted the stimulus, responses evoked by ACC stimulation were 'stimulus bound' in that they occurred with short latency (2–8 s) and promptly ceased when stimulation was stopped. Moreover, water intake occurred much more reliably when induced by ACC stimulation than by stimulation of other regions. The ACC is thought to be associated with affective motivation, whereby basic homeostatic modalities such as hunger or thirst can prompt reflexive autonomic adjustments much like those induced by pain or an itch[158,159]. Indeed, thirst is considered one of the primordial emotions[160].

The involvement of the prefrontal cortex in the perception of thirst has also received considerable support from human studies of brain activation using positron emission tomography (PET) and functional magnetic resonance imaging (fMRI). These studies have shown that intense thirst induced by systemic infusion of hypertonic saline[104,105,161] or exercise-induced dehydration[162,163] is consistently linked to activation of the ACC and other regions such as the insular cortex (IC). The observation that ACC activation occurs when thirst is driven by interoceptive sensory modalities

(such as, increases in osmolality, or decreases in blood volume) that flow in distinct neuroanatomical pathways suggests this site might be critical for the genesis of thirst perception at the level of the cortex. Further support for this hypothesis is provided by the observation that in humans the ACC and IC are immediately deactivated when thirst is satiated by the ingestion of water, well before water absorption from the digestive tract corrects the affected physiological parameter[162-166].

Studies in rodents have also provided support for the involvement of prefrontal regions in thirst. For example, autoradiographic metabolic trapping studies have shown that [^{14}C]glucose accumulates in the ACC of water-deprived rats[167], suggesting metabolic activation of the ACC. Moreover, hypovolaemic thirst induced by injection of the diuretic furosemide induces expression of the immediate early gene *c-Fos* in the rat IC, indicating neuronal activation[168]. Whether the activation of ACC and IC neurons is necessary and sufficient to mediate the sensation of thirst remains to be determined; however, taken together these studies suggest that the ACC and IC are putative primary sites for the perception of thirst in mammals.

Thalamic nuclei

The flow of somatosensory information to ACC and IC neurons in the cortex occurs through thalamic nuclei. Interoceptive signals that ascend from the viscera are relayed to cortical sites via the nucleus of the tractus solitaries (NTS), the parabrachial nucleus (PBN) and midline nuclei in the thalamus [158,169]. Similar to studies of the ACC and IC, functional imaging studies in humans have shown that medial thalamic nuclei become activated following stimulation of thirst by infusion of hypertonic saline [104] or exercise-induced dehydration [163]. Moreover, rat medial thalamic neurons that project to the ACC and IC express *c-Fos* in response to systemic hypertonicity, indicating their activation [103] . During the wake period, the thalamus transmits accurate real-time sensory information to the cortex by generating single action potentials; however, during the sleep period, thalamic neurons generate rhythmic oscillations which are thought to prevent the relay of sensory information to the cortex[170]. Therefore, the delivery of interoceptive information to the ACC and IC via thalamic relay cells could potentially provide an opportunity for these inputs to be gated according to the sleep–wake cycle[170] and thus prevent thirst from interfering with sleep — a hypothesis that remains to be proven. However, the activation of these regions in response to thirst suggests that a neuronal network linking the medial thalamus with the ACC and IC might represent

the core thirst-promoting module of the brain. It is therefore reasonable to speculate that the feedback and feed-forward mechanisms that drive thirst might do so via distinct anatomical pathways that engage the thalamo–ACC/IC circuit.

Homeostatic mechanisms

As mentioned above, thirst is perceived whenever water intake is required to counteract an increase in ECF sodium concentration or osmolality, or to correct a deficit in ECF volume (FIG. 1). Thus, specialized molecular and cellular systems have evolved to enable sodium-sensitive, osmosensitive and volume-sensitive neurons to encode quantitative changes in these parameters by altering the rate of action potential firing, thereby regulating the electrical activity of thirst-promoting neurons via negative feedback. The below sections outline our understanding of these homeostatic mechanisms.

Natraemic thirst

Increases in ECF [Na^+] can stimulate thirst (FIG. 1b), implying that sodium-specific detectors can initiate neural signals that are capable of activating thirst-encoding neurons. Early studies showed that afferent fibers in the hepatic branch of the vagus nerve can detect changes in extracellular [Na^+][171]; however, whether these axons carry information from sodium-specific detectors or osmoreceptors to the brain remains unclear[172-174]. Moreover sensory fibers that innervate the liver[173,174], local mesentery[175,176], and hepatic portal vein[177-179] are presumably exposed to high concentrations of substances that are absorbed from the digestive tract prior to their dilution into the general circulation. Thus, sensory afferents from these areas are ideally poised to contribute to anticipatory responses related to the ingestion of water or food (see below), and might be better suited to such a purpose than to the dynamic monitoring of steady-state values of ECF [Na^+].

A series of classic experiments in the 1960s and 1970s[180],[181-184] showed that thirst can be specifically regulated by sodium receptors expressed within the brain[182,185]. The molecular mechanisms responsible for sodium detection are not fully understood, but presumably involve proteins that can mediate an increase in the rate of action potential firing of specialized neurons that

are exposed to small increases in extracellular [Na^+][186-189]. At least four subtypes of ion channels could mediate such effects. These include epithelial-like Na^+ channels (ENaCs)[91,190-192], slowly-inactivating voltage-gated Na^+ channels such as Nav1.6[193], the persistent and weakly voltage-sensitive Na^+ channel Na_X[93,194-197], and non-selective cation channels[187,189,198]. In most cases, these channels contribute small amounts of inward (depolarizing) Na^+ current under resting conditions. Changes in the driving force resulting from changes in external [Na^+] could modulate the amplitude of this current, causing proportional and Na^+-specific changes in membrane potential and the rate of action potential firing[187].

Non-selective cation channels[199-201], ENacs[91,190,202] and Na_X channels[203] are expressed in the organum vasculosum lamina terminalis (OVLT) and subfornical organ (SFO) — a pair of midline circumventricular organs that have key roles in the control of fluid balance[107,122,204-206]. Electrophysiological recordings have shown that neurons in the OVLT[186,207,208] and SFO[195,209] can be depolarized or excited by increases in extracellular [Na^+]. Interestingly, Na_X is also expressed in the median preoptic nucleus (MnPO)[210], a structure that is interposed between the SFO and OVLT, and whose neurons also display intrinsic sensitivity to changes in extracellular [Na^+][210,211]. Although these observations support the hypothesis that detection of changes in [Na^+] could occur in any or all of these nuclei, the specificity of responses observed in OVLT and SFO remains to be formally established because most of these experiments were performed under conditions in which osmolality was also affected by changes in extracellular [Na^+]. Additionally, whereas Na_X channels directly mediate the excitation of MnPO neurons[212], Na_X-dependent excitation of SFO neurons has been shown to be mediated indirectly by the release of lactate from adjacent glial cells[188,213]. Thus, Na_X might mediate [Na^+] detection through distinct cell autonomous and non-cell autonomous mechanisms in different areas

Anatomical studies have shown that that neurons in the MnPO, OVLT and SFO are extensively and reciprocally interconnected[102,107,206,214-218] (FIG. 2), and functional studies have shown that activation of neurons in any of these areas using optogenetic or chemogenetic approaches can stimulate thirst[101,102,215,219,220]. Since neurons in the MnPO, OVLT and SFO project to the medial paraventricular and mediodorsal nuclei of the thalamus[103], it is tempting to speculate that changes in ECF [Na^+] might modulate thirst through these nuclei via proportional feedback regulation of the thalamo–cortical thirst circuit (FIG. 2). Further studies are required to explore this hypothesis,

and to fully define the network, cellular and molecular mechanisms that specifically mediate the sodium-dependent negative feedback control of thirst.

Osmotic thirst

The specific involvement of ECF osmolality as a factor that regulates thirst (FIG. 1) was first established in pioneering studies by Gilman[221] and Wolf[222] who showed that cellular dehydration (that is, shrinking) at an unidentified locus was required to induce thirst during ECF hypertonicity in dogs and humans. Conversely, dilution of the ECF (hypotonicity) was recognized as an inhibitory factor for thirst[223]. Classic work in goats and sheep revealed that hypertonic solutions could induce water intake when injected directly into the third ventricle[180,181], thus identifying the brain as a key site for osmosensory detection. Subsequent work demonstrated that a central osmosensitive system could stimulate water intake in a manner that was independent of changes in extracellular [Na^+][181] and further indicated that the osmosensory sites were present in a brain region that lacks a blood–brain barrier[182]. Although SFO neurons display intrinsic osmosensitivity[200,224] and are activated by systemic hypertonicity as detected by increased *c-Fos* expression[103] and *in vivo* fiber photometry[107], lesions of the SFO fail to prevent water intake induced by systemic hypertonicity[225,226]. Thus, activation of SFO neurons under such conditions might not be essential for the induction of osmotic thirst. By contrast, lesions encompassing the OVLT and MnPO were found to cause adipsia[227] and prevented water intake induced by a hyperosmotic stimulus[228-230]. Since the OVLT is a circumventricular organ (whereas the MnPO is not), the OVLT was identified as the putative osmoreceptor region responsible for the control of thirst[231,232]. Indeed, fMRI studies in humans have shown that the ventral portion of the lamina terminalis, which encloses the OVLT, is activated in response to systemic hyperosmotic stimuli [164,233].

In agreement with a role in the regulation of osmotic thirst neurons in the rodent OVLT are excited by hypertonic solutions infused into the internal carotid artery *in vivo* [208], or bath applied *in vitro*[186,199,207]. The mechanisms that mediate this effect are not completely understood. Neurons freshly isolated from the OVLT of adult mice are intrinsically sensitive to hypertonic solutions containing excess mannitol. Exposure to such solutions induces OVLT neurons to undergo membrane depolarization and increase the rate of action potential firing through the mechanical

activation of ΔN-Trpv1[86,199,234-236], an N-terminal variant of the transient receptor potential vanilloid type 1 (Trpv1) channel. However, systemic administration of hyperosmotic stimuli *in vivo* induces equivalent water intake and expression of *c-Fos* in the OVLT of wild type and Trpv1$^{-/-}$ mice[237,238]. Thus, additional network and non-cell autonomous mechanisms are likely to participate in the detection of osmotic stimuli by OVLT neurons *in situ*. For example, studies of osmosensitive neurons in the supraoptic nucleus (SON) have shown that hypotonic stimuli applied locally can inhibit electrical activity through the activation of glycine receptors in response to taurine release by surrounding glial cells[239-241], and that hypertonic stimuli can cause excitation by suppressing taurine release[242]. Although OVLT neurons are densely wrapped by glial processes[243], whether neuro–glial interactions contribute to the osmotic control of OVLT neurons is unknown. Additionally, afferent signals from peripheral sodium receptors or osmoreceptors that rely on channels other than □N-Trpv1 are likely to contribute to the regulation of OVLT neurons and thirst. Indeed, systemic hypertonicity can induce *c-Fos* expression in brainstem regions that relay interoceptive sensory signals, such as the PBN, NTS and ventrolateral medulla (VLM), in animals that have full lesions of the lamina terminalis (that is, the region encompassing the MnPO, OVLT and SFO)[244]. This observation indicates that the lamina terminalis is not the only source of systemic osmosensory information, and that the thirst-promoting ACC/IC network might also receive such signals via vagal[173] or spinal[245] afferents that project via the brainstem.

As mentioned earlier, studies in rats have shown that systemic hyperosmotic stimuli increase the expression of *c-Fos* in MnPO and OVLT neurons that project to midline thalamic nuclei, and in midline thalamic neurons that project to the ACC and IC[103]. Studies in humans using fMRI have also indicated that the ventral part of the lamina terminalis (that is, the OVLT and MnPO) is functionally connected to the medial thalamus, and that functional connectivity within this network is enhanced during thirst perception stimulated by systemic hypertonicity[163]. Thus, the activation of thirst by systemic hyperosmotic stimuli might involve the osmotic excitation of OVLT neurons and interconnected neurons in the MnPO and SFO, as well as neurons in brainstem nuclei, which together engage the medial thalamic–ACC–IC network (FIG. 2).

Volaemic thirst

Perhaps the most intuitive form of hydration deficit is hypovolaemia, a term that designates a net loss of ECF volume regardless of its composition. In its simplest form, hypovolaemia can be caused by haemorrhage, a condition that leads to a loss of isotonic ECF. Experiments in rats have shown that haemorrhage is a potent stimulus for thirst[119,246,247]. As mentioned previously, mammals incur an incessant fluid loss through the evaporation of lung exudate and the production of sweat. Since these fluids are hypotonic in comparison to ECF[109-111,248], the impact of restricting water intake for a significant amount of time is typically a dehydration that combines hypovolaemia with ECF hyperosmolality. Regardless of cause, it is now well established that mammals have evolved sensitive systems that monitor ECF volume independently of osmolality or natraemia, and that these systems can either promote or inhibit thirst via negative feedback (FIG. 1).

Changes in ECF volume are monitored indirectly by pressure receptors that detect stretch forces within the walls of the vasculature. Specifically, low pressure 'cardiopulmonary' receptors located in the atria, pulmonary artery and vena cava[249,250] detect blood volume, whereas high pressure 'baroreceptors' in the walls of the aortic arch and carotid sinus detect arterial pressure. The contribution of these two receptor systems to volume homeostasis varies under different pathological conditions[119,250]. Detailed discussion of the mechanism of action of these two systems is beyond the scope of this Review; however, their global contribution to the control of thirst in healthy individuals can be simplified as follows. Decreases in vascular stretch forces associated with an ECF volume deficit (that is, hypovolaemia or hypotension) induce a number of compensatory responses that maintain blood pressure and ECF volume, including an increase in the perception of thirst (FIG. 1). Conversely, an increase in stretch forces associated with overfilling (hypervolaemia or hypertension), induces opposite responses, including a suppression of thirst[251,252]. While hypotension or hypovolaemia may stimulate thirst via both sets of receptors, a study has demonstrated that baroreceptors play a greater role than volume receptors in the suppression of thirst during hypervolaemia or hypertension[253].

The neural circuitry through which thirst is stimulated by volume receptors and baroreceptors is unknown, but likely involves neurons in the NTS, PBN and VLM[121,249,254-256]. Neurons in these areas receive afferents from low and high pressure receptors and project axons to the medial thalamus[158,169] and MnPO[216,217,249]. The possible involvement of the lamina terminalis in mediating

the effects of hypovolaemia is supported by the observation that neurons in the MnPO, OVLT and SFO all express *c-Fos* in response to volume depletion[256,257]. Moreover, optogenetic activation of glutamatergic neurons in these areas can promote thirst[101,102,107,258]. Efferent signals from the lamina terminalis target the paraventricular nuclei of the thalamus[103,216] and could therefore activate thirst via the thalamic–ACC/IC circuit (FIG. 2). Interestingly, a new study has shown that optogenetic inhibition of glutamatergic thirst-promoting MnPO neurons is sufficient to suppress water intake in mice that have been water deprived for 48 h[258]. The output of these neurons might therefore provide an excitatory drive that is required to activate the thalamo–cortical circuitry either directly, or indirectly (for example, via the OVLT or SFO) under conditions of water deprivation. If true, then brainstem cardiopulmonary afferent signals are likely to be relayed via the MnPO, rather than the medial thalamus.

The networks responsible for the inhibition of thirst during hypervolaemia remain obscure. Isoosmotic volume expansion in rats induces *c-Fos* expression in a number of brainstem areas including the NTS, PBN and VLM[259-261]. In principle, neurons in these areas could inhibit thirst by reducing the activity of thirst-promoting neurons throughout the lamina terminalis (that is, in the MnPO, OVLT or SFO)[101,102,107,215,262], or through activation of thirst-inhibiting neurons in the MnPO or SFO[101,102] (FIG. 2). Further work is required to resolve the specific networks that modulate thirst in response to changes in ECF volume.

Hypovolaemia can also stimulate thirst through the release of renin from the kidney[119,250]. Specifically, when renal arterial perfusion is reduced as a consequence of hypovolaemia, renin is released into the circulation by the juxtaglomerular apparatus. Renin is a protease that cleaves angiotensinogen, a precursor protein produced by the liver to yield angiotensin I, which is then catalyzed into angiotensin II (Ang II) by angiotensin-converting enzyme. Circulating Ang II promotes a wide spectrum of responses that enhance vasomotor tone; moreover, classic studies from the 1970s showed that circulating Ang II can also serve as a powerful stimulator of thirst[250] through actions mediated via the SFO[263,264].

Hypervolaemia associated with excess ECF volume can also inhibit thirst through humoral mechanisms, whereby stretching of specialized cardiac myocytes causes the release atrial natriuretic peptide (ANP) into the bloodstream. ANP is well known to promote a decrease in ECF volume by stimulating renal natriuresis[265,266], but is also recognized for its potent inhibition of

thirst[265]. Although the location at which ANP acts to inhibit thirst is not completely clear, studies have shown that ANP can oppose the dipsogenic effect of Ang II when injected into the SFO of rats[267]. Additional work is required to define the mechanisms by which ANP inhibits thirst, but it seems likely that this peptide hormone mediates this effect through actions at a circumventricular organ, such as the SFO (FIG. 2).

THIRST-PROMOTING ANTICIPATORY MECHANISMS

The above sections examined the primary feedback mechanisms through which thirst is bi-directionally regulated in response to changes in the volume or composition of the ECF. Although these mechanisms are important to maintain ECF volume, natraemia and osmolality near desired set points (FIG. 1), they are by definition delayed consequences of on-going physiological perturbations. A host of feed-forward responses are now understood to drive water intake in anticipation of impending systemic solute loads or water deficits associated with various behavioural and environmental conditions[119-121,268,269]. These types of mechanisms are important because they can blunt the impact of physiological perturbations before they occur.

Prandial thirst

Rats consume approximately 70% of their daily water intake immediately before (pre-prandial), during (prandial) and following a meal (post-prandial)[270]. This behaviour is appropriate because food absorption creates a solute load that must be complemented with water intake to preserve ECF isotonicity. Indeed, food ingestion without water causes plasma to become hypertonic within minutes following a meal[271,272]. Post-prandial water intake therefore reflects in part the osmotic thirst triggered by solute absorption. However, water intake before and during the early part of a meal occurs well before ECF osmolality is increased by solute ingestion[107,271] and is therefore stimulated by mechanisms other than osmotic thirst. The existence of pre-prandial thirst implies the influence of a learned behaviour, or perhaps of a subconscious learned anticipatory benefit. The basis for pre-prandial thirst will not be further considered here. Prandial water intake, however, is directly proportional to the salt content of a meal[273], suggesting the presence of solute sensors in the upper gastrointestinal tract, liver or the interposed hepato−portal system, which can provide

ascending feed-forward information to stimulate prandial thirst in accordance with prevailing water requirements. Indeed, intragastric solute loads delivered by cannula can stimulate drinking in a dose-dependent manner[274-276], and removal of water ingested during a meal through a gastric fistula enhances water intake[277].

The cellular and network mechanisms that drive prandial thirst remain to be established but studies have shown that Na^+ receptors and osmoreceptors are present within the mesenteric hepatic portal area[175,278-280], which is innervated by side branches of the major splanchnic nerves[175] and vagal afferent nerves[280]. The involvement of this system in the regulation of prandial thirst is illustrated by the fact that water intake stimulated by intra−gastric NaCl can be inhibited by vagotomy [274] Activation of hepatic portal receptors with hypertonic NaCl in rats also affects the firing of NTS neurons *in vivo*[278,279] and induces *c-Fos* expression in the NTS as well as other brain regions involved in the control of thirst (such as the lamina terminalis)[281]. Moreover, a 2011 study identified hepatic osmoreceptors that send ascending signals to the brainstem via dorsal root ganglia, indicating a possible contribution of spinal pathways in the control of prandial thirst[245]. Additional work is needed to identify the cellular location and molecular mechanisms responsible for the detection of ingested solutes and the networks that control prandial thirst.

Although projections that ascend from the NTS could mediate prandial thirst by activating the ACC or IC via projections to the OVLT, MnPO or medial thalamus (FIG. 3), additional pathways might also be involved. Specifically, lesions of the SFO reduce prandial thirst in rats[282] whereas thirst-promoting SFO neurons are activated at the onset of feeding in mice[107,122]. Remarkably, optogenetic inhibition of these neurons reduces prandial water intake[107], suggesting that the firing of these SFO neurons is necessary to stimulate this behaviour. How thirst neurons in the SFO receive and integrate these signals to mediate prandial thirst remains to be established. Although a 2016 study observed only few direct projections from the PBN to thirst-promoting SFO neurons[107], these neurons might receive signals from PBN inputs to other local non thirst-promoting SFO neurons[283-285]. Taken together, these findings indicate that hepato−portal sensors that monitor the solute load associated with food intake can adaptively mediate an anticipatory feed-forward stimulation of water intake to mitigate the increase in ECF osmolality that would otherwise occur as a result of eating.

Thermal thirst

Hyperthermia caused by exercise or heat exposure in homeotherms leads to a loss of ECF solutes and water due to the evaporation of fluids during cooling responses such as sweating, panting or the spreading of saliva[286]. These responses can cause dehydration (resulting in ECF hypertonicity and hypovolaemia) since the fluids that are secreted and evaporated are hypotonic relative to the osmolality of ECF[109-111,287]. Several studies have shown that rodents exposed to high ambient temperatures drink considerable quantities of water before ECF osmolality or volume is increased[288-291], and that the magnitude of the observed water intake is proportionate to the change in core body temperature[290]. Together, these observations suggest that hyperthermia can provoke a feed-forward anticipatory stimulation of water intake that could mitigate the dehydrating effect of thermoregulatory cooling.

Although the specific mechanisms by which increases in temperature can induce thirst remain unknown, a considerable amount of information is available concerning cellular thermosensation and neural pathways that carry thermosensory information to the brain[292]. Thermosensitive neurons located in the brain and periphery can detect changes in temperature owing to the expression of various heat-sensitive and cold-sensitive ion channels[236,293,294]. Cutaneous thermoreceptors, for example, can detect the wide range of ambient temperatures that skin can be exposed to, and relay this sensory information to the brain via projections that ascend in the lamina I spino–thalamo–cortical pathway[158,169,295] or via thermal somatosensory afferent collaterals that transmit signals to the PBN via dense projections from the dorsal horn[292,296]. Thermoreceptor afferents are also located in various organs (for example, skeletal muscle[297]) and the viscera[298-301], where they presumably detect changes in local or core body temperature. Visceral afferents of this type, including those that innervate the splanchnic mesentery[301], probably project to the NTS and/or PBN via spinal or vagal pathways[158]. Neurons in the PBN project directly to the preoptic area (POA)[296] — a large region of the hypothalamus that encompasses several structures involved in the control of fluid balance, including the OVLT and MnPO (FIG. 3). *In vivo* electrophysiological recordings in cats have shown that a subset of POA neurons can be activated by heating cutaneous thermoreceptors in the absence of changes in core body temperature[302]; indicating information regarding ambient temperature can potentially access the thirst-promoting regions of the brain via neurons in this area; however, it remains to be determined whether increases in cutaneous temperature can stimulate thirst via such a pathway(FIG. 3).

Although a role for cutaneous receptors in the stimulation of thirst cannot be fully excluded, experiments have shown that humans report significantly greater subjective thirst following injections of hypertonic saline in the presence of elevated core body temperature, and that this effect is not observed when skin temperature is elevated[303]. Sensors responsible for the detection of core body temperature might therefore be particularly relevant for the control of thermal thirst. Although thirst-promoting neurons within the POA may receive information concerning core temperature via visceral afferents, the hypothalamus is also recognized as a key site for detection and regulation of core body temperature[304-307]. Indeed, studies performed over a century ago established the hypothalamus as the only brain region that is capable of responding to local thermal stimulation by promoting peripheral thermoregulatory responses (such as panting, sweating on footpads, shivering)[308]. Since these pioneering observations, ample evidence has established the POA as the main locus of the central thermostat[308-310]. Specifically, POA warming activates heat dissipating mechanisms, whereas cooling drives thermogenesis[296,309,311-314]. Moreover, structures within the POA and other areas of the hypothalamus orchestrate the thermoregulatory responses induced by heating or cooling of the periphery[292,296,306,314,315].

Interestingly, local heating of the ventral medial part of the POA (vmPOA) using a thermode can elicit intense thirst in euhydrated goats, whereas cooling inhibits water intake[316], suggesting that heat-sensitive neurons within this area can drive thermal thirst. A 2016 study showed that vmPOA neurons that express the neuropeptides brain-derived neurotrophic factor and pituitary adenylate cyclase-activating polypeptide are activated by heat exposure and that optogenetic stimulation of these neurons induces heat dissipating behaviours[314]. In addition, we showed that thirst can be induced by optogenetic activation of OVLT neurons that express the heat-sensitive channel ΔN-Trpv1[215] are functionally activated during hyperthermia to drive thermal thirst remains to be established.

Circadian thirst

Prolonged sleep is a potential cause of dehydration because fluid losses caused by breathing and urine production at this time are not opposed by regular water intake. However, mammals, including rodents and humans, can mitigate this effect through circadian responses that optimize

osmoregulation during sleep[83,317,318]. For example, studies in humans and rodents have shown that renal water reabsorption is progressively enhanced during the sleep period[317-321]. This effect is caused by an increase in vasopressin release from the neurohypophysis[318,322], which might result in part from enhanced synaptic excitation of magnocellular neurosecretory neurons[82]. This topic has been reviewed elsewhere[83] and is not further considered here. Another important adaptation observed in rodents is a substantial increase in water intake that occurs just before sleep (that is, circadian thirst), which creates a fluid reserve that compensates for the absence of water intake during sleep.

In agreement with previous reports in rats[323] and mice[324,325], we have shown that mice drink significantly more water during the last 2 h of their active period, compared to the 2-h period preceding it (that is, the basal period)[215]. Mice that were denied this enhanced intake were significantly dehydrated on waking, indicating this behaviour is physiologically adaptive. Moreover, control experiments showed that increased water intake during the active period was not driven by osmotic, prandial, volaemic or thermal thirst, supporting the hypothesis that water intake at this time is an anticipatory behaviour driven by the circadian clock, the suprachiasmatic nucleus (SCN).

The SCN are a pair of midline nuclei that each comprise thousands of neurons that mainly contain the inhibitory neurotransmitter GABA (γ-aminobutyric acid), and can also express, or co-express a number of different neuropeptides such as vasopressin, vasoactive intestinal peptide or gastric releasing peptide[11,14]. Findings from anatomical tracing studies have prompted the suggestion that vasopressin-containing neurons located in the outer shell of the SCN serve as the main output neurons that mediate a variety of circadian rhythms[10,14,326]. Vasopressin-expressing neurons of the SCN communicate with many parts of the brain, but notably send direct projections to the paraventricular nucleus of the thalamus, SFO and OVLT[14]. In principle, projections to any of these areas might be involved in the control of circadian thirst. However, results from our group have shown that projections from SCN vasopressin-expressing neurons to the OVLT are necessary and sufficient to mediate circadian thirst[215] (FIG. 4).

In *in vitro* studies of brain slices, we showed that the electrical activity of OVLT neurons is significantly increased during the active period compared to the basal period, and specifically, that the firing rate of vasopressin-expressing SCN neurons was significantly increased during the active

period. Analysis of whole-cell currents revealed that OVLT neurons are depolarized (that is, excited) by electrical stimulation of the SCN. Surprisingly, these effects did not involve fast neurotransmission by GABA or glutamate, but were mediated by the vasopressin V1a receptor (V1aR) and activation of downstream non-selective cation channels. *In vivo* experiments subsequently showed that optogenetic stimulation of vasopressin release from the axon terminals of SCN neurons within the OVLT during the basal period could increase water intake to a level equivalent to that observed during the active period. Conversely, optogenetic inhibition of vasopressin release from these terminals abolished water intake during the active period. These results indicate that circadian thirst during the active period is driven by an excitatory effect of vasopressin released by SCN neurons on thirst-promoting neurons in the OVLT (FIG. 4).

SATIATION OF THIRST

The above sections describe how homeostatic (feedback) and anticipatory (feed-forward) mechanisms can promote water intake in response to existing or impending fluid deficits. However, dehydrated animals that are given free access to water will stop drinking well before ECF volume and osmolality are restored[153,269,280,327]. Indeed, the negative valence associated with thirst and the motivation to drink declines rapidly upon water intake to terminate fluid ingestion and avoid overhydration[165,166,258,262,328]. In agreement with these observations, imaging studies in humans have shown that the ACC and IC are rapidly deactivated upon water ingestion[104,105,162,164,166]. Remarkably, however, the OVLT remains activated even after the ACC and IC are deactivated upon satiation prompted by water intake in hyperosmotic humans [164], suggesting that osmosensory OVLT neurons that monitor systemic tonicity continue to signal the hyperosmotic state until it is fully corrected by water absorption, and that satiety must occur at another level. Interestingly, use of fiber photometry to monitor cellular calcium levels *in vivo* has shown that the activity of thirst-promoting neurons in the MnPO and SFO of thirsty mice can be rapidly suppressed by water intake[107,122,258], suggesting these sites may mediate satiety signals under some conditions. Notably, glutamatergic MnPO neurons seem to proportionally encode the aversive quality (negative valence) of thirst, and inhibition of these neurons is sufficient to quench thirst in water-deprived mice[258,262]. Signals that mediate early satiety probably originate from oropharyngeal afferents, perhaps via the

trigeminal nerve[329], since cold metal placed within the oral cavity can alone transiently reduce SFO neuron activity[107]. Moreover, gustatory taste receptors can also modulate water intake[330].

Although oropharyngeal signals can mediate the rapid inhibition of thirst neurons in the SFO and MnPO following water intake, animals with open gastric fistulas ingest excessive amounts of water over the long term[277,331-333]. This finding suggests that the immediate inhibitory effect of oropharyngeal signals might be temporary and that thirst will re-emerge due to the persistent drive of feedback signals from homeostatic inputs, and also indicates that gastric and post-gastric signals have a key role in limiting the degree of water ingestion and can produce a long-lasting inhibition of water intake. The gastric signal that mediates satiety seems to specifically reflect the volume of the ingested fluid[269]; this process might be mediated by afferent signals from stretch receptors in the Vagus nerve that innervate the stomach and duodenum [334,335] [336]**.** In agreement with this hypothesis, gastric distension increases the rate of action potential firing[337] and expression of *c-Fos*[338] in NTS neurons. Moreover, this pathway can mediate an inhibitory effect on thirst, because water intake induced by hypertonicity or hypovolaemia is enhanced by lesions of the area postrema (AP) and NTS[339,340], or by blunting the function of the vagal NTS afferents by systemic administration of capsaicin[341]. In addition, gastric or hepato−portal osmoreceptors might be able to detect hypotonicity[172,173] and could also contribute to the osmotic inhibition of thirst via pathways that ascend through the NTS. Importantly, water intake in thirsty rats with AP/NTS lesions or in animals with gastric fistulas[277] eventually declines 15 – 30 min after the onset of drinking; thus, gastric distension or dilution signals provide the immediate inhibitory signal to cease drinking once sufficient fluid has been ingested. However, in the absence of this feed-forward effect, post-ingestive homeostatic signals (for example, ECF hypoosmolality or hypervolaemia) can act to suppress thirst should the ECF become hypoosmotic (FIG. 1).

Conclusions

Thirst is a complex behavioural response governed by multiple mechanisms that serve to correct ongoing and imminent homeostatic fluid perturbations. Maladaptive changes in the perception of thirst can lead to severe acute pathologies; thus, understanding the neural basis underlying this physiological response is crucial for the development of treatments and therapeutic strategies for these disorders. For example, hyperglycaemic patients experience polydipsia (excessive thirst) as a

result of concurrent hyperosmolality. Although this pathology is fairly well understood, other pathologies that affect thirst perception are not. For example, psychogenic polydipsia in patients with schizophrenia or obsessive–compulsive disorder can lead to severe states of hyponatraemia and hypoosmolality, which can result in seizures and even death. By contrast, adipsia — a condition that is particularly common in elderly individuals— leads to dehydration. This condition can be life-threatening during hot weather and is expected to contribute to the predicted 257% increase in the number of heat related deaths by 2050 as a result of climate change[342]. Although thirst has been a subject of study for decades, a lack of tools that enable the analysis of specific cell types has prevented the study of detailed neural circuits that underlie defined thirst behaviours. The development of tools, such as optogenetics and chemogenetics, to analyse neural networks has provided new insights into the mechanisms that govern thirst and will likely facilitate further advances this field in the future.

REFERENCES

1 Morgan, R. M., Patterson, M. J. & Nimmo, M. A. Acute effects of dehydration on sweat composition in men during prolonged exercise in the heat. *Acta physiologica Scandinavica* **182**, 37-43, doi:10.1111/j.1365-201X.2004.01305.x APS1305 [pii] (2004).

2 Effros, R. M. *et al.* Epithelial lining fluid solute concentrations in chronic obstructive lung disease patients and normal subjects. *J Appl Physiol* **99**, 1286-1292, doi:00362.2005 [pii] 10.1152/japplphysiol.00362.2005 (2005).

3 Griese, M., Noss, J. & Schramel, P. Elemental and ion composition of exhaled air condensate in cystic fibrosis. *J Cyst Fibros* **2**, 136-142, doi:S1569199303000626 [pii] 10.1016/S1569-1993(03)00062-6 (2003).

4 Bolt, E. E., Hagens, M., Willems, D. & Onwuteaka-Philipsen, B. D. Primary care patients hastening death by voluntarily stopping eating and drinking. *Annals of family medicine* **13**, 421-428, doi:10.1370/afm.1814 (2015).

5 Arima, H., Azuma, Y., Morishita, Y. & Hagiwara, D. Central diabetes insipidus. *Nagoya journal of medical science* **78**, 349-358, doi:10.18999/nagjms.78.4.349 (2016).

6 Cuesta, M., Hannon, M. J. & Thompson, C. J. Adipsic diabetes insipidus in adult patients. *Pituitary*, doi:10.1007/s11102-016-0784-4 (2017).

7 Eisenberg, Y. & Frohman, L. A. ADIPSIC DIABETES INSIPIDUS: A REVIEW. *Endocrine practice : official journal of the American College of Endocrinology and the American Association of Clinical Endocrinologists* **22**, 76-83, doi:10.4158/ep15940.ra (2016).

8 Manning, S., Shaffie, R. & Arora, S. Case Report: Severe hypernatremia from psychogenic adipsia. *F1000Research* **6**, 34, doi:10.12688/f1000research.9181.1 (2017).

9 Pereira, M. C., Vieira, M. M., Pereira, J. S. & Salgado, D. Adipsia in a Diabetes Insipidus Patient. *Case reports in oncology* **8**, 385-388, doi:10.1159/000440611 (2015).

10 Koch, C. A. & Fulop, T. Clinical aspects of changes in water and sodium homeostasis in the elderly. *Reviews in endocrine & metabolic disorders* **18**, 49-66, doi:10.1007/s11154-017-9420-5 (2017).

11 Fitzsimons, J. T. The physiology of thirst and sodium appetite. *Monogr Physiol Soc*, 1-572 (1979).

12 Johnson, A. K. The sensory psychobiology of thirst and salt appetite. *Med Sci Sports Exerc* **39**, 1388-1400, doi:10.1249/mss.0b013e3180686de8 00005768-200708000-00023 [pii] (2007).

13 McKinley, M. J. & Johnson, A. K. The physiological regulation of thirst and fluid intake. *News Physiol Sci* **19**, 1-6 (2004).

14 Zimmerman, C. A., Leib, D. E. & Knight, Z. A. Neural circuits underlying thirst and fluid homeostasis. *Nat Rev Neurosci*, doi:10.1038/nrn.2017.71 (2017).

15 Bourque, C. W. Central mechanisms of osmosensation and systemic osmoregulation. *Nature reviews. Neuroscience* **9**, 519-531, doi:nrn2400 [pii] 10.1038/nrn2400 (2008).

16 Verbalis, J. G. Disorders of body water homeostasis. *Best Pract Res Clin Endocrinol Metab* **17**, 471-503, doi:S1521690X03000496 [pii] (2003).

17 Lafontan, M., Visscher, T. L., Farpour-Lambert, N. & Yumuk, V. Opportunities for intervention strategies for weight management: global actions on fluid intake patterns. *Obesity facts* **8**, 54-76, doi:10.1159/000375103 (2015).

18 Popkin, B. M., D'Anci, K. E. & Rosenberg, I. H. Water, hydration, and health. *Nutrition reviews* **68**, 439-458, doi:10.1111/j.1753-4887.2010.00304.x (2010).
19 Orlandi, C., Zimmer, C. A. & Gheorghiade, M. Tolvaptan for the treatment of hyponatremia and congestive heart failure. *Future cardiology* **2**, 627-634, doi:10.2217/14796678.2.6.627 (2006).
20 Redondo, N., Gomez-Martinez, S. & Marcos, A. Sensory attributes of soft drinks and their influence on consumers' preferences. *Food & function* **5**, 1686-1694, doi:10.1039/c4fo00181h (2014).
21 Adler, S. M. & Verbalis, J. G. Disorders of body water homeostasis in critical illness. *Endocrinology and metabolism clinics of North America* **35**, 873-894, xi, doi:10.1016/j.ecl.2006.09.011 (2006).
22 Brvar, M. *et al.* Polydipsia as another mechanism of hyponatremia after 'ecstasy' (3,4 methyldioxymethamphetamine) ingestion. *European journal of emergency medicine : official journal of the European Society for Emergency Medicine* **11**, 302-304 (2004).
23 Kalantar-Zadeh, K., Nguyen, M. K., Chang, R. & Kurtz, I. Fatal hyponatremia in a young woman after ecstasy ingestion. *Nat Clin Pract Nephrol* **2**, 283-288, quiz 289, doi:ncpneph0167 [pii]
10.1038/ncpneph0167 (2006).
24 Traub, S. J., Hoffman, R. S. & Nelson, L. S. The "ecstasy" hangover: hyponatremia due to 3,4-methylenedioxymethamphetamine. *Journal of urban health : bulletin of the New York Academy of Medicine* **79**, 549-555, doi:10.1093/jurban/79.4.549 (2002).
25 Sandifer, M. G. Hyponatremia due to psychotropic drugs. *The Journal of clinical psychiatry* **44**, 301-303 (1983).
26 Lu, X. & Wang, X. Hyponatremia induced by antiepileptic drugs in patients with epilepsy. *Expert opinion on drug safety* **16**, 77-87, doi:10.1080/14740338.2017.1248399 (2017).
27 Furth, S. & Oski, F. A. Hyponatremia and water intoxication. *American journal of diseases of children (1960)* **147**, 932-933 (1993).
28 Kushnir, M., Schattner, A., Ezri, T. & Konichezky, S. Schizophrenia and fatal self-induced water intoxication with appropriately-diluted urine. *Am J Med Sci* **300**, 385-387 (1990).
29 Patel, J. K. Polydipsia, hyponatremia, and water intoxication among psychiatric patients. *Hospital & community psychiatry* **45**, 1073-1074 (1994).
30 Ofran, Y., Lavi, D., Opher, D., Weiss, T. A. & Elinav, E. Fatal voluntary salt intake resulting in the highest ever documented sodium plasma level in adults (255 mmol L-1): a disorder linked to female gender and psychiatric disorders. *J Intern Med* **256**, 525-528, doi:JIM1411 [pii]
10.1111/j.1365-2796.2004.01411.x (2004).
31 Turk, E. E., Schulz, F., Koops, E., Gehl, A. & Tsokos, M. Fatal hypernatremia after using salt as an emetic--report of three autopsy cases. *Leg Med (Tokyo)* **7**, 47-50, doi:S1344-6223(04)00030-6 [pii]
10.1016/j.legalmed.2004.06.005 (2005).
32 Kirkman, M. A., Albert, A. F., Ibrahim, A. & Doberenz, D. Hyponatremia and brain injury: historical and contemporary perspectives. *Neurocrit Care* **18**, 406-416, doi:10.1007/s12028-012-9805-y (2013).
33 De Smet, H. R., Menadue, M. F., Oliver, J. R. & Phillips, P. A. Increased thirst and vasopressin secretion after myocardial infarction in rats. *American journal of physiology.*

Regulatory, integrative and comparative physiology **285**, R1203-1211, doi:10.1152/ajpregu.00098.2003
285/5/R1203 [pii] (2003).
34 Sonneville, R. *et al.* Understanding brain dysfunction in sepsis. *Ann Intensive Care* **3**, 15, doi:10.1186/2110-5820-3-15 (2013).
35 Lyons, O. D., Bradley, T. D. & Chan, C. T. Hypervolemia and Sleep Apnea in Kidney Disease. *Seminars in nephrology* **35**, 373-382, doi:10.1016/j.semnephrol.2015.06.008 (2015).
36 Iwasa, M. & Takei, Y. Pathophysiology and management of hepatic encephalopathy 2014 update: Ammonia toxicity and hyponatremia. *Hepatology research : the official journal of the Japan Society of Hepatology* **45**, 1155-1162, doi:10.1111/hepr.12495 (2015).
37 Wier, L. M. *et al.* 1-99 (Agency for Healthcare and Research and Quality, Rockville, MD, 2011).
38 Magder, S. Volume and its relationship to cardiac output and venous return. *Critical care (London, England)* **20**, 271, doi:10.1186/s13054-016-1438-7 (2016).
39 Moranville, M. P., Mieure, K. D. & Santayana, E. M. Evaluation and management of shock States: hypovolemic, distributive, and cardiogenic shock. *Journal of pharmacy practice* **24**, 44-60, doi:10.1177/0897190010388150 (2011).
40 Senay Jr., L. C. & Christensen, M. L. Changes in blood plasma during progressive dehydration. *Journal of Applied Physiology* **20**, 1136-1140 (1965).
41 Bedford, J. J. & Leader, J. P. Response of tissues of the rat to anisosmolality in vivo. *The American journal of physiology* **264**, R1164-1179 (1993).
42 Ayus, J. C., Varon, J. & Arieff, A. I. Hyponatremia, cerebral edema, and noncardiogenic pulmonary edema in marathon runners. *Ann Intern Med* **132**, 711-714, doi:200005020-00005 [pii] (2000).
43 Machino, T. & Yoshizawa, T. Brain shrinkage due to acute hypernatremia. *Neurology* **67**, 880, doi:67/5/880 [pii]
10.1212/01.wnl.0000221726.41727.06 (2006).
44 Spigset, O. & Hedenmalm, K. Hyponatraemia and the syndrome of inappropriate antidiuretic hormone secretion (SIADH) induced by psychotropic drugs. *Drug safety* **12**, 209-225 (1995).
45 Sterns, R. H. Disorders of plasma sodium--causes, consequences, and correction. *The New England journal of medicine* **372**, 55-65, doi:10.1056/NEJMra1404489 (2015).
46 Stricker, E. M. & Sved, A. F. Thirst. *Nutrition (Burbank, Los Angeles County, Calif.)* **16**, 821-826 (2000).
47 Rullier, S. Dictionaire des Sciences Medicales pas un Societé de Médecines et de Chirurgiens. **51**, 448-490 (1821).
48 Cannon, W. B. Croonian Lecture: The Physiological Basis of Thirst. *Proceedings of the Royal Society of London. Series B, Containing Papers of a Biological Character* **90**, 283-301 (1918).
49 Wettendorff, H. Travaux du Laboratorie de physiologie *Instituts Solvay* **4**, 353 (1901).
50 Robinson, B. W. & Mishkin, M. Alimentary responses to forebrain stimulation in monkeys. *Exp Brain Res* **4**, 330-366 (1968).
51 Craig, A. D. How do you feel? Interoception: the sense of the physiological condition of the body. *Nature reviews. Neuroscience* **3**, 655-666, doi:10.1038/nrn894
nrn894 [pii] (2002).

52 Craig, A. D. A new view of pain as a homeostatic emotion. *Trends in neurosciences* **26**, 303-307, doi:S0166223603001231 [pii] (2003).
53 Denton, D. A., McKinley, M. J., Farrell, M. & Egan, G. F. The role of primordial emotions in the evolutionary origin of consciousness. *Consciousness and cognition* **18**, 500-514, doi:10.1016/j.concog.2008.06.009 (2009).
54 Denton, D. *et al.* Correlation of regional cerebral blood flow and change of plasma sodium concentration during genesis and satiation of thirst. *Proceedings of the National Academy of Sciences of the United States of America* **96**, 2532-2537 (1999).
55 Denton, D. *et al.* Neuroimaging of genesis and satiation of thirst and an interoceptor-driven theory of origins of primary consciousness. *Proceedings of the National Academy of Sciences of the United States of America* **96**, 5304-5309 (1999).
56 Farrell, M. J. *et al.* Unique, common, and interacting cortical correlates of thirst and pain. *Proceedings of the National Academy of Sciences of the United States of America* **103**, 2416-2421, doi:10.1073/pnas.0511019103 (2006).
57 Saker, P. *et al.* Regional brain responses associated with drinking water during thirst and after its satiation. *Proceedings of the National Academy of Sciences of the United States of America* **111**, 5379-5384, doi:10.1073/pnas.1403382111 (2014).
58 Farrell, M. J. *et al.* Cortical activation and lamina terminalis functional connectivity during thirst and drinking in humans. *American journal of physiology. Regulatory, integrative and comparative physiology* **301**, R623-631, doi:10.1152/ajpregu.00817.2010 (2011).
59 Egan, G. *et al.* Neural correlates of the emergence of consciousness of thirst. *Proceedings of the National Academy of Sciences of the United States of America* **100**, 15241-15246, doi:10.1073/pnas.2136650100
2136650100 [pii] (2003).
60 Saker, P., Farrell, M. J., Egan, G. F., McKinley, M. J. & Denton, D. A. Overdrinking, swallowing inhibition, and regional brain responses prior to swallowing. *Proceedings of the National Academy of Sciences of the United States of America* **113**, 12274-12279, doi:10.1073/pnas.1613929113 (2016).
61 Becker, C. A., Flaisch, T., Renner, B. & Schupp, H. T. From Thirst to Satiety: The Anterior Mid-Cingulate Cortex and Right Posterior Insula Indicate Dynamic Changes in Incentive Value. *Frontiers in human neuroscience* **11**, 234, doi:10.3389/fnhum.2017.00234 (2017).
62 Duncan, G. E. *et al.* Metabolic mapping of functional activity in rat brain and pituitary after water deprivation. *Neuroendocrinology* **49**, 489-495 (1989).
63 Pastuskovas, C. V., Cassell, M. D., Johnson, A. K. & Thunhorst, R. L. Increased cellular activity in rat insular cortex after water and salt ingestion induced by fluid depletion. *American journal of physiology. Regulatory, integrative and comparative physiology* **284**, R1119-1125, doi:10.1152/ajpregu.00189.2002
00189.2002 [pii] (2003).
64 Craig, A. D. Interoception: the sense of the physiological condition of the body. *Current opinion in neurobiology* **13**, 500-505, doi:S0959438803000904 [pii] (2003).
65 Hollis, J. H., McKinley, M. J., D'Souza, M., Kampe, J. & Oldfield, B. J. The trajectory of sensory pathways from the lamina terminalis to the insular and cingulate cortex; a neuroanatomical framework for the generation of thirst. *American journal of physiology. Regulatory, integrative and comparative physiology* **294**, R1390-1401, doi:00869.2007 [pii]
10.1152/ajpregu.00869.2007 (2008).

66 McCormick, D. A. & Bal, T. Sensory gating mechanisms of the thalamus. *Current opinion in neurobiology* **4**, 550-556 (1994).
67 Andrews, W. H. & Orbach, J. Sodium receptors activating some nerves of perfused rabbit livers. *The American journal of physiology* **227**, 1273-1275 (1974).
68 Adachi, A. Thermosensitive and osmoreceptive afferent fibers in the hepatic branch of the vagus nerve. *Journal of the autonomic nervous system* **10**, 269-273 (1984).
69 Adachi, A., Niijima, A. & Jacobs, H. L. An hepatic osmoreceptor mechanism in the rat: electrophysiological and behavioral studies. *The American journal of physiology* **231**, 1043-1049 (1976).
70 Andrews, W. H. & Orbach, J. Effect of osmotic pressure on spontaneous afferent discharge in the nerves of the perfused rabbit liver. *Pflugers Archiv : European journal of physiology* **361**, 89-94 (1975).
71 Choi-Kwon, S. & Baertschi, A. J. Splanchnic osmosensation and vasopressin: mechanisms and neural pathways. *The American journal of physiology* **261**, E18-25 (1991).
72 King, M. S. & Baertschi, A. J. Central neural pathway mediating splanchnic osmosensation. *Brain research* **550**, 268-278 (1991).
73 Haberich, F. J. Osmoreception in the portal circulation. *Fed Proc* **27**, 1137-1141 (1968).
74 Chwalbinska-Moneta, J. Role of hepatic portal osmoreception in the control of ADH release. *The American journal of physiology* **236**, E603-609 (1979).
75 Baertschi, A. J. & Vallet, P. G. Osmosensitivity of the hepatic portal vein area and vasopressin release in rats. *The Journal of physiology* **315**, 217-230 (1981).
76 Andersson, B., Jobin, M. & Olsson, K. A study of thirst and other effects of an increased sodium concentration in the 3rd brain ventricle. *Acta Physiol Scand.* **69**, 29-36 (1967).
77 McKinley, M. J., Blaine, E. H. & Denton, D. A. Brain osmoreceptors, cerebrospinal fluid electrolyte composition and thirst. *Brain research* **70**, 532-537, doi:0006-8993(74)90264-9 [pii] (1974).
78 McKinley, M. J., Denton, D. A. & Weisinger, R. S. Sensors for antidiuresis and thirst--osmoreceptors or CSF sodium detectors? *Brain research* **141**, 89-103, doi:0006-8993(78)90619-4 [pii] (1978).
79 Olsson, K. Further evidence for the importance of CSF Na+ concentration in central control of fluid balance. *Acta physiologica Scandinavica* **88**, 183-188, doi:10.1111/j.1748-1716.1973.tb05445.x (1973).
80 Olsson, K. Attenuation of dehydrative thirst by lowering of the CSF (Na+). *Acta physiologica Scandinavica* **94**, 536-538, doi:10.1111/j.1748-1716.1975.tb05913.x (1975).
81 Weisinger, R. S., Considine, P., Denton, D. A. & McKinley, M. J. Rapid effect of change in cerebrospinal fluid sodium concentration on salt appetite. *Nature* **280**, 490-491 (1979).
82 Vivas, L., Chiaraviglio, E. & Carrer, H. F. Rat organum vasculosum laminae terminalis in vitro: responses to changes in sodium concentration. *Brain research* **519**, 294-300, doi:0006-8993(90)90091-O [pii] (1990).
83 Voisin, D. L. & Bourque, C. W. Integration of sodium and osmosensory signals in vasopressin neurons. *Trends in neurosciences* **25**, 199-205, doi:S0166223602021422 [pii] (2002).
84 Noda, M. & Hiyama, T. Y. Sodium sensing in the brain. *Pflugers Archiv : European journal of physiology* **467**, 465-474, doi:10.1007/s00424-014-1662-4 (2015).

85 Voisin, D. L., Chakfe, Y. & Bourque, C. W. Coincident detection of CSF Na+ and osmotic pressure in osmoregulatory neurons of the supraoptic nucleus. *Neuron* **24**, 453-460, doi:S0896-6273(00)80858-2 [pii] (1999).
86 Miller, R. L. & Loewy, A. D. ENaC gamma-expressing astrocytes in the circumventricular organs, white matter, and ventral medullary surface: sites for Na+ regulation by glial cells. *Journal of chemical neuroanatomy* **53**, 72-80, doi:10.1016/j.jchemneu.2013.10.002 (2013).
87 Miller, R. L., Wang, M. H., Gray, P. A., Salkoff, L. B. & Loewy, A. D. ENaC-expressing neurons in the sensory circumventricular organs become c-Fos activated following systemic sodium changes. *American journal of physiology. Regulatory, integrative and comparative physiology* **305**, R1141-1152, doi:10.1152/ajpregu.00242.2013 (2013).
88 Ruiz, C., Gutknecht, S., Delay, E. & Kinnamon, S. Detection of NaCl and KCl in TRPV1 Knockout Mice. *Chemical Senses*, bjl024 (2006).
89 Teruyama, R., Sakuraba, M., Wilson, L. L., Wandrey, N. E. & Armstrong, W. E. Epithelial Na(+) sodium channels in magnocellular cells of the rat supraoptic and paraventricular nuclei. *Am J Physiol Endocrinol Metab* **302**, E273-285, doi:10.1152/ajpendo.00407.2011 (2012).
90 Tanaka, M. *et al.* Molecular and functional remodeling of electrogenic membrane of hypothalamic neurons in response to changes in their input. *Proceedings of the National Academy of Sciences of the United States of America* **96**, 1088-1093 (1999).
91 Hiyama, T. Y. *et al.* Autoimmunity to the sodium-level sensor in the brain causes essential hypernatremia. *Neuron* **66**, 508-522, doi:S0896-6273(10)00288-6 [pii] 10.1016/j.neuron.2010.04.017 (2010).
92 Hiyama, T. Y., Watanabe, E., Okado, H. & Noda, M. The subfornical organ is the primary locus of sodium-level sensing by Na(x) sodium channels for the control of salt-intake behavior. *The Journal of neuroscience : the official journal of the Society for Neuroscience* **24**, 9276-9281, doi:24/42/9276 [pii] 10.1523/JNEUROSCI.2795-04.2004 (2004).
93 Hiyama, T. Y. *et al.* Na(x) channel involved in CNS sodium-level sensing. *Nature neuroscience* **5**, 511-512, doi:10.1038/nn856 nn856 [pii] (2002).
94 Matsumoto, M. *et al.* Channel properties of Nax expressed in neurons. *PloS one* **10**, e0126109, doi:10.1371/journal.pone.0126109 (2015).
95 Goldin, A. L. Resurgence of sodium channel research. *Annual review of physiology* **63**, 871-894, doi:10.1146/annurev.physiol.63.1.871 (2001).
96 Bourque, C. W., Voisin, D. L. & Chakfe, Y. Stretch-inactivated cation channels: cellular targets for modulation of osmosensitivity in supraoptic neurons. *Progress in brain research* **139**, 85-94 (2002).
97 Ciura, S. & Bourque, C. W. Transient receptor potential vanilloid 1 is required for intrinsic osmoreception in organum vasculosum lamina terminalis neurons and for normal thirst responses to systemic hyperosmolality. *The Journal of neuroscience : the official journal of the Society for Neuroscience* **26**, 9069-9075, doi:26/35/9069 [pii] 10.1523/JNEUROSCI.0877-06.2006 (2006).
98 Bourque, C. W., Oliet, S. H. & Richard, D. Osmoreceptors, osmoreception, and osmoregulation. *Front Neuroendocrinol* **15**, 231-274, doi:S0091-3022(84)71010-7 [pii] 10.1006/frne.1994.1010 (1994).

99 Desson, S. E. & Ferguson, A. V. Interleukin 1beta modulates rat subfornical organ neurons as a result of activation of a non-selective cationic conductance. *The Journal of physiology* **550**, 113-122, doi:10.1113/jphysiol.2003.041210 (2003).
100 Amin, M. S. *et al.* Distribution of epithelial sodium channels and mineralocorticoid receptors in cardiovascular regulatory centers in rat brain. *American journal of physiology. Regulatory, integrative and comparative physiology* **289**, R1787-1797, doi:10.1152/ajpregu.00063.2005 (2005).
101 Watanabe, E. *et al.* Nav2/NaG channel is involved in control of salt-intake behavior in the CNS. *The Journal of neuroscience : the official journal of the Society for Neuroscience* **20**, 7743-7751, doi:20/20/7743 [pii] (2000).
102 Coble, J. P., Grobe, J. L., Johnson, A. K. & Sigmund, C. D. Mechanisms of brain renin angiotensin system-induced drinking and blood pressure: importance of the subfornical organ. *American journal of physiology. Regulatory, integrative and comparative physiology* **308**, R238-249, doi:10.1152/ajpregu.00486.2014 (2015).
103 Mimee, A., Smith, P. M. & Ferguson, A. V. Circumventricular organs: targets for integration of circulating fluid and energy balance signals? *Physiology & behavior* **121**, 96-102, doi:10.1016/j.physbeh.2013.02.012 (2013).
104 Zimmerman, C. A. *et al.* Thirst neurons anticipate the homeostatic consequences of eating and drinking. *Nature* **537**, 680-684, doi:10.1038/nature18950 (2016).
105 Miselis, R. R., Shapiro, R. E. & Hand, P. J. Subfornical organ efferents to neural systems for control of body water. *Science (New York, N.Y.)* **205**, 1022-1025 (1979).
106 Nissen, R., Bourque, C. W. & Renaud, L. P. Membrane properties of organum vasculosum lamina terminalis neurons recorded in vitro. *The American journal of physiology* **264**, R811-815 (1993).
107 Kinsman, B. J., Simmonds, S. S., Browning, K. N. & Stocker, S. D. Organum Vasculosum of the Lamina Terminalis Detects NaCl to Elevate Sympathetic Nerve Activity and Blood Pressure. *Hypertension (Dallas, Tex. : 1979)* **69**, 163-170, doi:10.1161/hypertensionaha.116.08372 (2017).
108 Sibbald, J. R., Hubbard, J. I. & Sirett, N. E. Responses from osmosensitive neurons of the rat subfornical organ in vitro. *Brain research* **461**, 205-214, doi:0006-8993(88)90251-X [pii] (1988).
109 Grob, M., Drolet, G. & Mouginot, D. Specific Na+ sensors are functionally expressed in a neuronal population of the median preoptic nucleus of the rat. *The Journal of neuroscience : the official journal of the Society for Neuroscience* **24**, 3974-3984, doi:10.1523/JNEUROSCI.3720-03.2004
24/16/3974 [pii] (2004).
110 Tremblay, C. *et al.* A neuronal sodium leak channel is responsible for the detection of sodium in the rat median preoptic nucleus. *J Neurophysiol*, doi:jn.00417.2010 [pii]
10.1152/jn.00417.2010 (2010).
111 Tremblay, C. *et al.* Neuronal sodium leak channel is responsible for the detection of sodium in the rat median preoptic nucleus. *J.Neurophysiol.* **105**, 650-660, doi:jn.00417.2010 [pii];10.1152/jn.00417.2010 [doi] (2011).
112 Shimizu, H. *et al.* Glial Nax channels control lactate signaling to neurons for brain [Na+] sensing. *Neuron* **54**, 59-72, doi:S0896-6273(07)00210-3 [pii]
10.1016/j.neuron.2007.03.014 (2007).

113 Camacho, A. & Phillips, M. I. Horseradish peroxidase study in rat of the neural connections of the organum vasculosum of the lamina terminalis. *Neuroscience letters* **25**, 201-204 (1981).
114 Oka, Y., Ye, M. & Zuker, C. S. Thirst driving and suppressing signals encoded by distinct neural populations in the brain. *Nature* **520**, 349-352, doi:10.1038/nature14108 (2015).
115 Gizowski, C., Zaelzer, C. & Bourque, C. W. Clock-driven vasopressin neurotransmission mediates anticipatory thirst prior to sleep. *Nature* **537**, 685-688, doi:10.1038/nature19756 (2016).
116 McKinley, M. J. *et al.* The median preoptic nucleus: front and centre for the regulation of body fluid, sodium, temperature, sleep and cardiovascular homeostasis. *Acta Physiol (Oxf)* **214**, 8-32, doi:10.1111/apha.12487 (2015).
117 Saper, C. B. & Levisohn, D. Afferent connections of the median preoptic nucleus in the rat: anatomical evidence for a cardiovascular integrative mechanism in the anteroventral third ventricular (AV3V) region. *Brain research* **288**, 21-31 (1983).
118 Lind, R. W., Van Hoesen, G. W. & Johnson, A. K. An HRP study of the connections of the subfornical organ of the rat. *The Journal of comparative neurology* **210**, 265-277, doi:10.1002/cne.902100306 (1982).
119 Nation, H. L., Nicoleau, M., Kinsman, B. J., Browning, K. N. & Stocker, S. D. DREADD-induced activation of subfornical organ neurons stimulates thirst and salt appetite. *J Neurophysiol* **115**, 3123-3129, doi:10.1152/jn.00149.2016 (2016).
120 Abbott, S. B., Machado, N. L., Geerling, J. C. & Saper, C. B. Reciprocal Control of Drinking Behavior by Median Preoptic Neurons in Mice. *The Journal of neuroscience : the official journal of the Society for Neuroscience* **36**, 8228-8237, doi:10.1523/JNEUROSCI.1244-16.2016 (2016).
121 Allen, W. E. *et al.* Thirst-associated preoptic neurons encode an aversive motivational drive. *Science (New York, N.Y.)* **357**, 1149-1155, doi:10.1126/science.aan6747 (2017).
122 Gilman, A. The relation between blood osmotic pressure, fluid distribution and voluntary water intake. *The American journal of physiology* **120**, 323-328 (1937).
123 Wolf, A. V. Osmometric analysis of thirst in man and dog. *Am. J. Physiol.*, 75-86 (1950).
124 Stricker, E. M. Osmoregulation and volume regulation in rats: inhibition of hypovolemic thirst by water. *Am.J.Physiol* **217**, 98-105 (1969).
125 Anderson, J. W., Washburn, D. L. & Ferguson, A. V. Intrinsic osmosensitivity of subfornical organ neurons. *Neuroscience* **100**, 539-547, doi:S0306-4522(00)00313-4 [pii] (2000).
126 Kucharczyk, J., Assaf, S. Y. & Mogenson, G. J. Differential effects of brain lesions on thirst induced by the administration of angiotensin-II to the preoptic region, subfornical organ and anterior third ventricle. *Brain research* **108**, 327-337 (1976).
127 Thrasher, T. N., Simpson, J. B. & Ramsay, D. J. Lesions of the subfornical organ block angiotensin-induced drinking in the dog. *Neuroendocrinology* **35**, 68-72 (1982).
128 Johnson, A. K. & Buggy, J. Periventricular preoptic-hypothalamus is vital for thirst and normal water economy. *The American journal of physiology* **234**, R122-129 (1978).
129 Buggy, J. & Jonhson, A. K. Preoptic-hypothalamic periventricular lesions: thirst deficits and hypernatremia. *The American journal of physiology* **233**, R44-52 (1977).
130 Thrasher, T. N., Keil, L. C. & Ramsay, D. J. Lesions of the organum vasculosum of the lamina terminalis (OVLT) attenuate osmotically-induced drinking and vasopressin secretion in the dog. *Endocrinology* **110**, 1837-1839 (1982).

131 Mangiapane, M. L., Thrasher, T. N., Keil, L. C., Simpson, J. B. & Ganong, W. F. Deficits in drinking and vasopressin secretion after lesions of the nucleus medianus. *Neuroendocrinology* **37**, 73-77 (1983).
132 Johnson, A. K., Cunningham, J. T. & Thunhorst, R. L. Integrative role of the lamina terminalis in the regulation of cardiovascular and body fluid homeostasis. *Clin Exp Pharmacol Physiol* **23**, 183-191 (1996).
133 McKinley, M. J. *et al.* Efferent neural pathways of the lamina terminalis subserving osmoregulation. *Progress in brain research* **91**, 395-402 (1992).
134 McKinley, M. J., Denton, D. A., Oldfield, B. J., De Oliveira, L. B. & Mathai, M. L. Water intake and the neural correlates of the consciousness of thirst. *Seminars in nephrology* **26**, 249-257, doi:S0270-9295(06)00012-X [pii]
10.1016/j.semnephrol.2006.02.001 (2006).
135 Ciura, S., Liedtke, W. & Bourque, C. W. Hypertonicity sensing in organum vasculosum lamina terminalis neurons: a mechanical process involving TRPV1 but not TRPV4. *The Journal of neuroscience : the official journal of the Society for Neuroscience* **31**, 14669-14676, doi:10.1523/jneurosci.1420-11.2011 (2011).
136 Zaelzer, C. *et al.* DeltaN-TRPV1: A Molecular Co-detector of Body Temperature and Osmotic Stress. *Cell reports* **13**, 23-30, doi:10.1016/j.celrep.2015.08.061 (2015).
137 Sharif-Naeini, R., Ciura, S., Zhang, Z. & Bourque, C. W. Contribution of TRPV channels to osmosensory transduction, thirst, and vasopressin release. *Kidney Int* **73**, 811-815, doi:5002788 [pii]
10.1038/sj.ki.5002788 (2008).
138 Sudbury, J. R., Ciura, S., Sharif-Naeini, R. & Bourque, C. W. Osmotic and thermal control of magnocellular neurosecretory neurons--role of an N-terminal variant of trpv1. *The European journal of neuroscience* **32**, 2022-2030, doi:10.1111/j.1460-9568.2010.07512.x (2010).
139 Kinsman, B. *et al.* Osmoregulatory thirst in mice lacking the transient receptor potential vanilloid type 1 (TRPV1) and/or type 4 (TRPV4) receptor. *American journal of physiology. Regulatory, integrative and comparative physiology* **307**, R1092-1100, doi:10.1152/ajpregu.00102.2014 (2014).
140 Taylor, A. C., McCarthy, J. J. & Stocker, S. D. Mice Lacking the Transient Receptor Vanilloid Potential 1 (TRPV1) Channel Display Normal Thirst Responses and Central Fos Activation to Hypernatremia. *American journal of physiology. Regulatory, integrative and comparative physiology*, doi:00003.2008 [pii]
10.1152/ajpregu.00003.2008 (2008).
141 Hussy, N., Deleuze, C., Pantaloni, A., Desarmenien, M. G. & Moos, F. Agonist action of taurine on glycine receptors in rat supraoptic magnocellular neurones: possible role in osmoregulation. *The Journal of physiology* **502 (Pt 3)**, 609-621 (1997).
142 Choe, K. Y., Olson, J. E. & Bourque, C. W. Taurine release by astrocytes modulates osmosensitive glycine receptor tone and excitability in the adult supraoptic nucleus. *The Journal of neuroscience : the official journal of the Society for Neuroscience* **32**, 12518-12527, doi:10.1523/JNEUROSCI.1380-12.2012 (2012).
143 Choe, K. Y., Trudel, E. & Bourque, C. W. Effects of Salt Loading on the Regulation of Rat Hypothalamic Magnocellular Neurosecretory Cells by Ionotropic GABA and Glycine Receptors. *Journal of neuroendocrinology* **28**, doi:10.1111/jne.12372 (2016).

144 Hussy, N., Deleuze, C., Desarmenien, M. G. & Moos, F. C. Osmotic regulation of neuronal activity: a new role for taurine and glial cells in a hypothalamic neuroendocrine structure. *Prog Neurobiol* **62**, 113-134, doi:S0301-0082(99)00071-4 [pii] (2000).
145 Prager-Khoutorsky, M. & Bourque, C. W. ANATOMICAL ORGANIZATION OF THE RAT ORGANUM VASCULOSUM LAMINAE TERMINALIS. *American journal of physiology. Regulatory, integrative and comparative physiology*, ajpregu 00134 02015, doi:10.1152/ajpregu.00134.2015 (2015).
146 Hochstenbach, S. L. & Ciriello, J. Effect of lesions of forebrain circumventricular organs on c-fos expression in the central nervous system to plasma hypernatremia. *Brain research* **713**, 17-28 (1996).
147 Lechner, S. G. *et al.* The Molecular and Cellular Identity of Peripheral Osmoreceptors. *Neuron* **69**, 332-344, doi:S0896-6273(10)01076-7 [pii] 10.1016/j.neuron.2010.12.028 (2011).
148 Russell, P. J., Abdelaal, A. E. & Mogenson, G. J. Graded levels of hemorrhage, thirst and angiotensin II in the rat. *Physiology & behavior* **15**, 117-119 (1975).
149 Fitzsimons, J. T. Drinking by rats depleted of body fluid without increase in osmotic pressure. *The Journal of physiology* **159**, 297-309 (1961).
150 Joris, L., Dab, I. & Quinton, P. M. Elemental composition of human airway surface fluid in healthy and diseased airways. *The American review of respiratory disease* **148**, 1633-1637, doi:10.1164/ajrccm/148.6_Pt_1.1633 (1993).
151 Zardetto-Smith, A. M., Thunhorst, R. L., Cicha, M. Z. & Johnson, A. K. Afferent signaling and forebrain mechanisms in the behavioral control of extracellular fluid volume. *Ann N Y Acad Sci* **689**, 161-176 (1993).
152 Fitzsimons, J. T. Angiotensin, thirst, and sodium appetite. *Physiol Rev.* **78**, 583-686 (1998).
153 Stocker, S. D., Stricker, E. M. & Sved, A. F. Arterial baroreceptors mediate the inhibitory effect of acute increases in arterial blood pressure on thirst. *American journal of physiology. Regulatory, integrative and comparative physiology* **282**, R1718-1729, doi:10.1152/ajpregu.00651.2001 (2002).
154 Stocker, S. D., Stricker, E. M. & Sved, A. F. Acute hypertension inhibits thirst stimulated by ANG II, hyperosmolality, or hypovolemia in rats. *American journal of physiology. Regulatory, integrative and comparative physiology* **280**, R214-224 (2001).
155 Stricker, E. M. & Sved, A. F. Controls of vasopressin secretion and thirst: similarities and dissimilarities in signals. *Physiology & behavior* **77**, 731-736 (2002).
156 Dampney, R. A., Polson, J. W., Potts, P. D., Hirooka, Y. & Horiuchi, J. Functional organization of brain pathways subserving the baroreceptor reflex: studies in conscious animals using immediate early gene expression. *Cell Mol.Neurobiol.* **23**, 597-616 (2003).
157 Thunhorst, R. L., Xu, Z., Cicha, M. Z., Zardetto-Smith, A. M. & Johnson, A. K. Fos expression in rat brain during depletion-induced thirst and salt appetite. *The American journal of physiology* **274**, R1807-1814 (1998).
158 Badoer, E., McKinley, M. J., Oldfield, B. J. & McAllen, R. M. Distribution of hypothalamic, medullary and lamina terminalis neurons expressing Fos after hemorrhage in conscious rats. *Brain research* **582**, 323-328 (1992).
159 Potts, P. D., Ludbrook, J., Gillman-Gaspari, T. A., Horiuchi, J. & Dampney, R. A. Activation of brain neurons following central hypervolaemia and hypovolaemia: contribution of baroreceptor and non-baroreceptor inputs. *Neuroscience* **95**, 499-511, doi:S0306452299004261 [pii] (2000).

160 Allen, W. E. *et al.* Thirst-Associated Preoptic Neurons Encode an Aversive Motivational Drive. *Science (New York, N.Y.)* **in press** (2017).
161 Godino, A., Giusti-Paiva, A., Antunes-Rodrigues, J. & Vivas, L. Neurochemical brain groups activated after an isotonic blood volume expansion in rats. *Neuroscience* **In Press, Corrected Proof**.
162 Howe, B. M., Bruno, S. B., Higgs, K. A., Stigers, R. L. & Cunningham, J. T. FosB expression in the central nervous system following isotonic volume expansion in unanesthetized rats. *Experimental neurology* **187**, 190-198, doi:10.1016/j.expneurol.2004.01.020 (2004).
163 Randolph, R. R., Li, Q., Curtis, K. S., Sullivan, M. J. & Cunningham, J. T. Fos expression following isotonic volume expansion of the unanesthetized male rat. *The American journal of physiology* **274**, R1345-1352 (1998).
164 Gizowski, C. & Bourque, C. W. Neurons that drive and quench thirst. *Science (New York, N.Y.)* **in press** (2017).
165 Simpson, J. B. & Routtenberg, A. Subfornical organ: a dipsogenic site of action of angiotensin II. *Science (New York, N.Y.)* **201**, 379-381 (1978).
166 Simpson, J. B. & Routtenberg, A. Subfornical organ: site of drinking elicitation by angiotensin II. *Science (New York, N.Y.)* **181**, 1172-1175 (1973).
167 Antunes-Rodrigues, J., de Castro, M., Elias, L. L., Valenca, M. M. & McCann, S. M. Neuroendocrine control of body fluid metabolism. *Physiol Rev* **84**, 169-208, doi:10.1152/physrev.00017.2003
84/1/169 [pii] (2004).
168 Kuwahara, K. & Nakao, K. Regulation and significance of atrial and brain natriuretic peptides as cardiac hormones. *Endocrine journal* **57**, 555-565 (2010).
169 Ehrlich, K. J. & Fitts, D. A. Atrial natriuretic peptide in the subfornical organ reduces drinking induced by angiotensin or in response to water deprivation. *Behavioral neuroscience* **104**, 365-372 (1990).
170 Stanhewicz, A. E. & Kenney, W. L. Determinants of water and sodium intake and output. *Nutrition reviews* **73 Suppl 2**, 73-82, doi:10.1093/nutrit/nuv033 (2015).
171 Stricker, E. M. & Stricker, M. L. Pre-systemic controls of fluid intake and vasopressin secretion. *Physiology & behavior* **103**, 86-88, doi:10.1016/j.physbeh.2010.11.019 (2011).
172 Fitzsimons, T. J. & Le Magnen, J. Eating as a regulatory control of drinking in the rat. *Journal of comparative and physiological psychology* **67**, 273-283 (1969).
173 Mandelblat-Cerf, Y. *et al.* Bidirectional Anticipation of Future Osmotic Challenges by Vasopressin Neurons. *Neuron* **93**, 57-65, doi:10.1016/j.neuron.2016.11.021 (2017).
174 Hatton, G. I. & Almli, C. R. Plasma osmotic pressure and volume changes as determinants of drinking thresholds. *Physiology & behavior* **4**, 207-214, doi:http://dx.doi.org/10.1016/0031-9384(69)90082-1 (1969).
175 Gamble J. L., P. M. C., McKhann C. F. The optimal water requirement in renal functions: 1. Measurements of water drinking by rats according to increments of urea and of several salts in the food. . *American Journal of Physiology* **88**, 571-580 (1929).
176 Kraly, F. S., Kim, Y. M., Dunham, L. M. & Tribuzio, R. A. Drinking after intragastric NaCl without increase in systemic plasma osmolality in rats. *The American journal of physiology* **269**, R1085-1092 (1995).

177 Stricker, E. M., Huang, W. & Sved, A. F. Early osmoregulatory signals in the control of water intake and neurohypophyseal hormone secretion. *Physiology & behavior* **76**, 415-421 (2002).
178 Manesh, R., Hoffmann, M. L. & Stricker, E. M. Water ingestion by rats fed a high-salt diet may be mediated, in part, by visceral osmoreceptors. *American journal of physiology. Regulatory, integrative and comparative physiology* **290**, R1742-1749, doi:10.1152/ajpregu.00865.2005 (2006).
179 Krause, E. G., de Kloet, A. D. & Sakai, R. R. Post-ingestive signals and satiation of water and sodium intake of male rats. *Physiology & behavior* **99**, 657-662, doi:10.1016/j.physbeh.2010.01.030 (2010).
180 Kobashi, M. & Adachi, A. Projection of nucleus tractus solitarius units influenced by hepatoportal afferent signal to parabrachial nucleus. *Journal of the autonomic nervous system* **16**, 153-158 (1986).
181 Kobashi, M. & Adachi, A. Convergence of hepatic osmoreceptive inputs on sodium-responsive units within the nucleus of the solitary tract of the rat. *J Neurophysiol* **54**, 212-219 (1985).
182 Stricker, E. M. & Hoffmann, M. L. Presystemic signals in the control of thirst, salt appetite, and vasopressin secretion. *Physiology & behavior* **91**, 404-412, doi:S0031-9384(07)00136-9 [pii]
10.1016/j.physbeh.2007.04.007 (2007).
183 Morita, H. *et al.* Fos induction in rat brain neurons after stimulation of the hepatoportal Na-sensitive mechanism. *The American journal of physiology* **272**, R913-923 (1997).
184 Starbuck, E. M. & Fitts, D. A. Influence of the subfornical organ on meal-associated drinking in rats. *American journal of physiology. Regulatory, integrative and comparative physiology* **280**, R669-677 (2001).
185 Gu, G. B. & Ju, G. The parabrachio-subfornical organ projection in the rat. *Brain research bulletin* **38**, 41-47 (1995).
186 Han, Z. S., Gu, G. B., Sun, C. Q. & Ju, G. Convergence of somatosensory and baroreceptive inputs onto parabrachio-subfornical organ neurons in the rat: an electrophysiological study. *Brain research* **566**, 239-247 (1991).
187 McKinley, M. J. *et al.* The sensory circumventricular organs of the mammalian brain. *Adv Anat Embryol Cell Biol* **172**, III-XII, 1-122, back cover (2003).
188 Sladek, C. D. & Johnson, A. K. Integration of thermal and osmotic regulation of water homeostasis: the role of TRPV channels. *American journal of physiology. Regulatory, integrative and comparative physiology* **305**, R669-678, doi:10.1152/ajpregu.00270.2013 (2013).
189 Bel'skaya, L. V., Kosenok, V. K. & Sarf, E. A. Chronophysiological features of the normal mineral composition of human saliva. *Archives of oral biology* **82**, 286-292, doi:10.1016/j.archoralbio.2017.06.024 (2017).
190 Lund, J. P., Barker, J. H., Dellow, P. G. & Stevenson, J. A. Water intake of normal and desalivate rats on exposure to environmental heat. *Canadian journal of physiology and pharmacology* **47**, 849-852 (1969).
191 Grace, J. E. & Stevenson, J. A. Thermogenic drinking in the rat. *The American journal of physiology* **220**, 1009-1015 (1971).
192 Box, B. M., Montis, F., Yeomans, C. & Stevenson, J. A. Thermogenic drinking in cold-acclimated rats. *The American journal of physiology* **225**, 162-165 (1973).

193 Barney, C. C. & Folkerts, M. M. Thermal dehydration-induced thirst in rats: role of body temperature. *The American journal of physiology* **269**, R557-564 (1995).
194 Morrison, S. F. & Nakamura, K. Central neural pathways for thermoregulation. *Frontiers in bioscience (Landmark edition)* **16**, 74-104 (2011).
195 Palkar, R., Lippoldt, E. K. & McKemy, D. D. The molecular and cellular basis of thermosensation in mammals. *Current opinion in neurobiology* **34**, 14-19, doi:10.1016/j.conb.2015.01.010 (2015).
196 Schepers, R. J. & Ringkamp, M. Thermoreceptors and thermosensitive afferents. *Neuroscience and biobehavioral reviews* **34**, 177-184, doi:10.1016/j.neubiorev.2009.10.003 (2010).
197 Craig, A. D., Bushnell, M. C., Zhang, E. T. & Blomqvist, A. A thalamic nucleus specific for pain and temperature sensation. *Nature* **372**, 770-773, doi:10.1038/372770a0 (1994).
198 Nakamura, K. & Morrison, S. F. A thermosensory pathway that controls body temperature. *Nature neuroscience* **11**, 62-71, doi:nn2027 [pii] 10.1038/nn2027 (2008).
199 Jessen, C., Feistkorn, G. & Nagel, A. Temperature sensitivity of skeletal muscle in the conscious goat. *Journal of applied physiology: respiratory, environmental and exercise physiology* **54**, 880-886 (1983).
200 Fajardo, O., Meseguer, V., Belmonte, C. & Viana, F. TRPA1 channels mediate cold temperature sensing in mammalian vagal sensory neurons: pharmacological and genetic evidence. *The Journal of neuroscience : the official journal of the Society for Neuroscience* **28**, 7863-7875, doi:10.1523/jneurosci.1696-08.2008 (2008).
201 Riedel, W. Warm receptors in the dorsal abdominal wall of the rabbit. *Pflugers Archiv : European journal of physiology* **361**, 205-206 (1976).
202 Rawson, R. O. & Quick, K. P. Localization of intra-abdominal thermoreceptors in the ewe. *The Journal of physiology* **222**, 665-667 (1972).
203 Adelson, D. W., Wei, J. Y. & Kruger, L. Warm-sensitive afferent splanchnic C-fiber units in vitro. *J Neurophysiol* **77**, 2989-3002 (1997).
204 Wit, A. & Wang, S. C. Temperature-sensitive neurons in preoptic-anterior hypothalamic region: effects of increasing ambient temperature. *The American journal of physiology* **215**, 1151-1159 (1968).
205 Takamata, A., Mack, G. W., Stachenfeld, N. S. & Nadel, E. R. Body temperature modification of osmotically induced vasopressin secretion and thirst in humans. *The American journal of physiology* **269**, R874-880 (1995).
206 Boulant, J. A. Cellular mechanisms of temperature sensitivity in hypothalamic neurons. *Progress in brain research* **115**, 3-8 (1998).
207 Fealey, R. D. Interoception and autonomic nervous system reflexes thermoregulation. *Handbook of clinical neurology* **117**, 79-88, doi:10.1016/b978-0-444-53491-0.00007-9 (2013).
208 Morrison, S. F. Central control of body temperature. *F1000Research* **5**, doi:10.12688/f1000research.7958.1 (2016).
209 Boulant, J. A. Hypothalamic mechanisms in thermoregulation. *Fed Proc* **40**, 2843-2850 (1981).
210 Barbour, H. G. Die Wirkung unmittelbarer Erwarmung und Abkuhlung der Warmezentra auf die Korpertemperatur. *Arch Exp Path Pharmak* **70**, 1-15 (1912).

211 Hammouda, M. The central and the reflex mechanism of panting. *The Journal of physiology* **77**, 319-336 (1933).
212 Magoun H. W., H. F., Brobeck J. R., Ranson S. W., Paolini P. Activation of heat loss mechanisms by local heating of the brain. *Journal of Neurophysiology* **87**, 885-905 (1986).
213 Jacobson, F. H. & Squires, R. D. Thermoregulatory responses of the cat to preoptic and environmental temperatures. *The American journal of physiology* **218**, 1575-1582 (1970).
214 Szczepanska-Sadowska, E. Plasma ADH increase and thirst suppression elicited by preoptic heating in the dog. *The American journal of physiology* **226**, 155-161 (1974).
215 Morrison, S. F., Nakamura, K. & Madden, C. J. Central control of thermogenesis in mammals. *Experimental physiology* **93**, 773-797, doi:expphysiol.2007.041848 [pii] 10.1113/expphysiol.2007.041848 (2008).
216 Tan, C. L. *et al.* Warm-Sensitive Neurons that Control Body Temperature. *Cell* **167**, 47-59.e15, doi:10.1016/j.cell.2016.08.028 (2016).
217 Nakamura, K. & Morrison, S. F. A thermosensory pathway mediating heat-defense responses. *Proceedings of the National Academy of Sciences of the United States of America* **107**, 8848-8853, doi:0913358107 [pii] 10.1073/pnas.0913358107 (2010).
218 Andersson, B. & Larsson, B. Influence of local temperature changes in the preoptic area and rostral hypothalamus on the regulation of food and water intake. *Acta physiologica Scandinavica* **52**, 75-89, doi:10.1111/j.1748-1716.1961.tb02203.x (1961).
219 Trudel, E. & Bourque, C. W. Circadian modulation of osmoregulated firing in rat supraoptic nucleus neurones. *Journal of neuroendocrinology* **24**, 577-586, doi:10.1111/j.1365-2826.2012.02298.x (2012).
220 Moon, D. G. *et al.* Antidiuretic hormone in elderly male patients with severe nocturia: a circadian study. *BJU Int* **94**, 571-575, doi:10.1111/j.1464-410X.2004.05003.x BJU5003 [pii] (2004).
221 Miller, M. Nocturnal polyuria in older people: pathophysiology and clinical implications. *J Am Geriatr Soc* **48**, 1321-1329 (2000).
222 Tokonami, N. *et al.* Local renal circadian clocks control fluid-electrolyte homeostasis and BP. *Journal of the American Society of Nephrology : JASN* **25**, 1430-1439, doi:10.1681/asn.2013060641 (2014).
223 Firsov, D., Tokonami, N. & Bonny, O. Role of the renal circadian timing system in maintaining water and electrolytes homeostasis. *Molecular and cellular endocrinology* **349**, 51-55, doi:10.1016/j.mce.2011.06.037 (2012).
224 Asplund, R. Nocturia, nocturnal polyuria, and sleep quality in the elderly. *J Psychosom Res* **56**, 517-525, doi:10.1016/j.jpsychores.2004.04.003 (2004).
225 Windle, R. J., Forsling, M. L. & Guzek, J. W. Daily rhythms in the hormone content of the neurohypophysial system and release of oxytocin and vasopressin in the male rat: effect of constant light. *J Endocrinol* **133**, 283-290 (1992).
226 Trudel, E. & Bourque, C. W. Central clock excites vasopressin neurons by waking osmosensory afferents during late sleep. *Nature neuroscience* **13**, 467-474, doi:nn.2503 [pii] 10.1038/nn.2503 (2010).
227 Spiteri, N. J. Circadian patterning of feeding, drinking and activity during diurnal food access in rats. *Physiology & behavior* **28**, 139-147 (1982).

228 Satinoff, E. & Prosser, R. A. Suprachiasmatic nuclear lesions eliminate circadian rhythms of drinking and activity, but not of body temperature, in male rats. *Journal of biological rhythms* **3**, 1-22, doi:10.1177/074873048800300101 (1988).
229 Johnson, R. F., Beltz, T. G., Thunhorst, R. L. & Johnson, A. K. Investigations on the physiological controls of water and saline intake in C57BL/6 mice. *American journal of physiology. Regulatory, integrative and comparative physiology* **285**, R394-403, doi:10.1152/ajpregu.00130.2003 (2003).
230 Lee, J. E. *et al.* Endogenous peptide discovery of the rat circadian clock: a focused study of the suprachiasmatic nucleus by ultrahigh performance tandem mass spectrometry. *Molecular & cellular proteomics : MCP* **9**, 285-297, doi:10.1074/mcp.M900362-MCP200 (2010).
231 Abrahamson, E. E. & Moore, R. Y. Suprachiasmatic nucleus in the mouse: retinal innervation, intrinsic organization and efferent projections. *Brain research* **916**, 172-191, doi:S0006-8993(01)02890-6 [pii] (2001).
232 Kalsbeek, A. & Buijs, R. M. Output pathways of the mammalian suprachiasmatic nucleus: coding circadian time by transmitter selection and specific targeting. *Cell Tissue Res* **309**, 109-118, doi:10.1007/s00441-002-0577-0 (2002).
233 Moore, R. Y., Speh, J. C. & Leak, R. K. Suprachiasmatic nucleus organization. *Cell Tissue Res* **309**, 89-98, doi:10.1007/s00441-002-0575-2 (2002).
234 Appelgren, B., Eriksson, S. & Jonasson, H. Oro-gastro-intestinal inhibition of hypernatremia-induced drinking in the goat. *Acta physiologica Scandinavica* **115**, 273-280, doi:10.1111/j.1748-1716.1982.tb07076.x (1982).
235 Wood, R. J., Rolls, E. T. & Rolls, B. J. Physiological mechanisms for thirst in the nonhuman primate. *The American journal of physiology* **242**, R423-428 (1982).
236 Krashes, M. J. Physiology: Forecast for water balance. *Nature* **537**, 626-627, doi:10.1038/537626a (2016).
237 Zocchi, D., Wennemuth, G. & Oka, Y. The cellular mechanism for water detection in the mammalian taste system. *Nature neuroscience* **20**, 927-933, doi:10.1038/nn.4575 (2017).
238 Blass, E. M., Jobaris, R. & Hall, W. G. Oropharyngeal control of drinking in rats. *Journal of comparative and physiological psychology* **90**, 909-916 (1976).
239 Maddison, S., Wood, R. J., Rolls, E. T., Rolls, B. J. & Gibbs, J. Drinking in the rhesus monkey: peripheral factors. *Journal of comparative and physiological psychology* **94**, 365-374 (1980).
240 Davis, J. D., Smith, G. P. & McCann, D. P. The control of water and sodium chloride intake by postingestional and orosensory stimulation in water-deprived rats. *Physiology & behavior* **75**, 7-14 (2002).
241 Paintal, A. S. Impulses in vagal afferent fibres from stretch receptors in the stomach and their role in the peripheral mechanism of hunger. *Nature* **172**, 1194-1195 (1953).
242 Malbert, C. H. & Leitner, L. M. Mechanoreceptors sensitive to flow at the gastroduodenal junction of the cat. *The American journal of physiology* **265**, G310-313 (1993).
243 Paintal, A. S. A study of gastric stretch receptors; their role in the peripheral mechanism of satiation of hunger and thirst. *The Journal of physiology* **126**, 255-270 (1954).
244 Raybould, H. E., Gayton, R. J. & Dockray, G. J. CNS effects of circulating CCK8: involvement of brainstem neurones responding to gastric distension. *Brain research* **342**, 187-190 (1985).

245 Olson, B. R. *et al.* c-Fos Expression in Rat Brain and Brainstem Nuclei in Response to Treatments That Alter Food Intake and Gastric Motility. *Molecular and cellular neurosciences* **4**, 93-106, doi:10.1006/mcne.1993.1011 (1993).
246 Hyde, T. M. & Miselis, R. R. Area postrema and adjacent nucleus of the solitary tract in water and sodium balance. *The American journal of physiology* **247**, R173-182 (1984).
247 Curtis, K. S., Verbalis, J. G. & Stricker, E. M. Area postrema lesions in rats appear to disrupt rapid feedback inhibition of fluid intake. *Brain research* **726**, 31-38 (1996).
248 Curtis, K. S. & Stricker, E. M. Enhanced fluid intake by rats after capsaicin treatment. *The American journal of physiology* **272**, R704-709 (1997).
249 Hajat, S., Vardoulakis, S., Heaviside, C. & Eggen, B. Climate change effects on human health: projections of temperature-related mortality for the UK during the 2020s, 2050s and 2080s. *Journal of epidemiology and community health* **68**, 641-648, doi:10.1136/jech-2013-202449 (2014).
250 Robertson, G. L., Shelton, R. L. & Athar, S. The osmoregulation of vasopressin. *Kidney Int* **10**, 25-37 (1976).

Acknowledgements

The authors' work is supported by a Foundation Grant from the Canadian Institutes of Health Research (CIHR, FDN 143337), an operating grant from the Heart and Stroke Foundation of Canada (G-16-00014197), a James McGill Chair to C.W.B., and by a Frederick Banting and Charles Best Canada Graduate Scholarship Doctoral Award to C.G. The Research Institute of the McGill University Health Centre receives generous funding from the Fonds de Recherche Québec Santé.

Author contributions

Both authors researched the data for the article, discussed its content, and contributed to writing and editing the manuscript before submission.

Competing interests

The authors declare no competing interests.

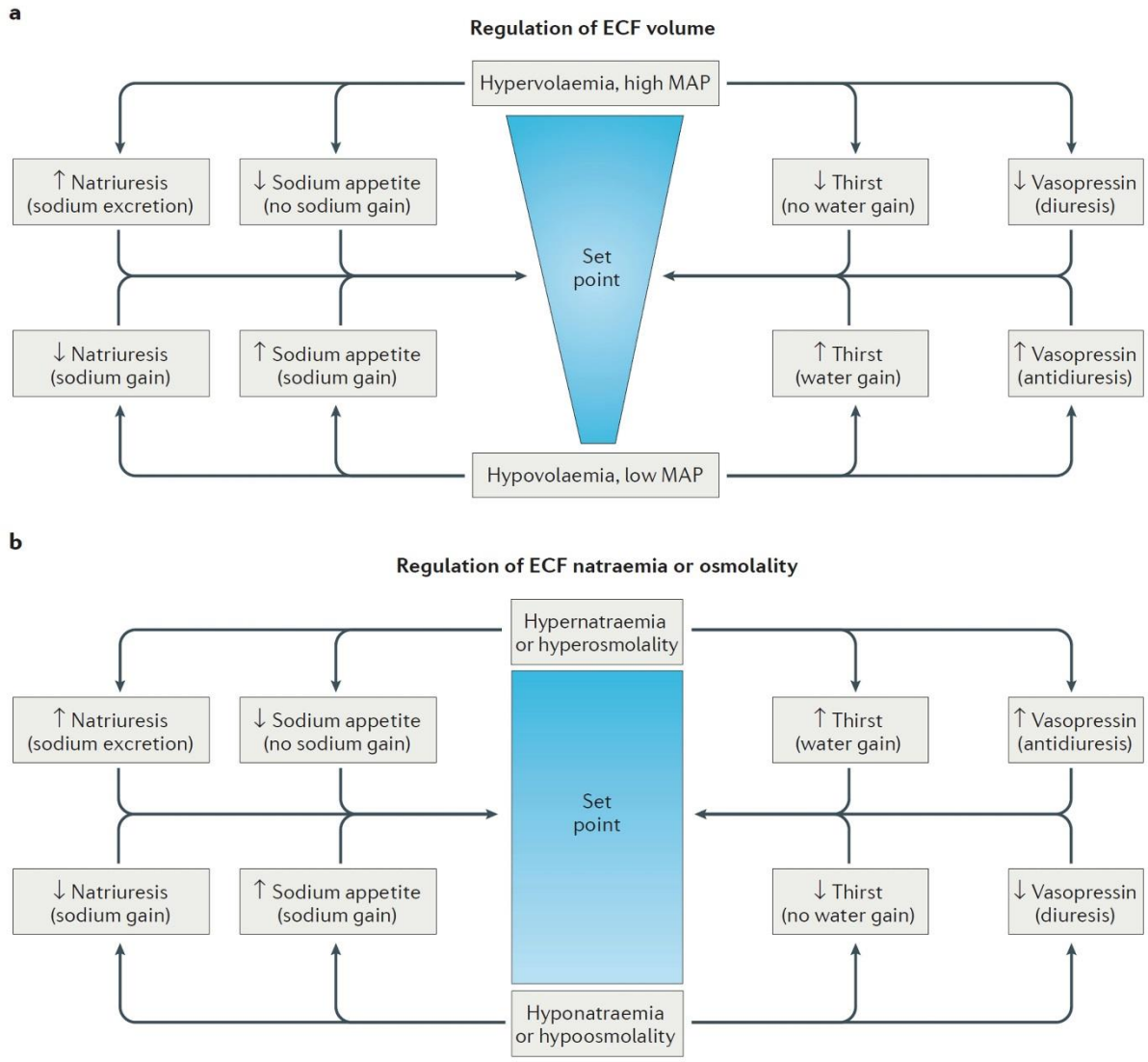

Figure 1. Feedback mechanisms to maintain body fluid balance. Perturbations in body fluid balance can involve changes in the osmolality and volume of the extracellular fluid (ECF), and their correction often requires the coordinated regulation of both parameters. Maintenance of volume and osmotic set points require the intake and excretion of sodium and water to be controlled through feedback mechanisms involving volume receptors, osmoreceptors and sodium (Na^+) detectors. **a |** When hypovolaemia occurs in the absence of a change in osmolality, for example as a result of blood loss, maintenance of fluid homeostasis requires a net accumulation of both salt and water to achieve a net gain of isotonic fluid. This effect is achieved through the stimulation of both sodium appetite and thirst, together with an increase in the reabsorption of sodium and water by the kidney. Sodium reabsorption is promoted by the renin–angiotensin–aldosterone system (RAAS), whereas

water reabsorption is stimulated by an increase in circulating levels of the antidiuretic hormone, vasopressin, which is released from the neurohypophysis. The stimulation of salt appetite and thirst during hypovolaemia is mediated in part by ascending neural inputs from blood volume sensors in the periphery and by the central effects of angiotensin II and aldosterone. By contrast, correction of isotonic hypervolaemia requires a net loss of isotonic fluid, which is achieved in part by suppression of thirst and salt appetite, and by stimulation of renal diuresis and natriuresis. Diuresis is provoked mainly by suppressing basal vasopressin release, which reduces water reabsorption[343]. Natriuresis on the other hand is enhanced by suppression basal RAAS activity, by the release of natriuretic peptides (ANP and BNP) from cardiac myocytes and through regulation of the kidney via renal nerves. **b** |) Increases in ECF osmolality (or natraemia can be readily induced in the absence of an altered ECF volume by the ingestion of salt or food. Appropriate homeostatic responses to hypernatraemia include the suppression of sodium appetite and an increase in natriuresis, combined with an increase and water intake and antidiuresis to promote dilution of the ECF. Conversely, a hypoosmotic status is corrected by suppressing thirst and antidiuresis while promoting sodium intake and its reabsorption by the kidney. MAP, mean arterial pressure

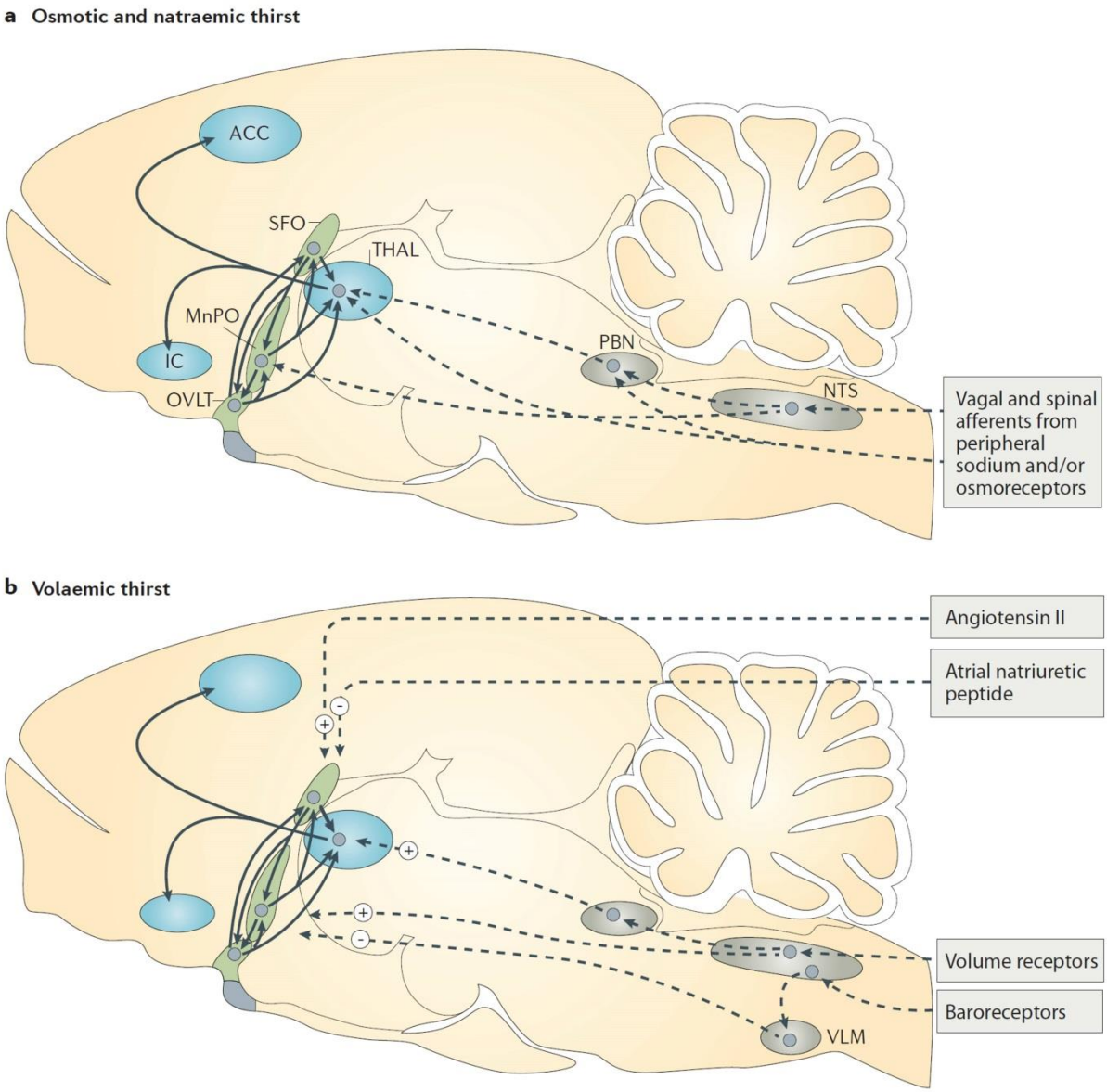

Figure 2. Neural pathways that control thirst homeostasis. Sagittal representation of anatomical pathways that contribute to the regulation of thirst during changes in extracellular fluid (ECF) osmolality and.or [Na^+] (part **a**) or volume (part **b**). The various signals that affect thirst integrate mainly within the region of the lamina terminalis, which includes the median preoptic nucleus (MnPO), organum vasculosum laminae terminalis (OVLT) and subfornical organ (SFO). Optogenetic or chemogenetic activation of thirst-promoting neurons in any of these structures can stimulate water intake. The perception of thirst seems to involve activation of the anterior cingulate cortex (ACC) and insular cortex (IC**)**, which might be mediated by relay neurons in the medial parts of the thalamus (THAL). Signals from peripheral sodium and osmoreceptors (part a), and

baroreceptors and volume receptors (part b) reach thirst promoting regions via visceral afferents that course through spinal or vagal pathways. These afferents may converge onto neurons within brain stem nuclei such as the nucleus tractus solitarius (NTS), the ventrolateral medulla (VLM) and/or the parabrachial nucleus (PBN), which then project to thirst-promoting regions. Alternatively, peripheral signals may be directly or indirectly relayed to the thalamus (THAL), whereby thalamic relay neurons transmit sensory information directly to the ACC and/or IC to promote thirst. Humoral signals like angiotensin II and atrial natriuretic peptide can influence the network by affecting the activity of neurons located in in the SFO.

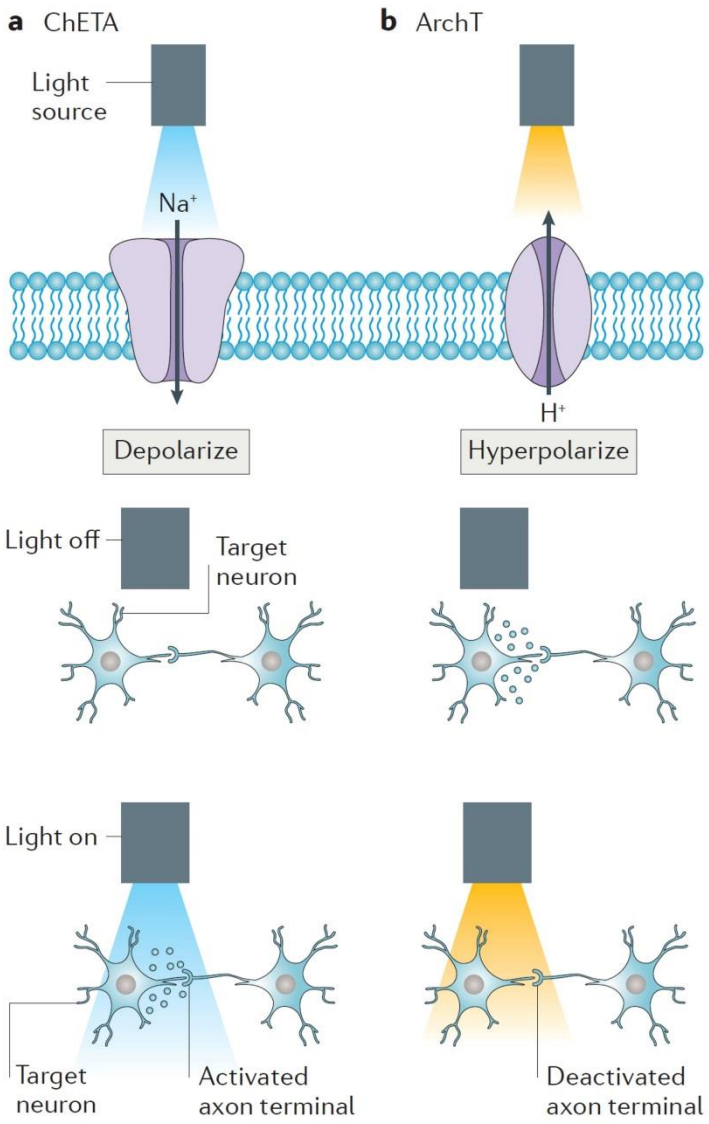

Figure 3. Optogenetic manipulation of neuronal activity Specialized light-sensitive ion channels or pumps genetically expressed in neurons can be activated by different wavelengths of light to cause membrane depolarization or hyperpolarization. When this process is induced in neuronal somata or dendrites these effects regulate the rate at which action potentials are discharged (not shown) However in this case, light is used to depolarize or hyperpolarize the axon terminals of the neuron and thus respectively stimulate or inhibit release of vasopressin. a) Channelrhodopsin is a blue light (~470 nm) sensitive ion channel, and when photoactivated enables the influx of sodium ions into the neuron in the direction of its electrochemical gradient. The influx of positive ions depolarizes the cell membrane, thereby activating voltage-gated calcium channels and stimulating

calcium-dependent release of neurotransmitters and neuropeptides. b) Archaerhodopsin is a yellow light (~589 nm) sensitive proton pump, and when photoactivated moves positively charged ions from the intracellular compartment to the extracellular space, resulting in a net hyperpolarization of the neuron. In this case, photoactivation of archaerhodopsin hyperpolarizes the axon terminals and prevents the opening of voltage-gated calcium channels, thereby inhibiting the release of neurochemicals.

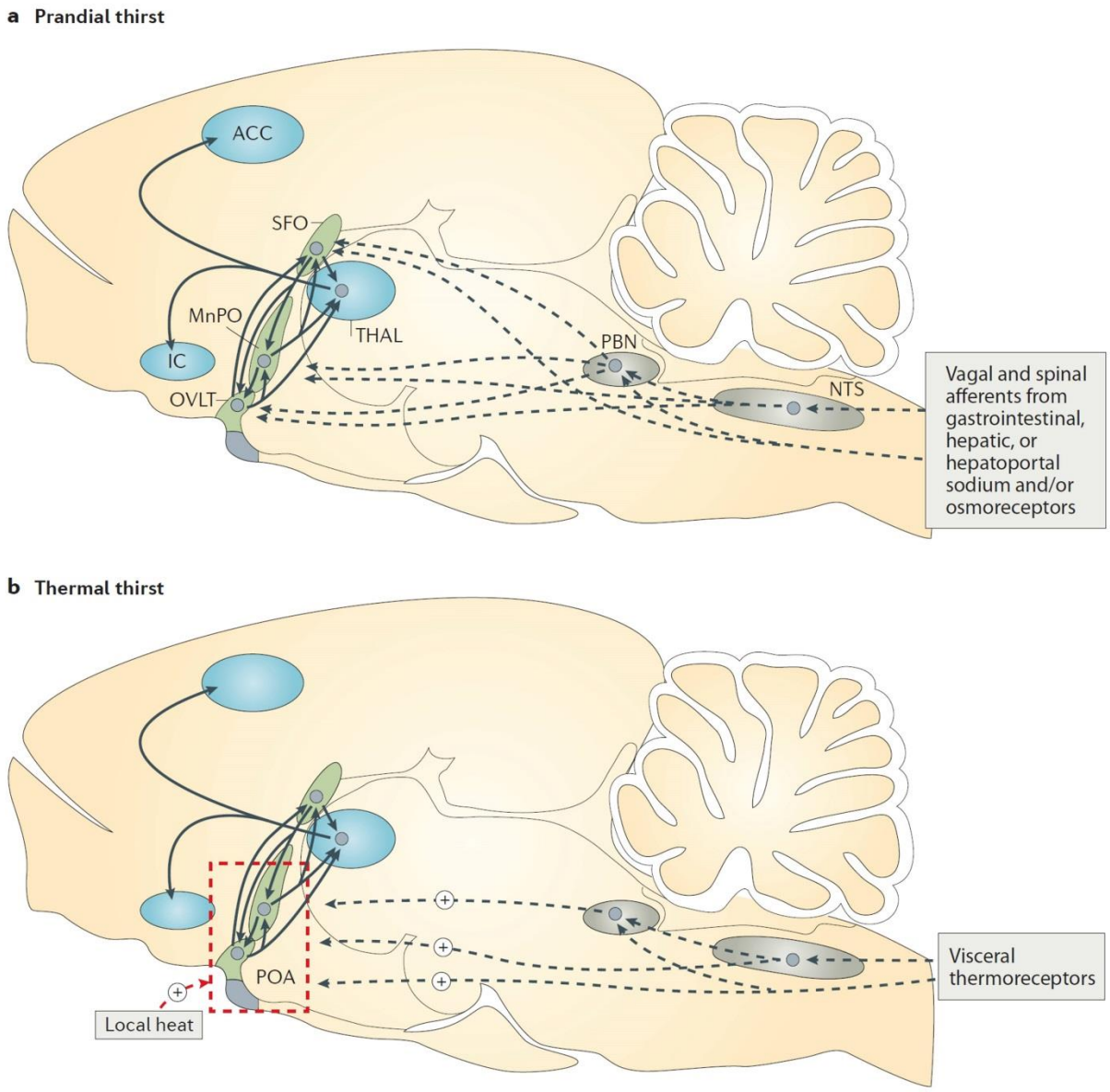

Figure 4. Neural pathways involved in the anticipatory stimulation of thirst during food intake and hyperthermia. a | Ingestion of solutes (such as salt or solid food) during a meal can provoke a marked increase in extracellular fluid (ECF) osmolality within minutes. Sensors that detect solutes within the stomach or duodenum can activate thirst-promoting brain regions, such as the median preoptic nucleus (MnPO), organum vasculosum laminae terminalis (OVLT) and subfornical organ (SFO) of the lamina terminalis, with subsequent actiation of the anterior cingulate cortex (ACC) and insular cortex (IC**)** via relay neurons in the medial parts of the thalamus (THAL), to stimulate prandial water intake and blunt this effect**. b** | Sustained increases in body temperature can lead to dehydration caused by evaporative water loss. Sensors of core body temperature in the

viscera project to the preoptic area (POA) via the nucleus tractor solitarius (NTS) and/or the parabrachial nucleus (PBN). Alternatively, the POA could potentially receive direct sensory inputs from visceral thermoreceptors, which encloses the OVLT and MnPO. Neurons in the POA are also temperature sensitive, and thus local activation of POA neurons due to intrinsic and synaptic responses could drive thirst via the activation of projections to the THAL–ACC/IC network.

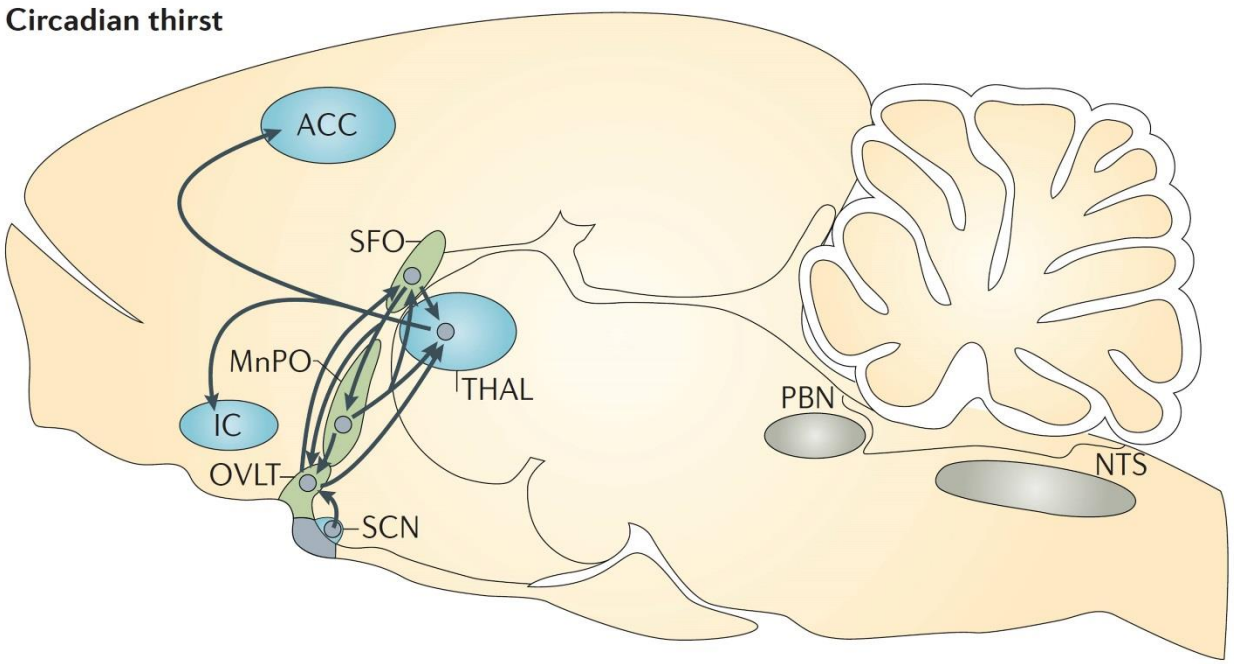

Figure 5. Circadian regulation of thirst. The circadian clock drives water intake prior to sleep to protect animals against overnight dehydration, which otherwise would occur due to the absence of water intake during sleep. **a** | Vasopressin-expressing neurons in the suprachiasmatic nucleus (SCN; the region of the brain that controls circadian rhythms) project to the OVLT. In mice, these neurons are suppressed during the active period but increase their firing rate toward the end of the active period. Vasopressin release at this time excites OVLT neurons to promote water intake ahead of a period of sleep during which no water intake occurs. ACC, anterior cingulate cortex; IC, insular cortex; MnPO, median preoptic nucleus; NTS, nucleus tractus solitarius; PBN, parabrachial nucleus; SFO, subfornical organ; THAL, thalamus.

Chapter 3 – Clock-driven vasopressin neurotransmission mediates anticipatory thirst prior to sleep

In section 1.2, I reference a quote that hypothesizes that water intake may be driven by a neural programmer with a circadian rhythm. Indeed, it has been shown that rats and mice display a robust daily pattern in water intake[323,325], and it has been proposed that the rise in water intake observed toward the end of the dark/active period rises in anticipation of the light onset. As mentioned in section 1.1.7, VP neurons in the SCN are thought to be the major output neurons. In section 1.2, I mention that the OVLT is a key central osmosensor and activation of these neurons are capable of driving water intake. There is also evidence suggesting the OVLT receives afferent input from the SCN[14]. Therefore, *I hypothesize that SCN^{VP} neurons drive an increase in the electrical activity of OVLT thirst neurons to drive an increase in water intake prior to sleep.* I performed 90% of the experiments and 80% of the writing.

Published in Nature, September 28, 2016

Clock-driven vasopressin neurotransmission mediates anticipatory thirst prior to sleep

C. Gizowski, C. Zaelzer, C. W. Bourque

Centre for Research in Neuroscience, Research Institute of the McGill University Health Centre, 1650 Cedar Avenue, Montreal, Canada, H3G 1A4

Circadian rhythms have evolved to anticipate and adapt animals to the constraints of earth's 24–hour light cycle[1]. Although molecular processes establishing periodicity in clock neurons of the suprachiasmatic nucleus (SCN) are well established, the mechanisms by which axonal projections from the central clock drive behavioural rhythms are unknown[2-4]. Here we reveal that the sleep period in mice (Zeitgeber time, ZT0–12) is preceded by an increase in water intake promoted entirely by the central clock, and not motivated by physiological need. Mice denied this surge experienced significant dehydration near the end of the sleep period, indicating this water intake contributes to the maintenance of overnight hydromineral balance. Furthermore, we show this effect relies specifically on the activity of SCN vasopressin (VP) neurons that project to thirst neurons in the OVLT (organum vasculosum lamina terminalis*)* where VP is released as a neurotransmitter. SCN VP neurons become electrically active during the anticipatory period (AP, ZT21.5–23.5), which depolarizes and excites OVLT neurons through the activation of postsynaptic VP V1a receptors (V1aR), and downstream non-selective cation channels. Optogenetic induction of VP release prior to AP (basal period, BP; ZT19.5-21.5) excited OVLT neurons and prompted a surge in water intake. Conversely, optogenetic inhibition of VP release during the AP inhibited the firing of OVLT neurons, and prevented the corresponding increase in water intake. Our findings reveal the existence of *anticipatory thirst,* and demonstrate this behaviour to be driven by excitatory peptidergic neurotransmission mediated by VP release from central clock neurons.

Nocturnal rodents display a surge in water intake prior to sleep[5,6]; however, whether the clock mediates this behaviour and serves an anticipatory physiological benefit remains to be determined. Water intake monitored in wild type (WT) mice confirmed that water intake increases significantly during the AP (ZT21.5–23.5) compared to the BP (ZT19.5–21.5; Fig. 1a, b). Increased intake during the AP was not motivated by physiological stimuli for thirst, such as hyperosmolality[7], increased core body temperature[8], or hypovolemia[9] (Fig. 1b). In addition, food

restriction throughout the BP–AP did not prevent a significant increase in water intake during the AP ($p<0.05$, n=8, paired t-test, data not shown), indicating increased water intake at this time does not simply reflect prandial drinking. These data suggest this behaviour is need-free, and may be driven directly by the central clock. To assess if this behaviour is physiologically relevant, we examined the impact of denying the water intake surge during the AP on serum osmolality and hematocrit measured near the end of the light period (ZT10; Fig. 1c). Animals subjected to this procedure displayed a significantly elevated serum osmolality and hematocrit, indicating a state of dehydration (Fig. 1d). These data indicate that increased water intake during the AP mitigates the impact of reduced water intake during sleep, and therefore serves an important homeostatic function.

Previous work established that the OVLT critically regulates water intake in mammals[10-12], and increased activity in this area orchestrates thirst perception in humans[13-15]. Due to the circadian nature of AP water intake[16,17], we hypothesized that this behaviour relies on connections between the SCN and OVLT. In support of this hypothesis, cell-attached recordings in slices of mouse hypothalamus that retain both nuclei (Extended Data Fig. 1, 2) revealed that the average firing rate and proportions of active OVLT neurons are significantly increased during the subjective AP compared to BP *in vitro* (Fig. 2a–c). Equivalent results were obtained in rat OVLT neurons (data not shown). In agreement with these observations, the density of OVLT neurons expressing c-Fos protein was increased during the AP compared to the BP in mice, providing *in vivo* support for increased neuronal activation (Fig. 2d). Anatomical studies have suggested that VP neurons in the shell of the SCN serve as major output cells of the clock[18-21]. We therefore examined if such neurons projected to the OVLT by injecting fluorescent microspheres into this nucleus (Fig. 2e, Extended Data Fig. 3). Confocal analysis of tissue sections obtained one week post-injection revealed the presence of microspheres in VP neurons in the shell of the SCN (Fig. 2f–h), but not in other regions containing VP neurons (Extended Data Fig. 3). Thus, the VP-containing fibers observed in the OVLT specifically emanated from SCN VP neurons (Extended Data Fig. 4). To determine if the activity of SCN VP neurons increased during the AP, we obtained visually guided cell-attached recordings from these neurons in slices prepared from mice in which fluorescent reporters are driven by the VP promoter (Fig. 2i, Extended Data Fig. 4). The data revealed that the average firing rate and proportions of active SCN VP neurons are significantly increased during the AP compared to the BP (Fig. 2j, k). Equivalent results were obtained in rat hypothalamic slices (data not shown).

In agreement with these *in vitro* data, the density of SCN VP neurons expressing c-Fos protein was increased during the AP compared to the BP *in vivo* (Fig. 2l).

The above findings suggest that the increased firing of OVLT neurons may rely on excitatory neurotransmission mediated by the increased activity of SCN VP neurons during the AP. To determine if VP is released within the OVLT, we examined the effects of SCN stimulation on the fluorescence of VP sensors plated over rat hypothalamic slices (Fig. 3a). These sensors consisted of HEK293 cells co-expressing the calcium indicator GCaMP6m[22] and the V1aR, which together promoted a dose-dependent calcium response to exogenous VP (Extended data Fig. 5). Electrical stimulation of the SCN significantly increased fluorescence in cells containing V1aRs, but not in the presence of the selective V1aR blocker, SR49059[23] (SR), or in HEK293 cells lacking V1aRs (Fig. 3a–c). Importantly, stimulation induced VP release was only observed in discreet regions of the slice (Extended Data Fig. 6), indicating that VP sensor activation over the OVLT did not result from volume transmission, but reflected local and activity dependent release at this site.

We next investigated the effects of SCN stimulation on OVLT neurons using whole cell voltage recordings. Electrical stimulation of the SCN (30 s at 10 Hz) caused a reversible depolarization and excitation of OVLT neurons in either mouse or rat hypothalamic slices (data not shown). These effects persisted during blockade of ionotropic glutamate and □-aminobutyric acid receptors (Fig. 3d, f), supporting our hypothesis that OVLT neurons may be directly depolarized and excited by a postsynaptic action of VP itself. Single−cell RT−PCR revealed that OVLT neurons express V1aRs (Extended Data Fig. 7); therefore, we examined if such receptors mediated these excitatory effects. Indeed, the effects of SCN stimulation were abolished by SR (Fig. 3e, f). Moreover, voltage clamp analysis revealed that SCN stimulation caused a V1aR dependent increase in membrane conductance associated with the appearance of an inward current reversing near –25 mV (Fig. 3g–i). The reversal potential of the current was unaffected by changes in the intracellular concentrations of potassium or chloride (Fig. 3j), indicating that VP released by the axon terminals of SCN neurons excites OVLT neurons by V1aR dependent activation of non-selective cation channels.

To determine if the increased firing rate of OVLT neurons during the AP is caused by the SCN–OVLT projection, we examined the impact of manipulating VP release using optogenetic approaches in mice expressing excitatory E123T mutant channelrhodopsin 2 (ChETA)[24], or

inhibitory archaerhodopsin-3 (ArchT)[25] driven by the VP promoter (Extended Data Fig. 4 and Extended Data Fig. 8). Application of blue light (473 nm) over the OVLT in hypothalamic slices prepared from ChETA mice caused VP release as measured by VP sensors (Fig. 4a–c). In agreement, blue light significantly increased the firing rate of OVLT neurons in ChETA preparations during the BP (Fig. 4d). Consistent with the involvement of VP release and V1aRs, the firing rate in the presence of blue light was significantly reduced by bath application of SR (Fig. 4d), but was unaffected by the selective V1bR antagonist SSR149415[26] (10 nM, n=24, $p>0.05$, Mann-Whitney, data not shown). Conversely, activation of ArchT with yellow light (589 nm) reduced the firing of OVLT neurons during the AP, and this effect was occluded and mimicked by SR (Fig. 4d). Taken together, these data support our hypothesis that increased OVLT firing during the AP is specifically dependent on postsynaptic V1aRs and VP release from the axon terminals of SCN VP neurons.

To further investigate the involvement of V1aRs in increasing the activity of OVLT neurons and water intake during the AP *in vivo*, additional experiments were performed on V1aR knockout ($V1aR^{-/-}$) mice. Although a rise in c-Fos expression was observed in SCN VP neurons of $V1aR^{-/-}$ mice during the AP (BP n= 11, AP n=12, $p<0.001$, Mann-Whitney, data not shown), this effect was absent in OVLT neurons (Fig. 4e). In agreement, $V1aR^{-/-}$ mice also failed to show an increase in water intake during the AP (Fig. 4f, Extended Data Fig. 7), indicating that V1aRs are necessary to activate OVLT neurons and generate this behaviour.

Finally, to determine if increased water intake during the AP is driven by the central clock, we examined the effects of optogenetically regulating VP release *in vivo* via light delivery through an implanted fiberoptic cannula targeting the OVLT (Extended Data Fig. 9). As in WT animals, implanted, but unphotostimulated ChETA and ArchT displayed significant increases in water intake during the AP (Extended Data Fig. 10). Application of blue light to the OVLT in ChETA mice, but not adjacent sites (Extended Data Fig. 9), significantly increased water intake when delivered during the BP, whereas yellow light had no effect (Fig 4g). Notably, water intake induced by blue light (0.50 ± 0.16 ml/hr) was equivalent to that observed during the AP in implanted but unstimulated ChETA mice (0.43 ± 0.09 ml/hr, $p>0.05$, Mann-Whitney, data not shown), suggesting light induced VP release is sufficient to cause a surge in water intake such as that observed during the AP. Conversely, application of yellow light to the OVLT abolished the water intake surge

observed during the AP in ArchT mice (Fig. 4h), indicating that VP released from the axon terminals of SCN neurons is necessary to drive *anticipatory thirst*.

Our study reveals that increased water intake during the AP is not motivated by physiological need, but anticipates and protects against the impact of overnight dehydration. How the central clock mediates adaptive behaviours of this kind was heretofore unknown. Our findings indicate that activity-dependent VP release from the axon terminals of clock neurons onto OVLT neurons is necessary and sufficient to generate *anticipatory thirst.* Whether the SCN drives other behaviours by VP neurotransmission remains to be determined.

Acknowledgements This work was supported by a Foundation Grant from the Canadian Institutes of Health Research (FDN 143337), a James McGill Chair, and a Studentship awarded by the Research Institute of the McGill University Health Centre (RIMUHC). The RIMUHC receives generous funding from the Fonds de Recherche Québec Santé. We would like to thank Dr. Michel Bouvier for supplying the human V1aR (Université de Montréal), and Dr. Hal Gainer for providing anti-VP neurophysin primary antibodies (National Institutes of Health). We would like to thank Drs. N. Cermakian, K-F. Storch, and M. Prager-Khoutorsky for constructive comments on an early draft of the manuscript.

Author Contributions C.G. and C.W.B. designed the study, interpreted the results, and wrote the manuscript. C.Z. contributed to experiments involving HEK cells and single cell RT PCR, C.G. performed all other experiments.

References

1 Mills, J. N. Human circadian rhythms. *Physiol Rev* **46**, 128-171, (1966).

2 Mohawk, J. A., Green, C. B. & Takahashi, J. S. Central and peripheral circadian clocks in mammals. *Annu Rev Neurosci* **35**, 445-462, (2012).

3 Hastings, M. H., Maywood, E. S. & O'Neill, J. S. Cellular circadian pacemaking and the role of cytosolic rhythms. *Curr Biol* **18**, R805-R815, (2008).

4 Antle, M. C. & Silver, R. Orchestrating time: arrangements of the brain circadian clock. *Trends Neurosci* **28**, 145-151, (2005).

5 Johnson, R. F., Beltz, T. G., Thunhorst, R. L. & Johnson, A. K. Investigations on the physiological controls of water and saline intake in C57BL/6 mice. *Am J Physiol Regul Integr Comp Physiol* **285**, R394-403, (2003).

6 Spiteri, N. J. Circadian patterning of feeding, drinking and activity during diurnal food access in rats. *Physiol Behav* **28**, 139-147, (1982).

7 Bourque, C. W. Central mechanisms of osmosensation and systemic osmoregulation. *Nat Rev Neurosci* **9**, 519-531, (2008).

8 Barney, C. C. & Folkerts, M. M. Thermal dehydration-induced thirst in rats: role of body temperature. *Am J Physiol* **269**, R557-564, (1995).

9 Fitzsimons, J. T. Angiotensin, thirst, and sodium appetite. *Physiol Rev.* **78**, 583-686, (1998).

10 Johnson, A. K. & Buggy, J. Periventricular preoptic-hypothalamus is vital for thirst and normal water economy. *Am J Physiol* **234**, R122-129, (1978).

11 McKinley, M. J., Denton, D. A. & Weisinger, R. S. Sensors for antidiuresis and thirst--osmoreceptors or CSF sodium detectors? *Brain Res* **141**, 89-103, (1978).

12 Ramsay, D. J., Thrasher, T. N. & Keil, L. C. The organum vasculosum laminae terminalis: a critical area for osmoreception. *Prog Brain Res* **60**, 91-98, (1983).

13 McKinley, M. J., Denton, D. A., Oldfield, B. J., De Oliveira, L. B. & Mathai, M. L. Water intake and the neural correlates of the consciousness of thirst. *Semin Nephrol* **26**, 249-257, (2006).

14 Farrell, M. J. *et al.* Cortical activation and lamina terminalis functional connectivity during thirst and drinking in humans. *Am J Physiol Regul Integr Comp Physiol* **301**, R623-631, (2011).

15 Hollis, J. H., McKinley, M. J., D'Souza, M., Kampe, J. & Oldfield, B. J. The trajectory of sensory pathways from the lamina terminalis to the insular and cingulate cortex; a neuroanatomical framework for the generation of thirst. *Am J Physiol Regul Integr Comp Physiol* **294**, R1390-1401, (2008).

16 Stephan, F. K. Circadian rhythms in the rat: constant darkness, entrainment to T cycles and to skeleton photoperiods. *Physiol Behav* **30**, 451-462, (1983).

17 Satinoff, E. & Prosser, R. A. Suprachiasmatic nuclear lesions eliminate circadian rhythms of drinking and activity, but not of body temperature, in male rats. *J Biol Rhythms* **3**, 1-22, (1988).

18 Kalsbeek, A. *et al.* SCN outputs and the hypothalamic balance of life. *J Biol Rhythms* **21**, 458-469, (2006).

19 Moore, R. Y., Speh, J. C. & Leak, R. K. Suprachiasmatic nucleus organization. *Cell Tissue Res* **309**, 89-98, (2002).

20 Abrahamson, E. E. & Moore, R. Y. Suprachiasmatic nucleus in the mouse: retinal innervation, intrinsic organization and efferent projections. *Brain Res* **916**, 172-191, (2001).

21 Buijs, R. M. & Kalsbeek, A. Hypothalamic integration of central and peripheral clocks. *Nat Rev Neurosci* **2**, 521-526, (2001).
22 Chen, T. W. *et al.* Ultrasensitive fluorescent proteins for imaging neuronal activity. *Nature* **499**, 295-300, (2013).
23 Serradeil-Le Gal, C. *et al.* Nonpeptide vasopressin receptor antagonists: development of selective and orally active V1a, V2 and V1b receptor ligands. *Prog Brain Res* **139**, 197-210, (2002).
24 Gunaydin, L. A. *et al.* Ultrafast optogenetic control. *Nat Neurosci* **13**, 387-392, (2010).
25 Han, X. *et al.* A high-light sensitivity optical neural silencer: development and application to optogenetic control of non-human primate cortex. *Front Syst Neurosci* **5**, 18, (2011).
26 Serradeil-Le Gal, C. *et al.* An overview of SSR149415, a selective nonpeptide vasopressin V(1b) receptor antagonist for the treatment of stress-related disorders. *CNS Drug Rev* **11**, 53-68, (2005).

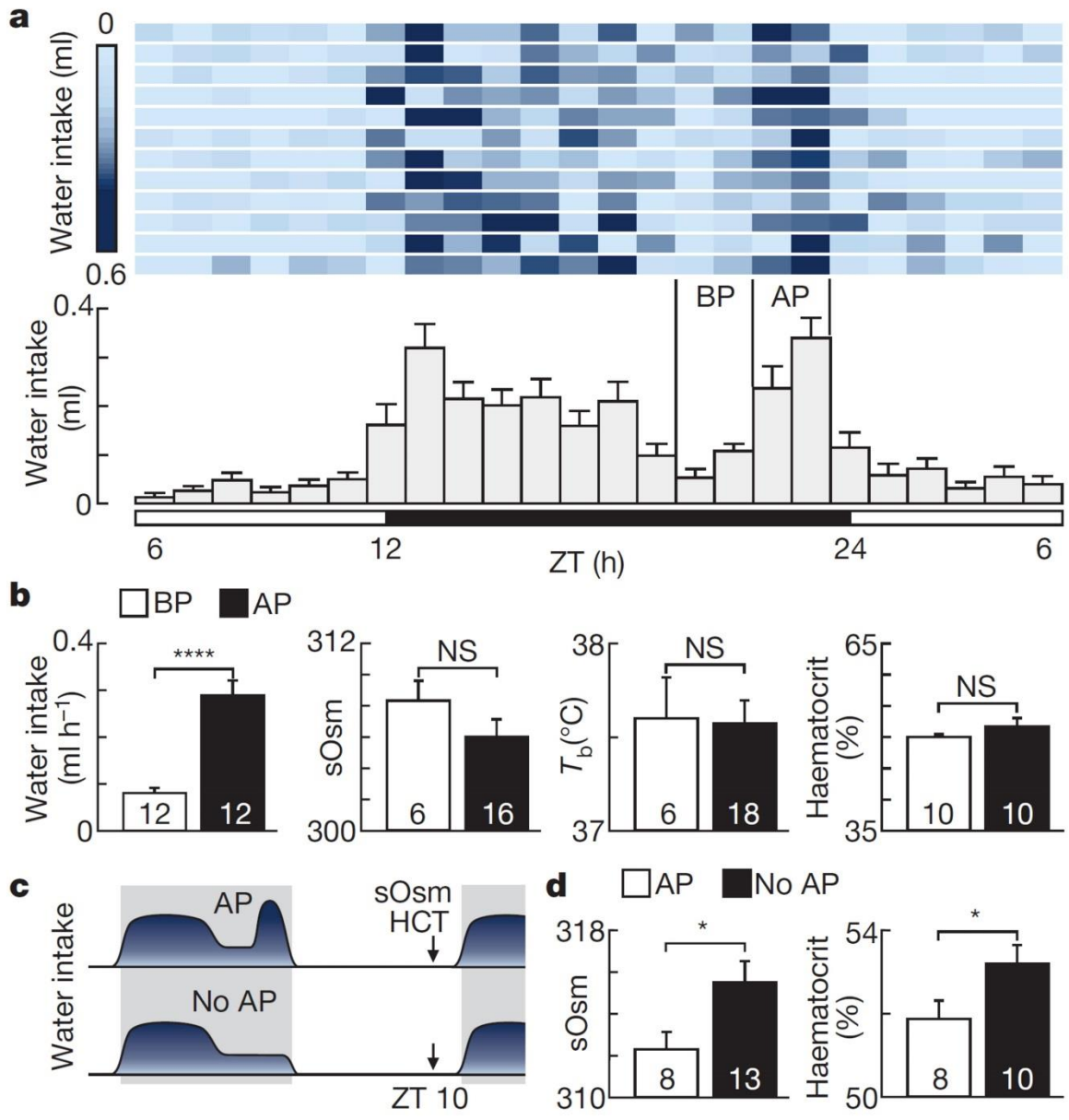

Figure 1 | Mice display anticipatory thirst during the AP. a, Raster plot shows daily water intake in 12 wild-type mice. Histogram plots mean ± s.e.m. water intake. b, Bar graphs compare water intake (****P < 0.0001, paired t-test) and physiological parameters during BP and AP (mean ± s.e.m.; serum osmolality, sOsm, t-test; core body temperature, Tb, t-test; volaemia, haematocrit, Mann–Whitney test; NS, P > 0.05). c, Schematic of protocol used to compare the impact of allowing (AP) or denying (No AP) water intake on serum osmolality and haematocrit at ZT10. d, Serum osmolality and haematocrit in mice subjected to protocol in c (mean ± s.e.m.; *P < 0.05, t-test). n as indicated

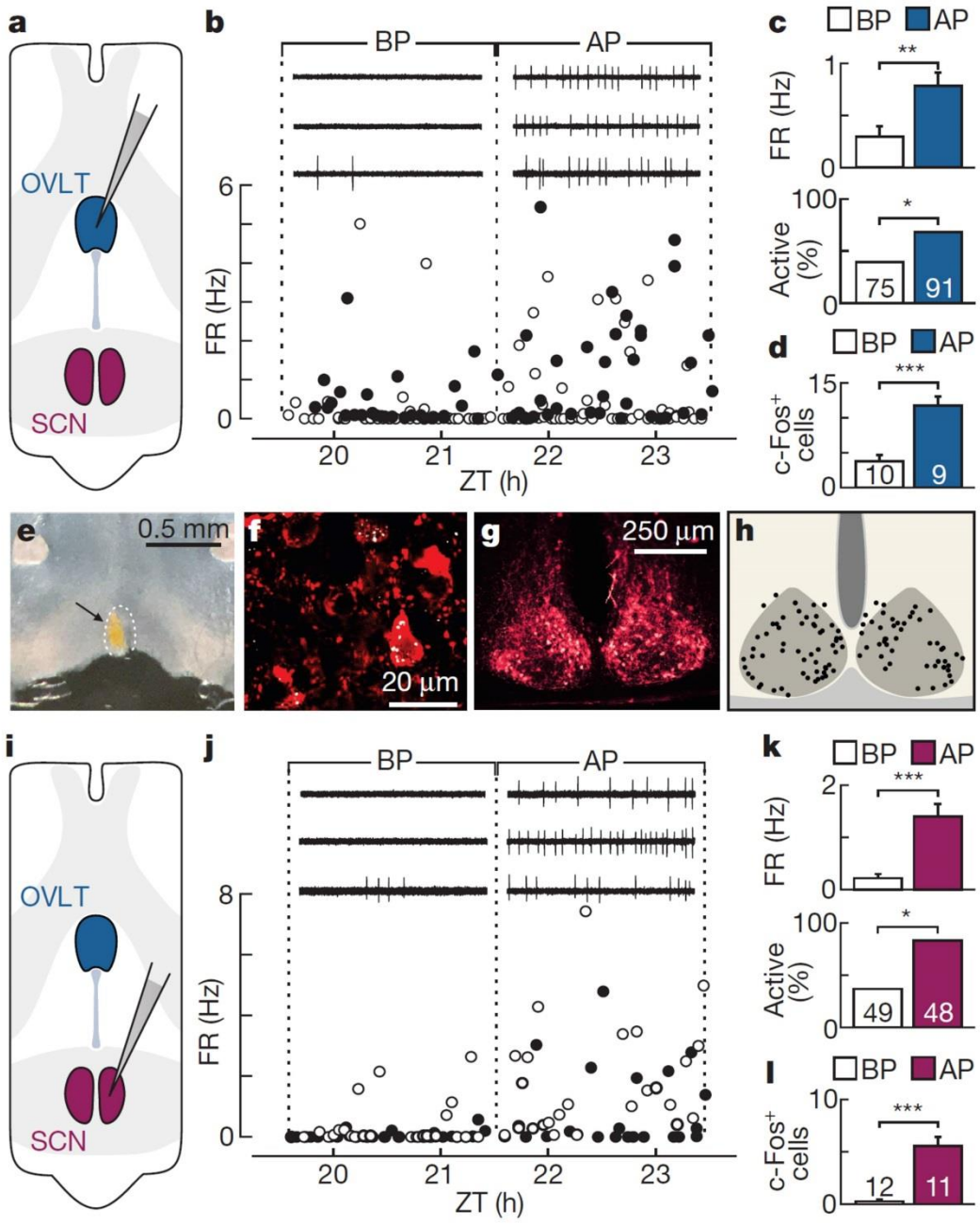

Figure 2 | OVLT and SCN VP neurons show increased activity during the AP. a, Schematic illustrating recording from OVLT neurons. **b**, Closed and opened circles plot firing rate (FR) of individual OVLT neurons in slices from ChETA and ArchT mice, respectively (5-s excerpts shown above). **c**, Plots show firing rate (mean ± s.e.m., Mann–Whitney test) and percentages of active cells ($\chi 2$ test; *P < 0.05, **P < 0.01). **d**, Number of c-Fos+ cells per section (mean ± s.e.m.; ***P < 0.001, Mann–Whitney test). **e**, Image of injection site (arrow) of microspheres into OVLT (dotted line). **f**, SCN VP neurons (red) containing microspheres (white). **g**, VP-labelled neurons in mouse

SCN. **h**, Positions of VP neurons containing microspheres (total of 109 cells from three separate experiments). **i**, Schematic illustrating recording from SCN VP neurons. **j**, Closed and open circles plot firing rate of individual SCN VP neurons in slices from ChETA and ArchT mice, respectively (5-s excerpts shown above). **k**, Plots show firing rate (mean ± s.e.m., Mann–Whitney test) and percentages of active cells ($\chi 2$ test). **l**, Number of c-Fos+ SCN VP neurons (mean ± s.e.m., Mann–Whitney test). n as indicated.

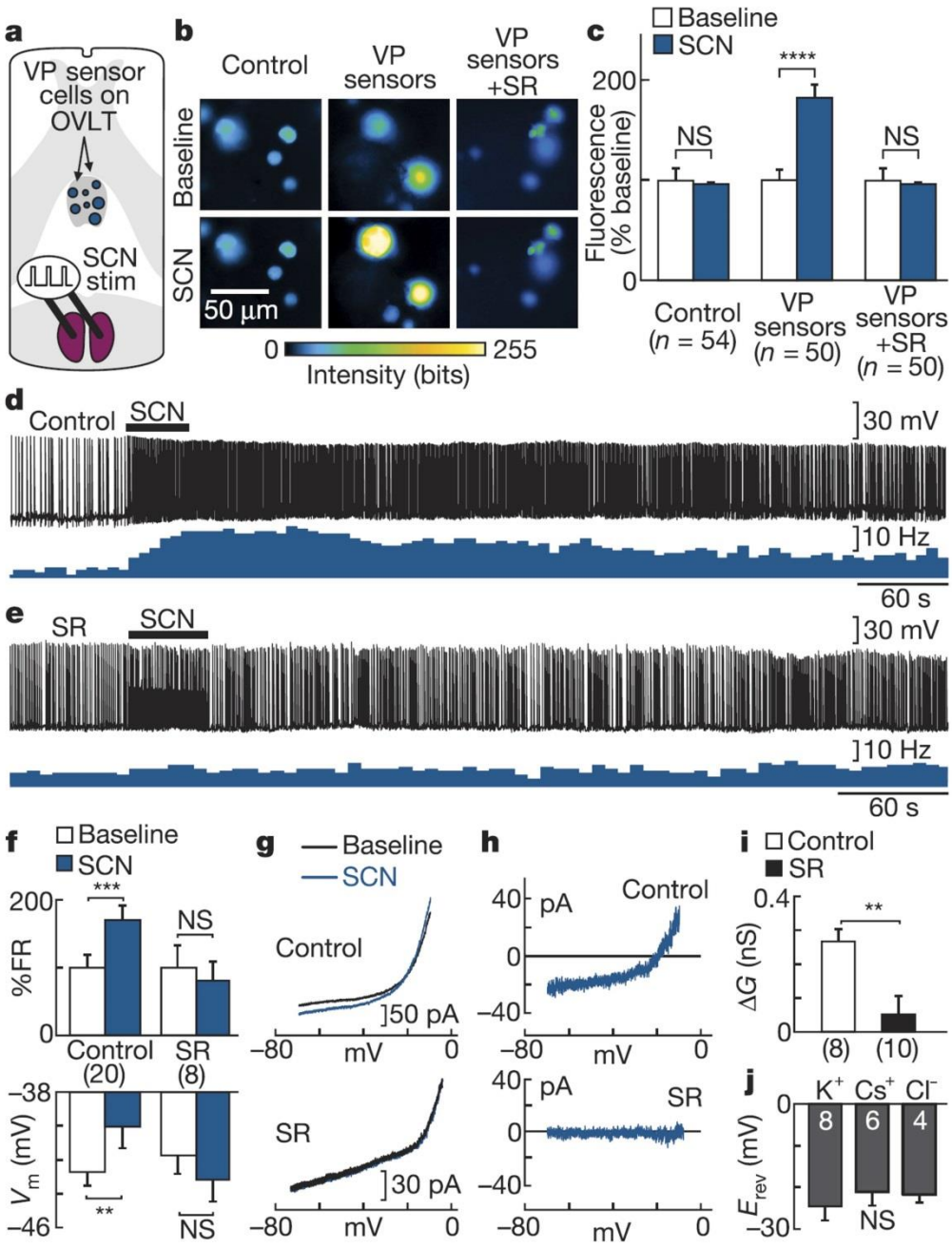

Figure 3 | VP released by SCN axon terminals excites OVLT neurons via non-selective cation channels. a, Schematic illustrating detection of SCN-mediated VP release in the rat OVLT. **b**, GCaMP6m fluorescence in HEK293 cells before (baseline) and after SCN stimulation (SCN; 40 s, 10 Hz). Control cells lack V1aR, VP sensors contain both GCaMP6m and V1aR, and VP sensors + SR are tested in the presence of SR49059 (10 µm). **c**, SCN stimulation-induced changes in

fluorescence (mean ± s.e.m.; ****P < 0.0001; NS, P > 0.05; paired t-test). Similar results were obtained in mouse Extended Data Fig. 6). **d**, Voltage response of OVLT neuron to SCN stimulation (bar; 30 s, 10 Hz) in the presence of kynurenate (3 mM) and bicuculline (10 μm). Lower trace shows firing rate. **e**, Recording from an OVLT neuron in the presence of SR49059 (with kynurenate and bicuculline), layout as in d. **f**, Firing rate expressed as percentage of respective baseline (%FR) before and after SCN stimulation (30 s, 10 hz) without (control) or with SR49059 (mean ± s.e.m., paired t-test). Lower graph shows corresponding changes in membrane voltage (Vm; control, Wilcoxon test; SR, paired t-test; **P < 0.01, ***P < 0.001). **g**, Steady-state current−voltage (I−V) relations in OVLT neurons before (baseline) and after (SCN) SCN stimulation in control conditions or with SR49059. **h**, Difference currents obtained from corresponding I−V curves in g. **i**, Mean ± s.e.m. change in membrane conductance (ΔG) caused by SCN stimulation in control conditions or with SR49059 (**P < 0.01, Mann– Whitney test). **j**, Reversal potentials (Erev) of SCN-induced currents measured with pipettes containing K+, Cs+, or high Cl− solutions (mean ± s.e.m., one-way ANOVA). n as indicated.

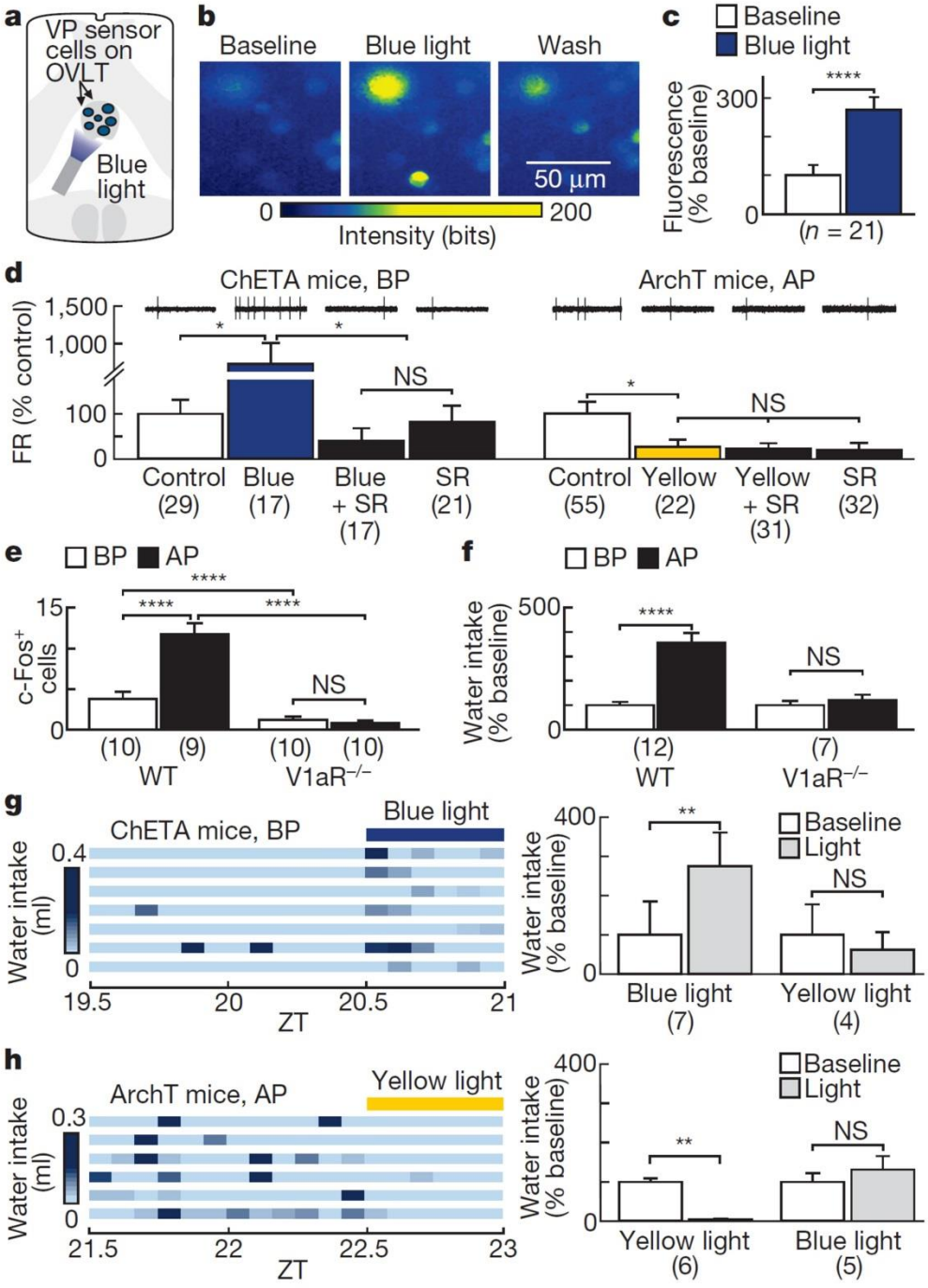

Figure 4 | Optogenetic and V1aR-dependent control of OVLT neuron firing and water intake. **a,** Schematic illustrating detection of light mediated SCN VP release in the OVLT. **b**, GCaMP6m fluorescence in VP sensors before (baseline) and after application of blue light (50 ms, 22 mW, 5 Hz, 30 s) and after wash. **c**, Changes in fluorescence induced by blue light (mean ± s.e.m.; ****P < 0.0001, paired t-test). **d**, Firing rate (mean ± s.e.m.) of OVLT neurons recorded in slices with or without light and/or SR49059 expressed as percent of average firing rate of control cells during BP

in ChETA mice (Kruskal–Wallis one-way ANOVA on ranks and Dunn's post-hoc test; *P < 0.05; NS, P > 0.05) or during AP in ArchT mice (control vs. yellow light, Mann–Whitney test; other comparisons, Kruskal– Wallis one-way ANOVA; 2-s excerpts shown above bars). **e**, Number of c-Fos+ OVLT cells in wild-type and V1aR−/− mice (mean ± s.e.m.; two-way ANOVA and Holm Sidak post-hoc test). **f**, Changes in the rate of water intake expressed as percent of average values in BP in wild-type and V1aR−/− mice (mean ± s.e.m.; paired t-test). **g**, Water intake (5-min bins) in seven trials from six ChETA mice in which blue light was applied at ZT20.5 (30 min, 22 mW). Changes in water intake induced by blue or yellow light (ZT20.5−21) expressed as percent of average intake during corresponding baselines (ZT19.5−20.5; mean ± s.e.m.; **P < 0.01; blue light, paired t-test; yellow light, Wilcoxon test). **h**, Water intake (5-min bins) in six trials from four ArchT mice in which yellow light was applied at ZT22.5 (30 min, 13 mW). Changes in water intake induced by yellow or blue light (ZT22.5−23) expressed as a percent of average intake during corresponding baselines (ZT21.5−22.5; mean ± s.e.m.; paired t-test). n as indicated.

Methods

Animals. Animals were treated in strict accordance with the guidelines outlined by the Canadian Council on Animal Care (http://www.ccac.ca/), and experiments adhered to protocols approved by the Facility Animal Care Committee of McGill University (protocol no. 1190). Long-Evans rats (80−50 g), and C57/B6 mice (60−90 d) were obtained from Charles River Laboratories, St−Constant, QC). VP-Cre (VP-IRES2-Cre-D) knock in mice were bred in our colony with either ChETA (R26-CAG-LSL-2XChETA-tdTomato) or ArchT mice (Ai40D; obtained from Jackson Laboratories, Bar Harbor, ME). V1aR knock out ($V1aR^{-/-}$) mice were bred in our colony (obtained from Jaqueline N. Crawley, National Institute of Mental Health, Bethesda, MD)[27]. All experiments were performed on male animals, except for one experiment (Extended Data Fig. 8) where a female was used. *In vitro* experiments were performed on mice aged 2−4 months, experiments on rats were done on animals weighing 80−150 g, and *in vivo* mouse experiments were done on animals aged 2−3 months. Animals were subjected to a strict 12:12 light:dark cycle.

Water Intake Monitoring. C57/B6 mice were individually housed in computer interfaced metabolic Oxylet cages from PanLab (Harvard Apparatus, St−Laurent, QC) to measure water intake. Animals were placed in cages and allowed to habituate to the cages for 4−6 days. To obtain the average circadian profile of water intake, we obtained hourly averages from each subject between ZT6.5 to ZT6.5 on the following day. Data files were analyzed using Metabolism (version 2.1.04; PanLab) and Microsoft Excel. Statistical analysis was performed in Sigmaplot (Version 12.3, Systat Software, Inc., Chicago, IL).

Physiological Parameters. Since we cannot obtain serial measures of serum osmolality in individual C57/B6 mice, we used a group approach whereby data were collected from multiple (3−9) subjects that were sacrificed at each time point tested. To this end, mice were anesthetized with isoflurane and rapidly decapitated to obtain blood samples, core body temperature using a digital thermometer, and hematocrit using a ZipCombo Centrifuge from LW Scientific Lawrenceville, GA). Blood samples were placed on ice and allowed to clot in 2−4°C for 60 minutes, after which they were centrifuged for 5 minutes, and serum osmolality was measured in duplicate using a micro-osmometer (Advanced Instruments Inc., Norwood, ME).

Water Restriction. The objective of this experiment (Fig. 1c, d), was to deny the surge in water intake, while preserving water intake levels during the AP equivalent to levels during the BP. Because water intake between ZT21.5-22.5 is equivalent to water intake from ZT19.5-21.5 (BP), we allowed water intake to proceed until ZT22.5 before removing access to water. Water was removed from C57/B6 mouse cages at either ZT22.5 (No AP surge allowed) or ZT23.5 (AP surge allowed). Access to water overnight was denied to prevent compensatory drinking and allow a specific evaluation of the impact of the AP surge alone. Animals were then sacrificed at ZT10 whereby blood samples were collected to measure serum osmolality and hematocrit as explained above.

OVLT Firing Rate. Horizontal hypothalamic slices containing the OVLT and SCN were prepared from 2−4 months male ArchT or ChETA mice. These animals were not subjected to any behavioural or optogenetic experiments prior to slice preparation. Mice anesthetized with isoflurane were killed by decapitation at ZT18-18.5. The brain was rapidly removed and immersed in near freezing (0 to 4°C) oxygenated (95% O_2, 5% CO_2) artificial mouse cerebrospinal fluid (AMCSF) composed of the following (in mM): 128 NaCl, 3 KCl, 1.23 NaH_2PO_4, 1.48 $MgCl_2$, 2 $CaCl_2$, 25.95 $NaHCO_3$ and 10 D-glucose (all obtained from Sigma Chemical Corp., St-Louis, MO, except for NaCl and $CaCl_2$, which were purchased from Fisher Scientific, St-Laurent, QC). A trimmed block of brain was glued cortex down with the rostral pole facing upwards to a mounting block angled 34° relative to the horizontal plane. A single 350-μm slice was then obtained (Extended Data Fig. 2) and transferred dorsal side up to a beaker containing warmed (32 °C) oxygenated AMCSF and allowed to incubate for 60 min. It was then transferred dorsal side up to a recording chamber where it was perfused with warmed (32 °C) oxygenated AMCSF at a rate of 2–3 ml min^{-1}. Cells were observed on a black and white monitor using an Olympus BX51WI upright microscope coupled to a video camera. Electrodes were visually guided to the cell using a motorized micromanipulator (SD Instruments Inc., Grants Pass, OR) and cell-attached recordings were made using a MultiClamp 700B amplifier (Molecular Devices Corp., Sunnyvale, CA). Membrane voltage was digitized via a Digidata 1440A interface coupled to a personal computer running Clampex 10.3 software (Molecular Devices). A bandpass filter was applied during cell-attached recordings (800 Hz–1.8

kHz). Patch pipettes were back filled with AMCSF and their resistance in the bath were 5.5−7.5 MΩ. Cell-attached recordings for firing rates of OVLT neurons during the BP were performed from ZT19.5−21.5 and AP period were from ZT21.5−23.5. Cell-attached recordings from OVLT neurons were obtained by making a loose seal. If cells did not fire during the recording, a brief zap of 25 μs was delivered at the end of the recording to evoke firing in order to confirm they were indeed silent cells that were otherwise capable of firing detectable action potentials. The average firing rate was calculated by dividing the total number of spikes recorded over a period of 60 s. One cell was excluded from this analysis because its firing rate was more than 4 times greater than the standard deviation of the group.

Evans blue injection. Evans blue was used to evaluate the boundaries of the OVLT in mice as previously reported for rat[28]. Briefly, mice were anesthetized with isoflurane and injected intravenously with 0.2 ml of 1% Evans blue dissolved in phosphate buffered saline (PBS). After 15 min, the animals were transcardially perfused with 20 ml PBS, and then the brain was extracted and fixed by immersion for at least 48 h in 4% paraformaldehyde (PFA) dissolved in PBS. Serial sections (50 μm thick) were cut and mounted onto slides, and Evans blue fluorescence was visualized using RS Image (version 1.9.2; Roper Scientific, Planegg, DE) using a 10X objective (na=0.4) attached to an Olympus BX51WI upright microscope (Richmond Hill, ON), and a CoolSnap HQ^2 camera (Photometrics, Tucson, AZ). Fluorescence was observed at 700 nm and excited at 650 nm using an X-Cite XLED1 system (Lumen Dynamics, Excelitas Canada Inc., Montreal, QC) and a BrightLine Pinkel filter set (DA/FI/TR/Cy5-4X-B-OMF; Semrock, Inc., Rochester, NY).

Retrograde fluorescent microspheres. C57/B6 mice (60 d) were anesthetized with isoflurane and stereotaxically injected with FluoSpheres (0.04um, yellow-green fluorescent 488 nm, 5% solids, azide free, ThermoFisher Scientific, Waltham, MA) into the OVLT (100−200 nl; from Bregma with a 7° vertical angle, X: 1.2 mm, Y: 0 mm, Z: -4.6 or -4.7; Extended Data Fig. 3) with a Neuros syringe (0.5 μL, 32 gauge, Hamilton Co., Reno, NV) over 5−10 minutes. The spheres were allowed to be retrogradely transported for 7 days, after which the animals were anesthetized with isoflurane and perfused via the heart with 10 ml of PBS followed by 300 ml of PBS containing 4% PFA. The

brains were extracted and postfixed by immersion for 48 h in 4% PFA in PBS. A vibratome was used to obtain serial coronal tissue sections (50 µm thick). Sections were blocked with 10% normal goat serum (in PBS containing 0.3% Triton-X) and incubated overnight at 4°C with primary antibodies. Following wash, sections were incubated for 1 h with fluorescently labeled secondary antibodies. Sections were then washed and mounted on coverslips using Prolong Gold Antifade reagent (Life Technologies, Carlsbad, CA). All images were acquired using a confocal microscope (FV1000, Olympus Canada). The following primary antibodies were used: PS41 anti-VP neurophysin mouse monoclonal antibody (1:50), and VA4 anti-VP neurophysin rabbit polyclonal antibody (1:1000) developed and generously contributed by Hal Gainer (National Institutes of Health, Bethesda, MD). Secondary antibodies were fluorescently labeled Alexa Fluor-conjugated [568 nm, and 647 nm; (Life Technologies; 1:500)].

c-Fos analysis. Brains were extracted from WT and V1aR$^{-/-}$ mice at ZT21.5-22 (for BP analysis) and ZT23.5-24 (for AP analysis) and immersion fixed in 4% PFA. Tissue sections (50 µm thick) from WT and V1aR$^{-/-}$ mice were processed using a rabbit polyclonal c-Fos antibody (EMD Millipore, Billerica MA; 1:5000) together with a chicken anti-NeuN (Hexaribonucleotide Binding Protein-3a) polyclonal antibody (ABN91, 1:500; EMD Millipore; in OVLT), or with PS41 (as above) in the SCN. Secondary antibodies were fluorescently labeled Alexa Fluor-conjugated [488 nm, 568 nm, and 647 nm; (Life Technologies; 1:500)]. Cells were considered c-Fos positive if they were >100% above background. For OVLT analysis, cells were counted in a 200 x 200 µm field centered over the nucleus. For SCN, density was assessed over the entire nucleus. Ns refer to the number of sections analyzed, and were obtained from 2 animals in each group.

SCN Firing Rate. Coronal 300-µm slices were obtained from mouse brain as described above. These animals were not subjected to any behavioural or optogenetic experiments prior to slice preparation. Cell-attached recordings were obtained from visually identified fluorescent VP cells (see extended data Figure 4). Green fluorescence in ArchT mice was detected using EN GFP 41017 filter cube (Chroma Technology Corp., Bellows Falls, VT) and red fluorescence in ChETA mice was detected using 49004 (Chroma Technology Corp., Bellows Falls, VT). Firing rate was assessed

as explained in "OVLT firing rate". One cell was excluded from this analysis because its firing rate was more than 4 times greater than the standard deviation of the group.

Rat Hypothalamic Slices. Horizontal hypothalamic slices were obtained from male rats as previously described[29]. Briefly, rats were killed by decapitation using a small rodent guillotine. The brain was rapidly removed and immersed in near freezing (0 to 4 °C) oxygenated (95% O_2, 5% CO_2) artificial rat cerebrospinal fluid (ARCSF) composed of the following (in mM) 120 NaCl, 3 KCl, 1.23 NaH_2PO_4, 1.48 $MgCl_2$, 2 $CaCl_2$, 25.95 $NaHCO_3$ and 10 D-glucose. A trimmed block of brain was glued cortex down with the rostral pole facing upwards to a mounting block angled 38° relative to the horizontal plane. The assembly was then placed in a vibratome and a first cut was made to discard the tissue lying anterior and ventral to the optic tracts and most of the optic chiasma. A single 400-µm slice was then obtained and transferred dorsal side up to a beaker containing warmed (32 °C) oxygenated ARCSF and allowed to rest for 60 mins. Slices were then placed in a warmed (32 °C) recording chamber perfused at a rate of 2–3 ml min^{-1}.

VP Detection with HEK293 Biosensors in Rat Brain slices. HEK293 cells were kept on DMEM media (Wysent) at 37°C and 5% CO_2. The co-transfection of pGP-CMV-avp 6m (AddGene, Cambridge, MA) and the human V1aR (provided by Dr. Michel Bouvier, University of Montreal, QC) (2.5 µg each) was done using Lipofectamine 3000 (Invitrogen). 24 to 48 hours after transfection the cultures were treated with trypsin, cells were lifted and plated over recently cut rat horizontal brain slices resting in beakers as explained above. Preparations were allowed to rest for 2 hours, allowing cells to attach to the slice prior to starting the experiment. Experiments were completed during the subjective BP (ZT19.5−21.5) when VP release was low. Slices were carefully placed in the recording chamber, and a bipolar electrical stimulating electrode (pair of 65 µm o.d. platinum wire) was placed in the SCN. Electrical pulses (20–80 µA, 0.1−0.5 ms; 10 Hz, 40 s) were delivered via an isolated stimulator (DS2, Digitimer Ltd., Welwyn Garden City, UK) triggered via a programmable digital timer (D4030, Digitimer). Fluorescence of GcaMP6m in HEK293 cells was observed using the EN GFP 41017 filter cube. Images were collected using Imaging Workbench 6.0 (INDEC BioSystems, Santa Clara, CA) at a rate of 1 image every 5 s (exposure 0.2 s). In control conditions, only pGP-CMV-GcaMP6m was transfected and not V1aR. Dose response analysis and

specificity were assessed on HEK293 cells plated on glass coverslips (Extended Data Fig. 5). VP dissolved in water (0.1 mM) was kept frozen until required. All images were analyzed using Fiji[30]. Fluorescence in regions of interests (HEK cells) was corrected for bleaching determined by fitting a single exponential. Background fluorescence was subtracted from all values. Values of fluorescence at various time points were expressed relative to baseline. Changes in fluorescence relative to baseline (average of 30 s before stimulation) were determined from the average of values observed during a 30 s period following the onset of the response.

Electrophysiological Analysis of Rat Brain Slices. Slices were obtained as mentioned above. Bicuculline (Bic) was dissolved directly into the ARCSF at the required concentration (10 μM). Kynurenate (Kyn) was first dissolved into a small volume (<0.5 ml) of 1 N NaOH and subsequently diluted into a larger volume of ARCSF at the required concentration (3 mM). All whole-cell experiments were performed in the presence of Kyn and Bic. All recordings were made during subjective night (ZT5−11). Whole-cell recordings from OVLT neurons were made using patch pipettes prepared from glass capillary tubes (1.2-mm outer diameter, A-M Systems, Sequim, WA) filled with the appropriate internal solution. Pipette resistance in the bath was 3.5−5.5 MΩ. Series resistance was 10−30 MΩ. A bipolar stimulating electrode was placed in the SCN at the beginning of each recording session. Electrical pulses (20–80 μA, 0.1−0.5 ms; 10Hz, 30s) were delivered as described above. For gap-free whole cell current clamp recordings, pipettes were back-filled with a solution containing the following (in mM) 140 K^+-gluconate, 2 $MgCl_2$, 10 HEPES, 2 ATP(Na_2), 0.4 GTP(Na_2) (pH adjusted to 7.25 with NaOH). Baseline average firing rates were calculated over a window of 60 s immediately preceding SCN stimulation, and the corresponding voltage was obtained from the peak of an all-points voltage histogram. SCN stimulation evoked firing rates were calculated over a window of 60 s during the maximal firing response within 2 min of the end of stimulation. Post-stimulation voltage was obtained during the corresponding period. Current clamp analysis (Fig. 3f) was restricted to cells maintained by current injection between -35 to -50 mV (values not corrected for liquid junction). Aliquots of SR49059 dissolved in DMSO (10 mM) we diluted into ARCSF to achieve a final concentration of 10 μM. For whole-cell voltage clamp experiments, steady state current-voltage (I−V) relations were obtained from the current responses induced by slow voltage ramps (−110 to +10 mV; 2s, V_h −50mV). Pipettes were backfilled with solutions corresponding to the experiment in question. K^+ internal solutions were composed of the

following (in mM): 140 K^+-gluconate, 2 $MgCl_2$, 10 HEPES, 2 ATP(Na_2), 0.4 GTP(Na_2) and 5 QX314-Br (pH adjusted to 7.25 with NaOH). Cs^+ internal solutions were composed of the following (in mM): 140 CsMeS, 10 HEPES, 2 $MgCl_2$, 2 ATP(Na_2), 0.4 GTP(Na_2) and 5 QX314-Br (pH adjusted to 7.25 with NaOH). Cl^- internal solutions were composed of the following (in mM): 100 CsMeS, 40 CsCl, 10 HEPES, 2 $MgCl_2$, 2 ATP(Na_2), 0.4 GTP(Na_2) and 5 QX314-Br (pH adjusted to 7.25 with NaOH). Currents induced in OVLT neurons induced by SCN stimulation were evaluated as the difference current obtained by subtracting the average of two I−Vs taken 1 min after SCN stimulation from the average of two I−Vs recorded preceding SCN stimulation. When required, a low pass filter was applied to the difference current trace (lowpass 80−200 Hz). SCN induced changes in membrane conductance were quantified as the slope of the difference current I−V, measured over a range of 20 mV below the reversal potential. In the analysis of Fig. 3i, and j, 2 cells were excluded because SCN induced currents did not show a reversal potential.

VP Detection Using Biosensors in Mouse Brain Slices. VP release caused by light induced depolarization of SCN VP axon was performed using co-transfected HEK293 cells prepared as described above, in horizontal slices prepared from ChETA mice. Blue light (473 nm DPSS Laser system, Laserglow Technologies, Toronto, ON) was delivered over the OVLT (50 ms, 22 mW, 5 Hz) for 30 s through a fiberoptic probe (slim titanium magnetic receptacle, 200 µm fiber optic diameter/240 µm diameter with coating/5.5 mm length numerical aperture 0.22, Doric Lenses, Quebec, QC), connected to a mono fiberoptic patchcord (2 m) via a fiberoptic rotary joint.

Optogenetic Manipulation of OVLT neuron firing. Horizontal slices were prepared from either ChETA or ArchT mice. Cell-attached recordings were performed as previously described. Blue light was delivered over the OVLT as previously described (50 ms, 22 mW, 5 Hz) for 30−60 s in ChETA slices during BP (ZT19.5−21.5). Additional light intensities were used to determine threshold sensitivity (Extended Data Fig. 9). Yellow light (589 nm, 13 mW, constant light, DPSS laser system, Laserglow Technologies) was delivered over the OVLT in ArchT slices during the AP (ZT21.5−23.5). SR (10 µm) was bath applied during experiments as noted. Firing rates were calculated by counting the number of spikes during 30−60 s. Firing rates were normalized to the average baseline firing of the time period in question.

Optogenetic Manipulation of SCN neuron firing. Coronal slices were prepared from either ChETA or ArchT male or female mouse brains. Cell-attached recordings were performed on identified VP neurons as previously described. Once sufficient baseline was recorded (2-3 min), either blue light (for ChETA) or yellow light (for ArchT) was delivered to the slice. Analysis of light induced changes in firing rate was performed by comparing firing rates averaged during 30−60 s periods recorded before and during light stimulation.

In Vivo Optogenetics. ChETA and ArchT male mice (60–90 d) were stereotaxically implanted with a slim magnetic receptacle fiberoptic cannulas (5.5 mm, Doric Lenses) above the OVLT (from Bregma with a 7° vertical angle, X: 1.18 mm, Y: 0 mm, Z: –4.5[31]). Cannulas were initially glued to the brain using Metabond (C&B Metabond, Parkell Inc., Edgewood, NY), allowed to dry, then covered with a generous coat of dental cement (Stoelting Co., Wood Dale, IL). Animals recovered for 7 days, after which they are handled for one week to allow habituation to handling and to the fiberoptic patchcord. For testing, animals are placed in metabolic cages on Thursday afternoons. On Mondays, the animals were trained by being connected to the patchcord during the appropriate test period (2.5 hr), 1 hour post-handling rest, 1 hour baseline, 30 min test. Actual testing started on the following Tuesday. ChETA mice were tested from ZT 18.5−21, and ArchT mice were tested from ZT 20.5−23. During the test period they either received blue light (either 22 mW continuous or 50 ms, 22 mW, 5 Hz), or yellow light (13 mW continuous) on separate days. Water intake analysis is performed as described above. Following the last day of testing, animals were anesthetized and decapitated. Optical implants were removed and brains were fixed by immersion for at least 48 h in 4% PFA dissolved in PBS. Serial coronal sections (50 µm thick) were cut to determine the position of the tip of the fiberoptic cannula. Experiments were rejected if the fiberoptic tip terminated rostral or caudal to the OVLT, or more than 200 µm dorsal from the dorsal surface of the OVLT.

Characterization of Transgene Expression in VP Neurons. Serial coronal sections (50 µm thick) were cut from an ArchT brain to analyze the expression of GFP in VP neurons. Sections were processed for 90mmune histochemistry as described above. A chicken anti-GFP primary antibody

(1:1000, AB13970, Abcam Inc., Toronto, ON) was used to enhance detection of the fluorescence reporter and the PS41 mouse monoclonal anti-VP neurophysin antibody (1:50; Hal Gainer, NIH[32,33]) was used to detect VP. Secondary antibodies were fluorescently labeled Alexa Fluor-conjugated [568 nm, and 647 nm; (Life Technologies; 1:500)]. Images were analysed using ImageJ 1.50a (NIH, Bethesda, MD) to count the number of VP labeled SCN neurons and anti-GFP labeled SCN neurons.

Single Cell RT-PCR. As previously described[34], Single OVLT neurons were aspirated from the slice using large autoclaved micropipettes (1−2 MW), which were backfilled with 1.5 µl of a solution containing RnaseIN (10 U/µl; Life Technologies). Upon contact and gigaseal formation, cells that fired action potentials (neurons) were sucked by negative pressure to collect cytoplasm, then lifted and completely suctioned into the electrode. The contents were then expelled by positive pressure into a 250-µl microcentrifuge tube containing 0.5 µl Dnase I (1 U/µl; Fisher Scientific) and 1× $MgCl_2$ buffer and stored over dry ice. Tubes were incubated at 37 °C for 30 min, and the reaction was stopped by adding 1 µl EDTA (25 mM) and incubated at 65 °C for 10 min. The RT reaction was then performed by adding 1 µl 50 µM Random Hexamer primers (Life Technologies), 0.25 µl RnaseIN (10 U/µl), 1 µl 0.1M DTT, 1 µl 50 mM MgCl2, 1 µl 10 mM (each) dNTPs mix (QIAGEN, Hilden, DE), 2 µl 5× First Strand Buffer, and 0.25 µl SuperscriptIII (200 U/µl; ThermoFisher). The mix was incubated at 50 °C for 2 hr and then the cDNA was stored at −20°C. Nested PCR and nested multiplex single-cell PCR were performed using the following primers:

Avpr1a ForOUT3	5’ATCCCATCCAAAACCACTCTGAGCG 3’
Avpr1a RevOUT3	5’GGTAACACTTGGAAGAAGGCGACCG 3’
Avpr1a ForIN3	5’GAAGAGAGCGAGGTAAGGAAGGACGG 3’
Avpr1a RevIN3	5’TGCGGGATGTCTTGCGTGGC 3’
V1v ForOUT	5’ATGTGGTAGACATGAGGGAGCTAGAGGC 3’
V1v RevOUT	5’AATCTTCCCACTGCTGGCAGCC 3’
V1v ForIN	5’TCCAGGGACTAGCCTCATTGGTGGG 3’
V1v RevIN	5’TGAGTTCTTCTAGCTTCAGTGTGGGGTG 3’

PCR amplicons were analyzed on 2.5% agarose.

Statistical analysis.

All group data are reported or displayed as means ± s.e.m. and the exact sample size is provided for each experimental group or condition either in the text or as indicated within or below bar graphs. Information about sample collection is also provided where relevant (e.g. number of trials per animals, or sections per brain). Differences between groups (two-sided) were compared using Sigmaplot 12.0 (Systat Software, Inc., San Jose, CA). The software first assessed normality of the data distribution. In all cases where the normality test failed, a suitable non-parametric test was performed. All tests used for comparisons are specified in the text.

References

27 Hu, S. B. *et al.* Vasopressin receptor 1a-mediated negative regulation of B cell receptor signaling. *Journal of Neuroimmunology* **135**, 72-81, (2003).

28 Prager-Khoutorsky, M. & Bourque, C. W. Anatomical organization of the rat organum vasculosum laminae terminalis. *Am J Physiol Regul Integr Comp Physiol* **309**, R324-337, (2015).

29 Trudel, E. & Bourque, C. W. A rat brain slice preserving synaptic connections between neurons of the suprachiasmatic nucleus, organum vasculosum lamina terminalis and supraoptic nucleus. *J Neurosci Methods* **128**, 67-77, (2003).

30 Schindelin, J. *et al.* Fiji: an open-source platform for biological-image analysis. *Nature Methods* **9**, 676-682, (2012).

31 Franklin, K. B. & Paxinos, G. *The mouse brain in stereotaxic coordinates*. Third edn, 1-364 (Elsevier, 2008).

32 Altstein, M. & Gainer, H. Differential biosynthesis and posttranslational processing of vasopressin and oxytocin in rat brain during embryonic and postnatal development. *Journal of Neuroscience* **8**, 3967-3977, (1988).

33 Altstein, M., Whitnall, M. H., House, S., Key, S. & Gainer, H. An immunochemical analysis of oxytocin and vasopressin prohormone processing in vivo. *Peptides* **9**, 87-105, (1988).

34 Zaelzer, C. *et al.* DeltaN-TRPV1: A Molecular Co-detector of Body Temperature and Osmotic Stress. *Cell Reports* **13**, 23-30, (2015).

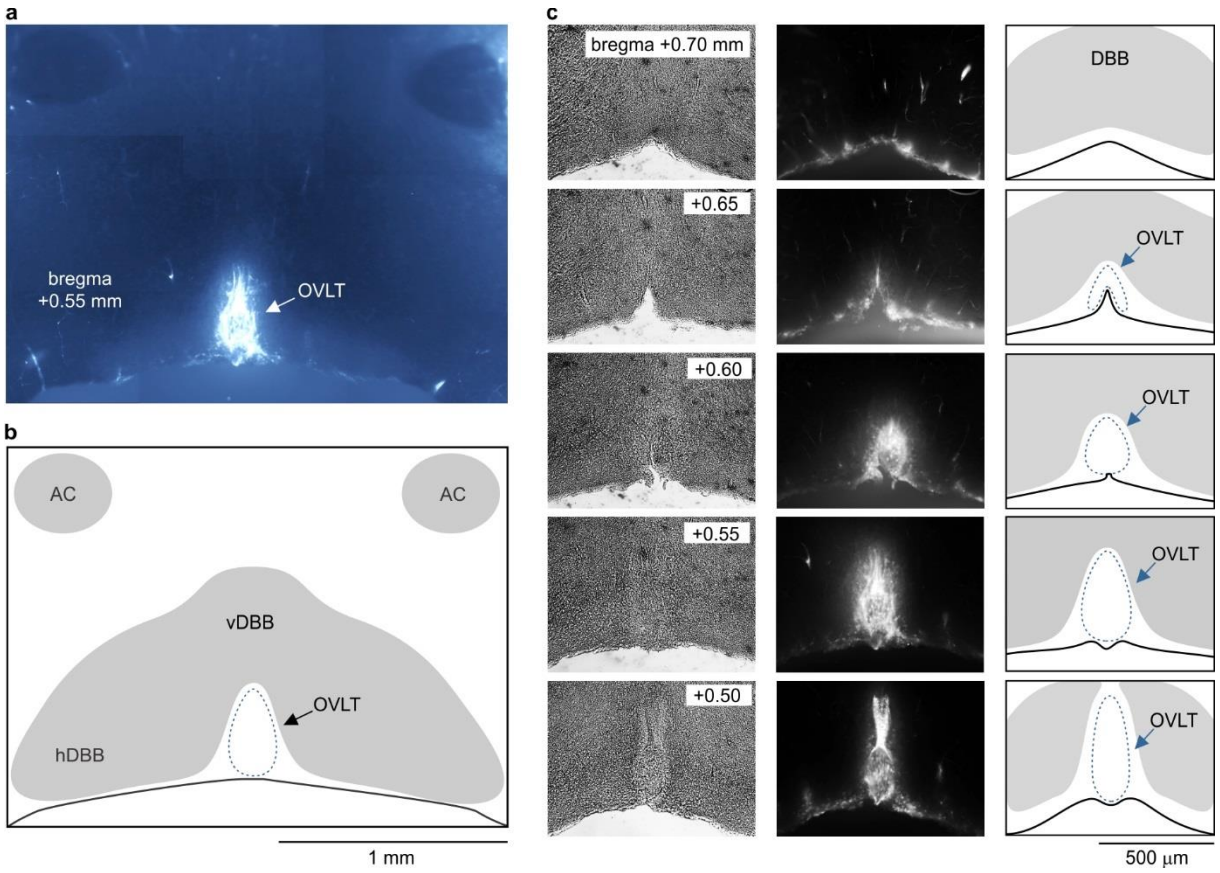

Extended Data Figure 1 | Anatomical outline of the mouse OVLT determined with Evans Blue. A, Micrograph shows fluorescence (excitation 650 nm, emission 700 nm) in a 50 µm thick coronal section taken through the anterior hypothalamus of a mouse injected intravenously with 1% Evans Blue. The section corresponds to a plane lying 0.55 mm rostral to Bregma as defined elsewhere[31]. **B**, Schematic illustrating the outline of the OVLT and surrounding structures including the anterior commissure (AC), ventral Diagonal Band of Broca (vDBB), horizontal Diagonal Band of Broca (hDBB). Scale bar applies to a and b. **c**, Panels show brightfield images (left column), Evans Blue fluorescence (middle), and schematics (right) in consecutive coronal sections spanning the entire rostro-caudal extent of the OVLT. Position relative to Bregma is indicated on brightfield panels.

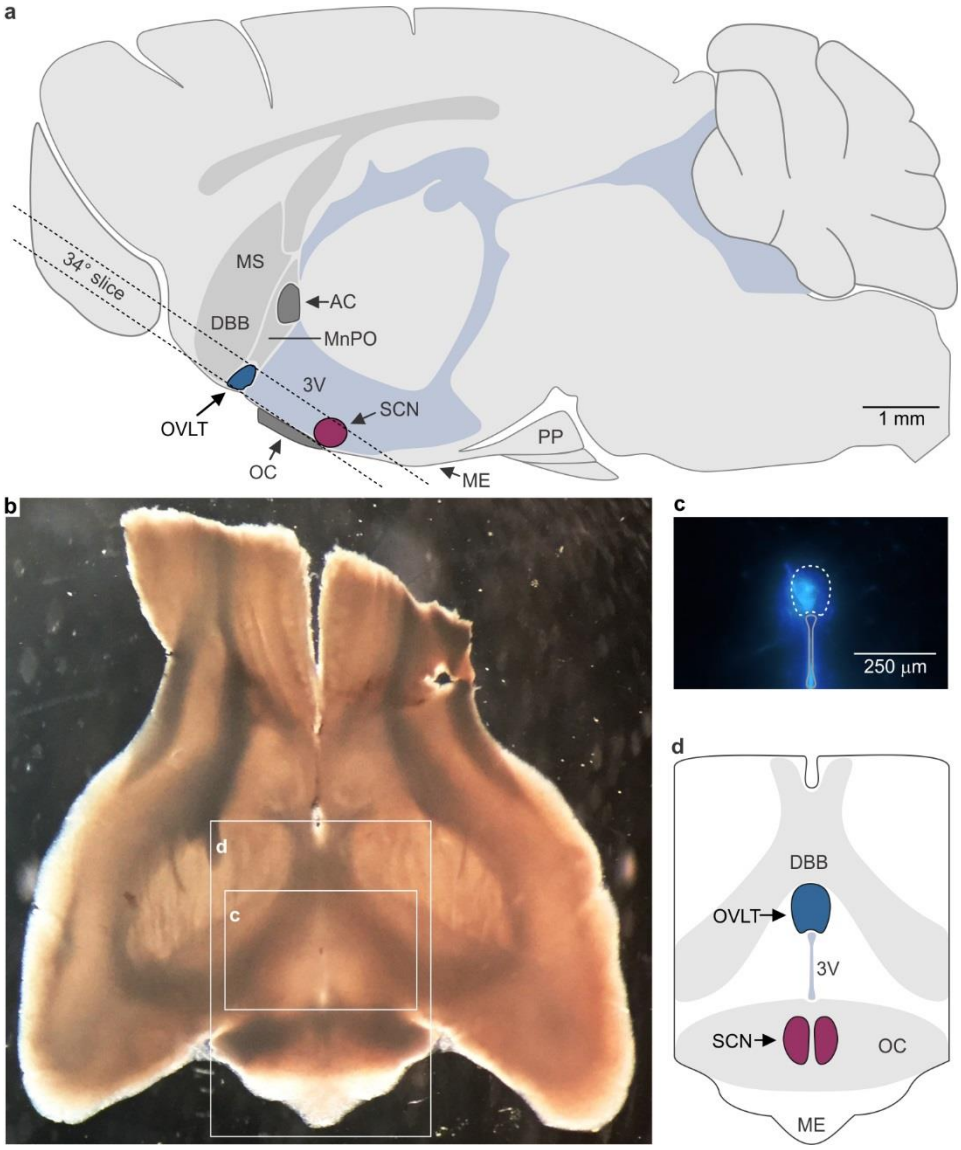

Extended Data Figure 2 | Preparation of angled slices of mouse hypothalamus that retain the OVLT and SCN. A, Schematic diagram showing the relative positions of the OVLT, SCN and other structures in the sagittal plane as defined elsewhere[31]. Anterior commissure (AC), Diagonal Band of Broca (DBB), Median eminence (ME), Median preoptic nucleus (MnPO), Medial septum (MS), Optic chiasma (OC), posterior pituitary (PP), third ventricle (3V). The brain slice was obtained at an angle of 34° relative to the horizontal plane. **B**, Brightfield image of a horizontal slice (plane as shown in a) obtained from a mouse injected intravenously with 1% Evan's Blue. **C**, Evans Blue fluorescence observed in the same slice in the small rectangular region identified in b. **d**, Schematic diagram illustrating various structures retained in the slice preparation (area shown by large rectangle in b).

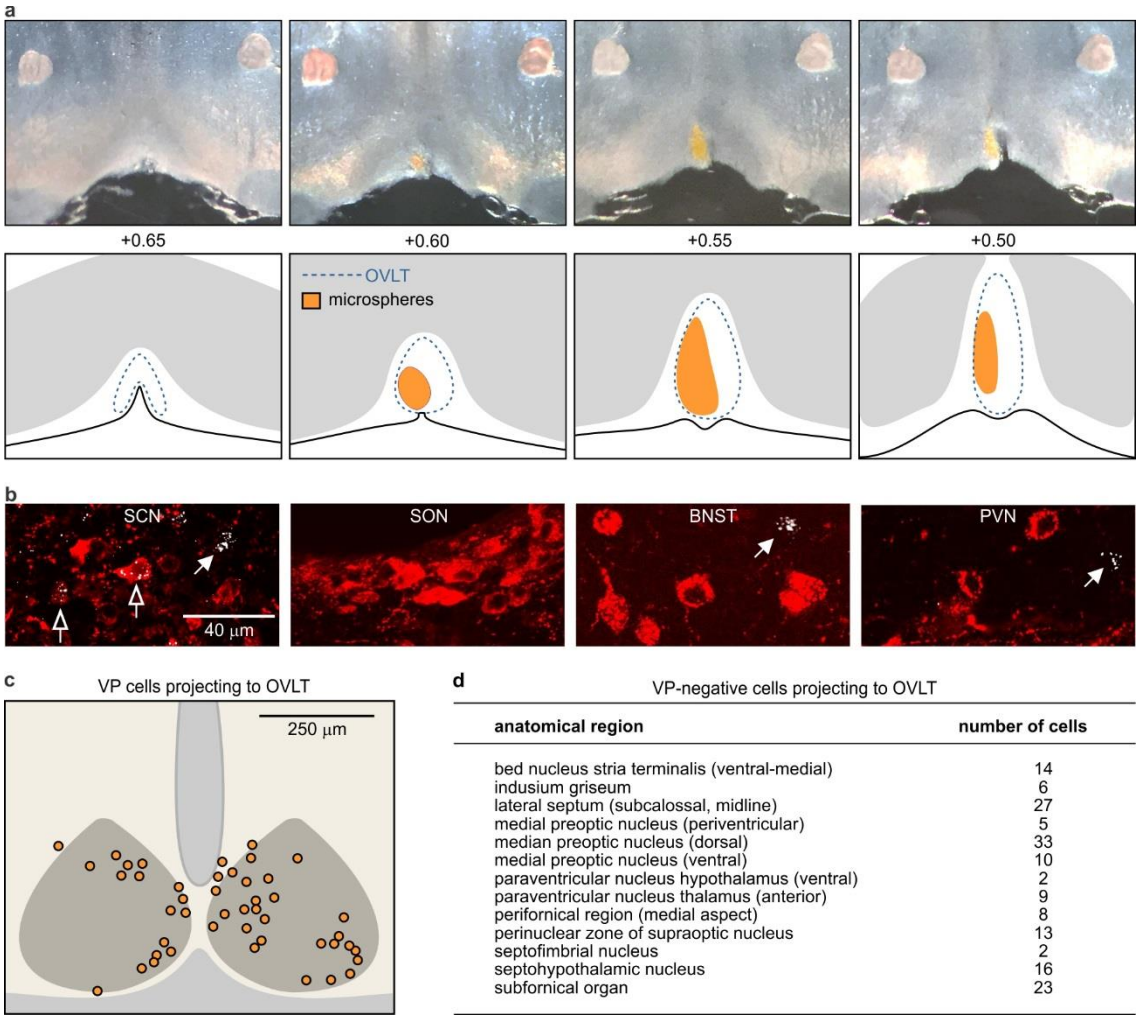

d

VP-negative cells projecting to OVLT

anatomical region	number of cells
bed nucleus stria terminalis (ventral-medial)	14
indusium griseum	6
lateral septum (subcalossal, midline)	27
medial preoptic nucleus (periventricular)	5
median preoptic nucleus (dorsal)	33
medial preoptic nucleus (ventral)	10
paraventricular nucleus hypothalamus (ventral)	2
paraventricular nucleus thalamus (anterior)	9
perifornical region (medial aspect)	8
perinuclear zone of supraoptic nucleus	13
septofimbrial nucleus	2
septohypothalamic nucleus	16
subfornical organ	23

Extended Data Figure 3 | Identification of SCN VP neurons projecting to the OVLT. A, Top panels are consecutive coronal brightfield micrographs showing the site of microsphere injection in one of three mice tested. Note the presence of material (orange) in three of the sections. Lower panels are schematics illustrating the location of the microspheres (orange) within the area encompassing the OVLT. **B,** Representative sections from four brain areas containing VP immunoreactive neurons (red) obtained from the brain shown in a: suprachiasmatic nucleus (SCN), supraoptic nucleus (SON), bed nucleus of the stria terminalis (BNST) and the hypothalamic paraventricular nucleus (PVN). Note that only the SCN contains retrogradely labeled VP neurons (open arrows), whereas neurons containing retrogradely transported beads in BNST and PVN are VP-negative (arrows). **C**, Schematic diagram illustrating the positions of all 46 VP-positive neurons projecting to the OVLT for the brain shown in a. **d**, Table lists other brain areas containing neurons projecting the OVLT for the brain shown in a. Only coronal sections positioned between +0.14 and -0.7 mm relative to Bregma were analyzed (sites identified according to ref [31]).

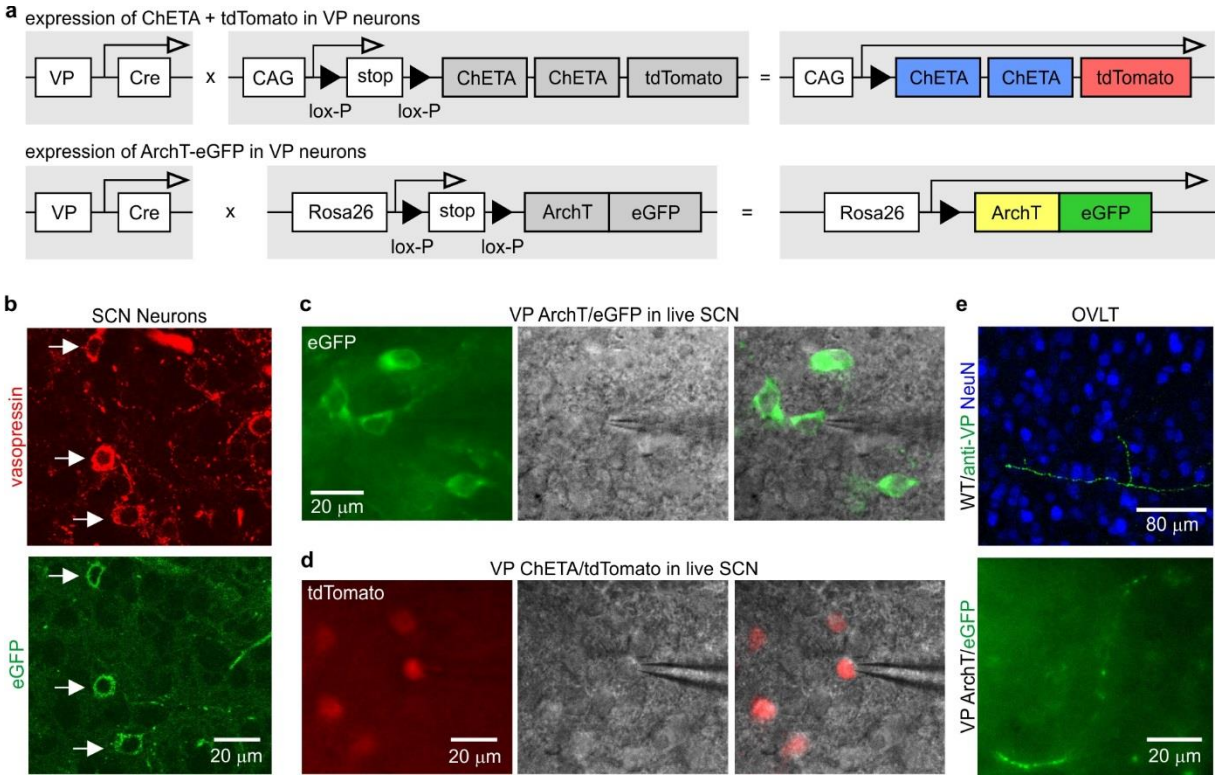

Extended Data Figure 4 | Transgenic mice expressing optogenetic probes and fluorescent reporters in VP neurons. A, Schematic illustrating the strategies used to produce mice in which VP neurons selectively express ChETA and tdTomato, or ArchT and eGFP. **B**, Panels show the presence of VP (red, upper) and eGFP (green, lower) in an immunolabeled section through the SCN. Note that neurons containing eGFP are VP-positive (arrows), but that not all VP neurons contain eGFP. An analysis of 5 sections indicated that 41% of the VP SCN neurons (93/225 cells) express the fluorescent reporter. **C**, The left panel shows live VP neurons identified by the presence eGFP in the SCN of a hypothalamic slice prepared from an ArchT mouse. One cell is being targeted with a patch clamp micropipette (middle panel shows brightfield; right panel is a merge). **D**, Patch clamping of SCN VP neurons identified by the expression of tdTomato in ChETA mice (layout as in c). **e**, VP containing fibers are visible by immunolabeling in the WT OVLT (upper panel; VP in green, NeuN in blue), and by eGFP expression in the OVLT of ArchT mice (lower) or tdTomato expression in ChETA mice (not shown).

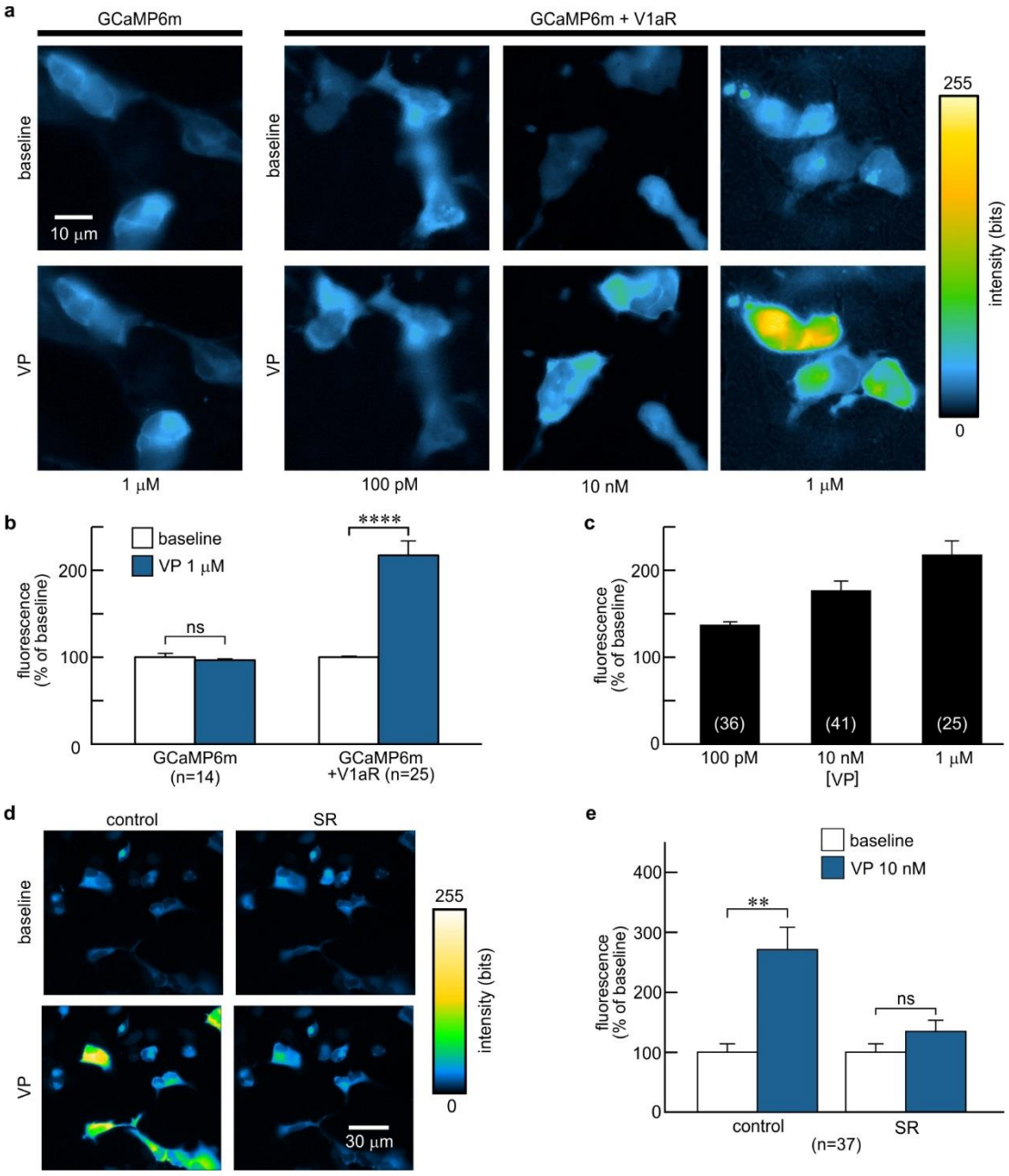

Extended Data Figure 5 | Specificity and calibration of VP sensor cells. A, Panels show the effects of bath-applied VP (concentrations shown below) on GcaMP6m fluorescence in HEK293 cells transfected with GcaMP6m alone, or co-transfected with GcaMP6m and the human V1aR. Note that VP has no effect in the absence of V1aR, but that dose-dependent increases were observed in the VP sensors co-transfected with GcaMP6m + V1aR. **B**, Bar graphs show mean ± s.e.m. values of fluorescence changes (relative to baseline) caused by 1 μM VP in both types of cells (****$p < 0.0001$, ns not significant; paired t-test; n shown in brackets). **C**, Bar graphs show

mean ± s.e.m. values of fluorescence (relative to baseline) induced by different concentrations of VP in HEK293 cells transfected with GcaMP6m and V1aR (n shown in brackets). **D**, Examples of GcaMP6m fluorescence in VP sensor cells treated with 10 nM VP in the absence (Control) and presence of 10 μM SR. **e**, Bar graphs show mean ± s.e.m. values of GcaMP6m fluorescence (relative to baseline) induced by 10 nM VP cells in the absence and presence of 10 μM SR. Cells were first tested in the presence of SR, then SR was washed and cells were retested in the absence of SR (**p<0.01; two-way RM ANOVA and Holm-Sidak post-hoc test).

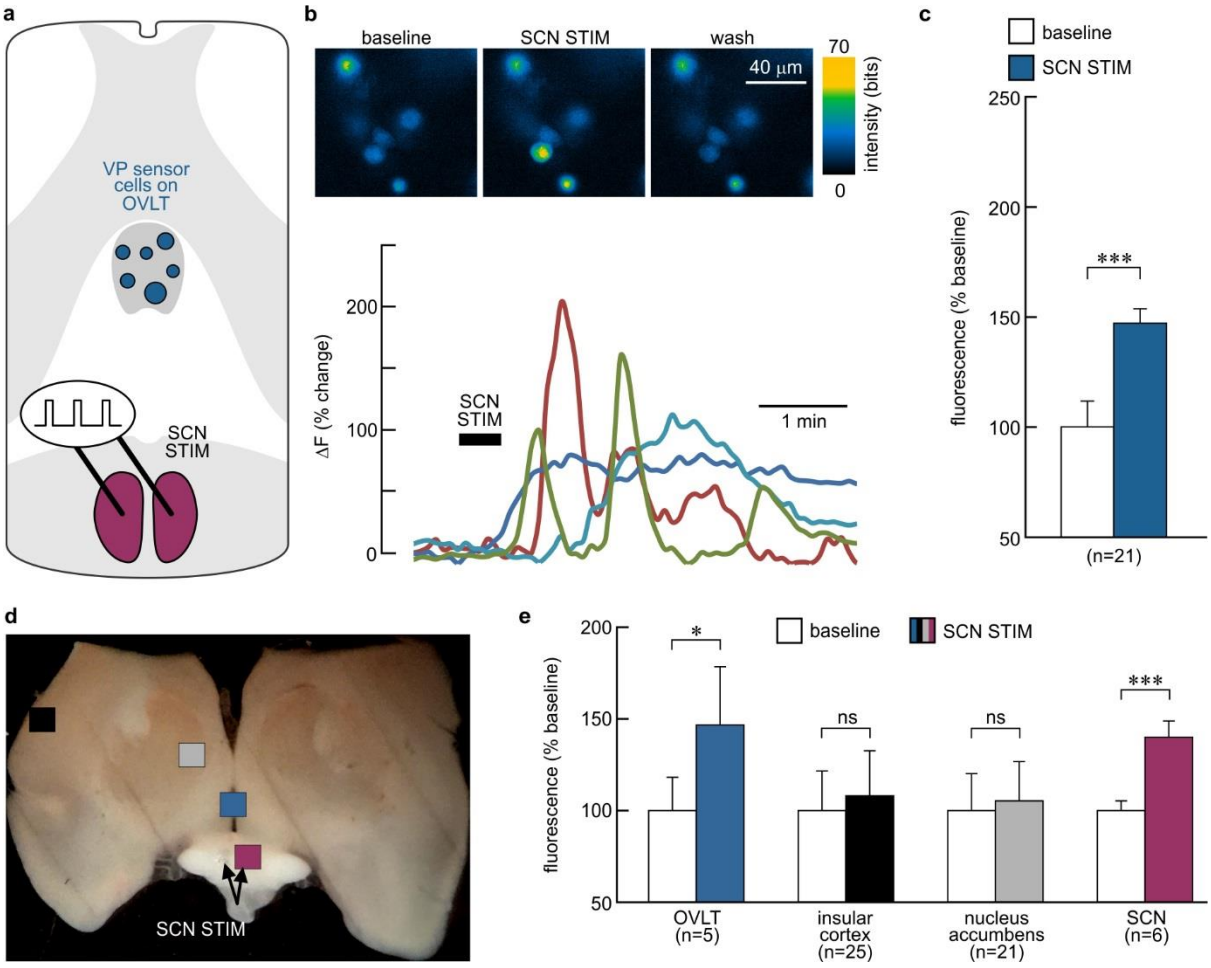

Extended Data Figure 6 | Detection of VP release in slices of mouse and rat hypothalamus. **A**, Schematic diagram illustrates the configuration of the experiment. HEK293 cells transfected with GcaMP6m +V1aR (VP sensors) were plated over the slice and GcaMP6m fluorescence was imaged over various regions (OVLT illustrated here). **B**, Upper panels show GcaMP6m fluorescence in VP sensors overlying the OVLT before (Baseline) and after electrical stimulation of the SCN (SCN STIM; 10 Hz, 30 s) in a slice of mouse hypothalamus. The lower graph plots the time course of changes in fluorescence (ΔF; expressed as percent of basal fluorescence, % Change) induced by SCN STIM (bar) in a number of cells. **C**, Bar graphs show mean ± s.e.m. values of fluorescence changes induced by SCN stimulation in slices of mouse hypothalamus relative to baseline (***p< 0.001; n shown in brackets, paired t-test). **D**, Photo of a horizontal rat hypothalamic slice depicting 4 regions where VP sensor fluorescence was measured after SCN STIM: OVLT (blue), insular cortex (black), nucleus accumbens (gray) and SCN (magenta). **E**, Bar graphs show mean ± s.e.m. GcaMP6m fluorescence before and after SCN STIM in 5

representative sensor cells lying over the OVLT, and all cells imaged over the other areas sampled. Note significant release in SCN and OVLT, but not in the other regions (paired t-test used for analysis of OVLT and SCN, and Wilcoxon test used for other regions, *$p<0.05$, ns not significant).

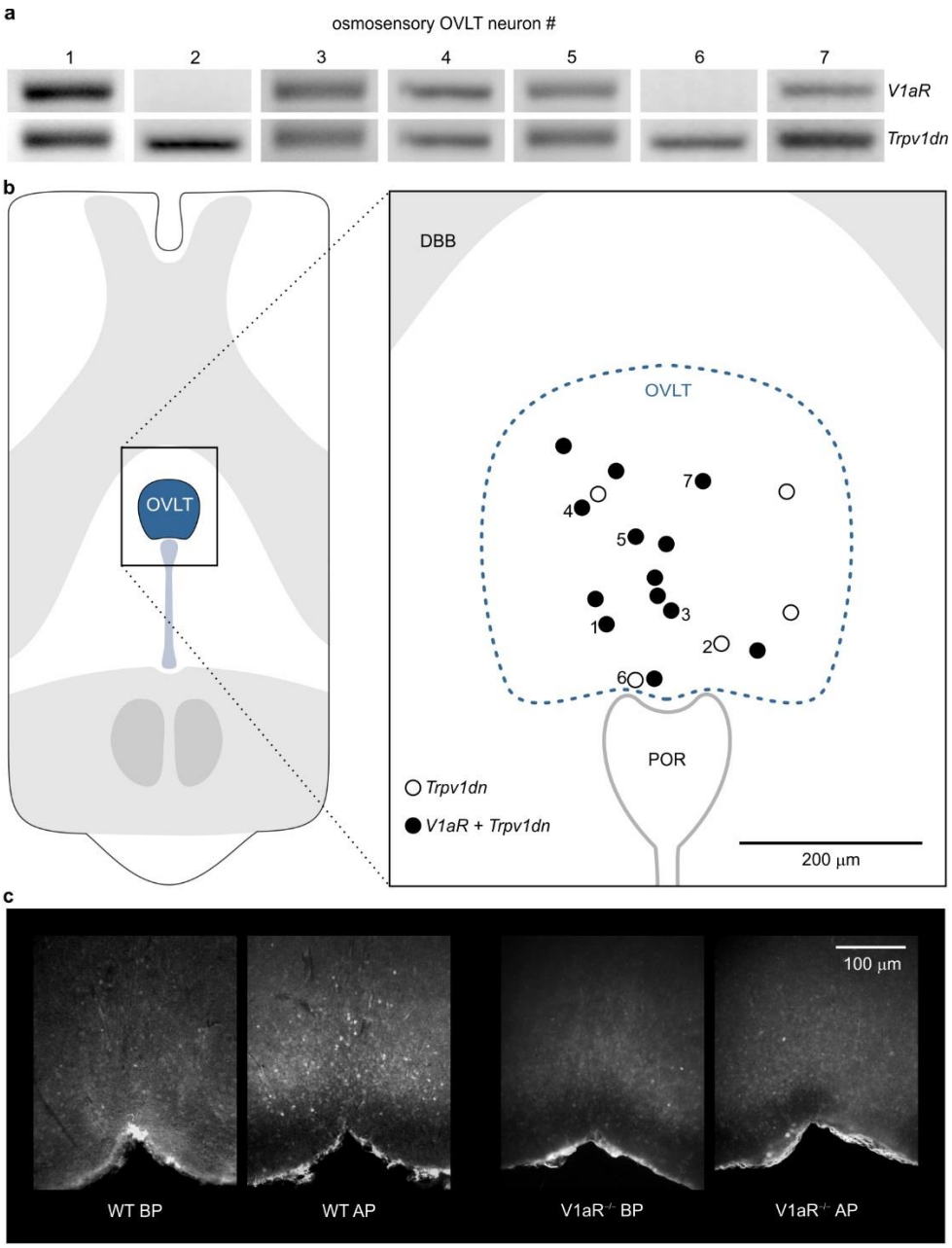

Extended Data Figure 7 | V1aRs are necessary for c-Fos activation during the AP in OVLT neurons. A, Single cell RT-PCR bands reveal the presence or absence of mRNA encoding VP V1aRs (upper panels) in seven (of 18) individual osmosensory OVLT neurons aspirated via patch pipette in a horizontal slice of rat hypothalamus. The positions of all sampled neurons were measured relative to the rostral part of the preoptic recess (POR) of the third ventricle, and mapped according to ref[28]. Most neurons were sampled in the core of the OVLT. **B**, OVLT

neurons were identified as osmosensory neurons by the presence of PCR products reflecting expression of the channel *Trpv1dn* (lower panels)[34]. In total, 13 of 18 *Trpv1dn* positive OVLT neurons (72%) were found to express V1aRs. **C**, Micrographs show expression of immunolabeled c-Fos in the OVLT of WT and $V1aR^{-/-}$ mice during the BP and AP. Note that the increase in c-Fos density observed in WT AP mice is absent in $V1aR^{-/-}$ mice.

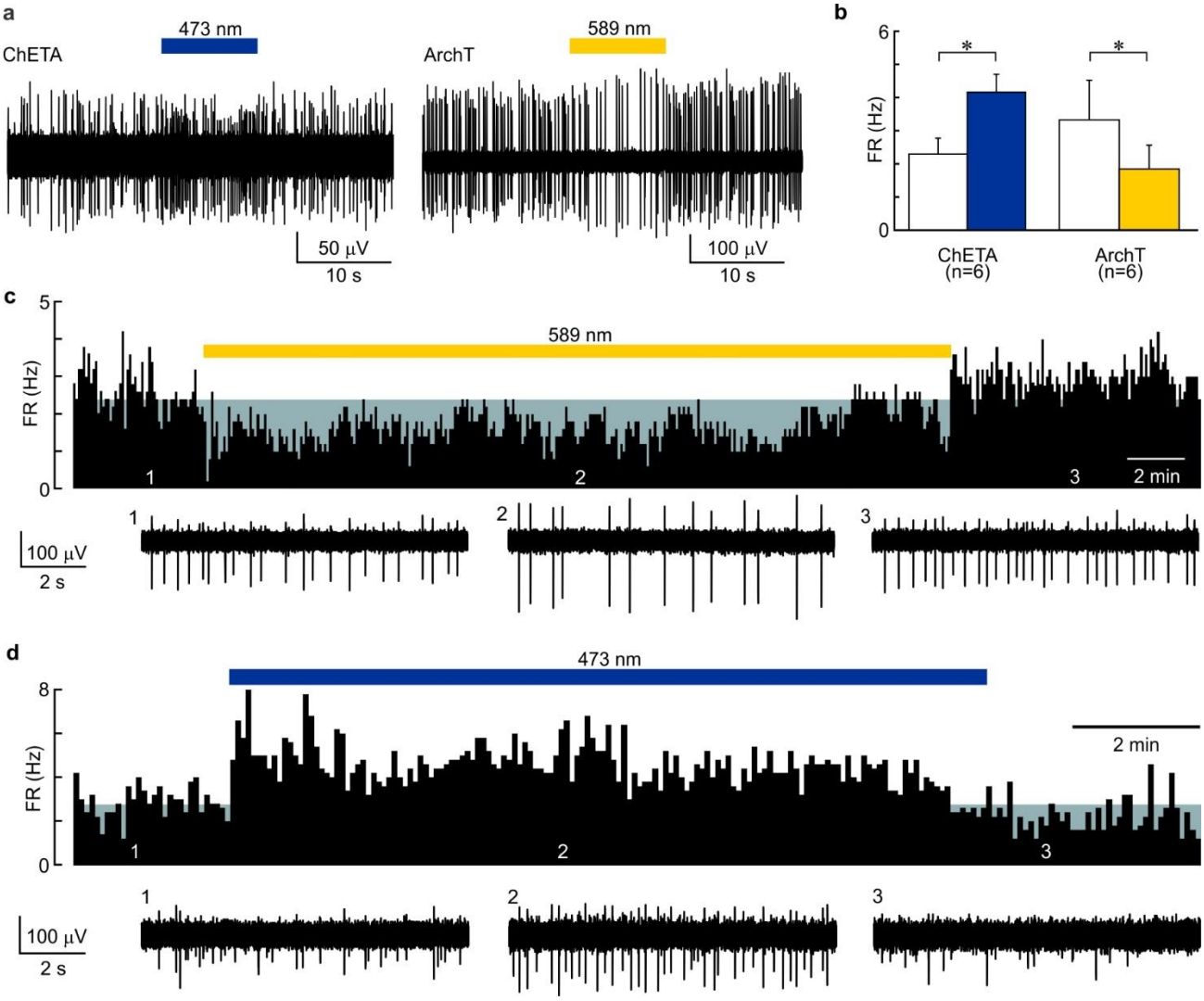

Extended Data Figure 8 | Optogenetic control of SCN VP neurons in ChETA and ArchT mice. A, Cell-attached recordings of spontaneous action potential firing in identified SCN VP neurons in slices prepared from ChETA and ArchT mice. Note how application of blue light (473 nm, blue bar) causes excitation of the ChETA neuron whereas application of yellow light (589 nm, yellow bar) inhibits the ArchT neuron. **B**, Bar graphs show mean ± s.e.m. values of firing rate (FR) measured in SCN VP neurons from both genotypes in the absence (white) and presence of light (blue for ChETA; yellow for ArchT; n shown in brackets; *$p<0.05$, ChETA paired t-test, ArchT Wilcoxon test). **C**, Upper trace is a rate meter record (5 s bins) showing the effects of a prolonged application of yellow light (bar) on FR of an SCN VP neuron from an ArchT mouse. Traces below show samples of neuronal activity recorded at the times indicated by the numbers. Note that the inhibitory effect of light on FR is sustained for >20 min but diminishes thereafter.

D, Upper trace is a rate meter record (5 s bins) showing the effects of a prolonged application of blue light (bar) on FR of an SCN VP neuron from a ChETA mouse. Traces below show samples of neuronal activity recorded at the times indicated by the numbers. Note that the excitatory effect of light on FR is sustained for >10 min but declines before the end of the stimulus.

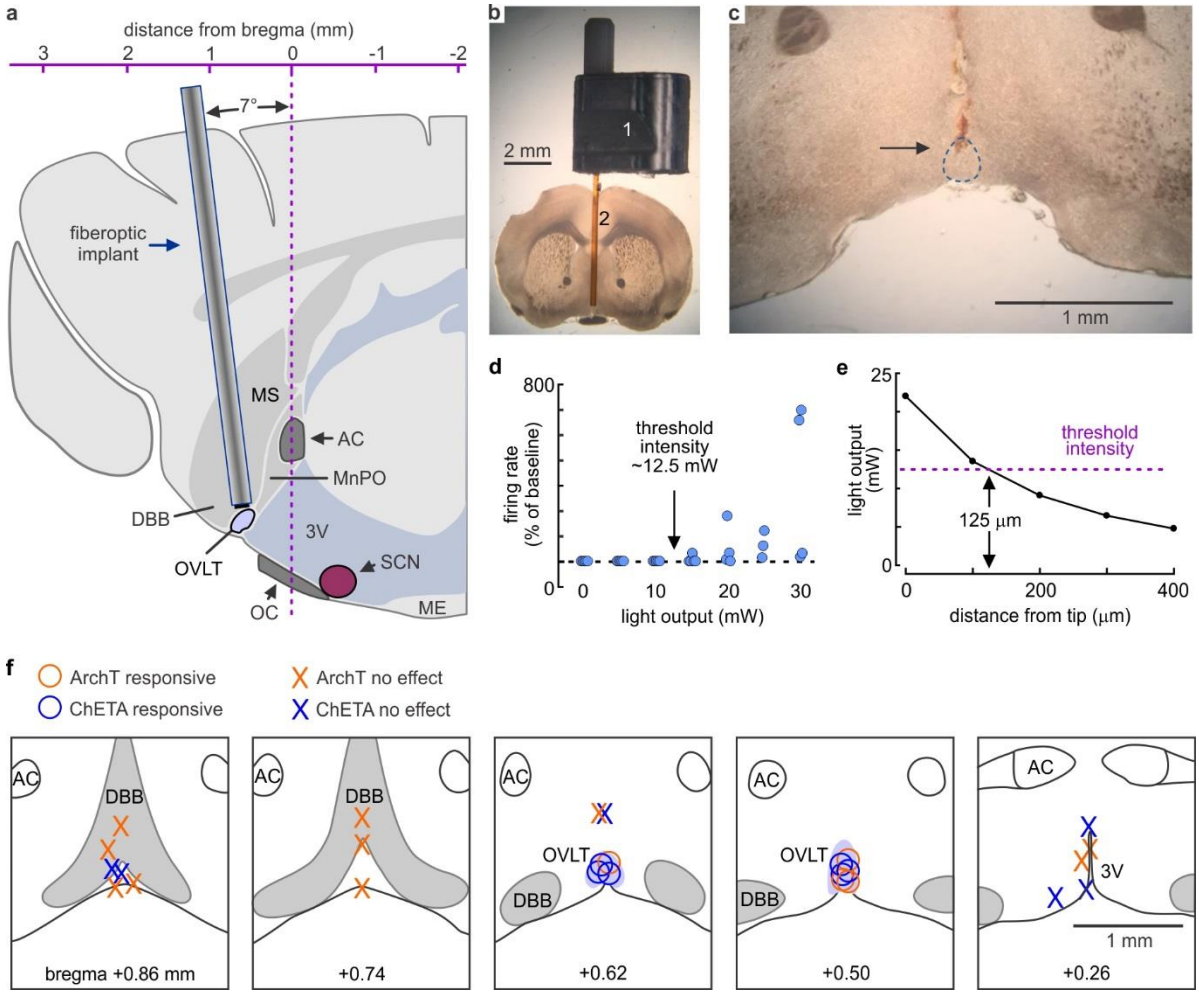

Extended Data Figure 9 | Optogenetic control of OVLT neurons in mice. A, Schematic diagram illustrating midline structures surrounding the mouse OVLT in the sagittal plane (AC, anterior commissure; DBB, Diagonal Band of Broca; ME, median eminence; MnPO, median preoptic nucleus; MS, medial septum; OC, optic chiasma; 3V, third ventricle). Positions illustrated as described elsewhere[31]. Fiberoptic cannula attached to a slim titanium magnetic receptacle was implanted by insertion at an angle of 7° relative to the vertical plane. **B**, Photograph shows the slim titanium magnetic receptacle and fiberoptic cannula superimposed on a coronal brain slice at the level of the OVLT. **C**, Coronal section from the paraformaldehyde-fixed brain of a mouse that was implanted with a fiberoptic cannula. Inspection of the section revealed that that the tip of the cannula had reached the most dorsal part (arrow) of the OVLT (dashed line). **D**, Plot shows the effect of blue light delivered for 1-2 mins at different intensities on the firing rate of OVLT neurons in slices from a ChETA mouse *in vitro*. Each dot is a different cell. Note that threshold intensity is ~12.5 mW. **E**, Plot shows theoretical decay of light intensity

through brain tissue as a function of distance using our specific parameters and the calculator module provided at optogenetic.org. Note that with a light output set at 22 mW (used in our *in vivo* experiments with ChETA mice), light intensity drops below threshold at a distance of ~125 µm from the tip of the fiberoptic probe. **F**, Coronal schematics (adapted with permission ref[31]) illustrate implantation sites for all *in vivo* optogenetic experiments determined by post-hoc histological inspection (as in c). Distance from Bregma in the rostro-caudal axis is shown below each panel. Note that experiments were only successful when the tip of the fiberoptic probe was placed directly into or above the OVLT.

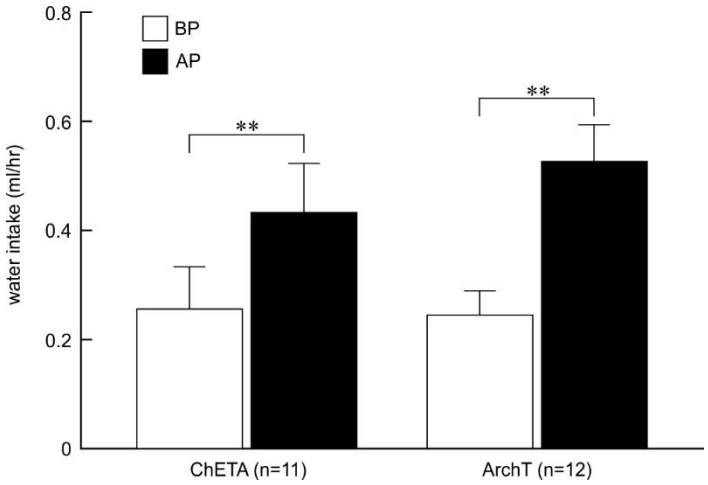

Extended Data Figure 10 | Transgenic ChETA and ArchT mice implanted with fiberoptic cannulae displayed increases in water intake during the AP. Bar graphs show mean ± s.e.m. values of water intake during the BP (ZT19.5–21.5) and AP (ZT21.5–23.5) in groups of ChETA and ArchT mice (paired t-test, **p<0.01; n shown in brackets).

Chapter 4 – Salt regulates clock time and output via an excitatory GABAergic neural circuit

Perhaps one of the most pronounced diurnal rhythms that mammals exhibit is the daily cycle in core body temperature[344]. It is likely that the clock mediates this rhythm, at least in part, via its outputs. The decrease in body temperature observed during the sleep period is thought to play an important role in opposing overnight adipsia by reducing water loss. Interestingly, it has been shown that an acute rise in osmolality drives a significant drop in core body temperature in mice and humans[345-347]. As mentioned in section 1.1.6, the shell region of the SCN, where VP neurons are located, receives abundant afferent non-retinal input from brain areas such as the hypothalamus. The OVLT, which located in the hypothalamus, is one of the major central osmo and sodium-sensors (section 1.2), therefore *I hypothesize that salt-dependent excitation of OVLT neurons can drive an increase in the electrical activity of SCN^{VP} neurons and regulate clock time and output.* I performed 100% of the experiments and 90% of the writing.

Submitted Oct 1st, 2019

Salt regulates clock time and output via an excitatory GABAergic neural circuit

Claire Gizowski and Charles W. Bourque

Brain Repair and Integrative Neuroscience Program, Research Institute of the McGill University Health Centre, 1650 Cedar Avenue, Montreal QC, Canada H3G1A4.

The suprachiasmatic nucleus (SCN) serves as the body's master circadian clock which adaptively coordinates changes in physiology and behaviour in anticipation of changing requirements throughout the 24h day-night cycle[348-351]. For example, the SCN opposes overnight adipsia by driving water intake prior to sleep[215,352], and by secreting anti-diuretic hormone[322,353] and lowering body temperature[345,354] to reduce water loss during sleep[355]. These responses can also be driven by central osmosensors to oppose an unscheduled rise in osmolality during the active phase[84,122,216,346]. However, it is unknown whether osmosensors require clock-output networks to drive homeostatic responses. Here we show that a systemic salt injection given at ZT19 (Zeitgeber Time), a time when SCN^{VP} (vasopressin) neurons are inactive, excited SCN^{VP} neurons and decreased non-shivering thermogenesis (NST) and body temperature (T_b). The effects of salt on NST and T_b were prevented by chemogenetic inhibition of SCN^{VP} neurons and mimicked by optogenetic stimulation of SCN^{VP} neurons *in vivo*. Combined anatomical and electrophysiological experiments revealed that salt sensing OVLT (organum vasculosum lamina terminalis) neurons expressing glutamic acid decarboxylase ($OVLT^{GAD}$) relay this information to SCN^{VP} neurons via an excitatory effect of GABA (*γ*-aminobutyric acid). Optogenetic activation of $OVLT^{GAD}$ neuron axon terminals excited SCN^{VP} neurons *in vitro* and mimicked the effects of salt on NST and T_b *in vivo*. Furthermore, chemogenetic inhibition of $OVLT^{GAD}$ neurons blunted the effects of systemic salt on NST and T_b. Lastly, we show salt significantly phase advanced the circadian locomotor activity onset of mice. This effect was mimicked by optogenetic activation of the $OVLT^{GAD}$→ SCN^{VP} pathway and prevented by chemogenetic inhibition of $OVLT^{GAD}$ neurons. Collectively, our findings provide the first demonstration that clock time can be regulated by non-photic, physiologically-relevant cues, and that such cues can drive unscheduled homeostatic responses via clock-output networks.

To determine if an acute rise in osmolality can recruit clock-output networks to drive a homeostatic response when the clock is otherwise silent, we first determined a time at which SCN neurons are electrically inactive. Specifically, we targeted SCN^{VP} neurons as these have been shown to drive homeostatic responses related to fluid balance[82,215]. To examine this question, we obtained cell-attached recordings from identified neurons in brain slices from mice in which a fluorescent reporter is driven by the *Avp* gene promoter[215] (Fig. 1a). Our results show that SCN^{VP} neurons were largely inactive from ZT17–22 (Fig. 1b), therefore we selected ZT19 as an appropriate time-point. Subcutaneous injection of salt, but not saline, at ZT19 significantly lowered T_b as assessed by infrared thermography (IRT; Fig. 1c–e; Extended Data Fig. 1, 2). This effect was associated with a significant reduction in NST, as revealed by a lowering in brown adipose tissue (BAT) temperature (T_{BAT}; Fig. 1f). Notably, NaCl did not reduce locomotor activity (Extended Data Fig. 2), indicating that salt-induced decreases in T_b and T_{BAT} were not simply caused by a reduction in energy expenditure. The effects of salt on T_b and T_{BAT} were significantly reduced by silencing SCN^{VP} neurons using a chemogenetic approach (Fig. 1g–i; Extended Data Fig. 3). Conversely, the effects of salt could be mimicked by optogenetic activation of SCN^{VP} neurons (Fig. 1j,k), which was not accompanied by a reduction in locomotor activity (Extended Data Fig. 4). These results indicate that an increase in SCN^{VP} neuron activity at ZT19 is necessary and sufficient to mediate the effects of salt on T_b and T_{BAT}.

To address whether SCN^{VP} neurons are intrinsically sodium-sensitive, we examined the effects of NaCl on action potential firing rate in coronal slices in the presence of glutamate and $GABA_A$ receptor (GluR, $GABA_AR$) antagonists. These experiments revealed no significant effect of NaCl on firing rate (data not shown, from 1 slice, n=7, paired *t*-test p=0.88), suggesting that salt-dependent activation of SCN^{VP} neurons may be mediated by a network effect. Previous studies have shown that systemic salt can be detected by glutamatergic OVLT neurons[90], however whole-cell patch recordings of spontaneous synaptic activity revealed little evidence that SCN^{VP} neurons receive afferent glutamatergic input *in vitro* (data not shown). We therefore examined if $OVLT^{GAD}$ neurons project to the SCN and if such neurons are intrinsically sodium-sensitive. Unilateral SCN injection of a retrograde virus[356] driving Cre dependent expression of tdTomato in GAD^{cre} mice induced expression of tdTomato in $OVLT^{GAD}$ neurons (Fig. 2a–c). Moreover, systemic salt induced expression of c-Fos in numerous $OVLT^{GAD}$→SCN neurons (Fig. 2b,c). Equivalent results were obtained with retrograde microspheres and GAD/c-Fos immunocytochemistry (Extended

Data Fig. 5). These results indicate that salt-responsive $OVLT^{GAD}$ neurons project to the SCN. To establish if $OVLT^{GAD}$ neurons are intrinsically salt-sensitive, we used calcium imaging and electrophysiological approaches *in vitro*. Bath application of NaCl to $OVLT^{GAD}$ neurons expressing the calcium reporter GCaMP6f significantly increased fluorescence and electrical activity in the presence of GluR and $GABA_AR$ blockers (Fig. 2d–g).

If the excitatory effects of salt on SCN^{VP} neurons are mediated by an $OVLT^{GAD}\rightarrow SCN^{VP}$ pathway, this would suggest GABA is excitatory on SCN^{VP} neurons during the dark period. Although previous studies have shown that a subset of SCN neurons can be excited by GABA[357,358], it is unknown if SCN^{VP} neurons can be specifically excited by GABA afferents at this time. To address this question, we examined the reversal potential of the electrically evoked GABAergic post-synaptic current (PSC; E_{GABA}) using gramicidin perforated patch clamp recordings of SCN^{VP} neurons between ZT17−24 (Fig. 2h). The vast majority of SCN^{VP} neurons displayed E_{GABA} values above spike threshold (Fig. 2i), suggesting that GABA is depolarizing. In agreement, cell-attached recordings revealed robust excitation of SCN^{VP} neurons in response to afferent stimulation in the presence of GluR blockers (Fig. 2j), and this effect was inhibited by bath application of a $GABA_AR$ antagonist (Fig. 2k). Furthermore, bath application of $GABA_AR$ antagonists decreased the spontaneous firing frequency of SCN^{VP} neurons (Extended Data Fig. 6). Together, these data demonstrate that GABA is excitatory on SCN^{VP} neurons during the dark period.

To determine if salt drives a network excitation of SCN^{VP} neurons, we examined the effects of bath applied NaCl on the rate of spontaneous PSCs (sPSC) and action potential firing frequency in horizontal slices of mouse brain that retain connectivity between the OVLT and the SCN[215]. Under voltage clamp, application of NaCl was found to significantly increase the rate of sPSCs in SCN^{VP} neurons (Fig. 2l–n). Moreover, when tested in cell-attached configuration with GluR blockers, NaCl significantly increased action potential firing in SCN^{VP} neurons (Fig. 3a,b). In agreement, optogenetic stimulation of OVLT GABAergic axon terminals within the SCN excited SCN^{VP} neurons (Fig. 3c,d; Extended Data Fig. 7), indicating that activation of this pathway is specifically capable of activating SCN^{VP} neurons *in vitro*. To determine if this pathway contributes to the sodium-dependent reduction of T_b and T_{BAT} *in vivo*, we compared the effects of NaCl in the absence or presence of chemogenetic inhibition of $OVLT^{GAD}$ neurons (Extended Data Fig. 8). These experiments revealed that silencing $OVLT^{GAD}$ neurons significantly reduced the effects of

salt on T_b and T_{BAT} (Fig. 3e,f). Moreover, optogenetic stimulation of axon terminals of $OVLT^{GAD}$ neurons within the SCN mimicked the effects of salt on T_b and T_{BAT} (Fig. 3g,h; Extended data Fig. 9), and did not significantly reduce locomotor activity (Extended Data Fig. 10). Collectively, the data presented so far, indicate the $OVLT^{GAD}\rightarrow SCN^{VP}$ pathway mediates the effects of NaCl on T_b and T_{BAT} *in vivo*. These findings demonstrate the clock not only serves as a pacemaker, but also receives inputs from central osmosensors that can drive clock-output neurons to command an unscheduled homeostatic response.

Classic experiments have shown that non-photic perturbations, such as drug injections, can cause phase shifts in the timing of the circadian clock as demonstrated by changes in the daily onset of locomotor activity in constant darkness[359]. To determine if salt can affect clock time when delivered at ZT19, we examined the effects of this manipulation on the onset of locomotor activity of mice monitored in the absence of light. In contrast to mice injected with saline, who displayed no significant shift in the time of onset on the day that followed the injection, salt injected mice showed a significant phase advance (Fig. 4a–c). Although the average offset time also occurred earlier in salt injected animals, this effect was not significant (Fig. 4d). The length of the active period (Fig. 4e) and the free-running period (Fig. 4f) were not significantly affected by salt, indicating this cue only affects clock time. Optogenetic and chemogenetic experiments were performed to examine if the effects of salt on clock time require $OVLT^{GAD}$ neuron activation. Chemogenetic inhibition of $OVLT^{GAD}$ neurons prevented the salt-induced phase advance, whereas optogenetic activation of $OVLT^{GAD}$ neuron axon terminals within the SCN mimicked this effect (Fig, 4g). Moreover, direct optogenetic activation of SCN^{VP} neurons also mimicked the effects of salt (Fig. 4g). Together, these results indicate that activation of the $OVLT^{GAD}\rightarrow SCN^{VP}$ pathway is necessary and sufficient to mediate salt-dependent changes in clock time.

Adaptation to a rise in systemic osmolality experienced during the active phase recruits a number of key homeostatic responses such as increased thirst[122,352], secretion of anti-diuretic hormone[216], and a reduction in T_b[346]. The latter response, in particular, limits evaporative water loss from the airway tract by reducing the thermal gradient between the organism and its environment[345,354]. Although the SCN engages these responses daily to anticipate the potential impact of adipsia during sleep[360], our findings reveal that central osmosensors can utilize clock-output networks to lower T_b at an unscheduled time. This unexpected finding indicates that the

central clock is instructed about physiological need and can acutely alter its output to cope with dynamic changes in an organism's internal environment.

Acknowledgements This work was supported by a Foundation Grant from the Canadian Institutes of Health Research (CIHR; FDN 143337) and a James McGill Chair to C.W.B, and a CIHR Banting and Best Canada Graduate Scholarship awarded to C.G. The RIMUHC receives generous funding from the Fonds de Recherche Québec Santé.

Author Contributions C.G. and C.W.B. designed the study, interpreted the results, and wrote the manuscript. C.G. performed all the experiments.

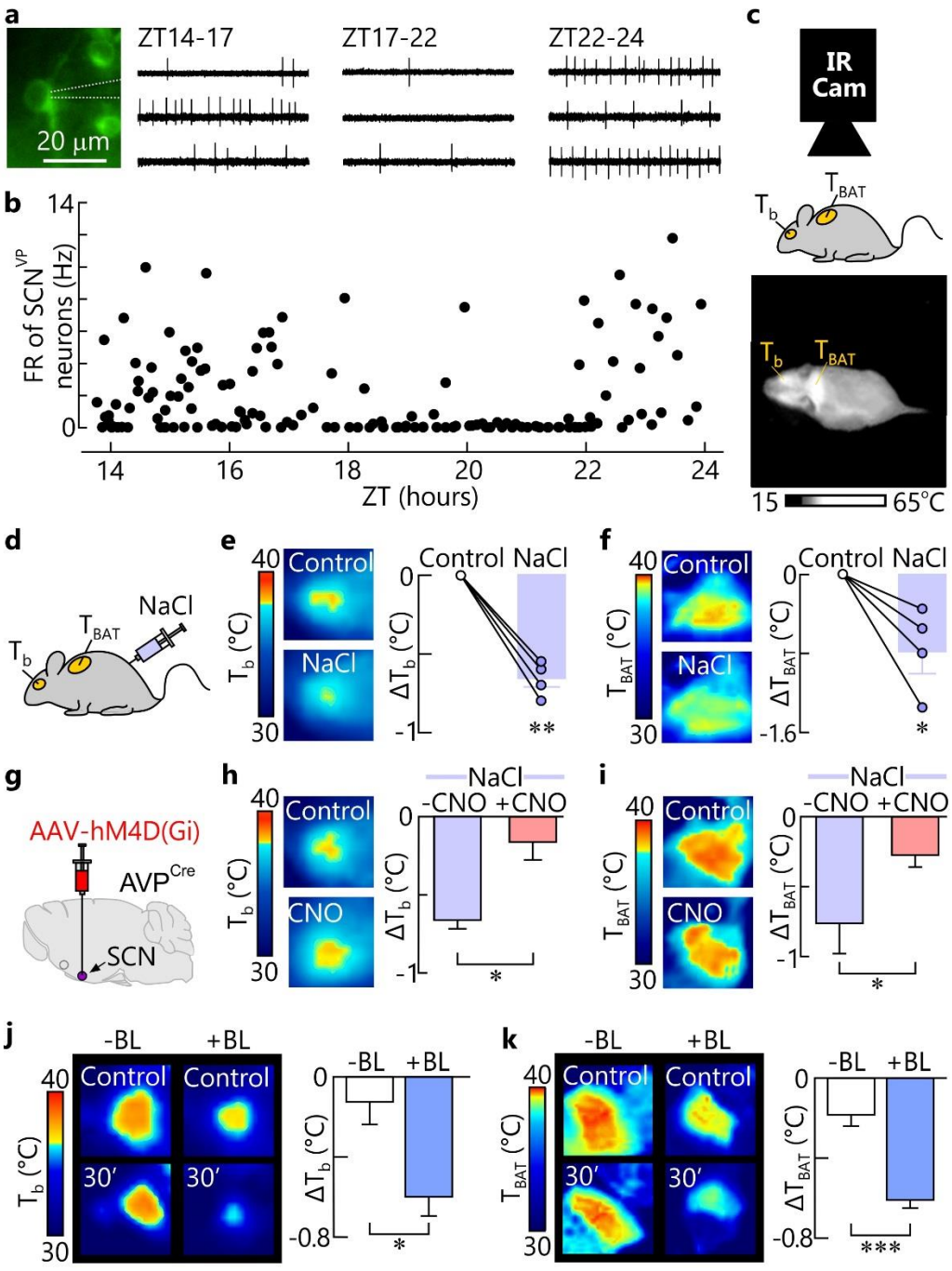

Figure 1. Salt loading reduces T_b and T_{BAT} via SCN^{VP} neurons. a, SCN^{VP} neurons in slices from AVP^{Cre} reporter mice were identified by green fluorescent protein (GFP; left panel) and cell-attached recordings of spontaneous action potential firing were obtained during three segments of the subjective dark phase (right panel shows representative sweeps). **b,** Plot shows the average action potential firing rate (FR) of individual SCN^{VP} neurons at different times (n = 141 neurons,

4 slices). **c**, Measurements of T_b (eye temperature) and T_{BAT} were obtained using an infrared thermographic camera (IRT). **d,** NaCl was injected subcutaneously. **e**, IRT images of T_b (left) before (Control) and 10 minutes after injection of 2M NaCl (8 µl/g). Right panel plots salt-induced changes in T_b (ΔT_b; n=4 AVP^{Cre} mice; mean ± s.e.m., paired *t*-test). **f,** left panels show IRT images of T_{BAT} in Control and after NaCl in the same mouse as **e**. Right panel plots salt-induced changes in T_{BAT} (ΔT_{BAT}) observed in the same mice as **e** (mean ± s.e.m., paired *t*-test). **g,** An AAV driving expression of an inhibitory DREADD [designer receptor exclusively activated by designer drugs; AAV DIO-hM4D(Gi)] was injected bilaterally into the SCN of AVP^{Cre} mice. **h,** IRT images of T_b (left) before and after injection of NaCl and the DREADD activator clozapine N-oxide (CNO 1 mg/Kg). Graph at right shows mean ± s.e.m. ΔT_b induced by NaCl in AVP^{Cre} mice or NaCl+CNO in AVP^{Cre} mice (paired *t*-test). **i**, IRT images of T_{BAT} (left) before and after injection of NaCl+CNO from same mouse as in **h**. Graph at right shows mean ± s.e.m. ΔT_{BAT} induced by NaCl in AVP^{Cre} mice or NaCl+CNO in AVP^{Cre} mice injected with AAV-DREADD in the SCN (paired *t*-test). **j**, IRT images at left show T_b in an AVP^{Cre} x $ChETA^{flex}$ mouse implanted with a fiberoptic probe delivering blue light (+BL) bilaterally to the SCN. Image sets -BL and +BL are tests of the same mouse on different days showing T_b before (Control) and 30 min after applying BL (+BL) or a time control without light (−BL). Graph at right shows mean ± s.e.m. ΔT_b (n=6; paired *t*-test). **k,** IRT images at left show T_{BAT} in in the same mouse and conditions as **j**. Graph at right shows mean ± s.e.m. ΔT_{BAT} (n=6; paired *t*-test). *p<0.05, **p<0.01, ***p<0.001.

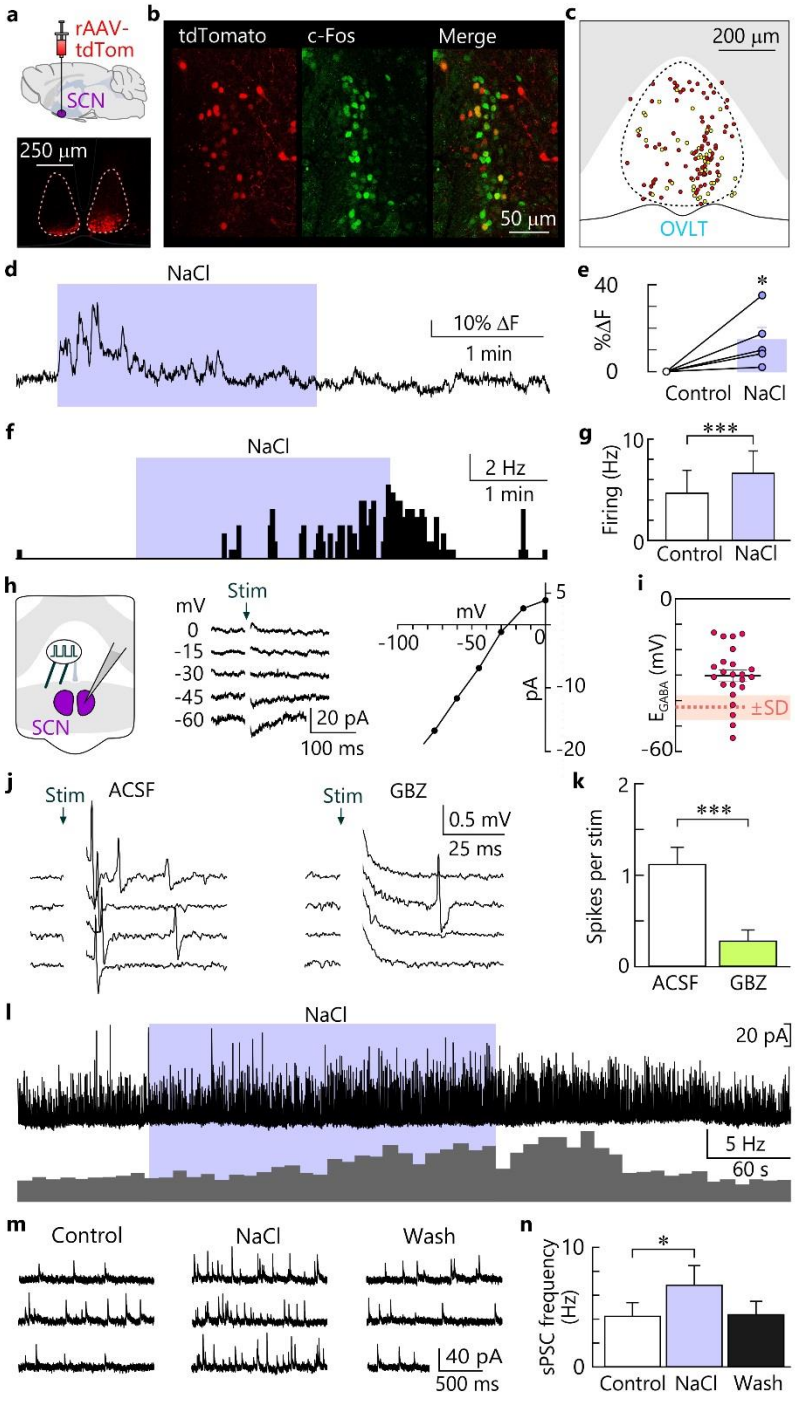

Figure 2. Salt sensitive OVLT^{GAD} neurons excite SCN^{VP} neurons at ZT19. a, GAD^{Cre} mice were injected with a retrograde AAV driving Cre dependent expression of tdTomato (rAAV-tdTom) into the right SCN. Three weeks later the mouse was injected with NaCl prior to perfusion. **b,** micrographs show the presence of many SCN-projecting retrogradely labelled OVLT^{GAD} neurons (red) in a single section, including several co-expressing c-Fos. **c,** Schematic shows the

location of c-Fos positive (yellow; n=44) or negative (red; n=88) SCN-projecting $OVLT^{GAD}$ neurons observed in this experiment. **d,** Percent changes in GCaMP6f fluorescence (%ΔF) relative to baseline induced by 10 mM NaCl (shaded area) in an $OVLT^{GAD}$ neuron in a brain slice (GAD^{Cre} x $GCaMP6f^{Flex}$) perfused with ACSF containing 3 mM Kynurenic acid (Kyn) and 20 µM Gabazine (GBZ). **e,** Graph plots values of %ΔF observed in 5 cells from 1 slice (paired *t*-test). **f,** Ratemeter plot showing effects of 10 mM NaCl on action potential FR in an $OVLT^{GAD}$ neuron tested as in **d**. **g,** Graph plots mean ± s.e.m. values of FR in the absence (Control) and presence of NaCl (4 cells from 1 slice; paired *t*-test). **h**, GABAergic responses of SCN^{VP} neurons recorded by perforated patch voltage clamp were evoked by electrical stimulation (Stim) in the presence of 3 mM Kyn (left). The effects of holding voltage on evoked GABAergic responses (e.g. middle traces) were plotted to determine E_{GABA} (right). **i,** Scatter plot shows values of E_{GABA} recorded from 23 neurons in 7 slices relative to the mean value of spike threshold (dotted line) and standard deviation (SD; shaded area). **j,** Effects of local stimulation on action potential firing detected by cell-attached recording of SCN^{VP} neurons in the presence of 3 mM Kyn. Note that robust excitation observed in the presence of ACSF and blocked by the addition of 20 µM GBZ. **k**, Bar graph shows mean ± s.e.m. number of spikes evoked by Stim in the absence (ACSF) and presence of GBZ (n = 9 cells from 3 slices; paired *t*-test). **l**, Graph (lower) plots frequency of spontaneous GABAergic synaptic events detected using whole cell current recording (upper) in an SCN^{VP} neuron treated with 10 mM NaCl (shaded area). **m,** Excerpts expanded from the trace in **l** illustrate GABAergic event frequency before, during (NaCl) and after (Wash) treatment with NaCl. **n,** Bar graphs plot frequencies of GABAergic synaptic events detected as in **l**, **m** for 8 cells in 7 slices (paired *t*-test). *p<0.05, ***p<0.001.

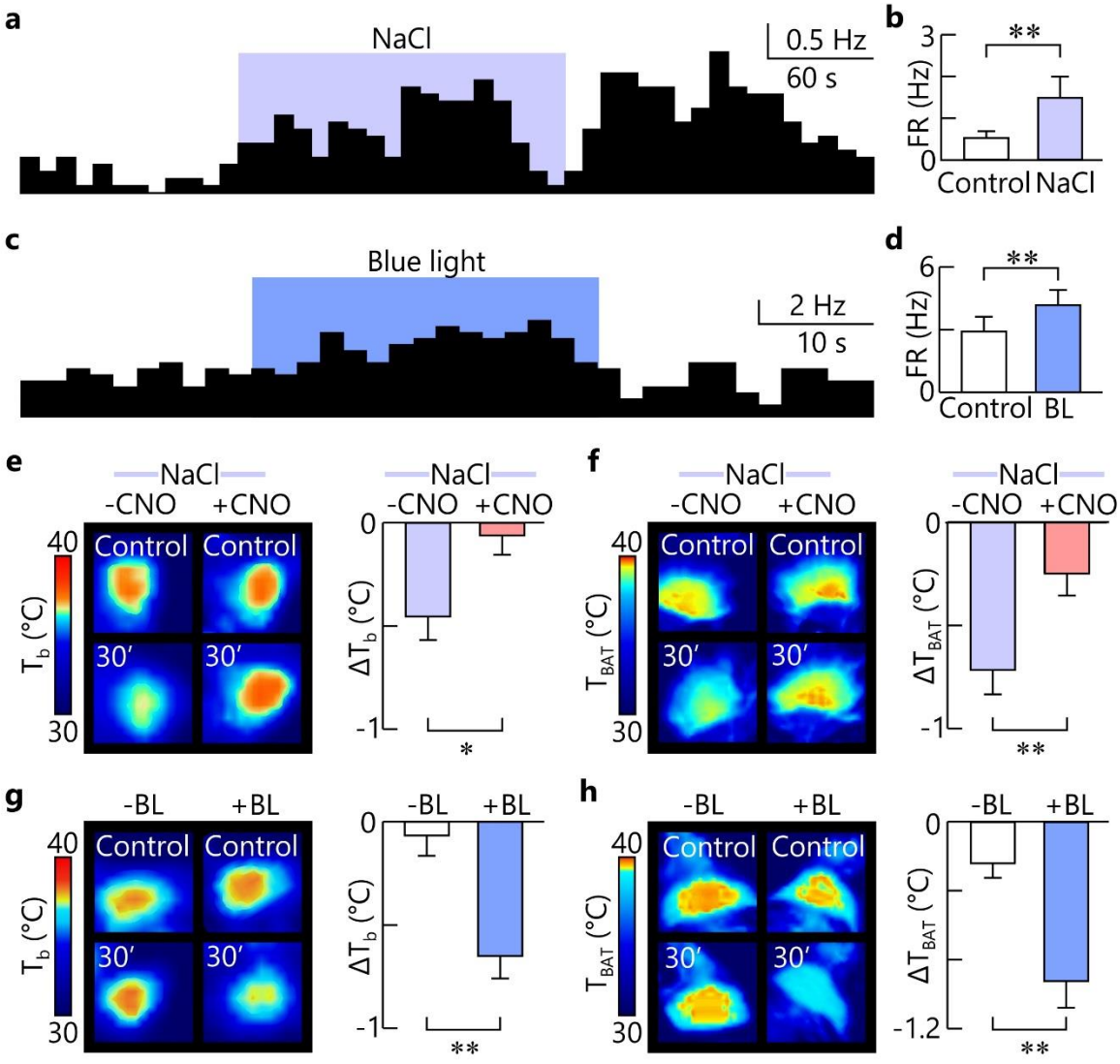

Figure 3. OVLT^{GAD} neurons mediate the effect of systemic salt on T_b and T_{BAT}. **a,** Frequency plot shows changes in FR evoked by 10 mM NaCl on an SCN^{VP} neuron in the presence of 3 mM Kyn. **b,** Bar graphs show mean ± s.e.m. FR observed in the absence (Control) and presence of NaCl in 10 neurons from 3 slices (paired *t*-test). **c,** The effect of activating axon terminals of OVLT^{GABA} neurons with blue light (BL) on SCN^{VP} neurons was examined in slices prepared from VGAT^{Flp} x AVP^{Cre} mice injected with AAV fDIO-ChR2 in the OVLT and AAV DIO-mCherry in the SCN. **d,** Bar graphs show mean ± s.e.m. FR observed in the absence (Control) and presence of BL in 5 neurons from 2 slices (paired *t*-test). **e,** IRT images of T_b (left) before and after (10 min) injection of NaCl without (NaCl−CNO) or with (NaCl+CNO) CNO (1 mg/Kg) in GAD^{Cre} mice injected with AAV DIO-hM4D(Gi) in the OVLT. Graph at right shows mean ± s.e.m. ΔT_b (n=8;

paired *t*-test). **f,** IRT images of T_{BAT} (left) in a mouse treated as in **e**. Graph at right shows mean ± s.e.m. ΔT_{BAT} (n=8; paired *t*-test). **g,** GAD^{Cre} animals injected with AAV DIO-ChR2 in the OVLT were implanted with a fiberoptic probe targeting the SCN bilaterally to optogenetically activate axon terminals of $OVLT^{GAD}$ neurons within the SCN. IRT image sets -BL and +BL tests of the same mouse on different days showing T_b before (Control) and 30 min (30') after applying BL (+BL) or a time control without light (−BL). Graph at right shows mean ± s.e.m. ΔT_b (n=5; paired *t*-test). **h,** IRT images at left show T_{BAT} in in the same mouse and conditions as **g**. Graph at right shows mean ± s.e.m. ΔT_{BAT} (n=5; paired *t*-test). *p<0.05, **p<0.01.

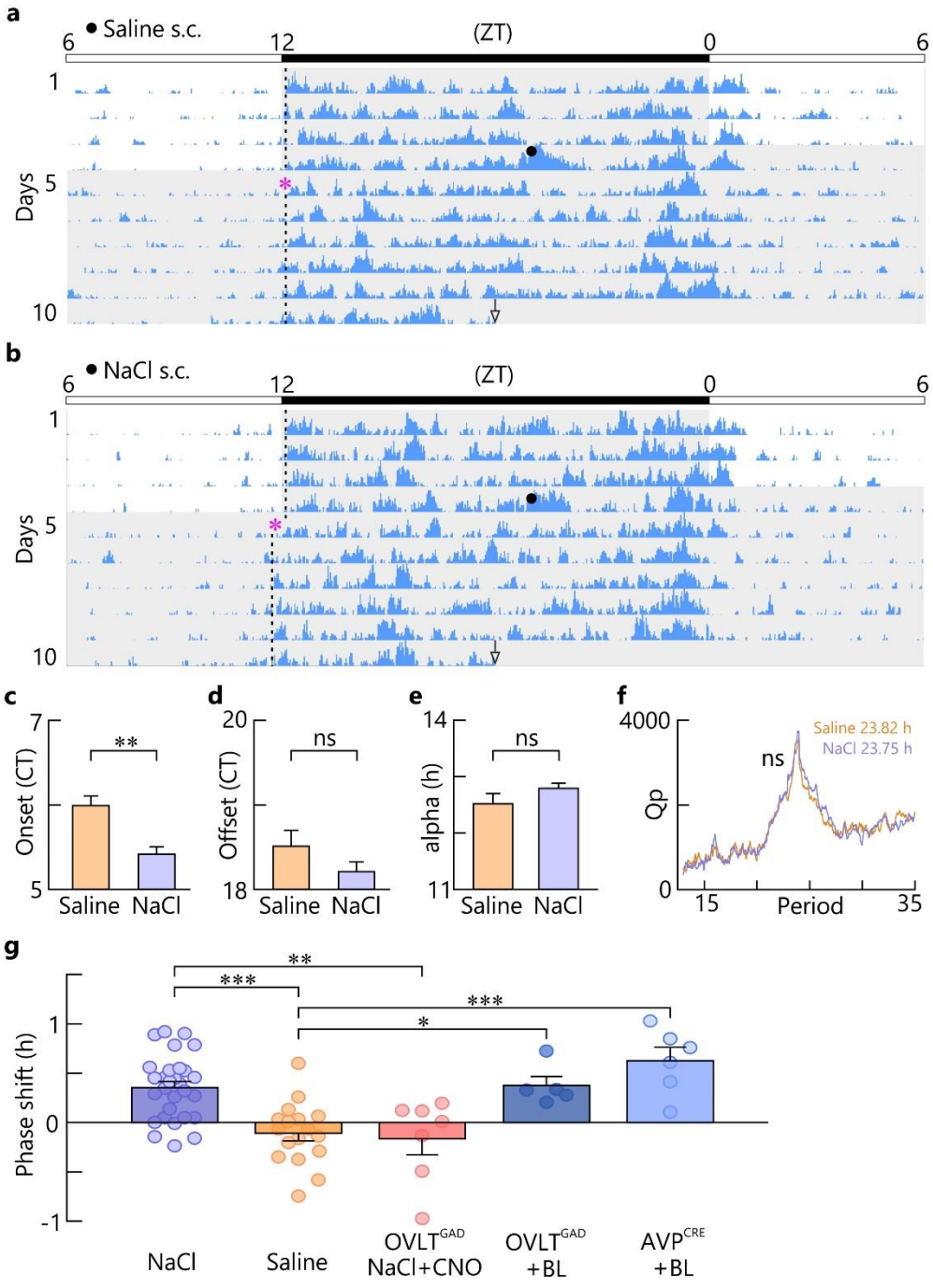

Figure 4. Activation of the OVLT^{GAD}→SCN^{VP} pathway advances the onset of locomotor activity. a, Averaged 24-h locomotor activity from 5 representative wild-type C57BL/6 mice over 10 consecutive days. Animals were injected with s.c. saline (0.9% NaCl; 8 µl/g) at ZT19. The upper dotted line represents the onset of locomotor activity during the four LD (Light:Dark) days and the lower dotted line represents activity onset in DD (Dark:Dark). The star represents the onset

on the first day in DD. The open arrow on day 10 signals the end of the experiment. **b,** Other trial with same mice, but injected with s.c. 2 M NaCl (8 µl/g) at ZT19. Symbols and parameters as in **a**. **c,** Bar graphs show mean ± s.e.m onset times during DD for those 5 mice. **d**, Bar graphs show offset times during DD for same mice. **e,** Bar graphs show active phase duration (alpha) for same mice. **f**, Plots show periodograms in DD after saline or NaCl injection in these 5 mice. Periods as indicated. **g**, Bar graphs show mean ± s.e.m shifts in activity onset times observed on DD 1 relative to LD in different conditions. Each data point represents an individual mouse. NaCl: 2 M NaCl ZT19, n=30. Saline: 0.9% NaCl ZT19, n=18. NaCl+CNO: 2 M NaCl+CNO (1 mg/kg) ZT19, n=7. GAD+BL: +BL (2.5 hz, 20 ms pulse, 5-10 mW) for 30 minutes within a time range from ZT19-20.5, n=5. AVP+BL: +BL (5 hz, 50 ms pulse, 23 mW) for 30 minutes within a time range from ZT19-20.5, n=6. (mean ± s.e.m., Holm-Sidak one-way ANOVA). * $p<0.05$, ** $p<0.01$, *** $p<0.001$.

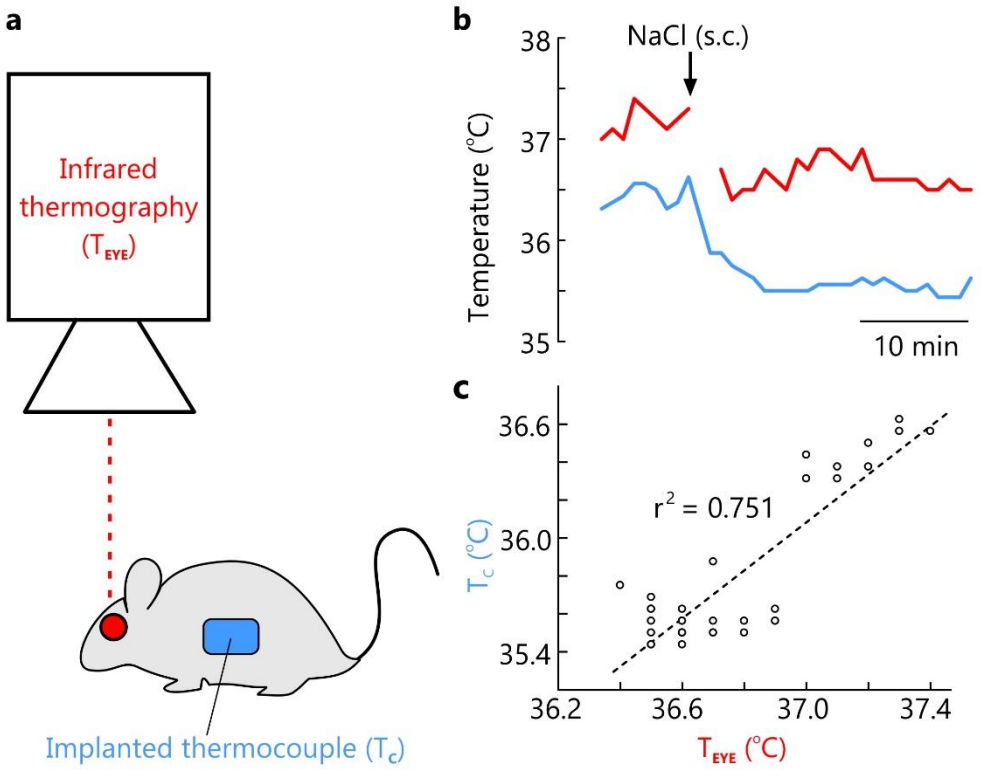

Extended Data 1. Validation of infrared thermography. **a**, schematic illustrates mouse with subcutaneously implanted NanoTag monitoring device used to track temperature via embedded thermocouple (T_C). Mouse was simultaneously filmed from above using a thermography camera and eye temperature (T_{EYE}) was assessed offline using FLIR software. **b**, plots show changes in T_C and T_{EYE} recorded simultaneously in a mouse injected with NaCl (s.c.) to provoke a lowering of body temperature. Note that changes in T_{EYE} and T_C parallel each other and that T_{EYE} is about 1°C higher than T_C. **c**, graph shows all T_C samples plotted as a function of T_{EYE}. Note the strong correlation between values obtained with the two methods.

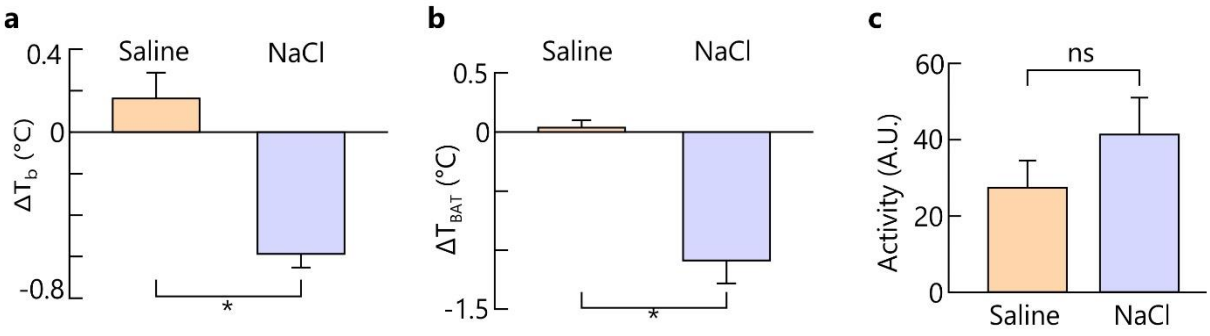

Extended Data Figure 2. Salt, but not saline, reduces T_b and T_{BAT} in mice. a, Bar graph shows T_b changes induced by s.c. saline or 2 M NaCl in GAD^{Cre} mice (n=4; mean ± s.e.m., paired *t*-test). **b**, Bar graph shows T_{BAT} changes induced by s.c. saline or 2M NaCl injection in these same mice (n=4; mean ± s.e.m., paired *t*-test). **c,** Average locomotor activity measured 10 minutes after s.c. injection of saline or 2 M NaCl in wild-type C57BL/6 mice (Saline n=8, NaCl n=8, *t*-test). ns $p>0.05$, *$p<0.05$

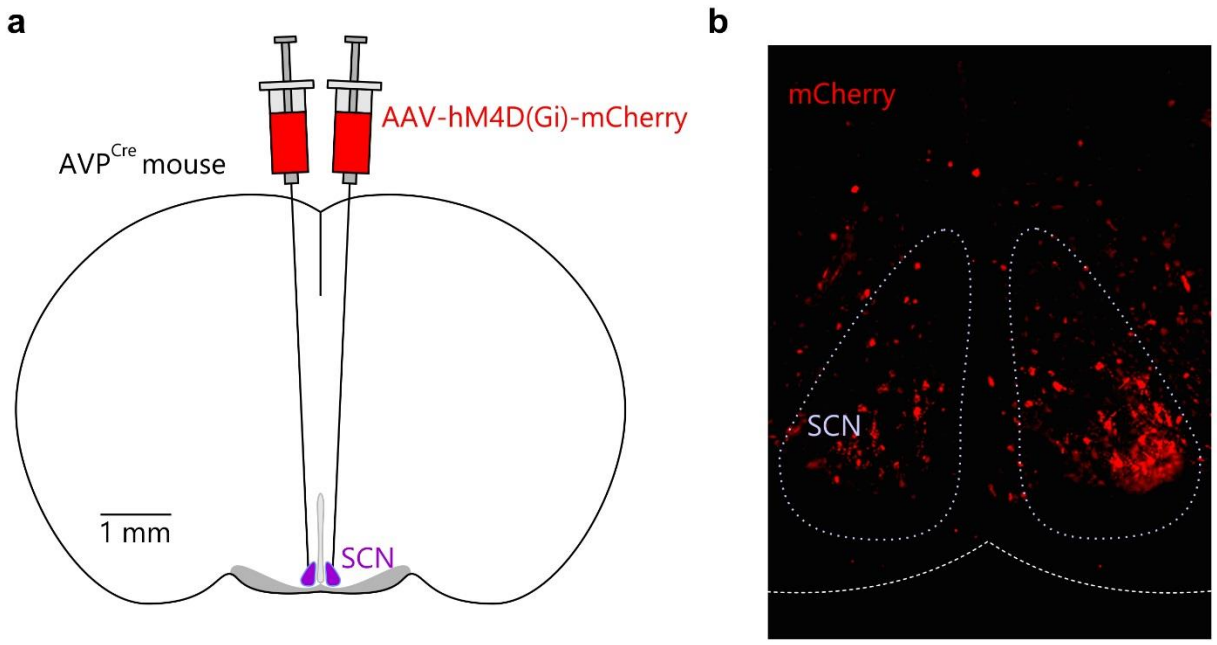

Extended Data Figure 3. Chemogenetic inhibition of SCN^{VP} neurons. a, Mice expressing Cre recombinase selectively in VP neurons (AVP^{Cre}) received bilateral injections of AAV DIO-hM4D(Gi) into the SCN and were allowed to recover for >3 weeks. **b,** The SCN of these animals contained many neurons which expressed the mCherry reporter.

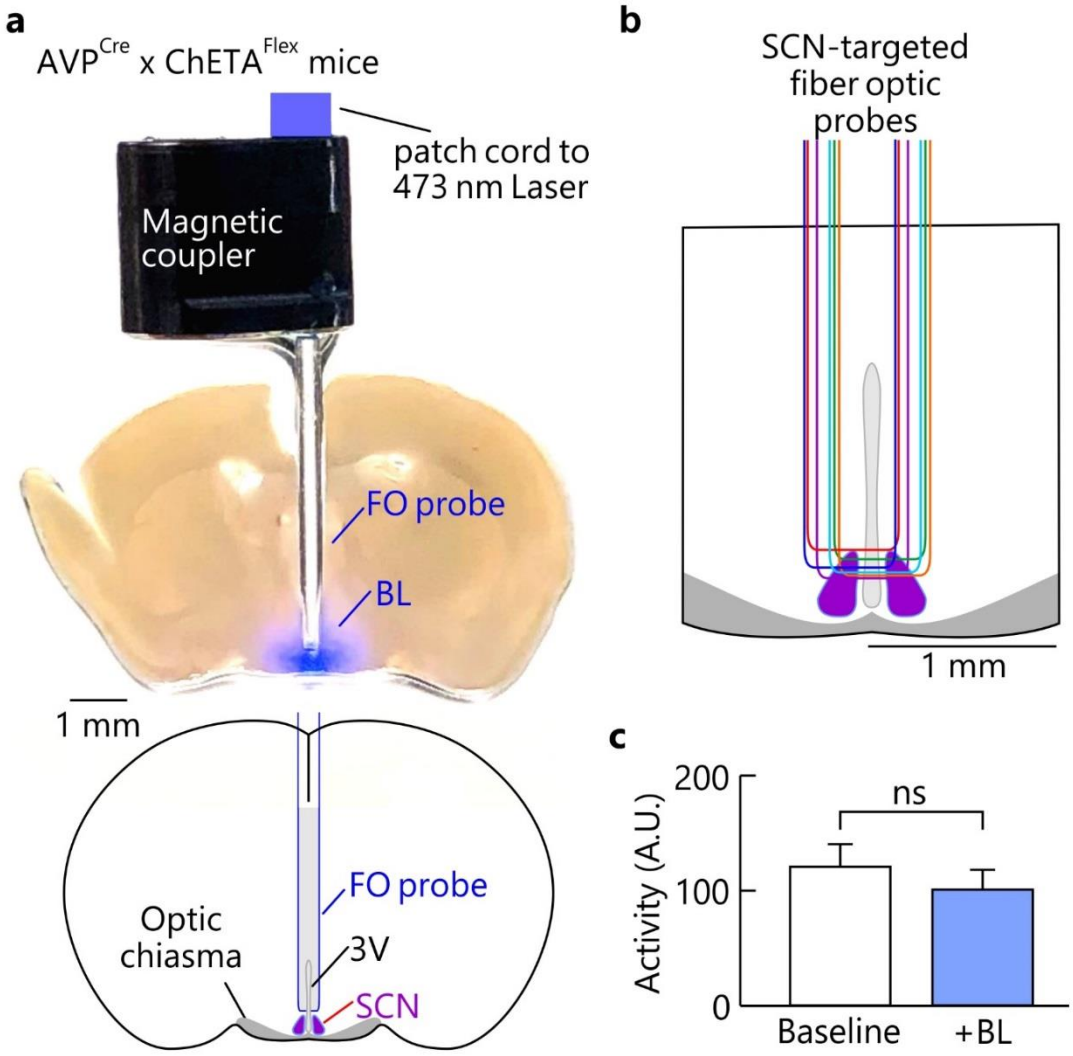

Extended Data Figure 4. Optogenetic activation of SCN^{VP} neurons. a, AVP^{Cre} x ChETA^{Flex} mice were implanted with a fiberoptic allowing optogenetic excitation of SCN^{VP} neurons using blue light (BL, 473 nm). These mice were implanted in the midline, through the third ventricle (3V), with a fiberoptic (FO) probe targeting the dorsal edge of the SCN (upper is a photo illustrated the arrangement shown as a schematic in the lower panel). Note from the photo that BL diffuses bilaterally to both SCNs. The FO probe was mounted through a magnetic coupler allowing attachment of the patch cord carrying BL from the 473 nm laser. **b,** Schematic diagram illustrates the histologically-determined position of the FO tip for the animals used in this study. **c,** Bar graph shows mean (±s.e.m.) changes in locomotor activity induced by BL (+BL; 5 hz, 50 ms pulse, 23 mW, 30 min) delivered to the SCNs of AVP^{Cre} x ChETA^{Flex} mice instrumented as shown in **a**. Stimulation of SCN^{VP} neurons with +BL did not significantly affect locomotor activity at 30 mins

compared to baseline (average locomotor activity measured before optogenetic stimulation; n=6, mean ± s.e.m., paired *t*-test). ns p>0.05

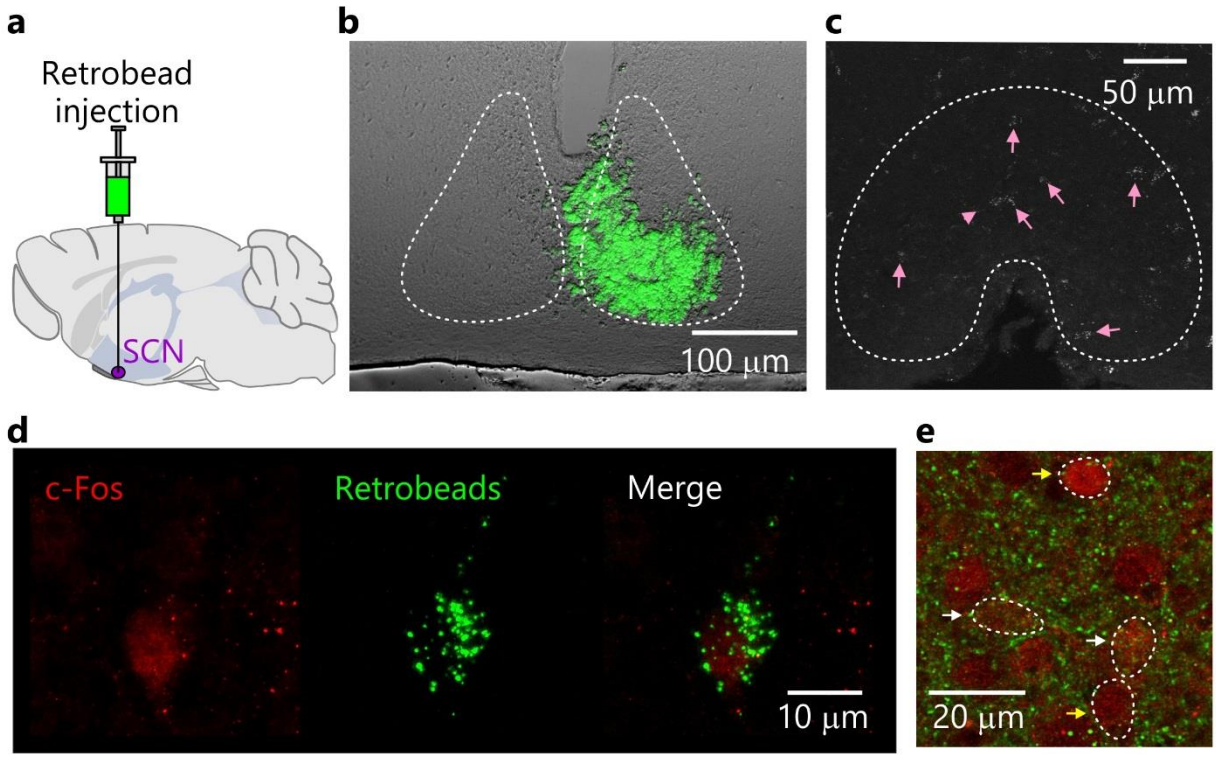

Extended Data Figure 5. OVLT→SCN neurons are sodium sensitive. a, Schematic of a unilateral injection of retrograde microspheres in the SCN of a wild-type C57BL/6 mouse. **b,** Merged brightfield and fluorescence micrograph showing the site of injection (beads in green) in one of 4 mice tested. **c,** Confocal image of a coronal OVLT section from the brain in **b.** The pink arrows point to OVLT neurons labelled with retrogradely transported beads. The dotted line delineates the OVLT. **d**, Animals were injected s.c. with 2 M NaCl and perfused with fixative 90 mins later. Expression of c-Fos was observed in retrogradely labelled OVLT neurons. **e**, Wild-type mice were injected s.c. with 2 M NaCl and perfused with fixative 90 mins later. Micrograph shows expression of immunolabelled c-Fos in red and GAD67, a marker for GABA neurons, in green in the OVLT. The yellow arrows point to c-Fos^{+}/GAD67^{-} neurons, and the white arrows point to c-FOS^{+}/GAD67^{+} neurons.

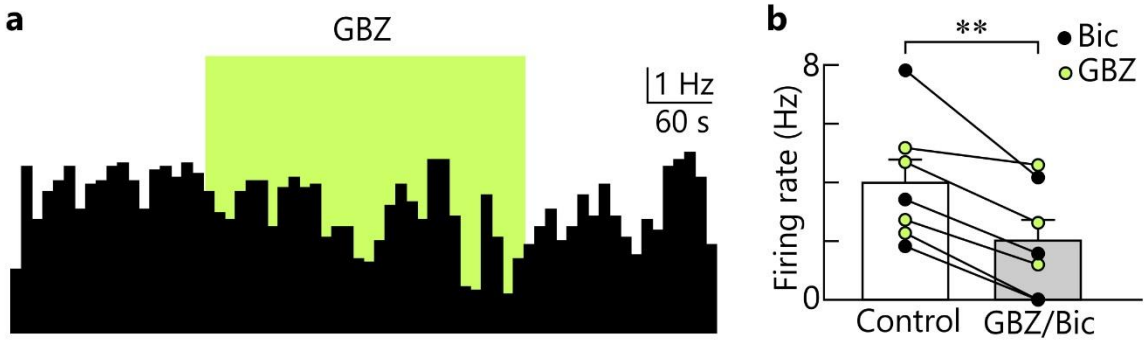

Extended Data Figure 6. **GABA$_A$R antagonists reduced spontaneous action potential firing rate of SCN^{VP} neurons. a**, Frequency plot shows changes in firing rate evoked by 20 µm gabazine (GBZ) on an SCN^{VP} neuron in the presence of 3 mM Kyn. **b,** Bar graph shows mean ± s.e.m. firing rate observed in the absence (control) and presence of GABA$_A$R antagonists (Bicuculine, Bic or GBZ), in 7 neurons from 5 slices. (paired *t*-test). ** $p<0.01$

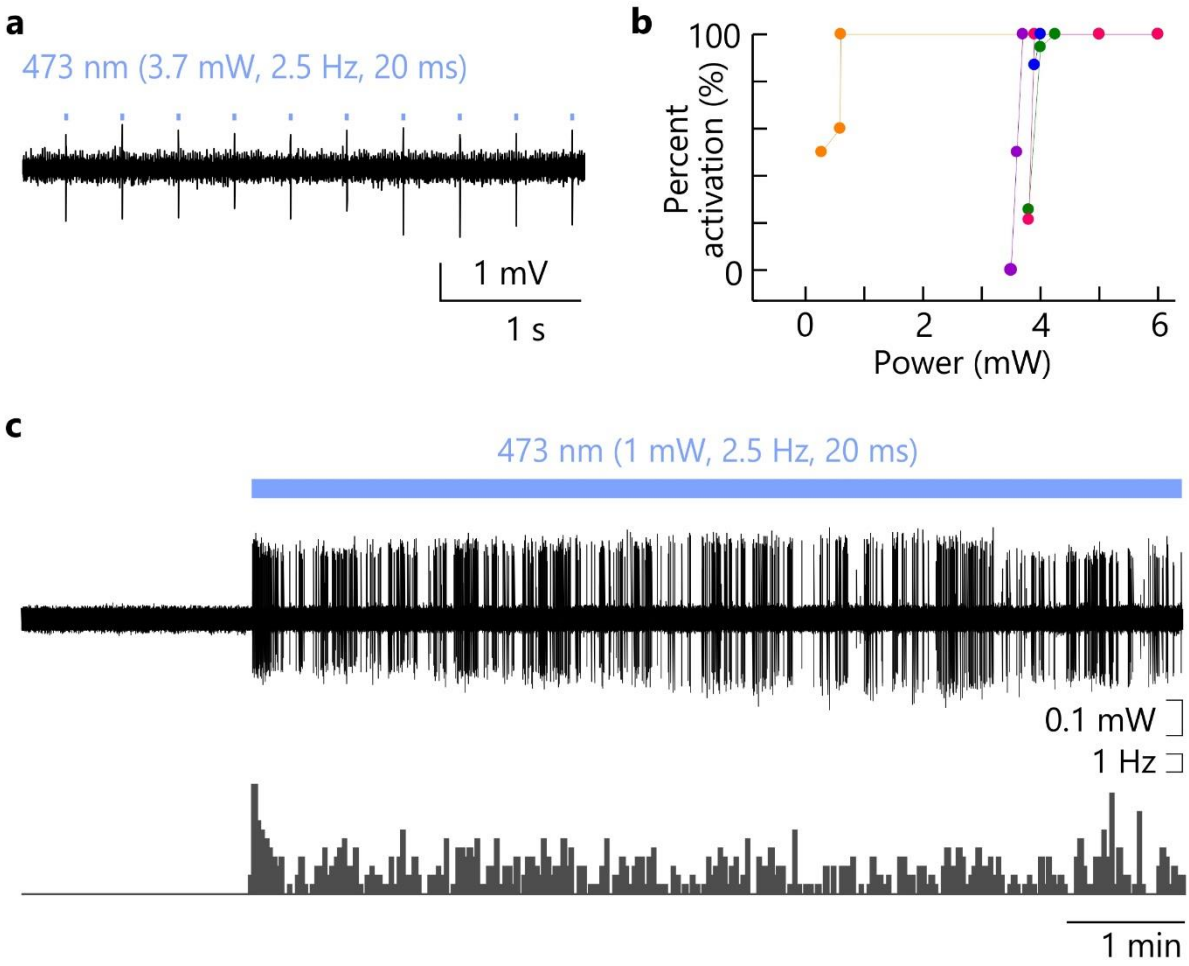

Extended Data Figure 7. Optogenetic stimulation of ChR2 expressing OVLT^{GABA} neurons. **a,** Cell-attached recording of an OVLT^{GABA} neuron expressing ChR2 driven by local delivery of AAV fDIO-ChR2-EYFP in a VGAT^{Flp} x AVP^{Cre} mouse. Note the spiking response to every light pulse. **b,** Plots of efficacy of optogenetic excitation (percent activation) measured in 5 neurons from 2 slices. Note that all cells display 100% excitation when exposed to blue light with an intensity >4 mW. **c,** Repetitive optogenetic stimulation at 2.5 Hz mediated sustained excitation for 20 minutes (only 10 mins shown).

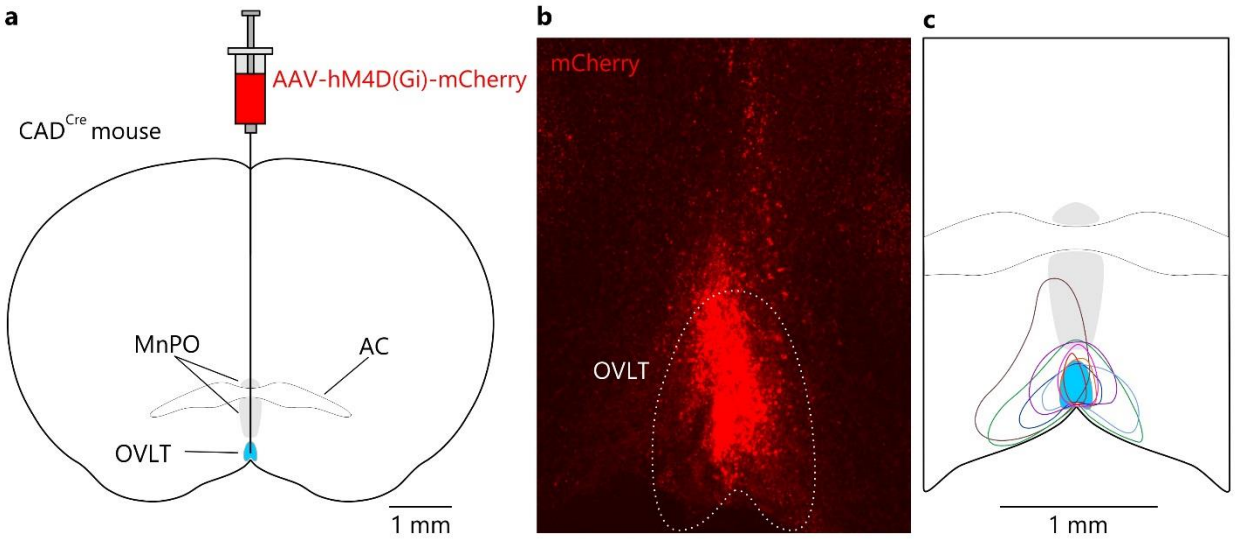

Extended Data Figure 8. Chemogenetic inhibition of OVLT^{GAD} neurons. a, Schematic illustrating a coronal view of the brain at the level of the OVLT, Median preoptic nucleus (MnPO) and anterior commissure (AC). GAD^{Cre} mice were injected with AAV DIO-hM4D(Gi) into the OVLT and were allowed to recover for >3 weeks. **b,** Animals showed intense expression of the mCherry reporter. **c,** Histological assessment of the location of AAV-driven expression based on inspection of mCherry signal in the 8 animals used in this study. Note that all injections included the OVLT.

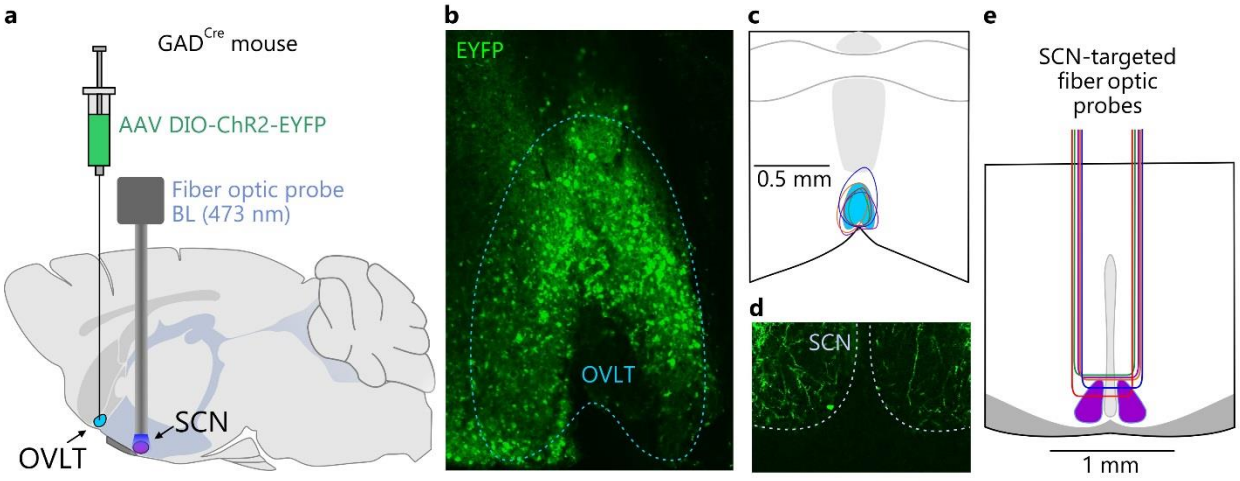

Extended Data Figure 9. Optogenetic activation of GABAergic OVLT neuron axon terminals in the SCN. a, GAD^{Cre} mice were injected with AAV DIO-ChR2-EYFP into the OVLT and were allowed to recover for >3 weeks. **b,** Animals showed intense expression of the EYFP reporter in the OVLT area. **c,** Histological assessment of the location of AAV-driven expression based on inspection of EYFP signal in the 5 animals used in this study. Note that all injections included the OVLT. **d,** Expression of EYFP containing axons of $OVLT^{GAD}$ neurons in the SCN. **e**, Relative placement of the fiberoptic probes in the same 5 animals.

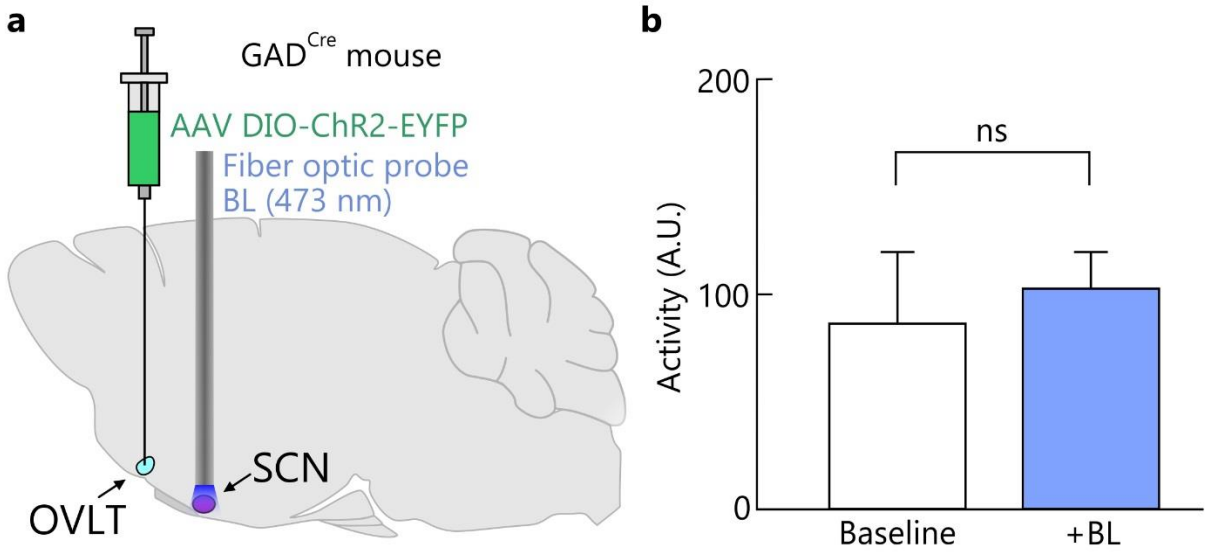

Extended Data Figure 10. Optogenetic stimulation of OVLT^{GAD} neurons does not reduce locomotor activity. a, GAD^{Cre} mice were injected with AAV DIO-ChR2-EYFP in the OVLT and implanted with a fiberoptic targeting the SCN. **b,** Averaged locomotor activity of these mice when blue light (+BL) was delivered bilaterally to the SCN. Stimulation of OVLT^{GAD} neuron axon terminals with +BL (2.5 hz, 20 ms pulse, 5-10mW, 30 min) did not significantly affect the average locomotor activity at 30 mins compared to baseline (average locomotor activity measured before optogenetic stimulation; n=5, mean ± s.e.m., paired *t*-test). ns $p>0.05$

Methods

Animals. Animals were treated in strict accordance with the guidelines outlined by the Canadian Council on Animal Care (http://www.ccac.ca/), and experiments adhered to protocols approved by the Facility Animal Care Committee of McGill University (protocol no. 1190). C57BL/6 mice (60−90 d) were obtained from Charles River Laboratories, St−Constant, QC). AVP^{Cre} (VP-IRES2-Cre-D) knock in mice were bred in our colony with ChETA (R26-CAG-LSL-2XChETA-tdTomato), ArchT mice (Ai40D), or with $VGAT^{Flp}$ (Slc32a1-2A-FlpO-D; obtained from Jackson Laboratories, Bar Harbor, ME). GAD^{Cre} (Gad2-IRES-Cre; obtained from Jackson laboratories) mice were bred in our colony and were also bred with GCaMP6f mice (Ai95(RCL-GCaMP6F)-D; obtained from Jackson Laboratories). All experiments were performed on male animals. *In vitro* experiments were performed on mice aged 2−6 months, and *in vivo* mouse experiments were done on animals aged 2−6 months. Animals were subjected to a strict 12:12 light:dark cycle unless they underwent the phase shift experiment, wherein they were exposed to constant darkness for up to 8 days.

SCN^{VP} Firing Rate. Horizontal hypothalamic slices containing the OVLT and SCN were prepared from 2−6-month-old male ArchT or ChETA mice. These animals were not subjected to any behavioural or optogenetic experiments prior to slice preparation. Mice anesthetized with isoflurane were killed by decapitation from ZT12−ZT16. The brain was rapidly removed and immersed in near freezing (0 to 4°C) oxygenated (95% O_2, 5% CO_2) artificial cerebrospinal fluid (ACSF) composed of the following (in mM): 128 NaCl, 3 KCl, 1.23 NaH_2PO_4, 1.48 $MgCl_2$, 2 $CaCl_2$, 25.95 $NaHCO_3$ and 10 D-glucose (all obtained from Sigma Chemical Corp., St-Louis, MO, except for NaCl and $CaCl_2$, which were purchased from Fisher Scientific, St-Laurent, QC). A trimmed block of brain was glued cortex down with the rostral pole facing upwards to a mounting block angled 34° relative to the horizontal plane. A single 350-μm slice was then obtained[215] and transferred dorsal side up to a beaker containing warmed (32 °C) oxygenated ACSF and allowed to incubate for 60 min. It was then transferred dorsal side up to a recording chamber where it was perfused with warmed (32 °C) oxygenated ACSF at a rate of 2–3 ml min^{-1}. Green fluorescence in ArchT mice was detected using EN GFP 41017 filter cube (Chroma Technology Corp., Bellows Falls, VT) and red fluorescence in ChETA mice was detected using 49004 (Chroma Technology

Corp., Bellows Falls, VT). Electrodes were visually guided to the cell using a motorized micromanipulator (SD Instruments Inc., Grants Pass, OR) and cell-attached recordings were made using a MultiClamp 700B amplifier (Molecular Devices Corp., Sunnyvale, CA). Membrane voltage was digitized via a Digidata 1440A interface coupled to a personal computer running Clampex 10.3 software (Molecular Devices). A bandpass filter was applied during cell-attached recordings (800 Hz–1.8 kHz). Patch pipettes were back filled with ACSF and their resistance in the bath were 5.5−7.5 MΩ. Cell-attached recordings for firing rates of SCN^{VP} neurons during the dark period were performed from ZT13−24. Cell-attached recordings from SCN^{VP} neurons were obtained by making a loose seal. If cells did not fire during the recording, a brief zap of 25 □s was delivered at the end of the recording to evoke firing in order to confirm they were indeed silent cells that were otherwise capable of firing detectable action potentials. The average firing rate was calculated by dividing the total number of spikes recorded over a period of 60−120 s. All analyses were done using pClamp 10.4 and Sigmaplot 12.0

Activity and temperature analysis. Activity (detected by accelerometry) and temperature (detected by thermocouple) of mice were recorded using NanoTag implantable recording devices (Stoelting, Chicago, IL). Mice were anesthetized with isoflurane and a small incision in the back was made to insert the NanoTag subcutaneously. Data were collected at 1-minute intervals for both temperature and activity for the duration of the experiment. To retrieve the data, NanoTag software and an RFID card reader/writer were used (Stoelting, Chicago, IL). To measure average activity levels (Extended Data Fig. 2, 4 and 10), activity units were averaged before the stimulus (40-50 mins), +10 mins post injections, or +30 mins post blue light (6 min averages).

Temperature analysis using thermography. Measurements of T_{BAT} and T_b were obtained using a thermal camera (E85: 384X288 Thermal Camera) with a 42° lens (FLIR, Wilsonville, OR). The upper dorsal region of mice was shaved in order to obtain accurate T_{BAT} values. T_{BAT} and T_b were analyzed using FLIR Tools V 6.4. For each frame analyzed, a 9 pixel ROI was centered over the BAT or EYE^{361} to achieve the maximal T value possible. Baseline T values were obtained from an average of 2 values obtained between -10 and 0 minutes. Values after stimulation were expressed as change in T relative to baseline (+10 minutes for chemogenetic experiments and +30

minutes for optogenetic experiments). Thermographic images were converted to 8-bit images and were assigned LUTs customized to facility viewing using ImageJ 1.50a (NIH,Bethesda, MD).

***In vivo* chemogenetic experiments.** For chemogenetic experiments, animals were injected at ZT19 with 2 M NaCl (8 µl/g) with DMSO (1 mg/kg) or with Clozapine-N-oxide (CNO; 1 mg/kg; Bio-Techne, Minneapolis, MN) dissolved in DMSO. Chemogenetic experiments were performed on AVP^{Cre} mice injected bilaterally in the SCN (from Bregma: X: + 0.1 mm, Y: +/- 0.1 mm, Z: -5.6 mm) and on GAD^{Cre} mice injected in the OVLT (X: + 0.9 mm, Y: 0 mm, Z: -4.85 mm) with AAV2/9-CAG-DIO-hM4D(Gi)-mCherry (Neurophotonics, Laval, QC). Following testing, serial coronal sections (200 µm thick) were cut to confirm the locus of virus expression. Imaging was performed using an FV3000 confocal microscope (Olympus Canada, Richmond Hill, ON).

***In vivo* optogenetic experiments.** Optogenetics experiments were performed on AVP^{Cre}x$ChETA^{Flex}$ transgenic mice and on GAD^{Cre} mice injected with AAV2/9-EF1a-DIO-hChR2(E123T/T159C)-EYFP in the OVLT (Neurophotonics). Blue light (473 nm DPSS Laser system, Laserglow technologies, Toronto, ON) was delivered over the SCN through an implanted fiberoptic probe (X: +0.1, Y: 0 mm, Z: -5.6 mm; slim titanium magnetic receptacle, 480 □m fiber optic diameter/500 µm diameter with coating/6.6 mm in length, numerical aperture 0.63, Doric Lenses, Quebec, QC), connected to a mono fiberoptic patchcord (0.25 m), which is connected to another mono fiberoptic patchcord (2 m) via a fiberoptic rotary joint. Blue light was delivered for 30 minutes within a time range from ZT19-20.5. Specs used for GAD^{Cre} mice: 2.5 Hz, 5-10 mW, 20 ms pulse; AVP^{Cre}x$ChETA^{Flex}$: 5 Hz, 23 mW, 50 ms pulse[215]. This same set up was used to test the effects of the patchcord alone on animals in the absence of blue light. Serial coronal sections (200 µm thick) were cut to determine the location of the virus injection in the OVLT and the position of the tip of the fiberoptic cannula in the SCN. Data from 1 animal was rejected because there was ChR2-EYFP labelling in the SCN following injection in the OVLT.

Retrograde fluorescent microspheres. C57BL/6 mice (60 d) were anesthetized with isoflurane and stereotaxically injected with FluoSpheres (0.04 µm, yellow-green fluorescent 488 nm, 5%

solids, azide free, ThermoFisher Scientific, Waltham, MA) unilaterally into the SCN (100−200 nl; from Bregma, X: 0.1 mm, Y: - 0.1 mm, Z: -5.6, Extended Data Fig. 6) with a Neuros syringe (0.5 µL, 32 gauge, Hamilton Co., Reno, NV) over 5−10 minutes. Retrograde transport was allowed for 7 days, after which the animals were injected with 2 M NaCl (8 µg/kg) 90 minutes prior to transcardial perfusion. Mice were anesthetized with isoflurane and perfused via the heart with 10 ml of PBS followed by 300 ml of PBS containing 4% PFA. The brains were extracted and postfixed by immersion for 48 h in 4% PFA in PBS. A vibratome was used to obtain serial coronal tissue sections (50 µm thick). Sections were blocked with 10% normal goat serum (in PBS containing 0.3% Triton-X) and incubated overnight at 4°C with primary antibodies. Following wash, sections were incubated for 1 h with fluorescently labeled secondary antibodies. Sections were then washed and mounted on coverslips using Prolong Gold Antifade reagent (Life Technologies, Carlsbad, CA). All images were acquired using a confocal microscope (FV1000, Olympus Canada). Tissue sections were processed using a rabbit polyclonal c-Fos antibody (EMD Millipore, Billerica MA; 1:5000; in OVLT). Secondary antibodies were fluorescently labeled Alexa Fluor-conjugated (568 nm; Life Technologies; 1:500).

c-Fos and GAD67 colocalization. C57BL/6 mice (60 d) were injected with 2 M NaCl and transcardially perfused as described above. Tissue sections from mice (50 µm) were processed using a rabbit polyclonal c-Fos antibody (EMD Millipore, Billerica MA; 1:5000) together with a mouse anti-GAD67 (Glutamic acid decarboxylase-67) monoclonal antibody (MAB5406, 1:200; EMD Millipore; in OVLT). Secondary antibodies were fluorescently labeled Alexa Fluor-conjugated (488 nm and 568 nm; Life Technologies; 1:500).

Retrograde labelling of OVLT^{GAD} neurons. GAD^{Cre} mice (2 mo) were anesthetized with isoflurane and stereotaxically injected with rAAV2-pCAG-FLEX-tdTomato virus (Janelia Research Campus, Ashburn, VA) unilaterally into the SCN (50 nl; X: -0.2 mm, Y: +0.2 mm, Z: -5.55 mm) with a Neuros syringe (0.5 µL, 32 gauge). Animals recovered for 3-4 weeks, after which they were injected with 2 M NaCl 90 minutes prior to transcardial perfusion. Immunocytochemistry was performed as previously described. Tissue sections were processed using a rabbit polyclonal c-Fos antibody (EMD Millipore; 1:5000; in OVLT). Secondary

antibodies were fluorescently labeled Alexa Fluor-conjugated (488 nm; Life Technologies; 1:500). Images were acquired with a FV1000 confocal microscope.

OVLT^{GAD} neurons are intrinsically osmo/sodium-sensitive in mouse brain slices. Horizontal slices from GAD^{Cre}xGCaMP6f^{Flex} transgenic mice were obtained at ZT4-6. Fluorescence of GCaMP6f in OVLT^{GAD} neurons was observed using the EN GFP 41017 filter cube. Images were collected using Imaging Workbench 6.0 (INDEC BioSystems, Santa Clara, CA) at a rate of 7 image every 1 s (exposure 0.1 s). All recordings were done in the presence of Kynurenic Acid (Kyn; 3 mM) and Gabazine (GBZ; 20 µm; all obtained from Sigma Chemical Corp.). Once adequate baseline was obtained, a 10 mM NaCl stimulus was bath applied over the slice. Changes in fluorescence (% ΔF) were determined from background corrected images of basal fluorescence (F_0) and peak fluorescence in the presence of NaCl (F_{NaCl}) using the equation $\%\Delta F=100[(F_{NaCl}-F_0)/F_0]$. To determine if OVLT^{GAD} neurons also showed an increase in electrical activity following 10 mM NaCl bath application, cell-attached recordings were obtained from GAD^{GCaMP6f} neurons as previously described. All recordings were done in the presence of Kyn and GBZ. The average firing rate during baseline and during NaCl application was calculated by dividing the total number of spikes recorded over a period of 60 s.

GABA is excitatory on SCN^{VP} neurons during the dark period. Brain slices from ChETA and ArchT mice were obtained as previously described and recordings were performed from ZT17−24 in the presence of Kyn (3 mM). Gramicidin (Sigma) was dissolved in DMSO at a concentration of 0.2 mg/µl and diluted 1:500 into internal pipette solution which was either normal ACSF (n=11) or K-gluconate internal (n=12) (in mM): 140 K^+-gluconate, 2 $MgCl_2$, 10 HEPES, 2 ATP(Na_2), 0.4 GTP(Na_2) (pH adjusted to 7.25 with NaOH). Patch pipettes (4−6 MΩ) were backfilled with the gramicidin mixed internal. Gigaohm-seals were quickly established with target cells, then E_{GABA} measurements were made after the pipette resistance dropped sufficiently, which typically took 10−15 minutes. Cells were voltage-clamped at -50 mV, and voltage steps were applied ranging from -100 to +10 mV during which electrical stimulation of focal GABA afferents were performed with a bipolar electrode coupled to a DS2 isolated stimulator (0.5 ms; 10-50 µA). The amplitudes of evoked or spontaneous postsynaptic currents at each voltage were measured from 1-3 trials and

plotted as a function of voltage. A linear fit was used to determine E_{GABA} for each cell tested. To confirm that E_{GABA} values observed by perforated patch were not affected by rupture of the patch, negative pressure was applied at the end of the recording to establish the whole cell configuration, and E_{GABA} was reassessed to confirm the value predicted by the Nernst equation (0 mV ACSF internal; -87 mV K-gluconate internal). Only cells in which E_{GABA} values were not affected by patch rupture were retained for analysis. To confirm that stimulation of GABA afferents causes excitation of SCN^{VP} neurons, cell-attached recordings were obtained using pipettes filled with ACSF in the presence of Kyn (ZT17−24). Afferents were typically stimulated at 0.03 to 1 Hz. Spiking response rate was determined by dividing the number of spikes elicited within a 30 ms window after stimulation, from 4-8 consecutive sweeps during baseline and during GBZ application. Spike threshold was determined in whole-cell current clamp mode as the baseline voltage at which the rising phase of a spontaneous action potential exceeded 10 V/s. The effects of GBZ or Bicuculine (Bic; 10 µM; Tocris Bioscience, Bristol, UK) on spontaneous action potential firing of SCN^{VP} neurons were determined by comparing firing rates during baseline and in the presence of drug.

Effects of NaCl on mouse brain slices. Brain slices from ChETA and ArchT mice were obtained as above and recordings were performed from ZT17−24. Whole-cell voltage clamp recordings from SCN^{VP} neurons were made using pipettes backfilled with either a K-gluconate internal (as above) or with a Cs^+ internal (in mM): 140 CsMeS, 10 HEPES, 2 $MgCl_2$, 2 ATP(Na_2), 0.4 GTP(Na_2) (pH adjusted to 7.25 with NaOH). Kyn (3 mM) was added to the ACSF when using a Cs^+ internal. The rate of spontaneous GABA events was determined using a template approach during 60-120 s of baseline, in the presence of 10 mM NaCl, and after wash. Cell-attached recording of the spontaneous firing rate of SCN^{VP} neurons during baseline and NaCl application were obtained in the presence of kyn.

***In vitro* Optogenetic stimulation of OVLT GABAergic neuron axon terminals within the SCN.** Horizontal slices were obtained from $VGAT^{Flp}xAVP^{Cre}$ mice previously injected with AAV2/5-EF1a-fDIO-hChR2(H134R)-eYFP in the OVLT (X: +0.9 mm, Y: 0 mm, Z: -4.85; Deisseroth Lab, Stanford) and AAV2/8-EF1a-DIO-mCherry bilaterally in the SCN (Z: +0.1 mm,

Y: +/- 0.1 mm, Z: -5.6 mm; Neurophotonics, Laval). Cell-attached recordings (ZT17−24) were obtained from identified SCN^{VP} neurons. Blue light was delivered over the SCN (2.5 Hz, 1-20 ms pulse, 2-5 mW) through a fiberoptic probe as previously described. The spike rates were determined during 15-60 s of baseline and during blue light stimulation.

Phase shift analysis. Animals were acclimated to the housing conditions for 4-7 days. Following 4 days of standard 12:12 light:dark (LD), animals were injected at ZT19 or optogenetically stimulated for 30 minutes between ZT19−20.5, after which animals were kept in constant darkness for the remainder of the experiment (DD). Onset times of locomotor activity were determined using ClockLab 6.0 (Actimetrics, Wilmette, IL) where onset time in LD was established as the average of software determined onset in days 1-4, and the onset time of the first day in DD was predicted by a linear fit based on the onset times of all days in DD. The phase shift was determined by subtracting the predicted onset time on day 1 in DD from the averaged onset time in LD. Offset times were determined using the same approach. ClockLab fit parameters were adjusted as required to obtain the best visual fit. Alpha was determined as the difference between the predicted offset and onset times in DD. The periodogram was constructed from days 1-5 in DD from an average of 5 mice that were tested with saline (0.9 % NaCl) or 2 M NaCl in separate phase analysis trials. Actograms in Fig.4a,b show accelerometer activity above 20 a.u. (to reduce noise; obtained with NanoTags).

Statistical analysis. All group data, other than spike threshold, are reported or displayed as means ± s.e.m. and the exact sample size is provided for each experimental group or condition either in the text. Spike threshold shows mean ± standard deviation. Information about sample collection is also provided where relevant (e.g. number of trials per animals, or sections per brain). Differences between groups (two-sided) were compared using Sigmaplot 12.0 (Systat Software, Inc., San Jose, CA). The software first assessed normality of the data distribution. In all cases where the normality test failed, a suitable non-parametric test was performed. All tests used for comparisons are specified in the text.

References

1 Mohawk, J. A., Green, C. B. & Takahashi, J. S. Central and peripheral circadian clocks in mammals. *Annu Rev Neurosci* **35**, 445-462, doi:10.1146/annurev-neuro-060909-153128 (2012).

2 Colwell, C. S. Linking neural activity and molecular oscillations in the SCN. *Nat Rev Neurosci* **12**, 553-569, doi:10.1038/nrn3086 (2011).

3 Reppert, S. M. & Weaver, D. R. Coordination of circadian timing in mammals. *Nature* **418**, 935-941, doi:10.1038/nature00965
nature00965 [pii] (2002).

4 Cuddapah, V. A., Zhang, S. L. & Sehgal, A. Regulation of the Blood-Brain Barrier by Circadian Rhythms and Sleep. *Trends Neurosci* **42**, 500-510, doi:10.1016/j.tins.2019.05.001 (2019).

5 Gizowski, C., Zaelzer, C. & Bourque, C. W. Clock-driven vasopressin neurotransmission mediates anticipatory thirst prior to sleep. *Nature* **537**, 685-688, doi:10.1038/nature19756 (2016).

6 Gizowski, C. & Bourque, C. W. The neural basis of homeostatic and anticipatory thirst. *Nat. Rev. Nephrol.* **14:** , 11-25 (2018).

7 Windle, R. J., Forsling, M. L. & Guzek, J. W. Daily rhythms in the hormone content of the neurohypophysial system and release of oxytocin and vasopressin in the male rat: effect of constant light. *J Endocrinol* **133**, 283-290 (1992).

8 Rittig, S. *et al.* Adult enuresis. The role of vasopressin and atrial natriuretic peptide. *Scand J Urol Nephrol Suppl* **125**, 79-86 (1989).

9 Willis, C. K., Menzies, A. K., Boyles, J. G. & Wojciechowski, M. S. Evaporative water loss is a plausible explanation for mortality of bats from white-nose syndrome. *Integrative and comparative biology* **51**, 364-373, doi:10.1093/icb/icr076 (2011).

10 Konishi, M., Nagashima, K. & Kanosue, K. Systemic salt loading decreases body temperature and increases heat-escape/cold-seeking behaviour via the central AT1 and V1 receptors in rats. *The Journal of physiology* **545**, 289-296, doi:PHY_027029 [pii] (2002).

11 Buijs, R. M., Guzman Ruiz, M. A., Mendez Hernandez, R. & Rodriguez Cortes, B. The suprachiasmatic nucleus; a responsive clock regulating homeostasis by daily changing the setpoints of physiological parameters. *Auton Neurosci* **218**, 43-50, doi:10.1016/j.autneu.2019.02.001 (2019).

12 McKinley, M. J. *et al.* The median preoptic nucleus: front and centre for the regulation of body fluid, sodium, temperature, sleep and cardiovascular homeostasis. *Acta Physiol (Oxf)* **214**, 8-32, doi:10.1111/apha.12487 (2015).

13 Bourque, C. W. Central mechanisms of osmosensation and systemic osmoregulation. *Nature reviews. Neuroscience* **9**, 519-531, doi:nrn2400 [pii]
10.1038/nrn2400 (2008).

14 Nagashima, K., Nakai, S., Konishi, M., Su, L. & Kanosue, K. Increased heat-escape/cold-seeking behavior following hypertonic saline injection in rats. *Am J Physiol Regul Integr Comp Physiol* **280**, R1031-1036, doi:10.1152/ajpregu.2001.280.4.R1031 (2001).

15 Zimmerman, C. A., Leib, D. E. & Knight, Z. A. Neural circuits underlying thirst and fluid homeostasis. *Nat Rev Neurosci*, doi:10.1038/nrn.2017.71 (2017).

16 Trudel, E. & Bourque, C. W. Central clock excites vasopressin neurons by waking osmosensory afferents during late sleep. *Nature neuroscience* **13**, 467-474, doi:nn.2503 [pii]
10.1038/nn.2503 (2010).
17 Nomura, K. *et al.* [Na(+)] Increases in Body Fluids Sensed by Central Nax Induce Sympathetically Mediated Blood Pressure Elevations via H(+)-Dependent Activation of ASIC1a. *Neuron* **101**, 60-75.e66, doi:10.1016/j.neuron.2018.11.017 (2019).
18 Tervo, D. G. *et al.* A Designer AAV Variant Permits Efficient Retrograde Access to Projection Neurons. *Neuron* **92**, 372-382, doi:10.1016/j.neuron.2016.09.021 (2016).
19 Wagner, S., Castel, M., Gainer, H. & Yarom, Y. GABA in the mammalian suprachiasmatic nucleus and its role in diurnal rhythmicity. *Nature* **387**, 598-603, doi:10.1038/42468 (1997).
20 Choi, H. J. *et al.* Excitatory actions of GABA in the suprachiasmatic nucleus. *The Journal of neuroscience : the official journal of the Society for Neuroscience* **28**, 5450-5459, doi:10.1523/jneurosci.5750-07.2008 (2008).
21 Mrosovsky, N. Locomotor activity and non-photic influences on circadian clocks. *Biological reviews of the Cambridge Philosophical Society* **71**, 343-372 (1996).
22 Gizowski, C., Trudel, E. & Bourque, C. W. Central and peripheral roles of vasopressin in the circadian defense of body hydration. *Best Pract Res Clin Endocrinol Metab* **31**, 535-546, doi:10.1016/j.beem.2017.11.001 (2017).
23 Meyer, C. W., Ootsuka, Y. & Romanovsky, A. A. Body Temperature Measurements for Metabolic Phenotyping in Mice. *Frontiers in physiology* **8**, 520, doi:10.3389/fphys.2017.00520 (2017).

Chapter 5 – Discussion

Summary of findings

There are multiple ways in which thirst can be stimulated to maintain fluid homeostasis in an organism. Until recent, thirst was generally thought of as a simple feedback reflex that occurred in response to perturbations such as a rise in osmolality or decrease in blood volume, however, as demonstrated in Chapters 2 and 3, need-free water intake is stimulated throughout the day to maintain body hydration near an optimal set point. Indeed, the findings in Chapter 3 reveal a new kind of thirst, termed "anticipatory thirst", whereby the central clock regulates water intake in anticipation of the sleep cycle and the associated reduced water consumption. It is interesting to note that water intake is essentially abolished by optogenetic inhibition of SCN^{VP} fibres within the OVLT during the AP. This begs the question, is water intake exclusively being driven by the clock at this time? Food intake also increases during the AP, which based on the literature would predict the occurrence of prandial thirst. However, our results indicate that AP-water intake is entirely clock driven. Our findings in Chapter 4 unexpectedly reveal that clock-output networks also drive homeostatic responses, such as a decrease in body temperature following a rise in plasma osmolality. Central osmosensors recruit clock-outputs to easily mediate adaptive responses that help animals cope with deviations from set point. It might just be the same for food intake, whereby brain nutrient sensors (e.g. those located in the arcuate nucleus[362]) might also recruit clock-outputs to drive prandial thirst to maintain fluid homeostasis.

The curious case of SCN^{VP} neuron firing

Anticipatory thirst is driven by an increase in the electrical activity of SCN^{VP} neurons, which occurs two hours prior to the dark/light transition thereby driving the excitation of OVLT neurons at this time. In addition, in Chapter 4, we revealed that SCN^{VP} neurons are only quiet from ZT17−22. This is surprising, as circadian canon characterizes the firing pattern of SCN neurons as high during the light and low during the dark period. Further, based on the current literature, one would expect the firing of these neurons to be driven and synchronized by the electrical activity of VIP neurons, whose activity, as mentioned in Section 1.1.4, is driven by light when housed in LD conditions. Perhaps as a whole, the activity pattern is as described; however, our findings would

suggest that subsets of neurons, particularly output neurons, might fire independently of the light cycle. For instance, it is possible that the period of the TTFL of SCN^{VP} neurons is intrinsically faster than 24 h and without synchronizing input from SCN^{VIP} neurons during the dark period, SCN^{VP} neurons fire ahead of the dark/light transition. Alternatively, perhaps their activity is regulated by a different subgroup of neurons during the dark period. It would be important to characterize the firing of all subgroups of identified SCN neurons (e.g. GRP, VIP) to gain a deeper understanding of the specific functions they regulate, instead of simply reporting the combined average firing rate of all neurons within the SCN. Indeed, it has been postulated that there are two functional classes of SCN^{VIP} neurons as defined by their firing patterns. These neurons fire either with tonic or irregular patterns[363], which might indicate that these two populations serve different roles. Our observation that SCN^{VP} neurons do not exhibit a 12 h bout of silence might be an artefact caused by a spatial wave, where not all SCN^{VP} neurons within a horizontal slice are time locked in phase. Indeed, there is evidence that VP expression density varies across the anteroposterior SCN[364]. To gain a better understanding of the activity profile of SCN^{VP} neurons, we would need to obtain 24 h recordings from individual neurons from defined anteroposterior locations.

Move it, there is a new neurotransmitter in town

An interesting finding about the SCN→OVLT pathway is the transmitter that mediates the increase in electrical activity of OVLT neurons. Typically, neuropeptides are thought to primarily modulate neuronal communication, such as bind presynaptic receptors, which can affect synaptic transmission. However, we clearly demonstrate that VP can act as a neurotransmitter on the postsynaptic cell and mediate direct changes in electrical activity. One of the classic criteria for a molecule to be considered a neurotransmitter is that the presynaptic cell must be able to release it in an activity dependent manner. Existing approaches, such as microdialysis and radioimmunoassay used to measure VP concentrations have poor temporal and spatial resolution. To this end, we developed a new technique allowing dynamic detection of peptide release within a specific brain site *in vitro*[365]. Using sniffer cells, we were able to conclusively determine that VP is released in an activity dependent way from the presynaptic neuron and is released within the OVLT.

It has long been hypothesized that neuropeptide release increases with spike frequency and that phasic firing is particularly effective[366]. Unlike neurotransmitters such as GABA and glutamate which are stored in small clear vesicles located within the active zone of the presynaptic neuron, neuropeptides are stored in dense core vesicles and are away further away from the synaptic bouton. It is thought that phasic firing enhances presynaptic calcium and enhances the probability of release of dense core vesicles[367]. However, we show that 5 Hz tonic stimulation can drive neuropeptide release, suggesting that perhaps phasic firing is only required for VP secretion from magnocellular neurosecretory neurons in the supraoptic and paraventricular nuclei. It is possible that non-magnocellular neurons, such as SCN neurons, have different presynaptic morphology or calcium entry dynamics thereby enabling the release of VP more readily.

Given the majority of neurons within the SCN are GABAergic, we initially investigated the possible effect that GABA might exert on OVLT neurons. Interestingly, at the beginning of the 5 Hz train, we observed an initial inhibition of on-ongoing electrical activity caused by summation of inhibitory postsynaptic potentials (IPSP) on OVLT neurons, however this effect would give way to a long-lasting depolarization and excitation of the OVLT neuron, which we then identified as a VP-dependent mechanism. It has been reported that not all SCN^{VP} neurons coexpress GABA[368], and it is highly probable that by using a non-specific approach, such as electrical stimulation, we are activating non-VPergic GABAergic fibres that originate from or adjacent to the SCN. To examine this more carefully, we optogenetically activated the axon terminals of SCN^{VP} neurons terminating within the OVLT and found no evidence of fast synaptic GABA transmission. Although preliminary in nature, this observation suggests the possibility that SCN^{VP} neurons that project to the OVLT do not contain GABA (data not shown). Future studies should investigate whether non-GABAergic SCN neurons can mediate the control of other circadian outputs via peptidergic signaling.

The excitatory action of VP on OVLT neurons is mediated via the activation of a non-selective cation channel. We show this specifically requires the activation of VP V1aRs. Upon VP binding to V1aRs, which is a G-q coupled GPCR, this leads to the activation of protein kinase C that can directly bind and activate non-selective cation channels[369]. Although we do not show that these

effects are directly mediated by ΔNTRPV1, we did observe a high rate of colocalisation between this channel and V1aRs in OVLT neurons (chapter 3). Furthermore, the reversal potential observed in our study (-25 mV) is similar to that reported in previous studies from our lab[370,371]. Despite this evidence, further experiments demonstrating that specific inhibition or knockdown of ΔNTRPV1 abolishes the effect of VP on OVLT neurons are required to conclusively determine that these are the downstream receptors mediating the excitatory effects.

OVLT circuits underlying thirst

Our *in vivo* $V1aR^{-/-}$ mouse data indicates that V1aRs are required to mediate c-Fos activation of OVLT neurons during the AP and drive anticipatory thirst. Importantly, c-Fos expression in SCN^{VP} neurons in $V1aR^{-/-}$ mice still significantly increased during the AP compared to the BP, indicating the disruption is specifically at the level of the OVLT (data not shown). Optogenetic activation of glutamatergic or nitric oxide synthase expressing OVLT neurons ($OVLT^{nNOS}$) has been shown to drive water intake in mice[101,372], however, it remains to be determined whether V1aR OVLT neurons ($OVLT^{V1aR}$) express glutamate and/or nNOS and if direct activation of these neurons can also drive thirst. Furthermore, it remains to be determined if $OVLT^{V1aR}$ neurons drive thirst via the same pathways as $OVLT^{nNOS}$ neurons. It has been shown that a pathway from $OVLT^{nNOS}$ neurons to nNOS MnPO neurons ($MnPO^{nNOS}$) robustly drives thirst. Specific ablation of $MnPO^{nNOS}$ neurons prevents water intake induced by optogenetic stimulation of $OVLT^{nNOS}$ neurons[372], indicating the MnPO is a critical step in the thirst pathway. The projection by which $MnPO^{nNOS}$ neurons drive thirst remains unknown, however it has been recently shown that MnPO neurons expressing PACAP project to the PVT[373]. It is not known whether nNOS and PACAP MnPO neurons represent the same neuronal population. Presumably, the PVT then orchestrates thirst via direct projections to the ACC and/or the IC (Chapter 2). Recent studies taking advantage of novel technologies have significantly advanced our understanding of the circuits underlying thirst; however further work is required to fully decipher these complex neural pathways.

Prevention of anticipatory thirst during sleep

A perplexing paradox arises from our work demonstrating SCN^{VP} neurons drive anticipatory thirst, such that the firing of SCN^{VP} neurons continues to be high during the light period, however water intake stops at the dark/light transition and is limited throughout this period. It is possible that homeostatic regulatory mechanisms are contributing to prevent thirst from occurring. For example, inhibitory osmosensory signals from the gastrointestinal tract might inhibit OVLT and/or MnPO neuron activity thereby preventing the activation of the PVT→ACC/IC pathway. It has been shown that dehydration can drive water intake via an excitatory projection from nNOS SFO neurons (SFO^{nNOS}) to $MnPO^{nNOS}$ neurons[372]. Water intake quickly activates GABAergic MnPO neurons, presumably via gastric signals, that send reciprocal inhibitory projections to SFO^{nNOS} neurons thereby inhibiting their activity and eliminating the excitatory drive from SFO^{nNOS} neurons to $MnPO^{nNOS}$ neurons. This inhibitory gating mechanism at the level of the MnPO prevents continued water intake and overhydration. In addition, it has also been shown that a small subpopulation of MnPO neurons expressing the *Nxph4* locus encodes blood osmolality, and that these neurons are activated by hyperosmolality and are quickly shut off upon water intake[374]. It is likely that the activity of these neurons is gated via oropharyngeal signals, satiation signals from the gastrointestinal tract and signals from the blood. Therefore, despite tonic excitatory input from SCN^{VP} neurons, input from the OVLT may be gated at the level of the MnPO to prevent water intake from occurring overnight. However, further work is required to determine whether GABAergic or *Nxph4* MnPO neurons also feedback onto $OVLT^{V1aR}$ neurons and inhibit their activity following water intake. On the other hand, it is difficult to comprehend how gastric signals only shutoff thirst at the light transition and not during the AP. For instance, mice drink a significant amount of water during a 2 h period in the absence of need, ultimately reducing plasma osmolality below set point. This might indicate that gastric osmosensory signal sensitivity is under clock control during the AP to enable preventative anticipatory thirst to occur. Alternatively, this could suggest that $OVLT^{V1aR}$ neurons do not receive gastric input and/or reciprocal inhibitory input from the MnPO, and bypass the MnPO to independently drive activity within the ACC/IC via the PVT to stimulate thirst during the AP. Moreover, throughout the sleep period, it is possible that the limited water intake is a result of VP depletion from SCN neurons resulting in a decrease in OVLT neuron activity. Another possibility is that $OVLT^{V1aR}$ neurons may feedback onto SCN^{VP} neurons to shut off their activity, however this is speculative. Alternatively, it has been shown that

SCN VIP neurons (SCN^{VIP}) also project to the OVLT[14,375]. It is possible that these are GABAergic in nature, and upon light input, these neurons provide tonic inhibitory input to OVLT neurons; however, if and how SCN^{VIP} output neurons function is entirely unknown. And most simply, perhaps none of these mechanisms occur and $OVLT^{V1aR}$ neurons are constitutively active throughout the light period, however their input to the PVT is gated by rhythmic oscillations generated in the thalamus during sleep, thus preventing thirst from interfering with sleep[170]. Clearly, further work is required to help us understand how anticipatory thirst is gated.

The osmolality switch-up

Although not reported in this thesis, we observed that the serum osmolality (sOsm) of mice is lower during the light period than during the dark period. For example, the average sOsm during the dark period is around 308 mOsm, whereas during the light period values are around 303 mOsm. This is counterintuitive to what one would expect as water intake is limited during sleep, however multiple clock-driven homeostatic mechanisms are in place to mediate this unexpected finding. First, it is likely that the initial reduction in osmolality observed during the dark/light transition occurs as a result of anticipatory thirst. Second, the surge in plasma VP during the late-sleep period enables water reabsorption via the kidneys and natriuresis to occur[84]. Lastly, the daily reduction in core body temperature observed during sleep is likely a key mechanism for maintaining hypoosmotic conditions. For example, in hibernating bats, core body temperature is reduced near ambient temperatures to minimize cutaneous evaporative water loss[376]. Conversely, when rats and humans are subjected to rises in plasma osmolality, their core body temperature decreases as a result[346,347], presumably to reduce the thermal gradient between internal and external environments, thus reducing evaporative water loss and preventing further rises in osmolality. Our findings in chapter 4 reveal that input from $OVLT^{GAD}$ neurons to SCN^{VP} neurons can mediate this homeostatic response.

BAT, but not that kind of bat, drives body temperature changes

Mice housed under standard conditions (20-23°C) are constantly generating heat as they are chronically cold stressed. Animals maintain optimal core body temperature (T_b) primarily via non-

shivering thermogenesis (NST) heat production mediated by BAT[377]. To examine the effects of systemic salt on T_b and the underlying thermoregulatory mechanisms contributing to the associated changes in T_b, we used infrared thermography (IRT) as a non-invasive approach to investigate this question. Although telemetry is considered the gold standard for measuring T_b, this method does not permit independent reporting of BAT temperature (T_{BAT}) changes. Furthermore, although T_b changes monitored using either method paralleled each other, we consistently measured T_b values 1°C lower with telemetry compared to those obtained with IRT. Presumably this is a consequence of the device being implanted subcutaneously and not intraperitoneally. Moreover, the ocular surface maintains the highest temperature and appears to be the most appropriate for rapid measurement of T_b with IRT[378]. Shaving the fur from the upper dorsal region of mice enabled accurate T_{BAT} measurements. Following a salt injection, we observed that mice turn off constitutively active NST, which results in a significant reduction in T_b. The preoptic area (POA), which comprises the OVLT, is thought to be a major coordinator of thermoregulation[379], therefore our experiments probing $OVLT^{GAD}$ neurons were not sufficient to conclusively determine if the $OVLT^{GAD}\rightarrow SCN^{VP}$ pathway is required to mediate this homeostatic response. For instance, photostimulation of $OVLT^{GAD}$ efferents might have antidromically activated neurons in the OVLT thereby regulating NST via SCN-independent pathways. In addition, chemogenetic silencing of $OVLT^{GAD}$ neurons does not eliminate the possibility that $OVLT^{GAD}$ neurons are regulating NST independently. Therefore, we further investigated how direct *in vivo* manipulation of SCN^{VP} neuron activity could mediate T_b. To this end, chemogenetic inhibition of SCN^{VP} neurons prevented the effects of salt on T_b and T_{BAT}, whereas optogenetic stimulation of these neurons mimicked these effects. These findings indicate that unscheduled changes in the electrical activity of SCN^{VP} neurons can indeed drive overt changes in T_b. It is tempting to speculate the activity profile of SCN^{VP} neurons might drive daily temperature rhythms by regulating NST. For instance, the reduced firing activity during the dark period permits an increase in T_b, whereas the high frequency activity during the light enables the drop in T_b. How SCN^{VP} neurons regulate NST remain unknown, however it is possible that SCN efferents project the POA or other hypothalamic nuclei such as the dorsal medial hypothalamus whereby neurons polysynaptically project to BAT[379].

Excited by GABA

An interesting feature of the OVLT→SCN this pathway is that the neurotransmitter involved is ubiquitously known as the classical inhibitory neurotransmitter. In healthy brains, the only non-SCN well characterized effects of excitatory GABA have been reported in the hippocampi of immature developing brains[380]. In the SCN, it has been reported that GABA exerts excitatory effects primarily on neurons located in the dorsal regions and during the dark period[358]. In Chapter 4, we show that GABA is excitatory on SCN^{VP} neurons during the dark period and reveal that the GABA reversal potential ($GABA_{Rev}$) is significantly depolarized (-30 mV), indicating that at resting membrane potentials (-50 mV), GABA is excitatory. Although we did not further investigate the mechanisms underlying why this occurs, there is strong evidence suggesting chloride transporters are differentially expressed within subregions of the SCN and their expression is rhythmically regulated. For instance, the chloride gradient of neurons in the core is primarily regulated by the KCC2 K^+/Cl^- cotransporter, which extrudes chloride out of the cell[381]. Upon GABA binding to $GABA_A$ receptors, chloride enters the neuron resulting in an outwardly hyperpolarizing current. Interestingly, it has been shown that SCN^{VP} neurons express little KCC2[381]. Instead, these neurons are thought to express mainly the NKCC1 $Na^+/K^+/2Cl^-$ cotransporter which drives chloride influx into the cell thereby depolarizing $GABA_{Rev}$[382]. In addition, it has been shown that NKCC1 protein measurements are two-fold higher within the dorsal regions during the dark compared to the light period[358]. Although the advantages of having bipolar effects of GABA within the SCN are unclear, it has been postulated that these differences are required for coupling between the core and shell such that SCN^{VIP} neurons can readily synchronize SCN^{VP} neurons via excitatory GABA[383]. On the other hand, perhaps excitatory GABA transmission is an effective way for neurons within the SCN to differentiate between photic glutamatergic input to the core and non-photic GABAergic input to the shell, enabling specific subsets of neurons to mediate their respective functions. For example, NMDA receptor activation by glutamate is associated with an increase in intracellular calcium, which might alter the timing of the TTFL, whereas GABA activation of $GABA_AR$ would not. Ultimately, further work is required to conclusively determine the functional basis of excitatory GABA within the SCN.

Salt sensing by OVLT neurons

Previous work investigating the neurochemical identity of OVLT neurons that can drive thirst[101], sense changes in extracellular sodium[90], and drive changes in the electrical firing of magnosecretory SON neurons[384] have exclusively reported that these responses are mediated by glutamatergic neurons ($OVLT^{Vglut}$). By contrast, our findings are the first to demonstrate that $OVLT^{GAD}$ neurons, in the absence of fast synaptic transmission, are intrinsically osmo and sodium-sensitive. It has been recently shown that OVLT glial cells expressing Na_x channels export H^+ upon salt detection thereby activating $OVLT^{Vglut}$ neurons via acid-sensing ion channels[90]. Recordings from isolated single $OVLT^{GAD}$ neurons are required to determine whether these neurons can be directly activated by salt and eliminate the possibility of glial-mediated activation. For example, the excitatory effects of salt may be directly mediated via a molecular transduction complex such as TRPV1[385]. Alternatively, these neurons may express channels that can mediate salt-dependent increases in firing such as ENaCs[190], Nav1.6[193] and Na_x[195]. The role of GABAergic OVLT neurons has been largely ignored, however we clearly show that these neurons are critical for transmitting salt-related information to the clock and recruit clock-output networks to drive adaptive homeostatic responses. The OVLT is not a simple homogenous nucleus, and it would be short-sighted to exclude the contributions of GABA neurons in circuits mediating fluid homeostasis.

The salt at the end of the tunnel

Placing animals in the absence of light (DD), is a tried-and-true experimental method that enables us to demonstrate that non-photic stimuli can cause phase shifts by altering clock time. However, in reality, light cycles are almost always present. It is difficult to conceptualize the benefits of non-photic phase shifting in DD and accept that experiments must be done in these conditions. Photic stimulus alone is clearly not sufficient to immediately realign the circadian time of those subjected to shift work or jet lag to local time[386], thus it is likely that non-photic stimuli, in conjunction with light, are key for rapidly reentraining the clock. It would be interesting to show that, under a jet lag protocol, daily salt intake at ZT19 relative to internal circadian time, accelerates recovery from jet lag. On the other hand, our data strongly suggests that non-photic inputs to the SCN can serve acute adaptive benefits. These unexpected findings challenge us to explore the possibility that the

clock is so much more than a simple pacemaker, and instead plays a critical role as an integrator and effector of homeostatic need.

Chapter 6 – Conclusion

The findings presented in this thesis address my key hypotheses of (i) how does the clock drive circadian water intake, and (ii) how does a physiologically relevant non-photic cue alter clock time and output. Although there are enough additional experiments and questions proposed in my discussion to fuel a life time and a half's worth of work, collectively my findings obtained within my short six-year stint provide fundamental new insights into the biology of behaviour, expand our current knowledge of synaptic transmission, and challenge our current view of the role of the circadian clock.

“Here’s to those who wish us well,

and those who don’t can go to hell”

Elaine Benes

The little Kicks

Bibliography

1 Xu, Y. & Pan, D. Interpretation of the Nobel Prize in Physiology or Medicine 2017. *Science China. Life sciences* **61**, 131-134, doi:10.1007/s11427-017-9216-0 (2018).

2 de Mairan, J. J. Observation botanique. *Histoire de l'Académie royale des sciences avec les mémoires de mathématique et de physique tirés des registres de cette Académie*, 35 (1729).

3 Turek, F. W. Circadian neural rhythms in mammals. *Annual review of physiology* **47**, 49-64, doi:10.1146/annurev.ph.47.030185.000405 (1985).

4 Ralph, M. R., Foster, R. G., Davis, F. C. & Menaker, M. Transplanted suprachiasmatic nucleus determines circadian period. *Science (New York, N.Y.)* **247**, 975-978 (1990).

5 Moore, R. Y. & Eichler, V. B. Loss of a circadian adrenal corticosterone rhythm following suprachiasmatic lesions in the rat. *Brain research* **42**, 201-206 (1972).

6 Stephan, F. K. & Zucker, I. Circadian rhythms in drinking behavior and locomotor activity of rats are eliminated by hypothalamic lesions. *Proceedings of the National Academy of Sciences of the United States of America* **69**, 1583-1586 (1972).

7 Silver, R., LeSauter, J., Tresco, P. A. & Lehman, M. N. A diffusible coupling signal from the transplanted suprachiasmatic nucleus controlling circadian locomotor rhythms. *Nature* **382**, 810-813, doi:10.1038/382810a0 (1996).

8 Meyer-Bernstein, E. L. *et al.* Effects of suprachiasmatic transplants on circadian rhythms of neuroendocrine function in golden hamsters. *Endocrinology* **140**, 207-218, doi:10.1210/endo.140.1.6428 (1999).

9 Antle, M. C. & Silver, R. Orchestrating time: arrangements of the brain circadian clock. *Trends in neurosciences* **28**, 145-151, doi:S0166-2236(05)00019-6 [pii] 10.1016/j.tins.2005.01.003 (2005).

10 Moore, R. Y., Speh, J. C. & Leak, R. K. Suprachiasmatic nucleus organization. *Cell Tissue Res* **309**, 89-98, doi:10.1007/s00441-002-0575-2 (2002).

11 Lee, J. E. *et al.* Endogenous peptide discovery of the rat circadian clock: a focused study of the suprachiasmatic nucleus by ultrahigh performance tandem mass spectrometry. *Molecular & cellular proteomics : MCP* **9**, 285-297, doi:10.1074/mcp.M900362-MCP200 (2010).

12 Fliers, E., Noppen, N. W., Wiersinga, W. M., Visser, T. J. & Swaab, D. F. Distribution of thyrotropin-releasing hormone (TRH)-containing cells and fibers in the human hypothalamus. *The Journal of comparative neurology* **350**, 311-323, doi:10.1002/cne.903500213 (1994).

13 Nakahara, K. *et al.* The gut-brain peptide neuromedin U is involved in the mammalian circadian oscillator system. *Biochemical and biophysical research communications* **318**, 156-161, doi:10.1016/j.bbrc.2004.04.014 (2004).

14 Abrahamson, E. E. & Moore, R. Y. Suprachiasmatic nucleus in the mouse: retinal innervation, intrinsic organization and efferent projections. *Brain research* **916**, 172-191, doi:S0006-8993(01)02890-6 [pii] (2001).

15 Moga, M. M. & Moore, R. Y. Organization of neural inputs to the suprachiasmatic nucleus in the rat. *The Journal of comparative neurology* **389**, 508-534 (1997).

16 Leak, R. K., Card, J. P. & Moore, R. Y. Suprachiasmatic pacemaker organization analyzed by viral transynaptic transport. *Brain research* **819**, 23-32 (1999).

17 Watts, A. G. & Swanson, L. W. Efferent projections of the suprachiasmatic nucleus: II. Studies using retrograde transport of fluorescent dyes and simultaneous peptide immunohistochemistry in the rat. *The Journal of comparative neurology* **258**, 230-252, doi:10.1002/cne.902580205 (1987).
18 Burgoon, P. W., Lindberg, P. T. & Gillette, M. U. Different patterns of circadian oscillation in the suprachiasmatic nucleus of hamster, mouse, and rat. *Journal of comparative physiology. A, Neuroethology, sensory, neural, and behavioral physiology* **190**, 167-171, doi:10.1007/s00359-003-0486-z (2004).
19 Green, D. J. & Gillette, R. Circadian rhythm of firing rate recorded from single cells in the rat suprachiasmatic brain slice. *Brain research* **245**, 198-200, doi:0006-8993(82)90361-4 [pii] (1982).
20 Gillette, M. U. & Reppert, S. M. The hypothalamic suprachiasmatic nuclei: circadian patterns of vasopressin secretion and neuronal activity in vitro. *Brain research bulletin* **19**, 135-139 (1987).
21 Groos, G. & Hendriks, J. Circadian rhythms in electrical discharge of rat suprachiasmatic neurones recorded in vitro. *Neuroscience letters* **34**, 283-288 (1982).
22 Shibata, S., Oomura, Y., Kita, H. & Hattori, K. Circadian rhythmic changes of neuronal activity in the suprachiasmatic nucleus of the rat hypothalamic slice. *Brain research* **247**, 154-158, doi:0006-8993(82)91041-1 [pii] (1982).
23 Shibata, S., Liou, S. Y. & Ueki, S. Development of the circadian rhythm of neuronal activity in suprachiasmatic nucleus of rat hypothalamic slices. *Neuroscience letters* **43**, 231-234 (1983).
24 Welsh, D. K., Logothetis, D. E., Meister, M. & Reppert, S. M. Individual neurons dissociated from rat suprachiasmatic nucleus express independently phased circadian firing rhythms. *Neuron* **14**, 697-706 (1995).
25 Schaap, J., Pennartz, C. M. & Meijer, J. H. Electrophysiology of the circadian pacemaker in mammals. *Chronobiology international* **20**, 171-188 (2003).
26 Herzog, E. D., Takahashi, J. S. & Block, G. D. Clock controls circadian period in isolated suprachiasmatic nucleus neurons. *Nature neuroscience* **1**, 708-713, doi:10.1038/3708 (1998).
27 Honma, S., Shirakawa, T., Katsuno, Y., Namihira, M. & Honma, K. Circadian periods of single suprachiasmatic neurons in rats. *Neuroscience letters* **250**, 157-160, doi:10.1016/s0304-3940(98)00464-9 (1998).
28 Webb, A. B., Angelo, N., Huettner, J. E. & Herzog, E. D. Intrinsic, nondeterministic circadian rhythm generation in identified mammalian neurons. *Proceedings of the National Academy of Sciences of the United States of America* **106**, 16493-16498, doi:10.1073/pnas.0902768106 (2009).
29 (NobelPrize.org, 2017).
30 Itri, J. N. *et al.* Circadian regulation of a-type potassium currents in the suprachiasmatic nucleus. *Journal of neurophysiology* **103**, 632-640, doi:10.1152/jn.00670.2009 (2010).
31 Alvado, L. & Allen, C. N. Tetraethylammonium (TEA) increases the inactivation time constant of the transient K+ current in suprachiasmatic nucleus neurons. *Brain research* **1221**, 24-29, doi:10.1016/j.brainres.2008.05.025 (2008).
32 Allen, C. N., Nitabach, M. N. & Colwell, C. S. Membrane Currents, Gene Expression, and Circadian Clocks. *Cold Spring Harbor perspectives in biology* **9**, doi:10.1101/cshperspect.a027714 (2017).

33 Granados-Fuentes, D., Norris, A. J., Carrasquillo, Y., Nerbonne, J. M. & Herzog, E. D. I(A) channels encoded by Kv1.4 and Kv4.2 regulate neuronal firing in the suprachiasmatic nucleus and circadian rhythms in locomotor activity. *The Journal of neuroscience : the official journal of the Society for Neuroscience* **32**, 10045-10052, doi:10.1523/jneurosci.0174-12.2012 (2012).
34 Belle, M. D., Diekman, C. O., Forger, D. B. & Piggins, H. D. Daily electrical silencing in the mammalian circadian clock. *Science (New York, N.Y.)* **326**, 281-284, doi:10.1126/science.1169657 (2009).
35 de Jeu, M., Hermes, M. & Pennartz, C. Circadian modulation of membrane properties in slices of rat suprachiasmatic nucleus. *Neuroreport* **9**, 3725-3729, doi:10.1097/00001756-199811160-00028 (1998).
36 Rudy, B. Diversity and ubiquity of K channels. *Neuroscience* **25**, 729-749, doi:10.1016/0306-4522(88)90033-4 (1988).
37 Clapham, D. E. Calcium signaling. *Cell* **131**, 1047-1058, doi:10.1016/j.cell.2007.11.028 (2007).
38 Noguchi, T. *et al.* Calcium Circadian Rhythmicity in the Suprachiasmatic Nucleus: Cell Autonomy and Network Modulation. *eNeuro* **4**, doi:10.1523/eneuro.0160-17.2017 (2017).
39 Welsh, D. K., Takahashi, J. S. & Kay, S. A. Suprachiasmatic nucleus: cell autonomy and network properties. *Annual review of physiology* **72**, 551-577, doi:10.1146/annurev-physiol-021909-135919 (2010).
40 Aguilar-Roblero, R., Morin, L. P. & Moore, R. Y. Morphological correlates of circadian rhythm restoration induced by transplantation of the suprachiasmatic nucleus in hamsters. *Experimental neurology* **130**, 250-260, doi:10.1006/exnr.1994.1203 (1994).
41 Aton, S. J., Colwell, C. S., Harmar, A. J., Waschek, J. & Herzog, E. D. Vasoactive intestinal polypeptide mediates circadian rhythmicity and synchrony in mammalian clock neurons. *Nature neuroscience* **8**, 476-483, doi:10.1038/nn1419 (2005).
42 Rash, J. E. *et al.* Connexin36 vs. connexin32, "miniature" neuronal gap junctions, and limited electrotonic coupling in rodent suprachiasmatic nucleus. *Neuroscience* **149**, 350-371, doi:10.1016/j.neuroscience.2007.06.052 (2007).
43 Long, M. A., Jutras, M. J., Connors, B. W. & Burwell, R. D. Electrical synapses coordinate activity in the suprachiasmatic nucleus. *Nature neuroscience* **8**, 61-66, doi:10.1038/nn1361 (2005).
44 Prosser, R. A., Edgar, D. M., Heller, H. C. & Miller, J. D. A possible glial role in the mammalian circadian clock. *Brain research* **643**, 296-301, doi:10.1016/0006-8993(94)90036-1 (1994).
45 Shinohara, K., Funabashi, T., Mitushima, D. & Kimura, F. Effects of gap junction blocker on vasopressin and vasoactive intestinal polypeptide rhythms in the rat suprachiasmatic nucleus in vitro. *Neuroscience research* **38**, 43-47, doi:10.1016/s0168-0102(00)00141-3 (2000).
46 Brancaccio, M. *et al.* Cell-autonomous clock of astrocytes drives circadian behavior in mammals. *Science (New York, N.Y.)* **363**, 187-192, doi:10.1126/science.aat4104 (2019).
47 De Coursey, P. J. Daily light sensitivity rhythm in a rodent. *Science (New York, N.Y.)* **131**, 33-35, doi:10.1126/science.131.3392.33 (1960).
48 Moore, R. Y. & Lenn, N. J. A retinohypothalamic projection in the rat. *The Journal of comparative neurology* **146**, 1-14, doi:10.1002/cne.901460102 (1972).

49 Hendrickson, A. E., Wagoner, N. & Cowan, W. M. An autoradiographic and electron microscopic study of retino-hypothalamic connections. *Zeitschrift fur Zellforschung und mikroskopische Anatomie (Vienna, Austria : 1948)* **135**, 1-26, doi:10.1007/bf00307084 (1972).
50 Freedman, M. S. *et al.* Regulation of mammalian circadian behavior by non-rod, non-cone, ocular photoreceptors. *Science (New York, N.Y.)* **284**, 502-504, doi:10.1126/science.284.5413.502 (1999).
51 Provencio, I., Jiang, G., De Grip, W. J., Hayes, W. P. & Rollag, M. D. Melanopsin: An opsin in melanophores, brain, and eye. *Proceedings of the National Academy of Sciences of the United States of America* **95**, 340-345, doi:10.1073/pnas.95.1.340 (1998).
52 Hatori, M. *et al.* Inducible ablation of melanopsin-expressing retinal ganglion cells reveals their central role in non-image forming visual responses. *PloS one* **3**, e2451, doi:10.1371/journal.pone.0002451 (2008).
53 Hannibal, J., Moller, M., Ottersen, O. P. & Fahrenkrug, J. PACAP and glutamate are co-stored in the retinohypothalamic tract. *The Journal of comparative neurology* **418**, 147-155 (2000).
54 Hannibal, J. *et al.* Pituitary adenylate cyclase-activating peptide (PACAP) in the retinohypothalamic tract: a potential daytime regulator of the biological clock. *The Journal of neuroscience : the official journal of the Society for Neuroscience* **17**, 2637-2644 (1997).
55 Reghunandanan, V. & Reghunandanan, R. Neurotransmitters of the suprachiasmatic nuclei. *Journal of circadian rhythms* **4**, 2, doi:10.1186/1740-3391-4-2 (2006).
56 Ding, J. M. *et al.* Resetting the biological clock: mediation of nocturnal circadian shifts by glutamate and NO. *Science (New York, N.Y.)* **266**, 1713-1717, doi:10.1126/science.7527589 (1994).
57 Harrington, M. E., Hoque, S., Hall, A., Golombek, D. & Biello, S. Pituitary adenylate cyclase activating peptide phase shifts circadian rhythms in a manner similar to light. *The Journal of neuroscience : the official journal of the Society for Neuroscience* **19**, 6637-6642 (1999).
58 Colwell, C. S. & Menaker, M. NMDA as well as non-NMDA receptor antagonists can prevent the phase-shifting effects of light on the circadian system of the golden hamster. *Journal of biological rhythms* **7**, 125-136, doi:10.1177/074873049200700204 (1992).
59 Takeuchi, Y., Takashima, M., Katoh, Y., Nishikawa, T. & Takahashi, K. N-methyl-D-aspartate, quisqualate and kainate receptors are all involved in transmission of photic stimulation in the suprachiasmatic nucleus in rats. *Brain research* **563**, 127-131, doi:10.1016/0006-8993(91)91524-5 (1991).
60 Tsuji, T. *et al.* Vasopressin casts light on the suprachiasmatic nucleus. *The Journal of physiology* **595**, 3497-3514, doi:10.1113/jp274025 (2017).
61 Yamaguchi, Y. *et al.* Mice genetically deficient in vasopressin V1a and V1b receptors are resistant to jet lag. *Science (New York, N.Y.)* **342**, 85-90, doi:10.1126/science.1238599 (2013).
62 Halberg, F., Visscher, M. B. & Bittner, J. J. Relation of visual factors to eosinophil rhythm in mice. *The American journal of physiology* **179**, 229-235, doi:10.1152/ajplegacy.1954.179.2.229 (1954).
63 Mistlberger, R. E. Circadian food-anticipatory activity: formal models and physiological mechanisms. *Neuroscience and biobehavioral reviews* **18**, 171-195 (1994).

64 Fuchikawa, T., Eban-Rothschild, A., Nagari, M., Shemesh, Y. & Bloch, G. Potent social synchronization can override photic entrainment of circadian rhythms. *Nature communications* **7**, 11662, doi:10.1038/ncomms11662 (2016).
65 Yasumoto, Y., Nakao, R. & Oishi, K. Free access to a running-wheel advances the phase of behavioral and physiological circadian rhythms and peripheral molecular clocks in mice. *PloS one* **10**, e0116476, doi:10.1371/journal.pone.0116476 (2015).
66 Teshima, K. *et al.* Nonphotic entrainment of the circadian body temperature rhythm by the selective ORL1 receptor agonist W-212393 in rats. *British journal of pharmacology* **146**, 33-40, doi:10.1038/sj.bjp.0706311 (2005).
67 Vansteensel, M. J. *et al.* The opioid fentanyl affects light input, electrical activity and Per gene expression in the hamster suprachiasmatic nuclei. *The European journal of neuroscience* **21**, 2958-2966, doi:10.1111/j.1460-9568.2005.04131.x (2005).
68 Mistlberger, R. E., Houpt, T. A. & Moore-Ede, M. C. The benzodiazepine triazolam phase-shifts circadian activity rhythms in a diurnal primate, the squirrel monkey (Saimiri sciureus). *Neuroscience letters* **124**, 27-30, doi:10.1016/0304-3940(91)90814-a (1991).
69 Johnson, R. F., Smale, L., Moore, R. Y. & Morin, L. P. Lateral geniculate lesions block circadian phase-shift responses to a benzodiazepine. *Proceedings of the National Academy of Sciences of the United States of America* **85**, 5301-5304 (1988).
70 Lewy, A. J., Ahmed, S., Jackson, J. M. & Sack, R. L. Melatonin shifts human circadian rhythms according to a phase-response curve. *Chronobiology international* **9**, 380-392 (1992).
71 Janik, D. & Mrosovsky, N. Intergeniculate leaflet lesions and behaviorally-induced shifts of circadian rhythms. *Brain research* **651**, 174-182 (1994).
72 Weaver, D. R. & Reppert, S. M. Direct in utero perception of light by the mammalian fetus. *Brain research. Developmental brain research* **47**, 151-155, doi:10.1016/0165-3806(89)90119-3 (1989).
73 Reppert, S. M. & Schwartz, W. J. Maternal suprachiasmatic nuclei are necessary for maternal coordination of the developing circadian system. *The Journal of neuroscience : the official journal of the Society for Neuroscience* **6**, 2724-2729 (1986).
74 Mistlberger, R. E. & Skene, D. J. Social influences on mammalian circadian rhythms: animal and human studies. *Biological reviews of the Cambridge Philosophical Society* **79**, 533-556 (2004).
75 Viswanathan, N. & Davis, F. C. Single prenatal injections of melatonin or the D1-dopamine receptor agonist SKF 38393 to pregnant hamsters sets the offsprings' circadian rhythms to phases 180 degrees apart. *Journal of comparative physiology. A, Sensory, neural, and behavioral physiology* **180**, 339-346 (1997).
76 Reppert, S. M., Artman, H. G., Swaminathan, S. & Fisher, D. A. Vasopressin exhibits a rhythmic daily pattern in cerebrospinal fluid but not in blood. *Science (New York, N.Y.)* **213**, 1256-1257 (1981).
77 Schwartz, W. J. & Reppert, S. M. Neural regulation of the circadian vasopressin rhythm in cerebrospinal fluid: a pre-eminent role for the suprachiasmatic nuclei. *The Journal of neuroscience : the official journal of the Society for Neuroscience* **5**, 2771-2778 (1985).
78 Groblewski, T. A., Nunez, A. A. & Gold, R. M. Circadian rhythms in vasopressin deficient rats. *Brain research bulletin* **6**, 125-130, doi:10.1016/s0361-9230(81)80036-6 (1981).

79 Brown, M. H. & Nunez, A. A. Vasopressin-deficient rats show a reduced amplitude of the circadian sleep rhythm. *Physiology & behavior* **46**, 759-762, doi:10.1016/0031-9384(89)90364-8 (1989).
80 Kalsbeek, A., van Heerikhuize, J. J., Wortel, J. & Buijs, R. M. A diurnal rhythm of stimulatory input to the hypothalamo-pituitary-adrenal system as revealed by timed intrahypothalamic administration of the vasopressin V1 antagonist. *The Journal of neuroscience : the official journal of the Society for Neuroscience* **16**, 5555-5565 (1996).
81 Kalsbeek, A., van der Vliet, J. & Buijs, R. M. Decrease of endogenous vasopressin release necessary for expression of the circadian rise in plasma corticosterone: a reverse microdialysis study. *Journal of neuroendocrinology* **8**, 299-307, doi:10.1046/j.1365-2826.1996.04597.x (1996).
82 Trudel, E. & Bourque, C. W. Central clock excites vasopressin neurons by waking osmosensory afferents during late sleep. *Nature neuroscience* **13**, 467-474, doi:nn.2503 [pii]
10.1038/nn.2503 (2010).
83 Trudel, E. & Bourque, C. W. Circadian modulation of osmoregulated firing in rat supraoptic nucleus neurones. *Journal of neuroendocrinology* **24**, 577-586, doi:10.1111/j.1365-2826.2012.02298.x (2012).
84 Bourque, C. W. Central mechanisms of osmosensation and systemic osmoregulation. *Nature reviews. Neuroscience* **9**, 519-531, doi:nrn2400 [pii]
10.1038/nrn2400 (2008).
85 Ciura, S. *et al.* Trpv4 Mediates Hypotonic Inhibition of Central Osmosensory Neurons via Taurine Gliotransmission. *Cell reports* **23**, 2245-2253, doi:10.1016/j.celrep.2018.04.090 (2018).
86 Ciura, S., Liedtke, W. & Bourque, C. W. Hypertonicity sensing in organum vasculosum lamina terminalis neurons: a mechanical process involving TRPV1 but not TRPV4. *The Journal of neuroscience : the official journal of the Society for Neuroscience* **31**, 14669-14676, doi:10.1523/jneurosci.1420-11.2011 (2011).
87 Toney, G. M. & Stocker, S. D. Hyperosmotic activation of CNS sympathetic drive: implications for cardiovascular disease. *The Journal of physiology* **588**, 3375-3384, doi:10.1113/jphysiol.2010.191940 (2010).
88 McKinley, M. J. *et al.* Osmoregulatory fluid intake but not hypovolemic thirst is intact in mice lacking angiotensin. *American journal of physiology. Regulatory, integrative and comparative physiology* **294**, R1533-1543, doi:10.1152/ajpregu.00848.2007 (2008).
89 Shi, P., Stocker, S. D. & Toney, G. M. Organum vasculosum laminae terminalis contributes to increased sympathetic nerve activity induced by central hyperosmolality. *American journal of physiology. Regulatory, integrative and comparative physiology* **293**, R2279-2289, doi:00160.2007 [pii]
10.1152/ajpregu.00160.2007 (2007).
90 Nomura, K. *et al.* [Na(+)] Increases in Body Fluids Sensed by Central Nax Induce Sympathetically Mediated Blood Pressure Elevations via H(+)-Dependent Activation of ASIC1a. *Neuron* **101**, 60-75.e66, doi:10.1016/j.neuron.2018.11.017 (2019).
91 Miller, R. L. & Loewy, A. D. ENaC gamma-expressing astrocytes in the circumventricular organs, white matter, and ventral medullary surface: sites for Na+ regulation by glial cells. *Journal of chemical neuroanatomy* **53**, 72-80, doi:10.1016/j.jchemneu.2013.10.002 (2013).

92 Noda, M. The subfornical organ, a specialized sodium channel, and the sensing of sodium levels in the brain. *Neuroscientist* **12**, 80-91, doi:12/1/80 [pii]
10.1177/1073858405279683 (2006).
93 Hiyama, T. Y., Watanabe, E., Okado, H. & Noda, M. The subfornical organ is the primary locus of sodium-level sensing by Na(x) sodium channels for the control of salt-intake behavior. *The Journal of neuroscience : the official journal of the Society for Neuroscience* **24**, 9276-9281, doi:24/42/9276 [pii]
10.1523/JNEUROSCI.2795-04.2004 (2004).
94 Vivas, L., Pastuskovas, C. V. & Tonelli, L. Sodium depletion induces Fos immunoreactivity in circumventricular organs of the lamina terminalis. *Brain research* **679**, 34-41 (1995).
95 Richard, D. & Bourque, C. W. Atrial natriuretic peptide modulates synaptic transmission from osmoreceptor afferents to the supraoptic nucleus. *The Journal of neuroscience : the official journal of the Society for Neuroscience* **16**, 7526-7532 (1996).
96 Ferguson, A. V. Angiotensinergic regulation of autonomic and neuroendocrine outputs: critical roles for the subfornical organ and paraventricular nucleus. *Neuroendocrinology* **89**, 370-376, doi:000211202 [pii];10.1159/000211202 [doi] (2009).
97 Grob, M., Trottier, J. F. & Mouginot, D. Heterogeneous co-localization of AT 1A receptor and Fos protein in forebrain neuronal populations responding to acute hydromineral deficit. *Brain research* **996**, 81-88, doi:S0006899303038538 [pii] (2004).
98 Moellenhoff, E. *et al.* Effect of repetitive icv injections of ANG II on c-Fos and AT(1)-receptor expression in the rat brain. *American journal of physiology. Regulatory, integrative and comparative physiology* **280**, R1095-1104 (2001).
99 Ferguson, A. V., Donevan, S. D., Papas, S. & Smith, P. M. Circumventricular structures: CNS sensors of circulating peptides and autonomic control centres. *Endocrinol.Exp.* **24**, 19-27 (1990).
100 Gutman, M. B., Ciriello, J. & Mogenson, G. J. Effects of plasma angiotensin II and hypernatremia on subfornical organ neurons. *The American journal of physiology* **254**, R746-754 (1988).
101 Abbott, S. B., Machado, N. L., Geerling, J. C. & Saper, C. B. Reciprocal Control of Drinking Behavior by Median Preoptic Neurons in Mice. *The Journal of neuroscience : the official journal of the Society for Neuroscience* **36**, 8228-8237, doi:10.1523/JNEUROSCI.1244-16.2016 (2016).
102 Oka, Y., Ye, M. & Zuker, C. S. Thirst driving and suppressing signals encoded by distinct neural populations in the brain. *Nature* **520**, 349-352, doi:10.1038/nature14108 (2015).
103 Hollis, J. H., McKinley, M. J., D'Souza, M., Kampe, J. & Oldfield, B. J. The trajectory of sensory pathways from the lamina terminalis to the insular and cingulate cortex; a neuroanatomical framework for the generation of thirst. *American journal of physiology. Regulatory, integrative and comparative physiology* **294**, R1390-1401, doi:00869.2007 [pii]
10.1152/ajpregu.00869.2007 (2008).
104 Denton, D. *et al.* Correlation of regional cerebral blood flow and change of plasma sodium concentration during genesis and satiation of thirst. *Proceedings of the National Academy of Sciences of the United States of America* **96**, 2532-2537 (1999).

105 Denton, D. *et al.* Neuroimaging of genesis and satiation of thirst and an interoceptor-driven theory of origins of primary consciousness. *Proceedings of the National Academy of Sciences of the United States of America* **96**, 5304-5309 (1999).
106 Denton, D. A., McKinley, M. & Weisinger, R. S. Hypothalamic integration of body fluid regulation. *Proc Nat Acad Sci USA* **93**, 7397-7404 (1996).
107 Zimmerman, C. A. *et al.* Thirst neurons anticipate the homeostatic consequences of eating and drinking. *Nature* **537**, 680-684, doi:10.1038/nature18950 (2016).
108 Oatley, K. Dissociation of the circadian drinking pattern from eating. *Nature* **229**, 494-496 (1971).
109 Morgan, R. M., Patterson, M. J. & Nimmo, M. A. Acute effects of dehydration on sweat composition in men during prolonged exercise in the heat. *Acta physiologica Scandinavica* **182**, 37-43, doi:10.1111/j.1365-201X.2004.01305.x
APS1305 [pii] (2004).
110 Effros, R. M. *et al.* Epithelial lining fluid solute concentrations in chronic obstructive lung disease patients and normal subjects. *J Appl Physiol* **99**, 1286-1292, doi:00362.2005 [pii]
10.1152/japplphysiol.00362.2005 (2005).
111 Griese, M., Noss, J. & Schramel, P. Elemental and ion composition of exhaled air condensate in cystic fibrosis. *J Cyst Fibros* **2**, 136-142, doi:S1569199303000626 [pii]
10.1016/S1569-1993(03)00062-6 (2003).
112 Bolt, E. E., Hagens, M., Willems, D. & Onwuteaka-Philipsen, B. D. Primary care patients hastening death by voluntarily stopping eating and drinking. *Annals of family medicine* **13**, 421-428, doi:10.1370/afm.1814 (2015).
113 Arima, H., Azuma, Y., Morishita, Y. & Hagiwara, D. Central diabetes insipidus. *Nagoya journal of medical science* **78**, 349-358, doi:10.18999/nagjms.78.4.349 (2016).
114 Cuesta, M., Hannon, M. J. & Thompson, C. J. Adipsic diabetes insipidus in adult patients. *Pituitary*, doi:10.1007/s11102-016-0784-4 (2017).
115 Eisenberg, Y. & Frohman, L. A. ADIPSIC DIABETES INSIPIDUS: A REVIEW. *Endocrine practice : official journal of the American College of Endocrinology and the American Association of Clinical Endocrinologists* **22**, 76-83, doi:10.4158/ep15940.ra (2016).
116 Manning, S., Shaffie, R. & Arora, S. Case Report: Severe hypernatremia from psychogenic adipsia. *F1000Research* **6**, 34, doi:10.12688/f1000research.9181.1 (2017).
117 Pereira, M. C., Vieira, M. M., Pereira, J. S. & Salgado, D. Adipsia in a Diabetes Insipidus Patient. *Case reports in oncology* **8**, 385-388, doi:10.1159/000440611 (2015).
118 Koch, C. A. & Fulop, T. Clinical aspects of changes in water and sodium homeostasis in the elderly. *Reviews in endocrine & metabolic disorders* **18**, 49-66, doi:10.1007/s11154-017-9420-5 (2017).
119 Fitzsimons, J. T. The physiology of thirst and sodium appetite. *Monogr Physiol Soc*, 1-572 (1979).
120 Johnson, A. K. The sensory psychobiology of thirst and salt appetite. *Med Sci Sports Exerc* **39**, 1388-1400, doi:10.1249/mss.0b013e3180686de8
00005768-200708000-00023 [pii] (2007).
121 McKinley, M. J. & Johnson, A. K. The physiological regulation of thirst and fluid intake. *News Physiol Sci* **19**, 1-6 (2004).
122 Zimmerman, C. A., Leib, D. E. & Knight, Z. A. Neural circuits underlying thirst and fluid homeostasis. *Nat Rev Neurosci*, doi:10.1038/nrn.2017.71 (2017).

123 Verbalis, J. G. Disorders of body water homeostasis. *Best Pract Res Clin Endocrinol Metab* **17**, 471-503, doi:S1521690X03000496 [pii] (2003).
124 Lafontan, M., Visscher, T. L., Farpour-Lambert, N. & Yumuk, V. Opportunities for intervention strategies for weight management: global actions on fluid intake patterns. *Obesity facts* **8**, 54-76, doi:10.1159/000375103 (2015).
125 Popkin, B. M., D'Anci, K. E. & Rosenberg, I. H. Water, hydration, and health. *Nutrition reviews* **68**, 439-458, doi:10.1111/j.1753-4887.2010.00304.x (2010).
126 Orlandi, C., Zimmer, C. A. & Gheorghiade, M. Tolvaptan for the treatment of hyponatremia and congestive heart failure. *Future cardiology* **2**, 627-634, doi:10.2217/14796678.2.6.627 (2006).
127 Redondo, N., Gomez-Martinez, S. & Marcos, A. Sensory attributes of soft drinks and their influence on consumers' preferences. *Food & function* **5**, 1686-1694, doi:10.1039/c4fo00181h (2014).
128 Adler, S. M. & Verbalis, J. G. Disorders of body water homeostasis in critical illness. *Endocrinology and metabolism clinics of North America* **35**, 873-894, xi, doi:10.1016/j.ecl.2006.09.011 (2006).
129 Brvar, M. *et al.* Polydipsia as another mechanism of hyponatremia after 'ecstasy' (3,4 methyldioxymethamphetamine) ingestion. *European journal of emergency medicine : official journal of the European Society for Emergency Medicine* **11**, 302-304 (2004).
130 Kalantar-Zadeh, K., Nguyen, M. K., Chang, R. & Kurtz, I. Fatal hyponatremia in a young woman after ecstasy ingestion. *Nat Clin Pract Nephrol* **2**, 283-288, quiz 289, doi:ncpneph0167 [pii]
10.1038/ncpneph0167 (2006).
131 Traub, S. J., Hoffman, R. S. & Nelson, L. S. The "ecstasy" hangover: hyponatremia due to 3,4-methylenedioxymethamphetamine. *Journal of urban health : bulletin of the New York Academy of Medicine* **79**, 549-555, doi:10.1093/jurban/79.4.549 (2002).
132 Sandifer, M. G. Hyponatremia due to psychotropic drugs. *The Journal of clinical psychiatry* **44**, 301-303 (1983).
133 Lu, X. & Wang, X. Hyponatremia induced by antiepileptic drugs in patients with epilepsy. *Expert opinion on drug safety* **16**, 77-87, doi:10.1080/14740338.2017.1248399 (2017).
134 Furth, S. & Oski, F. A. Hyponatremia and water intoxication. *American journal of diseases of children (1960)* **147**, 932-933 (1993).
135 Kushnir, M., Schattner, A., Ezri, T. & Konichezky, S. Schizophrenia and fatal self-induced water intoxication with appropriately-diluted urine. *Am J Med Sci* **300**, 385-387 (1990).
136 Patel, J. K. Polydipsia, hyponatremia, and water intoxication among psychiatric patients. *Hospital & community psychiatry* **45**, 1073-1074 (1994).
137 Ofran, Y., Lavi, D., Opher, D., Weiss, T. A. & Elinav, E. Fatal voluntary salt intake resulting in the highest ever documented sodium plasma level in adults (255 mmol L-1): a disorder linked to female gender and psychiatric disorders. *J Intern Med* **256**, 525-528, doi:JIM1411 [pii]
10.1111/j.1365-2796.2004.01411.x (2004).
138 Turk, E. E., Schulz, F., Koops, E., Gehl, A. & Tsokos, M. Fatal hypernatremia after using salt as an emetic--report of three autopsy cases. *Leg Med (Tokyo)* **7**, 47-50, doi:S1344-6223(04)00030-6 [pii]
10.1016/j.legalmed.2004.06.005 (2005).

139 Kirkman, M. A., Albert, A. F., Ibrahim, A. & Doberenz, D. Hyponatremia and brain injury: historical and contemporary perspectives. *Neurocrit Care* **18**, 406-416, doi:10.1007/s12028-012-9805-y (2013).
140 De Smet, H. R., Menadue, M. F., Oliver, J. R. & Phillips, P. A. Increased thirst and vasopressin secretion after myocardial infarction in rats. *American journal of physiology. Regulatory, integrative and comparative physiology* **285**, R1203-1211, doi:10.1152/ajpregu.00098.2003
285/5/R1203 [pii] (2003).
141 Sonneville, R. *et al.* Understanding brain dysfunction in sepsis. *Ann Intensive Care* **3**, 15, doi:10.1186/2110-5820-3-15 (2013).
142 Lyons, O. D., Bradley, T. D. & Chan, C. T. Hypervolemia and Sleep Apnea in Kidney Disease. *Seminars in nephrology* **35**, 373-382, doi:10.1016/j.semnephrol.2015.06.008 (2015).
143 Iwasa, M. & Takei, Y. Pathophysiology and management of hepatic encephalopathy 2014 update: Ammonia toxicity and hyponatremia. *Hepatology research : the official journal of the Japan Society of Hepatology* **45**, 1155-1162, doi:10.1111/hepr.12495 (2015).
144 Wier, L. M. *et al.* 1-99 (Agency for Healthcare and Research and Quality, Rockville, MD, 2011).
145 Magder, S. Volume and its relationship to cardiac output and venous return. *Critical care (London, England)* **20**, 271, doi:10.1186/s13054-016-1438-7 (2016).
146 Moranville, M. P., Mieure, K. D. & Santayana, E. M. Evaluation and management of shock States: hypovolemic, distributive, and cardiogenic shock. *Journal of pharmacy practice* **24**, 44-60, doi:10.1177/0897190010388150 (2011).
147 Senay Jr., L. C. & Christensen, M. L. Changes in blood plasma during progressive dehydration. *Journal of Applied Physiology* **20**, 1136-1140 (1965).
148 Bedford, J. J. & Leader, J. P. Response of tissues of the rat to anisosmolality in vivo. *The American journal of physiology* **264**, R1164-1179 (1993).
149 Ayus, J. C., Varon, J. & Arieff, A. I. Hyponatremia, cerebral edema, and noncardiogenic pulmonary edema in marathon runners. *Ann Intern Med* **132**, 711-714, doi:200005020-00005 [pii] (2000).
150 Machino, T. & Yoshizawa, T. Brain shrinkage due to acute hypernatremia. *Neurology* **67**, 880, doi:67/5/880 [pii]
10.1212/01.wnl.0000221726.41727.06 (2006).
151 Spigset, O. & Hedenmalm, K. Hyponatraemia and the syndrome of inappropriate antidiuretic hormone secretion (SIADH) induced by psychotropic drugs. *Drug safety* **12**, 209-225 (1995).
152 Sterns, R. H. Disorders of plasma sodium--causes, consequences, and correction. *The New England journal of medicine* **372**, 55-65, doi:10.1056/NEJMra1404489 (2015).
153 Stricker, E. M. & Sved, A. F. Thirst. *Nutrition (Burbank, Los Angeles County, Calif.)* **16**, 821-826 (2000).
154 Rullier, S. Dictionaire des Sciences Medicales pas un Societé de Médecines et de Chirurgiens. **51**, 448-490 (1821).
155 Cannon, W. B. Croonian Lecture: The Physiological Basis of Thirst. *Proceedings of the Royal Society of London. Series B, Containing Papers of a Biological Character* **90**, 283-301 (1918).
156 Wettendorff, H. Travaux du Laboratorie de physiologie *Instituts Solvay* **4**, 353 (1901).

157 Robinson, B. W. & Mishkin, M. Alimentary responses to forebrain stimulation in monkeys. *Exp Brain Res* **4**, 330-366 (1968).
158 Craig, A. D. How do you feel? Interoception: the sense of the physiological condition of the body. *Nature reviews. Neuroscience* **3**, 655-666, doi:10.1038/nrn894 nrn894 [pii] (2002).
159 Craig, A. D. A new view of pain as a homeostatic emotion. *Trends in neurosciences* **26**, 303-307, doi:S0166223603001231 [pii] (2003).
160 Denton, D. A., McKinley, M. J., Farrell, M. & Egan, G. F. The role of primordial emotions in the evolutionary origin of consciousness. *Consciousness and cognition* **18**, 500-514, doi:10.1016/j.concog.2008.06.009 (2009).
161 Farrell, M. J. *et al.* Unique, common, and interacting cortical correlates of thirst and pain. *Proceedings of the National Academy of Sciences of the United States of America* **103**, 2416-2421, doi:10.1073/pnas.0511019103 (2006).
162 Saker, P. *et al.* Regional brain responses associated with drinking water during thirst and after its satiation. *Proceedings of the National Academy of Sciences of the United States of America* **111**, 5379-5384, doi:10.1073/pnas.1403382111 (2014).
163 Farrell, M. J. *et al.* Cortical activation and lamina terminalis functional connectivity during thirst and drinking in humans. *American journal of physiology. Regulatory, integrative and comparative physiology* **301**, R623-631, doi:10.1152/ajpregu.00817.2010 (2011).
164 Egan, G. *et al.* Neural correlates of the emergence of consciousness of thirst. *Proceedings of the National Academy of Sciences of the United States of America* **100**, 15241-15246, doi:10.1073/pnas.2136650100 2136650100 [pii] (2003).
165 Saker, P., Farrell, M. J., Egan, G. F., McKinley, M. J. & Denton, D. A. Overdrinking, swallowing inhibition, and regional brain responses prior to swallowing. *Proceedings of the National Academy of Sciences of the United States of America* **113**, 12274-12279, doi:10.1073/pnas.1613929113 (2016).
166 Becker, C. A., Flaisch, T., Renner, B. & Schupp, H. T. From Thirst to Satiety: The Anterior Mid-Cingulate Cortex and Right Posterior Insula Indicate Dynamic Changes in Incentive Value. *Frontiers in human neuroscience* **11**, 234, doi:10.3389/fnhum.2017.00234 (2017).
167 Duncan, G. E. *et al.* Metabolic mapping of functional activity in rat brain and pituitary after water deprivation. *Neuroendocrinology* **49**, 489-495 (1989).
168 Pastuskovas, C. V., Cassell, M. D., Johnson, A. K. & Thunhorst, R. L. Increased cellular activity in rat insular cortex after water and salt ingestion induced by fluid depletion. *American journal of physiology. Regulatory, integrative and comparative physiology* **284**, R1119-1125, doi:10.1152/ajpregu.00189.2002 00189.2002 [pii] (2003).
169 Craig, A. D. Interoception: the sense of the physiological condition of the body. *Current opinion in neurobiology* **13**, 500-505, doi:S0959438803000904 [pii] (2003).
170 McCormick, D. A. & Bal, T. Sensory gating mechanisms of the thalamus. *Current opinion in neurobiology* **4**, 550-556 (1994).
171 Andrews, W. H. & Orbach, J. Sodium receptors activating some nerves of perfused rabbit livers. *The American journal of physiology* **227**, 1273-1275 (1974).
172 Adachi, A. Thermosensitive and osmoreceptive afferent fibers in the hepatic branch of the vagus nerve. *Journal of the autonomic nervous system* **10**, 269-273 (1984).

173 Adachi, A., Niijima, A. & Jacobs, H. L. An hepatic osmoreceptor mechanism in the rat: electrophysiological and behavioral studies. *The American journal of physiology* **231**, 1043-1049 (1976).
174 Andrews, W. H. & Orbach, J. Effect of osmotic pressure on spontaneous afferent discharge in the nerves of the perfused rabbit liver. *Pflugers Archiv : European journal of physiology* **361**, 89-94 (1975).
175 Choi-Kwon, S. & Baertschi, A. J. Splanchnic osmosensation and vasopressin: mechanisms and neural pathways. *The American journal of physiology* **261**, E18-25 (1991).
176 King, M. S. & Baertschi, A. J. Central neural pathway mediating splanchnic osmosensation. *Brain research* **550**, 268-278 (1991).
177 Haberich, F. J. Osmoreception in the portal circulation. *Fed Proc* **27**, 1137-1141 (1968).
178 Chwalbinska-Moneta, J. Role of hepatic portal osmoreception in the control of ADH release. *The American journal of physiology* **236**, E603-609 (1979).
179 Baertschi, A. J. & Vallet, P. G. Osmosensitivity of the hepatic portal vein area and vasopressin release in rats. *The Journal of physiology* **315**, 217-230 (1981).
180 Andersson, B., Jobin, M. & Olsson, K. A study of thirst and other effects of an increased sodium concentration in the 3rd brain ventricle. *Acta Physiol Scand.* **69**, 29-36 (1967).
181 McKinley, M. J., Blaine, E. H. & Denton, D. A. Brain osmoreceptors, cerebrospinal fluid electrolyte composition and thirst. *Brain research* **70**, 532-537, doi:0006-8993(74)90264-9 [pii] (1974).
182 McKinley, M. J., Denton, D. A. & Weisinger, R. S. Sensors for antidiuresis and thirst--osmoreceptors or CSF sodium detectors? *Brain research* **141**, 89-103, doi:0006-8993(78)90619-4 [pii] (1978).
183 Olsson, K. Further evidence for the importance of CSF Na+ concentration in central control of fluid balance. *Acta physiologica Scandinavica* **88**, 183-188, doi:10.1111/j.1748-1716.1973.tb05445.x (1973).
184 Olsson, K. Attenuation of dehydrative thirst by lowering of the CSF (Na+). *Acta physiologica Scandinavica* **94**, 536-538, doi:10.1111/j.1748-1716.1975.tb05913.x (1975).
185 Weisinger, R. S., Considine, P., Denton, D. A. & McKinley, M. J. Rapid effect of change in cerebrospinal fluid sodium concentration on salt appetite. *Nature* **280**, 490-491 (1979).
186 Vivas, L., Chiaraviglio, E. & Carrer, H. F. Rat organum vasculosum laminae terminalis in vitro: responses to changes in sodium concentration. *Brain research* **519**, 294-300, doi:0006-8993(90)90091-O [pii] (1990).
187 Voisin, D. L. & Bourque, C. W. Integration of sodium and osmosensory signals in vasopressin neurons. *Trends in neurosciences* **25**, 199-205, doi:S0166223602021422 [pii] (2002).
188 Noda, M. & Hiyama, T. Y. Sodium sensing in the brain. *Pflugers Archiv : European journal of physiology* **467**, 465-474, doi:10.1007/s00424-014-1662-4 (2015).
189 Voisin, D. L., Chakfe, Y. & Bourque, C. W. Coincident detection of CSF Na+ and osmotic pressure in osmoregulatory neurons of the supraoptic nucleus. *Neuron* **24**, 453-460, doi:S0896-6273(00)80858-2 [pii] (1999).
190 Miller, R. L., Wang, M. H., Gray, P. A., Salkoff, L. B. & Loewy, A. D. ENaC-expressing neurons in the sensory circumventricular organs become c-Fos activated following systemic sodium changes. *American journal of physiology. Regulatory, integrative and comparative physiology* **305**, R1141-1152, doi:10.1152/ajpregu.00242.2013 (2013).

191 Ruiz, C., Gutknecht, S., Delay, E. & Kinnamon, S. Detection of NaCl and KCl in TRPV1 Knockout Mice. *Chemical Senses*, bjl024 (2006).
192 Teruyama, R., Sakuraba, M., Wilson, L. L., Wandrey, N. E. & Armstrong, W. E. Epithelial Na(+) sodium channels in magnocellular cells of the rat supraoptic and paraventricular nuclei. *Am J Physiol Endocrinol Metab* **302**, E273-285, doi:10.1152/ajpendo.00407.2011 (2012).
193 Tanaka, M. *et al.* Molecular and functional remodeling of electrogenic membrane of hypothalamic neurons in response to changes in their input. *Proceedings of the National Academy of Sciences of the United States of America* **96**, 1088-1093 (1999).
194 Hiyama, T. Y. *et al.* Autoimmunity to the sodium-level sensor in the brain causes essential hypernatremia. *Neuron* **66**, 508-522, doi:S0896-6273(10)00288-6 [pii] 10.1016/j.neuron.2010.04.017 (2010).
195 Hiyama, T. Y. *et al.* Na(x) channel involved in CNS sodium-level sensing. *Nature neuroscience* **5**, 511-512, doi:10.1038/nn856 nn856 [pii] (2002).
196 Matsumoto, M. *et al.* Channel properties of Nax expressed in neurons. *PloS one* **10**, e0126109, doi:10.1371/journal.pone.0126109 (2015).
197 Goldin, A. L. Resurgence of sodium channel research. *Annual review of physiology* **63**, 871-894, doi:10.1146/annurev.physiol.63.1.871 (2001).
198 Bourque, C. W., Voisin, D. L. & Chakfe, Y. Stretch-inactivated cation channels: cellular targets for modulation of osmosensitivity in supraoptic neurons. *Progress in brain research* **139**, 85-94 (2002).
199 Ciura, S. & Bourque, C. W. Transient receptor potential vanilloid 1 is required for intrinsic osmoreception in organum vasculosum lamina terminalis neurons and for normal thirst responses to systemic hyperosmolality. *The Journal of neuroscience : the official journal of the Society for Neuroscience* **26**, 9069-9075, doi:26/35/9069 [pii] 10.1523/JNEUROSCI.0877-06.2006 (2006).
200 Bourque, C. W., Oliet, S. H. & Richard, D. Osmoreceptors, osmoreception, and osmoregulation. *Front Neuroendocrinol* **15**, 231-274, doi:S0091-3022(84)71010-7 [pii] 10.1006/frne.1994.1010 (1994).
201 Desson, S. E. & Ferguson, A. V. Interleukin 1beta modulates rat subfornical organ neurons as a result of activation of a non-selective cationic conductance. *The Journal of physiology* **550**, 113-122, doi:10.1113/jphysiol.2003.041210 (2003).
202 Amin, M. S. *et al.* Distribution of epithelial sodium channels and mineralocorticoid receptors in cardiovascular regulatory centers in rat brain. *American journal of physiology. Regulatory, integrative and comparative physiology* **289**, R1787-1797, doi:10.1152/ajpregu.00063.2005 (2005).
203 Watanabe, E. *et al.* Nav2/NaG channel is involved in control of salt-intake behavior in the CNS. *The Journal of neuroscience : the official journal of the Society for Neuroscience* **20**, 7743-7751, doi:20/20/7743 [pii] (2000).
204 Coble, J. P., Grobe, J. L., Johnson, A. K. & Sigmund, C. D. Mechanisms of brain renin angiotensin system-induced drinking and blood pressure: importance of the subfornical organ. *American journal of physiology. Regulatory, integrative and comparative physiology* **308**, R238-249, doi:10.1152/ajpregu.00486.2014 (2015).

205 Mimee, A., Smith, P. M. & Ferguson, A. V. Circumventricular organs: targets for integration of circulating fluid and energy balance signals? *Physiology & behavior* **121**, 96-102, doi:10.1016/j.physbeh.2013.02.012 (2013).
206 Miselis, R. R., Shapiro, R. E. & Hand, P. J. Subfornical organ efferents to neural systems for control of body water. *Science (New York, N.Y.)* **205**, 1022-1025 (1979).
207 Nissen, R., Bourque, C. W. & Renaud, L. P. Membrane properties of organum vasculosum lamina terminalis neurons recorded in vitro. *The American journal of physiology* **264**, R811-815 (1993).
208 Kinsman, B. J., Simmonds, S. S., Browning, K. N. & Stocker, S. D. Organum Vasculosum of the Lamina Terminalis Detects NaCl to Elevate Sympathetic Nerve Activity and Blood Pressure. *Hypertension (Dallas, Tex. : 1979)* **69**, 163-170, doi:10.1161/hypertensionaha.116.08372 (2017).
209 Sibbald, J. R., Hubbard, J. I. & Sirett, N. E. Responses from osmosensitive neurons of the rat subfornical organ in vitro. *Brain research* **461**, 205-214, doi:0006-8993(88)90251-X [pii] (1988).
210 Grob, M., Drolet, G. & Mouginot, D. Specific Na+ sensors are functionally expressed in a neuronal population of the median preoptic nucleus of the rat. *The Journal of neuroscience : the official journal of the Society for Neuroscience* **24**, 3974-3984, doi:10.1523/JNEUROSCI.3720-03.2004
24/16/3974 [pii] (2004).
211 Tremblay, C. *et al.* A neuronal sodium leak channel is responsible for the detection of sodium in the rat median preoptic nucleus. *J Neurophysiol*, doi:jn.00417.2010 [pii]
10.1152/jn.00417.2010 (2010).
212 Tremblay, C. *et al.* Neuronal sodium leak channel is responsible for the detection of sodium in the rat median preoptic nucleus. *J.Neurophysiol.* **105**, 650-660, doi:jn.00417.2010 [pii];10.1152/jn.00417.2010 [doi] (2011).
213 Shimizu, H. *et al.* Glial Nax channels control lactate signaling to neurons for brain [Na+] sensing. *Neuron* **54**, 59-72, doi:S0896-6273(07)00210-3 [pii]
10.1016/j.neuron.2007.03.014 (2007).
214 Camacho, A. & Phillips, M. I. Horseradish peroxidase study in rat of the neural connections of the organum vasculosum of the lamina terminalis. *Neuroscience letters* **25**, 201-204 (1981).
215 Gizowski, C., Zaelzer, C. & Bourque, C. W. Clock-driven vasopressin neurotransmission mediates anticipatory thirst prior to sleep. *Nature* **537**, 685-688, doi:10.1038/nature19756 (2016).
216 McKinley, M. J. *et al.* The median preoptic nucleus: front and centre for the regulation of body fluid, sodium, temperature, sleep and cardiovascular homeostasis. *Acta Physiol (Oxf)* **214**, 8-32, doi:10.1111/apha.12487 (2015).
217 Saper, C. B. & Levisohn, D. Afferent connections of the median preoptic nucleus in the rat: anatomical evidence for a cardiovascular integrative mechanism in the anteroventral third ventricular (AV3V) region. *Brain research* **288**, 21-31 (1983).
218 Lind, R. W., Van Hoesen, G. W. & Johnson, A. K. An HRP study of the connections of the subfornical organ of the rat. *The Journal of comparative neurology* **210**, 265-277, doi:10.1002/cne.902100306 (1982).

219 Nation, H. L., Nicoleau, M., Kinsman, B. J., Browning, K. N. & Stocker, S. D. DREADD-induced activation of subfornical organ neurons stimulates thirst and salt appetite. *J Neurophysiol* **115**, 3123-3129, doi:10.1152/jn.00149.2016 (2016).
220 Allen, W. E. *et al.* Thirst-associated preoptic neurons encode an aversive motivational drive. *Science (New York, N.Y.)* **357**, 1149-1155, doi:10.1126/science.aan6747 (2017).
221 Gilman, A. The relation between blood osmotic pressure, fluid distribution and voluntary water intake. *The American journal of physiology* **120**, 323-328 (1937).
222 Wolf, A. V. Osmometric analysis of thirst in man and dog. *Am. J. Physiol.*, 75-86 (1950).
223 Stricker, E. M. Osmoregulation and volume regulation in rats: inhibition of hypovolemic thirst by water. *Am.J.Physiol* **217**, 98-105 (1969).
224 Anderson, J. W., Washburn, D. L. & Ferguson, A. V. Intrinsic osmosensitivity of subfornical organ neurons. *Neuroscience* **100**, 539-547, doi:S0306-4522(00)00313-4 [pii] (2000).
225 Kucharczyk, J., Assaf, S. Y. & Mogenson, G. J. Differential effects of brain lesions on thirst induced by the administration of angiotensin-II to the preoptic region, subfornical organ and anterior third ventricle. *Brain research* **108**, 327-337 (1976).
226 Thrasher, T. N., Simpson, J. B. & Ramsay, D. J. Lesions of the subfornical organ block angiotensin-induced drinking in the dog. *Neuroendocrinology* **35**, 68-72 (1982).
227 Johnson, A. K. & Buggy, J. Periventricular preoptic-hypothalamus is vital for thirst and normal water economy. *The American journal of physiology* **234**, R122-129 (1978).
228 Buggy, J. & Jonhson, A. K. Preoptic-hypothalamic periventricular lesions: thirst deficits and hypernatremia. *The American journal of physiology* **233**, R44-52 (1977).
229 Thrasher, T. N., Keil, L. C. & Ramsay, D. J. Lesions of the organum vasculosum of the lamina terminalis (OVLT) attenuate osmotically-induced drinking and vasopressin secretion in the dog. *Endocrinology* **110**, 1837-1839 (1982).
230 Mangiapane, M. L., Thrasher, T. N., Keil, L. C., Simpson, J. B. & Ganong, W. F. Deficits in drinking and vasopressin secretion after lesions of the nucleus medianus. *Neuroendocrinology* **37**, 73-77 (1983).
231 Johnson, A. K., Cunningham, J. T. & Thunhorst, R. L. Integrative role of the lamina terminalis in the regulation of cardiovascular and body fluid homeostasis. *Clin Exp Pharmacol Physiol* **23**, 183-191 (1996).
232 McKinley, M. J. *et al.* Efferent neural pathways of the lamina terminalis subserving osmoregulation. *Progress in brain research* **91**, 395-402 (1992).
233 McKinley, M. J., Denton, D. A., Oldfield, B. J., De Oliveira, L. B. & Mathai, M. L. Water intake and the neural correlates of the consciousness of thirst. *Seminars in nephrology* **26**, 249-257, doi:S0270-9295(06)00012-X [pii]
10.1016/j.semnephrol.2006.02.001 (2006).
234 Zaelzer, C. *et al.* DeltaN-TRPV1: A Molecular Co-detector of Body Temperature and Osmotic Stress. *Cell reports* **13**, 23-30, doi:10.1016/j.celrep.2015.08.061 (2015).
235 Sharif-Naeini, R., Ciura, S., Zhang, Z. & Bourque, C. W. Contribution of TRPV channels to osmosensory transduction, thirst, and vasopressin release. *Kidney Int* **73**, 811-815, doi:5002788 [pii]
10.1038/sj.ki.5002788 (2008).
236 Sudbury, J. R., Ciura, S., Sharif-Naeini, R. & Bourque, C. W. Osmotic and thermal control of magnocellular neurosecretory neurons--role of an N-terminal variant of trpv1. *The*

European journal of neuroscience **32**, 2022-2030, doi:10.1111/j.1460-9568.2010.07512.x (2010).

237 Kinsman, B. *et al.* Osmoregulatory thirst in mice lacking the transient receptor potential vanilloid type 1 (TRPV1) and/or type 4 (TRPV4) receptor. *American journal of physiology. Regulatory, integrative and comparative physiology* **307**, R1092-1100, doi:10.1152/ajpregu.00102.2014 (2014).

238 Taylor, A. C., McCarthy, J. J. & Stocker, S. D. Mice Lacking the Transient Receptor Vanilloid Potential 1 (TRPV1) Channel Display Normal Thirst Responses and Central Fos Activation to Hypernatremia. *American journal of physiology. Regulatory, integrative and comparative physiology*, doi:00003.2008 [pii] 10.1152/ajpregu.00003.2008 (2008).

239 Hussy, N., Deleuze, C., Pantaloni, A., Desarmenien, M. G. & Moos, F. Agonist action of taurine on glycine receptors in rat supraoptic magnocellular neurones: possible role in osmoregulation. *The Journal of physiology* **502 (Pt 3)**, 609-621 (1997).

240 Choe, K. Y., Olson, J. E. & Bourque, C. W. Taurine release by astrocytes modulates osmosensitive glycine receptor tone and excitability in the adult supraoptic nucleus. *The Journal of neuroscience : the official journal of the Society for Neuroscience* **32**, 12518-12527, doi:10.1523/JNEUROSCI.1380-12.2012 (2012).

241 Choe, K. Y., Trudel, E. & Bourque, C. W. Effects of Salt Loading on the Regulation of Rat Hypothalamic Magnocellular Neurosecretory Cells by Ionotropic GABA and Glycine Receptors. *Journal of neuroendocrinology* **28**, doi:10.1111/jne.12372 (2016).

242 Hussy, N., Deleuze, C., Desarmenien, M. G. & Moos, F. C. Osmotic regulation of neuronal activity: a new role for taurine and glial cells in a hypothalamic neuroendocrine structure. *Prog Neurobiol* **62**, 113-134, doi:S0301-0082(99)00071-4 [pii] (2000).

243 Prager-Khoutorsky, M. & Bourque, C. W. ANATOMICAL ORGANIZATION OF THE RAT ORGANUM VASCULOSUM LAMINAE TERMINALIS. *American journal of physiology. Regulatory, integrative and comparative physiology*, ajpregu 00134 02015, doi:10.1152/ajpregu.00134.2015 (2015).

244 Hochstenbach, S. L. & Ciriello, J. Effect of lesions of forebrain circumventricular organs on c-fos expression in the central nervous system to plasma hypernatremia. *Brain research* **713**, 17-28 (1996).

245 Lechner, S. G. *et al.* The Molecular and Cellular Identity of Peripheral Osmoreceptors. *Neuron* **69**, 332-344, doi:S0896-6273(10)01076-7 [pii] 10.1016/j.neuron.2010.12.028 (2011).

246 Russell, P. J., Abdelaal, A. E. & Mogenson, G. J. Graded levels of hemorrhage, thirst and angiotensin II in the rat. *Physiology & behavior* **15**, 117-119 (1975).

247 Fitzsimons, J. T. Drinking by rats depleted of body fluid without increase in osmotic pressure. *The Journal of physiology* **159**, 297-309 (1961).

248 Joris, L., Dab, I. & Quinton, P. M. Elemental composition of human airway surface fluid in healthy and diseased airways. *The American review of respiratory disease* **148**, 1633-1637, doi:10.1164/ajrccm/148.6_Pt_1.1633 (1993).

249 Zardetto-Smith, A. M., Thunhorst, R. L., Cicha, M. Z. & Johnson, A. K. Afferent signaling and forebrain mechanisms in the behavioral control of extracellular fluid volume. *Ann N Y Acad Sci* **689**, 161-176 (1993).

250 Fitzsimons, J. T. Angiotensin, thirst, and sodium appetite. *Physiol Rev.* **78**, 583-686 (1998).

251 Stocker, S. D., Stricker, E. M. & Sved, A. F. Arterial baroreceptors mediate the inhibitory effect of acute increases in arterial blood pressure on thirst. *American journal of physiology. Regulatory, integrative and comparative physiology* **282**, R1718-1729, doi:10.1152/ajpregu.00651.2001 (2002).
252 Stocker, S. D., Stricker, E. M. & Sved, A. F. Acute hypertension inhibits thirst stimulated by ANG II, hyperosmolality, or hypovolemia in rats. *American journal of physiology. Regulatory, integrative and comparative physiology* **280**, R214-224 (2001).
253 Stricker, E. M. & Sved, A. F. Controls of vasopressin secretion and thirst: similarities and dissimilarities in signals. *Physiology & behavior* **77**, 731-736 (2002).
254 Dampney, R. A., Polson, J. W., Potts, P. D., Hirooka, Y. & Horiuchi, J. Functional organization of brain pathways subserving the baroreceptor reflex: studies in conscious animals using immediate early gene expression. *Cell Mol.Neurobiol.* **23**, 597-616 (2003).
255 Thunhorst, R. L., Xu, Z., Cicha, M. Z., Zardetto-Smith, A. M. & Johnson, A. K. Fos expression in rat brain during depletion-induced thirst and salt appetite. *The American journal of physiology* **274**, R1807-1814 (1998).
256 Badoer, E., McKinley, M. J., Oldfield, B. J. & McAllen, R. M. Distribution of hypothalamic, medullary and lamina terminalis neurons expressing Fos after hemorrhage in conscious rats. *Brain research* **582**, 323-328 (1992).
257 Potts, P. D., Ludbrook, J., Gillman-Gaspari, T. A., Horiuchi, J. & Dampney, R. A. Activation of brain neurons following central hypervolaemia and hypovolaemia: contribution of baroreceptor and non-baroreceptor inputs. *Neuroscience* **95**, 499-511, doi:S0306452299004261 [pii] (2000).
258 Allen, W. E. *et al.* Thirst-Associated Preoptic Neurons Encode an Aversive Motivational Drive. *Science (New York, N.Y.)* **in press** (2017).
259 Godino, A., Giusti-Paiva, A., Antunes-Rodrigues, J. & Vivas, L. Neurochemical brain groups activated after an isotonic blood volume expansion in rats. *Neuroscience* **In Press, Corrected Proof**.
260 Howe, B. M., Bruno, S. B., Higgs, K. A., Stigers, R. L. & Cunningham, J. T. FosB expression in the central nervous system following isotonic volume expansion in unanesthetized rats. *Experimental neurology* **187**, 190-198, doi:10.1016/j.expneurol.2004.01.020 (2004).
261 Randolph, R. R., Li, Q., Curtis, K. S., Sullivan, M. J. & Cunningham, J. T. Fos expression following isotonic volume expansion of the unanesthetized male rat. *The American journal of physiology* **274**, R1345-1352 (1998).
262 Gizowski, C. & Bourque, C. W. Neurons that drive and quench thirst. *Science (New York, N.Y.)* **in press** (2017).
263 Simpson, J. B. & Routtenberg, A. Subfornical organ: a dipsogenic site of action of angiotensin II. *Science (New York, N.Y.)* **201**, 379-381 (1978).
264 Simpson, J. B. & Routtenberg, A. Subfornical organ: site of drinking elicitation by angiotensin II. *Science (New York, N.Y.)* **181**, 1172-1175 (1973).
265 Antunes-Rodrigues, J., de Castro, M., Elias, L. L., Valenca, M. M. & McCann, S. M. Neuroendocrine control of body fluid metabolism. *Physiol Rev* **84**, 169-208, doi:10.1152/physrev.00017.2003
84/1/169 [pii] (2004).
266 Kuwahara, K. & Nakao, K. Regulation and significance of atrial and brain natriuretic peptides as cardiac hormones. *Endocrine journal* **57**, 555-565 (2010).

267 Ehrlich, K. J. & Fitts, D. A. Atrial natriuretic peptide in the subfornical organ reduces drinking induced by angiotensin or in response to water deprivation. *Behavioral neuroscience* **104**, 365-372 (1990).
268 Stanhewicz, A. E. & Kenney, W. L. Determinants of water and sodium intake and output. *Nutrition reviews* **73 Suppl 2**, 73-82, doi:10.1093/nutrit/nuv033 (2015).
269 Stricker, E. M. & Stricker, M. L. Pre-systemic controls of fluid intake and vasopressin secretion. *Physiology & behavior* **103**, 86-88, doi:10.1016/j.physbeh.2010.11.019 (2011).
270 Fitzsimons, T. J. & Le Magnen, J. Eating as a regulatory control of drinking in the rat. *Journal of comparative and physiological psychology* **67**, 273-283 (1969).
271 Mandelblat-Cerf, Y. *et al.* Bidirectional Anticipation of Future Osmotic Challenges by Vasopressin Neurons. *Neuron* **93**, 57-65, doi:10.1016/j.neuron.2016.11.021 (2017).
272 Hatton, G. I. & Almli, C. R. Plasma osmotic pressure and volume changes as determinants of drinking thresholds. *Physiology & behavior* **4**, 207-214, doi:http://dx.doi.org/10.1016/0031-9384(69)90082-1 (1969).
273 Gamble J. L., P. M. C., McKhann C. F. The optimal water requirement in renal functions: 1. Measurements of water drinking by rats according to increments of urea and of several salts in the food. . *American Journal of Physiology* **88**, 571-580 (1929).
274 Kraly, F. S., Kim, Y. M., Dunham, L. M. & Tribuzio, R. A. Drinking after intragastric NaCl without increase in systemic plasma osmolality in rats. *The American journal of physiology* **269**, R1085-1092 (1995).
275 Stricker, E. M., Huang, W. & Sved, A. F. Early osmoregulatory signals in the control of water intake and neurohypophyseal hormone secretion. *Physiology & behavior* **76**, 415-421 (2002).
276 Manesh, R., Hoffmann, M. L. & Stricker, E. M. Water ingestion by rats fed a high-salt diet may be mediated, in part, by visceral osmoreceptors. *American journal of physiology. Regulatory, integrative and comparative physiology* **290**, R1742-1749, doi:10.1152/ajpregu.00865.2005 (2006).
277 Krause, E. G., de Kloet, A. D. & Sakai, R. R. Post-ingestive signals and satiation of water and sodium intake of male rats. *Physiology & behavior* **99**, 657-662, doi:10.1016/j.physbeh.2010.01.030 (2010).
278 Kobashi, M. & Adachi, A. Projection of nucleus tractus solitarius units influenced by hepatoportal afferent signal to parabrachial nucleus. *Journal of the autonomic nervous system* **16**, 153-158 (1986).
279 Kobashi, M. & Adachi, A. Convergence of hepatic osmoreceptive inputs on sodium-responsive units within the nucleus of the solitary tract of the rat. *J Neurophysiol* **54**, 212-219 (1985).
280 Stricker, E. M. & Hoffmann, M. L. Presystemic signals in the control of thirst, salt appetite, and vasopressin secretion. *Physiology & behavior* **91**, 404-412, doi:S0031-9384(07)00136-9 [pii]
10.1016/j.physbeh.2007.04.007 (2007).
281 Morita, H. *et al.* Fos induction in rat brain neurons after stimulation of the hepatoportal Na-sensitive mechanism. *The American journal of physiology* **272**, R913-923 (1997).
282 Starbuck, E. M. & Fitts, D. A. Influence of the subfornical organ on meal-associated drinking in rats. *American journal of physiology. Regulatory, integrative and comparative physiology* **280**, R669-677 (2001).

283 Gu, G. B. & Ju, G. The parabrachio-subfornical organ projection in the rat. *Brain research bulletin* **38**, 41-47 (1995).
284 Han, Z. S., Gu, G. B., Sun, C. Q. & Ju, G. Convergence of somatosensory and baroreceptive inputs onto parabrachio-subfornical organ neurons in the rat: an electrophysiological study. *Brain research* **566**, 239-247 (1991).
285 McKinley, M. J. *et al.* The sensory circumventricular organs of the mammalian brain. *Adv Anat Embryol Cell Biol* **172**, III-XII, 1-122, back cover (2003).
286 Sladek, C. D. & Johnson, A. K. Integration of thermal and osmotic regulation of water homeostasis: the role of TRPV channels. *American journal of physiology. Regulatory, integrative and comparative physiology* **305**, R669-678, doi:10.1152/ajpregu.00270.2013 (2013).
287 Bel'skaya, L. V., Kosenok, V. K. & Sarf, E. A. Chronophysiological features of the normal mineral composition of human saliva. *Archives of oral biology* **82**, 286-292, doi:10.1016/j.archoralbio.2017.06.024 (2017).
288 Lund, J. P., Barker, J. H., Dellow, P. G. & Stevenson, J. A. Water intake of normal and desalivate rats on exposure to environmental heat. *Canadian journal of physiology and pharmacology* **47**, 849-852 (1969).
289 Grace, J. E. & Stevenson, J. A. Thermogenic drinking in the rat. *The American journal of physiology* **220**, 1009-1015 (1971).
290 Box, B. M., Montis, F., Yeomans, C. & Stevenson, J. A. Thermogenic drinking in cold-acclimated rats. *The American journal of physiology* **225**, 162-165 (1973).
291 Barney, C. C. & Folkerts, M. M. Thermal dehydration-induced thirst in rats: role of body temperature. *The American journal of physiology* **269**, R557-564 (1995).
292 Morrison, S. F. & Nakamura, K. Central neural pathways for thermoregulation. *Frontiers in bioscience (Landmark edition)* **16**, 74-104 (2011).
293 Palkar, R., Lippoldt, E. K. & McKemy, D. D. The molecular and cellular basis of thermosensation in mammals. *Current opinion in neurobiology* **34**, 14-19, doi:10.1016/j.conb.2015.01.010 (2015).
294 Schepers, R. J. & Ringkamp, M. Thermoreceptors and thermosensitive afferents. *Neuroscience and biobehavioral reviews* **34**, 177-184, doi:10.1016/j.neubiorev.2009.10.003 (2010).
295 Craig, A. D., Bushnell, M. C., Zhang, E. T. & Blomqvist, A. A thalamic nucleus specific for pain and temperature sensation. *Nature* **372**, 770-773, doi:10.1038/372770a0 (1994).
296 Nakamura, K. & Morrison, S. F. A thermosensory pathway that controls body temperature. *Nature neuroscience* **11**, 62-71, doi:nn2027 [pii]
10.1038/nn2027 (2008).
297 Jessen, C., Feistkorn, G. & Nagel, A. Temperature sensitivity of skeletal muscle in the conscious goat. *Journal of applied physiology: respiratory, environmental and exercise physiology* **54**, 880-886 (1983).
298 Fajardo, O., Meseguer, V., Belmonte, C. & Viana, F. TRPA1 channels mediate cold temperature sensing in mammalian vagal sensory neurons: pharmacological and genetic evidence. *The Journal of neuroscience : the official journal of the Society for Neuroscience* **28**, 7863-7875, doi:10.1523/jneurosci.1696-08.2008 (2008).
299 Riedel, W. Warm receptors in the dorsal abdominal wall of the rabbit. *Pflugers Archiv : European journal of physiology* **361**, 205-206 (1976).

300 Rawson, R. O. & Quick, K. P. Localization of intra-abdominal thermoreceptors in the ewe. *The Journal of physiology* **222**, 665-667 (1972).
301 Adelson, D. W., Wei, J. Y. & Kruger, L. Warm-sensitive afferent splanchnic C-fiber units in vitro. *J Neurophysiol* **77**, 2989-3002 (1997).
302 Wit, A. & Wang, S. C. Temperature-sensitive neurons in preoptic-anterior hypothalamic region: effects of increasing ambient temperature. *The American journal of physiology* **215**, 1151-1159 (1968).
303 Takamata, A., Mack, G. W., Stachenfeld, N. S. & Nadel, E. R. Body temperature modification of osmotically induced vasopressin secretion and thirst in humans. *The American journal of physiology* **269**, R874-880 (1995).
304 Boulant, J. A. Cellular mechanisms of temperature sensitivity in hypothalamic neurons. *Progress in brain research* **115**, 3-8 (1998).
305 Fealey, R. D. Interoception and autonomic nervous system reflexes thermoregulation. *Handbook of clinical neurology* **117**, 79-88, doi:10.1016/b978-0-444-53491-0.00007-9 (2013).
306 Morrison, S. F. Central control of body temperature. *F1000Research* **5**, doi:10.12688/f1000research.7958.1 (2016).
307 Boulant, J. A. Hypothalamic mechanisms in thermoregulation. *Fed Proc* **40**, 2843-2850 (1981).
308 Barbour, H. G. Die Wirkung unmittelbarer Erwarmung und Abkuhlung der Warmezentra auf die Korpertemperatur. *Arch Exp Path Pharmak* **70**, 1-15 (1912).
309 Hammouda, M. The central and the reflex mechanism of panting. *The Journal of physiology* **77**, 319-336 (1933).
310 Magoun H. W., H. F., Brobeck J. R., Ranson S. W., Paolini P. Activation of heat loss mechanisms by local heating of the brain. *Journal of Neurophysiology* **87**, 885-905 (1986).
311 Jacobson, F. H. & Squires, R. D. Thermoregulatory responses of the cat to preoptic and environmental temperatures. *The American journal of physiology* **218**, 1575-1582 (1970).
312 Szczepanska-Sadowska, E. Plasma ADH increase and thirst suppression elicited by preoptic heating in the dog. *The American journal of physiology* **226**, 155-161 (1974).
313 Morrison, S. F., Nakamura, K. & Madden, C. J. Central control of thermogenesis in mammals. *Experimental physiology* **93**, 773-797, doi:expphysiol.2007.041848 [pii] 10.1113/expphysiol.2007.041848 (2008).
314 Tan, C. L. *et al.* Warm-Sensitive Neurons that Control Body Temperature. *Cell* **167**, 47-59.e15, doi:10.1016/j.cell.2016.08.028 (2016).
315 Nakamura, K. & Morrison, S. F. A thermosensory pathway mediating heat-defense responses. *Proceedings of the National Academy of Sciences of the United States of America* **107**, 8848-8853, doi:0913358107 [pii] 10.1073/pnas.0913358107 (2010).
316 Andersson, B. & Larsson, B. Influence of local temperature changes in the preoptic area and rostral hypothalamus on the regulation of food and water intake. *Acta physiologica Scandinavica* **52**, 75-89, doi:10.1111/j.1748-1716.1961.tb02203.x (1961).
317 Moon, D. G. *et al.* Antidiuretic hormone in elderly male patients with severe nocturia: a circadian study. *BJU Int* **94**, 571-575, doi:10.1111/j.1464-410X.2004.05003.x BJU5003 [pii] (2004).
318 Miller, M. Nocturnal polyuria in older people: pathophysiology and clinical implications. *J Am Geriatr Soc* **48**, 1321-1329 (2000).

319 Tokonami, N. *et al*. Local renal circadian clocks control fluid-electrolyte homeostasis and BP. *Journal of the American Society of Nephrology : JASN* **25**, 1430-1439, doi:10.1681/asn.2013060641 (2014).
320 Firsov, D., Tokonami, N. & Bonny, O. Role of the renal circadian timing system in maintaining water and electrolytes homeostasis. *Molecular and cellular endocrinology* **349**, 51-55, doi:10.1016/j.mce.2011.06.037 (2012).
321 Asplund, R. Nocturia, nocturnal polyuria, and sleep quality in the elderly. *J Psychosom Res* **56**, 517-525, doi:10.1016/j.jpsychores.2004.04.003 (2004).
322 Windle, R. J., Forsling, M. L. & Guzek, J. W. Daily rhythms in the hormone content of the neurohypophysial system and release of oxytocin and vasopressin in the male rat: effect of constant light. *J Endocrinol* **133**, 283-290 (1992).
323 Spiteri, N. J. Circadian patterning of feeding, drinking and activity during diurnal food access in rats. *Physiology & behavior* **28**, 139-147 (1982).
324 Satinoff, E. & Prosser, R. A. Suprachiasmatic nuclear lesions eliminate circadian rhythms of drinking and activity, but not of body temperature, in male rats. *Journal of biological rhythms* **3**, 1-22, doi:10.1177/074873048800300101 (1988).
325 Johnson, R. F., Beltz, T. G., Thunhorst, R. L. & Johnson, A. K. Investigations on the physiological controls of water and saline intake in C57BL/6 mice. *American journal of physiology. Regulatory, integrative and comparative physiology* **285**, R394-403, doi:10.1152/ajpregu.00130.2003 (2003).
326 Kalsbeek, A. & Buijs, R. M. Output pathways of the mammalian suprachiasmatic nucleus: coding circadian time by transmitter selection and specific targeting. *Cell Tissue Res* **309**, 109-118, doi:10.1007/s00441-002-0577-0 (2002).
327 Appelgren, B., Eriksson, S. & Jonasson, H. Oro-gastro-intestinal inhibition of hypernatremia-induced drinking in the goat. *Acta physiologica Scandinavica* **115**, 273-280, doi:10.1111/j.1748-1716.1982.tb07076.x (1982).
328 Wood, R. J., Rolls, E. T. & Rolls, B. J. Physiological mechanisms for thirst in the nonhuman primate. *The American journal of physiology* **242**, R423-428 (1982).
329 Krashes, M. J. Physiology: Forecast for water balance. *Nature* **537**, 626-627, doi:10.1038/537626a (2016).
330 Zocchi, D., Wennemuth, G. & Oka, Y. The cellular mechanism for water detection in the mammalian taste system. *Nature neuroscience* **20**, 927-933, doi:10.1038/nn.4575 (2017).
331 Blass, E. M., Jobaris, R. & Hall, W. G. Oropharyngeal control of drinking in rats. *Journal of comparative and physiological psychology* **90**, 909-916 (1976).
332 Maddison, S., Wood, R. J., Rolls, E. T., Rolls, B. J. & Gibbs, J. Drinking in the rhesus monkey: peripheral factors. *Journal of comparative and physiological psychology* **94**, 365-374 (1980).
333 Davis, J. D., Smith, G. P. & McCann, D. P. The control of water and sodium chloride intake by postingestional and orosensory stimulation in water-deprived rats. *Physiology & behavior* **75**, 7-14 (2002).
334 Paintal, A. S. Impulses in vagal afferent fibres from stretch receptors in the stomach and their role in the peripheral mechanism of hunger. *Nature* **172**, 1194-1195 (1953).
335 Malbert, C. H. & Leitner, L. M. Mechanoreceptors sensitive to flow at the gastroduodenal junction of the cat. *The American journal of physiology* **265**, G310-313 (1993).
336 Paintal, A. S. A study of gastric stretch receptors; their role in the peripheral mechanism of satiation of hunger and thirst. *The Journal of physiology* **126**, 255-270 (1954).

337 Raybould, H. E., Gayton, R. J. & Dockray, G. J. CNS effects of circulating CCK8: involvement of brainstem neurones responding to gastric distension. *Brain research* **342**, 187-190 (1985).
338 Olson, B. R. *et al.* c-Fos Expression in Rat Brain and Brainstem Nuclei in Response to Treatments That Alter Food Intake and Gastric Motility. *Molecular and cellular neurosciences* **4**, 93-106, doi:10.1006/mcne.1993.1011 (1993).
339 Hyde, T. M. & Miselis, R. R. Area postrema and adjacent nucleus of the solitary tract in water and sodium balance. *The American journal of physiology* **247**, R173-182 (1984).
340 Curtis, K. S., Verbalis, J. G. & Stricker, E. M. Area postrema lesions in rats appear to disrupt rapid feedback inhibition of fluid intake. *Brain research* **726**, 31-38 (1996).
341 Curtis, K. S. & Stricker, E. M. Enhanced fluid intake by rats after capsaicin treatment. *The American journal of physiology* **272**, R704-709 (1997).
342 Hajat, S., Vardoulakis, S., Heaviside, C. & Eggen, B. Climate change effects on human health: projections of temperature-related mortality for the UK during the 2020s, 2050s and 2080s. *Journal of epidemiology and community health* **68**, 641-648, doi:10.1136/jech-2013-202449 (2014).
343 Robertson, G. L., Shelton, R. L. & Athar, S. The osmoregulation of vasopressin. *Kidney Int* **10**, 25-37 (1976).
344 Morf, J. & Schibler, U. Body temperature cycles: gatekeepers of circadian clocks. *Cell cycle (Georgetown, Tex.)* **12**, 539-540, doi:10.4161/cc.23670 (2013).
345 Konishi, M., Nagashima, K. & Kanosue, K. Systemic salt loading decreases body temperature and increases heat-escape/cold-seeking behaviour via the central AT1 and V1 receptors in rats. *The Journal of physiology* **545**, 289-296, doi:PHY_027029 [pii] (2002).
346 Nagashima, K., Nakai, S., Konishi, M., Su, L. & Kanosue, K. Increased heat-escape/cold-seeking behavior following hypertonic saline injection in rats. *Am J Physiol Regul Integr Comp Physiol* **280**, R1031-1036, doi:10.1152/ajpregu.2001.280.4.R1031 (2001).
347 Muller, M. D. *et al.* Effect of acute salt ingestion upon core temperature in healthy men. *Hypertension research : official journal of the Japanese Society of Hypertension* **34**, 753-757, doi:10.1038/hr.2011.27 (2011).
348 Mohawk, J. A., Green, C. B. & Takahashi, J. S. Central and peripheral circadian clocks in mammals. *Annu Rev Neurosci* **35**, 445-462, doi:10.1146/annurev-neuro-060909-153128 (2012).
349 Colwell, C. S. Linking neural activity and molecular oscillations in the SCN. *Nat Rev Neurosci* **12**, 553-569, doi:10.1038/nrn3086 (2011).
350 Reppert, S. M. & Weaver, D. R. Coordination of circadian timing in mammals. *Nature* **418**, 935-941, doi:10.1038/nature00965
nature00965 [pii] (2002).
351 Cuddapah, V. A., Zhang, S. L. & Sehgal, A. Regulation of the Blood-Brain Barrier by Circadian Rhythms and Sleep. *Trends Neurosci* **42**, 500-510, doi:10.1016/j.tins.2019.05.001 (2019).
352 Gizowski, C. & Bourque, C. W. The neural basis of homeostatic and anticipatory thirst. *Nat. Rev. Nephrol.* **14:** , 11-25 (2018).
353 Rittig, S. *et al.* Adult enuresis. The role of vasopressin and atrial natriuretic peptide. *Scand J Urol Nephrol Suppl* **125**, 79-86 (1989).

354 Willis, C. K., Menzies, A. K., Boyles, J. G. & Wojciechowski, M. S. Evaporative water loss is a plausible explanation for mortality of bats from white-nose syndrome. *Integrative and comparative biology* **51**, 364-373, doi:10.1093/icb/icr076 (2011).
355 Buijs, R. M., Guzman Ruiz, M. A., Mendez Hernandez, R. & Rodriguez Cortes, B. The suprachiasmatic nucleus; a responsive clock regulating homeostasis by daily changing the setpoints of physiological parameters. *Auton Neurosci* **218**, 43-50, doi:10.1016/j.autneu.2019.02.001 (2019).
356 Tervo, D. G. *et al.* A Designer AAV Variant Permits Efficient Retrograde Access to Projection Neurons. *Neuron* **92**, 372-382, doi:10.1016/j.neuron.2016.09.021 (2016).
357 Wagner, S., Castel, M., Gainer, H. & Yarom, Y. GABA in the mammalian suprachiasmatic nucleus and its role in diurnal rhythmicity. *Nature* **387**, 598-603, doi:10.1038/42468 (1997).
358 Choi, H. J. *et al.* Excitatory actions of GABA in the suprachiasmatic nucleus. *The Journal of neuroscience : the official journal of the Society for Neuroscience* **28**, 5450-5459, doi:10.1523/jneurosci.5750-07.2008 (2008).
359 Mrosovsky, N. Locomotor activity and non-photic influences on circadian clocks. *Biological reviews of the Cambridge Philosophical Society* **71**, 343-372 (1996).
360 Gizowski, C., Trudel, E. & Bourque, C. W. Central and peripheral roles of vasopressin in the circadian defense of body hydration. *Best Pract Res Clin Endocrinol Metab* **31**, 535-546, doi:10.1016/j.beem.2017.11.001 (2017).
361 Meyer, C. W., Ootsuka, Y. & Romanovsky, A. A. Body Temperature Measurements for Metabolic Phenotyping in Mice. *Frontiers in physiology* **8**, 520, doi:10.3389/fphys.2017.00520 (2017).
362 Andermann, M. L. & Lowell, B. B. Toward a Wiring Diagram Understanding of Appetite Control. *Neuron* **95**, 757-778, doi:10.1016/j.neuron.2017.06.014 (2017).
363 Mazuski, C. *et al.* Entrainment of Circadian Rhythms Depends on Firing Rates and Neuropeptide Release of VIP SCN Neurons. *Neuron* **99**, 555-563.e555, doi:10.1016/j.neuron.2018.06.029 (2018).
364 Bedont, J. L. *et al.* Asymmetric vasopressin signaling spatially organizes the master circadian clock. *The Journal of comparative neurology* **526**, 2048-2067, doi:10.1002/cne.24478 (2018).
365 Zaelzer, C., Gizowski, C., Salmon, C. K., Murai, K. K. & Bourque, C. W. Detection of activity-dependent vasopressin release from neuronal dendrites and axon terminals using sniffer cells. *Journal of neurophysiology* **120**, 1386-1396, doi:10.1152/jn.00467.2017 (2018).
366 Dutton, A. & Dyball, R. E. Phasic firing enhances vasopressin release from the rat neurohypophysis. *The Journal of physiology* **290**, 433-440 (1979).
367 van den Pol, A. N. Neuropeptide transmission in brain circuits. *Neuron* **76**, 98-115, doi:10.1016/j.neuron.2012.09.014 (2012).
368 Buijs, R. M., Wortel, J. & Hou, Y. X. Colocalization of gamma-aminobutyric acid with vasopressin, vasoactive intestinal peptide, and somatostatin in the rat suprachiasmatic nucleus. *The Journal of comparative neurology* **358**, 343-352, doi:10.1002/cne.903580304 (1995).
369 Numazaki, M., Tominaga, T., Toyooka, H. & Tominaga, M. Direct phosphorylation of capsaicin receptor VR1 by protein kinase Cepsilon and identification of two target serine residues. *J Biol Chem* **277**, 13375-13378, doi:10.1074/jbc.C200104200

C200104200 [pii] (2002).
370 Sharif Naeini, R., Witty, M. F., Seguela, P. & Bourque, C. W. An N-terminal variant of Trpv1 channel is required for osmosensory transduction. *Nature neuroscience* **9**, 93-98, doi:nn1614 [pii]
10.1038/nn1614 (2006).
371 Sharif-Naeini, R., Ciura, S. & Bourque, C. W. TRPV1 gene required for thermosensory transduction and anticipatory secretion from vasopressin neurons during hyperthermia. *Neuron* **58**, 179-185, doi:S0896-6273(08)00136-0 [pii]
10.1016/j.neuron.2008.02.013 (2008).
372 Augustine, V. *et al.* Hierarchical neural architecture underlying thirst regulation. *Nature* **555**, 204-209, doi:10.1038/nature25488 (2018).
373 Leib, D. E. *et al.* The Forebrain Thirst Circuit Drives Drinking through Negative Reinforcement. *Neuron* **96**, 1272-1281.e1274, doi:10.1016/j.neuron.2017.11.041 (2017).
374 Zimmerman, C. A. *et al.* A gut-to-brain signal of fluid osmolarity controls thirst satiation. *Nature* **568**, 98-102, doi:10.1038/s41586-019-1066-x (2019).
375 Campos, L. M., Cruz-Rizzolo, R. J., Watanabe, I. S., Pinato, L. & Nogueira, M. I. Efferent projections of the suprachiasmatic nucleus based on the distribution of vasoactive intestinal peptide (VIP) and arginine vasopressin (AVP) immunoreactive fibers in the hypothalamus of Sapajus apella. *Journal of chemical neuroanatomy* **57-58**, 42-53, doi:10.1016/j.jchemneu.2014.03.004 (2014).
376 Ben-Hamo, M., Munoz-Garcia, A., Williams, J. B., Korine, C. & Pinshow, B. Waking to drink: rates of evaporative water loss determine arousal frequency in hibernating bats. *The Journal of experimental biology* **216**, 573-577, doi:10.1242/jeb.078790 (2013).
377 Cannon, B. & Nedergaard, J. Nonshivering thermogenesis and its adequate measurement in metabolic studies. *The Journal of experimental biology* **214**, 242-253, doi:10.1242/jeb.050989 (2011).
378 Vogel, B. *et al.* Touch-free measurement of body temperature using close-up thermography of the ocular surface. *MethodsX* **3**, 407-416, doi:10.1016/j.mex.2016.05.002 (2016).
379 Labbe, S. M. *et al.* Hypothalamic control of brown adipose tissue thermogenesis. *Frontiers in systems neuroscience* **9**, 150, doi:10.3389/fnsys.2015.00150 (2015).
380 Ben-Ari, Y. Excitatory actions of gaba during development: the nature of the nurture. *Nature reviews. Neuroscience* **3**, 728-739, doi:10.1038/nrn920 (2002).
381 Belenky, M. A., Yarom, Y. & Pickard, G. E. Heterogeneous expression of gamma-aminobutyric acid and gamma-aminobutyric acid-associated receptors and transporters in the rat suprachiasmatic nucleus. *The Journal of comparative neurology* **506**, 708-732, doi:10.1002/cne.21553 (2008).
382 Belenky, M. A. *et al.* Cell-type specific distribution of chloride transporters in the rat suprachiasmatic nucleus. *Neuroscience* **165**, 1519-1537, doi:10.1016/j.neuroscience.2009.11.040 (2010).
383 Albus, H., Vansteensel, M. J., Michel, S., Block, G. D. & Meijer, J. H. A GABAergic mechanism is necessary for coupling dissociable ventral and dorsal regional oscillators within the circadian clock. *Current biology : CB* **15**, 886-893, doi:10.1016/j.cub.2005.03.051 (2005).
384 Bourque, C. W., Ciura, S., Trudel, E., Stachniak, T. J. & Sharif-Naeini, R. Neurophysiological characterization of mammalian osmosensitive neurones. *Experimental physiology* **92**, 499-505, doi:expphysiol.2006.035634 [pii]

10.1113/expphysiol.2006.035634 (2007).
385 Yang, F. & Zheng, J. Understand spiciness: mechanism of TRPV1 channel activation by capsaicin. *Protein & cell* **8**, 169-177, doi:10.1007/s13238-016-0353-7 (2017).
386 Eastman, C. I. & Burgess, H. J. How To Travel the World Without Jet lag. *Sleep medicine clinics* **4**, 241-255, doi:10.1016/j.jsmc.2009.02.006 (2009).

Appendix A

Permission requests from authors – Spring Nature

The author of articles published by Springer Nature do not usually need to seek permission for re-use of their material as long as the journal is credited with initial publication.

Ownership of copyright in in original research articles remains with the Author, and provided that, when reproducing the contribution or extracts from it or from the Supplementary Information, the Author acknowledges first and reference publication in the Journal, the Author retains the following non-exclusive rights:

To reproduce the contribution in whole or in part in any printed volume (book or thesis) of which they are the author(s).

The author and any academic institution where they work at the time may reproduce the contribution for the purpose of course teaching.

To reuse figures or tables created by the Author and contained in the Contribution in oral presentations and other works created by them.

To post a copy of the contribution as accepted for publication after peer review (in locked Word processing file, of a PDF version thereof) on the Author's own web site, or the Author's institutional repository, or the Author's funding body's archive, six months after publication of the printed or online edition of the Journal, provided that they also link to the contribution on the publisher's website.

The above use of the term 'Contribution' refers to the author's own version, not the final version as published in the Journal.